

**Direction des bibliothèques**

**AVIS**

Ce document a été numérisé par la Division de la gestion des documents et des archives de l'Université de Montréal.

L'auteur a autorisé l'Université de Montréal à reproduire et diffuser, en totalité ou en partie, par quelque moyen que ce soit et sur quelque support que ce soit, et exclusivement à des fins non lucratives d'enseignement et de recherche, des copies de ce mémoire ou de cette thèse.

L'auteur et les coauteurs le cas échéant conservent la propriété du droit d'auteur et des droits moraux qui protègent ce document. Ni la thèse ou le mémoire, ni des extraits substantiels de ce document, ne doivent être imprimés ou autrement reproduits sans l'autorisation de l'auteur.

Afin de se conformer à la Loi canadienne sur la protection des renseignements personnels, quelques formulaires secondaires, coordonnées ou signatures intégrées au texte ont pu être enlevés de ce document. Bien que cela ait pu affecter la pagination, il n'y a aucun contenu manquant.

**NOTICE**

This document was digitized by the Records Management & Archives Division of Université de Montréal.

The author of this thesis or dissertation has granted a nonexclusive license allowing Université de Montréal to reproduce and publish the document, in part or in whole, and in any format, solely for noncommercial educational and research purposes.

The author and co-authors if applicable retain copyright ownership and moral rights in this document. Neither the whole thesis or dissertation, nor substantial extracts from it, may be printed or otherwise reproduced without the author's permission.

In compliance with the Canadian Privacy Act some supporting forms, contact information or signatures may have been removed from the document. While this may affect the document page count, it does not represent any loss of content from the document.

Université de Montréal

Aspects spatial et temporel de l'intégration visuelle au niveau de la voie dorsale  
du système visuel du chat : le cortex suprasylvien latéral comme modèle

Par

Brian G. Ouellette

Département de Psychologie

Faculté des Arts et Science

Thèse présentée à la Faculté des études supérieures en vue de l'obtention du  
grade de doctorat en Psychologie option Sciences Cognitives et  
Neuropsychologie

Janvier, 2008

©, Brian G. Ouellette, 2008



Université de Montréal  
Faculté des études supérieures

Cette thèse intitulée :

Aspects spatial et temporel de l'intégration visuelle au niveau de la voie dorsale  
du système visuel du chat : le cortex suprasylvien latéral comme modèle

Présenté par :

Brian G. Ouellette

A été évalué par un jury composé des personnes suivantes ;

Maurice Ptito, Président-rapporteur

Christian Casanova, directeur de recherche

Jocelyn Faubert, co-directeur de recherche

Dave St-Amour, membre du jury

Stephen Lomber, examinateur externe

Martin Arguin, représentant du doyen de la FES

## Résumé

Depuis les 25 dernières années la notion d'une hiérarchie d'aires corticales a grandement influencé le contexte théorique dans lequel les études dans le domaine des neurosciences sont effectuées. Cette notion de hiérarchie propose qu'en observant un patron récurrent de couches d'origines et de terminaisons des projections entre les aires corticales il est possible d'établir un ordre relatif entre ces mêmes aires. Les aires de bas niveau seraient les principales afférences excitatrices aux aires de plus haut niveau alors que la rétroaction provenant de ces dernières aurait plutôt un rôle de modulateur. Cette notion permet en effet d'expliquer un grand nombre d'observations physiologiques, telle que la progression des propriétés visuelles des neurones dans différentes régions corticales. Cependant, certaines propriétés physiologiques ne correspondent pas à la hiérarchie. Afin d'infirmer ou confirmer l'existence d'une hiérarchie, trois hypothèses furent testées et les données comparées aux prédictions basées sur la hiérarchie. Comme modèle d'aire corticale, le cortex entourant la partie médiane du sulcus suprasylvien latéral (PMLS) fût choisi. Cette région reçoit des projections directes et massives de l'aire 17, ce qui permet de faire des prédictions précises quant aux changements des réponses du PMLS lors d'enregistrements extracellulaires. La technique d'enregistrement extracellulaire unitaire avec micro-électrodes chez le chat adulte anesthésié a été utilisée dans les trois études. Dans la première expérience, l'aire visuelle primaire du chaton fût lésée, puis des enregistrements dans le PMLS furent recueillis un an plus tard. La sélectivité à la direction

typique de cette région y était toujours présente, malgré l'élimination de sa principale afférence. Dans une deuxième étude, une comparaison de la latence des réponses neuronales a révélée une activation simultanée de plusieurs aires corticales, malgré leur appartenance à différents niveaux de la hiérarchie. Enfin, une étude des profils spatio-temporels des champs récepteurs du PMLS a mis en évidence que certaines cellules n'étaient pas de type complexe comme prédit. Les présentes études confirment donc que la hiérarchie anatomique ne correspond pas toujours aux propriétés physiologiques. Ceci suggère que des afférences autres que celles incluses dans la hiérarchie sont impliquées dans le transfert de l'information dans la voie dorsale chez le chat.

**Mots clés :** mouvement, vision, électrophysiologie, hiérarchie corticale, chat, voie dorsale, PMLS, latence, lésion, profils spatio-temporel

## Abstract

The notion of a hierarchy of cortical areas based on anatomical data has had a considerable influence on theories in neuroscience over the past 25 years. The hierarchies are based on the observation of recurrent projection patterns between cortical areas. Namely the lamina of origin and termination of projections allows one to establish a relative order between areas. Lower order areas are thought to be the main input to higher order areas, while higher order areas would feedback modulatory influences to lower order areas. This notion explains a large number of physiological observations, such as the progression of visual receptive field properties across different cortical areas. However, some neuronal response properties do not correspond with what would be expected from a hierarchically organised system. In order to further test the notion of a hierarchy, data was obtained relative to three different hypotheses and compared to predictions based on the hierarchy. The postero-medial lateral suprasylvian sulcus (PMLS) was chosen as a model structure. This area receives direct and massive projections from area 17, which allows for precise predictions in changes of neuronal responses while recording in PMLS cortex. The three studies were carried out using single unit extracellular recordings with micro-electrodes in the adult anaesthetised cat. In the first experiment, a neonatal lesion of primary visual cortex was performed, followed by recordings in PMLS cortex one year later. The typical direction selective responses of the latter were still present despite the removal of PMLS' putative main input. In a second study, a comparison of response latencies revealed a simultaneous

activation across cortical areas, despite the choice of areas that are situated at different levels of the hierarchy. Finally, a spatio-temporal analysis of PMLS receptive fields revealed that a subset of neurons did not have the complex type receptive fields expected. The three studies confirm that the anatomically based hierarchy does not always correspond with physiological response properties. This suggests that afferents other than those proposed within the classical hierarchy are involved in the transfer of information in the dorsal stream of the cat.

Keywords : movement, vision, electrophysiology, cortical hierarchy, cat, dorsal stream, PMLS, latency, lesion, spatio-temporal profiles

## Table des matières

Introduction.....	1
1. Deux voies visuelles .....	1
2. L'anatomie de la voie dorsale .....	3
2.1 La voie géniculéo-aies 17, 18 et 19 .....	3
2.1.1 La notion de hiérarchie corticale.....	4
2.1.2 La voie cortico-thalamo-corticale.....	8
2.1.3 La voie cortico-corticale.....	10
2.2 La voie rétino-thalamo-corticale .....	10
2.3 La voie tecto-thalamo-corticale .....	11
3. Physiologie des neurones du PMLS .....	14
3.1 Données électrophysiologiques .....	14
3.2 Données comportementales .....	15
3.3 Modèle d'analyse du mouvement.....	16
3.3.1 Modèle d'énergie.....	17
3.3.2 Modèle de sélection.....	20
3.3.2.1 La rétine .....	20
3.3.2.2 Le cortex visuel primaire .....	23
3.3.2.3 L'aire MT .....	23
3.3.2.4 La sortie .....	25
4. L'aspect parallèle du système.....	26



4.1 Lésion de l'aire visuelle primaire .....	26
4.1.1 Lésion chez l'adulte .....	26
4.1.2 Lésion chez le chaton .....	27
4.1.2.1 Nature des stimuli .....	27
4.1.2.2 Fondement anatomique .....	28
4.2 Profil temporel des réponses .....	30
4.2.1 Les latences neuronales .....	30
4.2.2 D'autres mesures temporelles .....	32
4.3 Profile spatio-temporel des champs récepteurs .....	33
4.3.1 La corrélation rétrograde .....	34
4.3.2 Les profils de l'aire 17 .....	40
4.3.3 Les profils du PMLS .....	41
5. Objectif et hypothèse .....	43
5.1 Première étude .....	43
5.2 Deuxième étude .....	44
5.3 Troisième étude .....	45
5.4 Résumé de l'objectif .....	45
Article 1 .....	47
Abstract .....	49
Introduction .....	51
Methods .....	52
Lesion protocol .....	52

Animal preparation .....	53
Recordings and visual stimulation .....	54
Receptive field properties .....	54
Plaid patterns .....	55
Random dot kinematograms .....	55
Data analysis.....	56
Histology .....	56
Results.....	57
Extent of the lesions .....	57
Basic receptive field properties .....	61
Sinewave gratings .....	61
Plaid patterns .....	64
RDKs .....	66
Stimulus dependent direction selectivity.....	68
Discussion .....	69
General observations .....	69
Unilateral nature of the lesions.....	70
Proportion of direction selective cells .....	70
Possible pathways .....	71
Role of feedback connections .....	76
Comparison with primate.....	76

Implications for motion processing .....	78
Conclusions.....	81
Acknowledgements.....	82
References .....	83
Article 2.....	89
Abstract.....	91
Introduction.....	93
Methods.....	96
Single unit recordings.....	96
Stimuli .....	96
Visual onset latencies.....	97
Results.....	100
Differences across areas.....	100
Differences between stimuli .....	104
Effect of primary visual cortex lesions .....	107
Discussion .....	109
General findings.....	109
Methodological considerations .....	110
Differences across areas.....	112
Differences across stimuli .....	114

Cortical versus thalamic latencies .....	116
PMLS-lesion .....	117
Conclusion .....	117
Acknowledgements.....	119
References .....	120
Article 3.....	125
Abstract.....	127
Introduction .....	128
Methods.....	130
Animal preparation .....	130
Recordings .....	132
Visual stimulation .....	132
Data analysis.....	134
Reverse correlation .....	134
Assessment of overlap .....	138
Cellular classification.....	140
Quantification of responses to gratings .....	141
Predicting RF parameters .....	143
Surface fitting .....	144
Results.....	145
Spatial organization of the RF .....	146

Basic RF parameters.....	146
Overlap.....	149
Cellular classification .....	153
Temporal response profile.....	156
Response latencies .....	156
Response phase .....	159
Response duration .....	163
Multi-lobed responses .....	164
Afferents.....	166
RF property prediction.....	167
Direction selectivity.....	168
Spatial frequency.....	169
Temporal frequency.....	170
Test of linear model.....	171
Subfield fits.....	174
Discussion .....	175
General conclusions.....	175
Methodological considerations.....	177
Spatial domain .....	177
Complex like RF profile .....	177
Other RF profiles .....	179
Spatial integration of motion signal.....	181
Temporal domain .....	184

Response duration .....	184
Response slope.....	185
Response latency.....	186
Phase shifted and multi-lobed response.....	186
Implications for system organization .....	187
The evidence against sole area 17 input.....	188
Direct LGN input.....	189
Direct input from the Pulvinar .....	190
Conclusion .....	193
Appendix.....	194
References .....	196
Acknowledgements.....	205
Grants.....	205
Discussion .....	206
1. Résumé des résultats .....	206
1.1 Études des effets d'une lésion de l'aire visuelle primaire .....	206
1.2 Études des latences .....	207
1.3 Étude des profils spatio-temporels .....	207
2. Considérations méthodologiques.....	208
2.1 Étude de lésions de l'aire visuelle primaire .....	208
2.1.1 Étendues des lésions .....	208
2.1.2 Âges des lésions .....	209

2.2 Étude de latence .....	210
2.2.1 La nature du processus étudié .....	210
2.2.2 La résolution temporelle .....	211
2.3 Profil spatio-temporel .....	212
2.3.1 Aspect linéaire de la méthode .....	212
2.3.2 La nature non-écologique de la stimulation impulsionnelle .....	213
3. Implication pour la hiérarchie des aires corticales .....	214
3.1 La voie du CGL .....	215
3.2 Les voies alternatives .....	219
3.2.1 Le collicule supérieur .....	219
3.2.2 Les boucles de rétroaction .....	221
3.2.3 La voie rétino-thalamo-corticale .....	221
3.3 Réconciliation de l'anatomie et de la physiologie .....	223
3.3.1 La proposition sensorielle .....	223
3.3.2 La proposition attentionnelle .....	226
4. Intégration spatiale dans le PMLS .....	228
4.1 Intégration linéaire versus non-linéaire .....	228
4.2 Intégration du mouvement .....	229
5. Études futures .....	233
5.1 Idées découlant de l'étude des profils .....	233
5.1.1 La corrélation rétrograde d'ordre supérieur .....	233
5.1.2 La corrélation rétrograde d'ordre supérieur et l'inactivation .....	234
5.1.3 Le mouvement fronto-parallèle versus le flux optique .....	237

5.2 Idées découlant de l'étude de lésion .....	240
5.2.1 L'identification de l'origine de la sélectivité résiduelle.....	240
5.2.2 Amélioration comportementale post-lésion.....	241
5.2.3 Mesure de l'effet des lésions par corrélation rétrograde.....	242
5.3 Idées découlant de l'étude de latences .....	243
5.3.1 Latence aux stimuli stationnaires et dynamiques .....	243
5.3.2 Confirmation et identification de deux sous-voies dorsales .....	243
5.4 Idées découlant de la synthèse des trois études.....	244
5.4.1 Anatomie : la nature des connexions.....	244
5.4.2 Comportement : le rôle comportemental du PMLS.....	246
5.4.3 Physiologie : rôle des voies <i>feedforward</i> et de rétroaction .....	247
6. Conclusions .....	248
Références .....	249



Liste des tableaux

Article 2

Table 1 : Measures of central tendency.....103

Figure 7 : Direction and velocity selectivity of the Reichardt model .....	80
----------------------------------------------------------------------------	----

## Article 2

Figure 1 : Cumulative sum technique .....	99
-------------------------------------------	----

Figure 2 : Latencies in different areas.....	101
----------------------------------------------	-----

Figure 3 : Mean and median latencies.....	102
-------------------------------------------	-----

Figure 4 : The cumulative percentage of latencies .....	105
---------------------------------------------------------	-----

Figure 5 : Latencies obtained when different stimuli are presented .....	108
--------------------------------------------------------------------------	-----

## Article 3

Figure 1 : Adaptive pixel-wise Wiener filter.....	136
---------------------------------------------------	-----

Figure 2 : Overlap of subfields.....	142
--------------------------------------	-----

Figure 3 : Spatio-temporal RF I.....	147
--------------------------------------	-----

Figure 4 : Spatio-temporal RF II.....	148
---------------------------------------	-----

Figure 5 : Receptive field parameters.....	150
--------------------------------------------	-----

Figure 6 : Examples of receptive field organization .....	152
-----------------------------------------------------------	-----

Figure 7 : Examples of receptive field organization .....	155
-----------------------------------------------------------	-----

Figure 8 : Response latencies .....	157
-------------------------------------	-----

Figure 9 : Temporal response profiles .....	161
---------------------------------------------	-----

Figure 10 : Temporal characteristics of the response .....	162
------------------------------------------------------------	-----

Figure 11 : Best RF descriptor .....176

## Discussion

Figure 1 : Corrélat physiologique du modèle de Reichardt.....232

Figure 2 : Corrélation rétrograde d'ordre supérieur.....236

Figure 3 : Surface de réponse de deux neurones idéalisés.....239

## Liste des abréviations

AEV : sulcus ectosylvien antérieur

ALLS : partie antéro-latérale du sulcus suprasylvien latéral

AMLS : partie antéro-médiane du sulcus suprasylvien latéral

CGLd : corps genouillé latéral

LPI : partie latérale du noyau latéro-postérieur thalamique

LPm : partie médiane du noyau latéro-postérieur thalamique

MT : sulcus médio-temporal

PMLS : partie postéro-médiane du sulcus suprasylvien latéral

PLLS : partie postéro-latérale du sulcus suprasylvien latéral

RDK : kinématogramme de points distribués aléatoirement

V1 : aire visuelle primaire

VLS : partie ventro-latérale du sulcus suprasylvien latéral

*Qui rogat, non errat*

*Education is what remains after one has forgotten what one has learned in school.*

Albert Einstein

## Remerciements

À tous, je souhaite que tous vos désirs se réalisent, au plan professionnel mais surtout personnel. Vous voyez, ça commence déjà, vous vous débarrassez de moi! Merci d'avoir partagé un bon moment de vie avec moi (bon... pas par choix, mais... quand même!). Ça a été très plaisant.

Christian, bien qu'un remerciement s'impose de par le contexte, celui-ci est des plus sincères. Ne serait-ce que pour la grande liberté de questions que tu nous permets d'aborder dans le laboratoire, et franchement, j'en ai eu des idées plutôt excentriques. Merci de m'avoir permis de faire un doctorat dans un laboratoire qui se concentre sur le LP-pulvinar, sans que je travaille sur le LP-pulvinar, cet enfer de l'électrophysiologiste. Merci pour l'encadrement, surtout lors des premières années, qui m'a poussé à me dépasser (parfois plus par peur du patron que par envie, mais bon...) et à devenir le penseur critique que je suis aujourd'hui. Merci d'avoir investi dans des objets qui *a priori* paraissent absurdes (la bête et la bête II). Surtout, n'arrête pas de crier tout seul dans ton bureau avec la porte ouverte. Enfin, je te promets que je ferai tout pour ne pas devenir un autre «celui dont il faut taire le nom».

Fred et Martin, si je peux me permettre d'utiliser l'expression d'un grand sage, je vous traiterais de «vieux meubles». Tout comme des vieux meubles

peuvent être vus comme étant d'une valeur inestimable, vous l'êtes tout autant dans un laboratoire. Jamais la qualité des travaux des autres étudiants n'aurait pu être la même sans votre présence. Ce fût un grand plaisir de travailler avec vous, mais les moments à l'extérieur du labo sont tout aussi mémorables. En espérant que nos chemins se recroisent un jour...

À Denis, merci. Merci pour les « cours » de statistiques, anatomiques et autres informations académiques. Tu es une vraie encyclopédie ambulante. Cependant, merci surtout pour nous avoir montré comment décortiquer un article, souvent pour le démolir de A à Z et ainsi détruire nos illusions par rapport à la noblesse de la démarche scientifique tout en nous poussant à faire des projets les mieux conçus possible afin de nous approcher de nos illusions originelles. Ce fût un des exercices les plus utiles lors de mes études graduées. Merci également pour les histoires macabres, les informations les plus excentriques, l'historique des potins de l'UdeM, ainsi que la diversité de faune (bien que morte) dans le laboratoire. Un safari pour repasser nos t-shirts sur un dos d'éléphant, ça te dis?

Karine, bien que tu n'étais pas là pour la grande partie de mon PhD, sans ton aide pour la maîtrise, le PhD aurait été bien plus difficile. Suite à ton départ le spectre de ta personne à eu un effet sur le labo bien plus longtemps que tu ne pourrais le penser.

Merci à Matthieu pour ce savant mélange d'idées de génie et de délires absolus, de bonne humeur permanente et de pessimisme sans borne. Merci aussi pour les multiples discussions qui ont permis au dernier volet de cette thèse d'aboutir. Finalement, le désir d'autoflagellation est une affliction qui se soigne. À bien y penser, ça fait parti de ton charme, n'y change rien. Même si ça te rend malheureux, ça amuse les autres.

À celle qui s'offusque beaucoup trop facilement, il ne faudrait surtout pas prendre des années et des années d'insultes trop au personnel. Surtout, ne perd pas cette passion que tu as lorsque tu parles de tes idées scientifiques, même si je n'y comprends strictement rien à ce que tu racontes et que je ne veux rien y comprendre. La biologie moléculaire c'est n'importe quoi Nawal! Merci beaucoup d'avoir corrigé l'autoGAFFE de ce texte. S'il y a des commentaires des membres du jury, je te les réfère en mentionnant ton incompétence.

Jonathan, je me souviendrai surtout de toutes ces bières dont tu ne te souviendras jamais! Pis tant qu'à y être, merci pour tout le reste.



Geneviève, toi qui sais tout à l'étage, dans l'immeuble, voire dans toute l'université, «la priorité numéro un» : garde moi au courant s.t.p. Ce fût bien plaisant de travailler avec toi et surtout d'observer ta relation inter-corridor avec le patron. Mon côté psy qui sort.

Sébastien, merci de danser le tango avec une balle de caoutchouc. J'aurais bien fini par détruire quelque chose dans le labo n'eut été du DÉFONÇAGE encadré hebdomadaire.

Aux deux seules véritables électrophysiologistes qui restent encore dans le laboratoire, Mélissa et Marilyse, je vous souhaite bonne chance dans vos deux projets qui requièrent chacun une patience hors norme. Que les dieux de l'électrophysiologie soient avec vous, mais n'oubliez pas de faire des sacrifices aux dieux aux moments opportuns. Il paraît qu'ils sont très friands du para.

Marouane, keep the faith, keep the dialogue, and keep up the beautiful idea of putting the two together. 2008 Inch Allah!

À la bête (Pulvinar), merci de m'avoir permis de sauver beaucoup de temps et accessoirement le réchauffage de pieds fût bien apprécié surtout dans

un immeuble trop climatisé. Je me souviendrai toujours de tes douces vibrations chaleureuses. Et je suis surtout heureux de partir avant l'arrivée de bête II, je le sais que tu serais bien trop jalouse si je te laissais tomber pour une autre.

So far, so good, so what...

## Introduction

Le présent ouvrage porte sur le système visuel chez le chat, notamment sur une région qui est la partie latérale du sulcus suprasylvien postéro-médian (PMLS). Cette aire corticale extrastriée est généralement associée au traitement de l'information spécifique au mouvement. L'introduction traitera en premier lieu de l'organisation générale du système visuel tel que nous le connaissons, pour se concentrer dans un deuxième temps sur le PMLS. Ces informations permettront la formulation de questions et d'hypothèses sur lesquelles porte ce travail.

### 1. Deux voies visuelles

Il a été proposé et généralement accepté qu'à partir de l'aire visuelle primaire, le système visuel se divise en deux voies distinctes, bien qu'interconnectées (Ungerleider & Mishkin, 1982; Goodale & Milner, 1992). La première voie étant celle du *quoi* (*what*), aussi connue sous le nom de la voie ventrale, qui serait spécialisée dans la reconnaissance et la discrimination des objets. La voie dorsale, quant à elle, servirait plutôt à l'analyse de la position spatiale des objets dans l'environnement. C'est sur cette dernière que nous nous concentrerons dans cette thèse. Cette voie porte deux noms descriptifs, soit la voie du *où* (*where*) ou du *comment* (*how*), selon la structure considérée comme le point terminal du système. Étant donné que la présente thèse se

limite au système visuel, et n'implique pas une sortie motrice, le terme de *où* sera utilisé.

Bien que le terme *où* soit représentatif du rôle joué par cette partie du système visuel, il est important de comprendre que cette voie traite l'information concernant l'emplacement spatial dans un sens plus large. C'est-à-dire, par exemple, que dans la mesure où le mouvement d'un objet est une séquence de passages par plusieurs positions, il tombe dans la catégorie de ce qui serait traité par la voie dorsale.

Ce schème de deux voies spécialisées dans le traitement de différents types d'information était basé sur des travaux chez le primate non-humain et dans une moindre mesure chez l'humain. La question se pose donc si cette dichotomie se reflète également chez le chat, qui est le modèle utilisé dans les présents travaux. Les travaux de Lomber (2001) où l'inactivation réversible par refroidissement du cortex a été utilisée de concert avec des tâches comportementales qui ciblaient spécifiquement soit la reconnaissance de forme, soit l'analyse du mouvement et l'orientation spatiale, ont permis une ségrégation des aires corticales selon leurs fonctions chez le chat. À cette élégante démonstration d'une similarité entre le chat et le primate, se joint l'apport d'autres études qui semblent confirmer cette séparation des voies (Pasternak *et al.*, 1995; Dreher *et al.*, 1996a; Rudolph & Pasternak, 1996; Vanduffel *et al.*, 1997b). Cependant, Scannell & Young (1993) ont démontré que les données anatomiques ne concordent pas avec cette dichotomie des voies visuelles.

## 2. L'anatomie de la voie dorsale

### 2.1 La voie géniculo-aies 17, 18 et 19

Suite à la transduction de la lumière en signal électrique par les photorécepteurs, l'information est traitée par les diverses couches de la rétine pour être relayée par les cellules ganglionnaires vers plusieurs structures visuelles. La voie la plus étudiée est celle où l'information visuelle est envoyée par les cellules ganglionnaires de la rétine vers la partie dorsale du corps genouillé latéral (CGLd) du thalamus et puis vers les aires 17, 18, 19. À partir de ces aires visuelles, l'information visuelle est redistribuée vers un grand nombre de structures visuelles, tant corticales que sous-corticales.

À des fins de concision, nous nous limiterons à la région corticale centrale aux trois études qui forment cette thèse, soit le PMLS. Nous verrons dans une section subséquente de l'introduction les raisons pour lesquelles cette région fût choisie. Donc, en ce qui concerne spécifiquement le PMLS, ce dernier reçoit des afférences de la part des aires 17, 18 et 19 (Henry *et al.*, 1978; Symonds & Rosenquist, 1984a, b; Einstein & Fitzpatrick, 1991; Grant & Shipp, 1991; Shipp & Grant, 1991; Norita *et al.*, 1996; Scannell, 1997; Scannell *et al.*, 1999; Grant & Hilgetag, 2005). La grande majorité de ces projections proviennent des couches supragranulaires des aires 17 et 18 (Figure 1), alors qu'elles sont issues des couches supra- et infragranulaire pour l'aire 19 (Figure 1). La plupart de ces projections aboutissent dans la couche IV du PMLS (Figure 1). En résumé, les neurones du PMLS reçoivent des projections directes et multiples

en provenance du système géniculo-aies 17, 18 et 19 et sont à seulement trois synapses de la rétine via cette voie.

### 2.1.1 La notion de hiérarchie corticale

La mention ci-dessus de projections cortico-cortiales qui ont leurs origines et terminaisons dans des couches spécifiques nécessite une explication particulière avant de procéder à la description des autres voies projetant vers le PMLS. Depuis la fin des années 70, la notion de hiérarchie entre des régions corticales est une idée qui influence grandement l'étude du système visuel. Cette notion de hiérarchie provient du fait qu'il semble y avoir un patron récurrent de couches d'origines et de terminaisons des projections entre les aires corticales (Rockland & Pandya, 1979; Maunsell & van Essen, 1983; Van Essen & Maunsell, 1983; Symonds & Rosenquist, 1984b; Felleman & Van Essen, 1991). Des analyses quantitatives plus poussées de ces résultats confirment la présence de patrons récurrent et supportent l'idée d'une hiérarchie des aires visuelles tant chez le primate que chez le chat (Scannell & Young, 1993; Scannell *et al.*, 1995; Scannell *et al.*, 1999; Hilgetag *et al.*, 2000a; Hilgetag *et al.*, 2000b; Grant & Hilgetag, 2005). Enfin, il a été démontré que la diminution de la concentration de 2-DG est plus grande dans les aires de haut niveau que dans celles de bas niveau suite à l'inactivation par cryoprobe d'une aire de niveau intermédiaire (Vanduffel *et al.*, 1997a). Ceci correspond aux prédictions faites à partir de la hiérarchie.

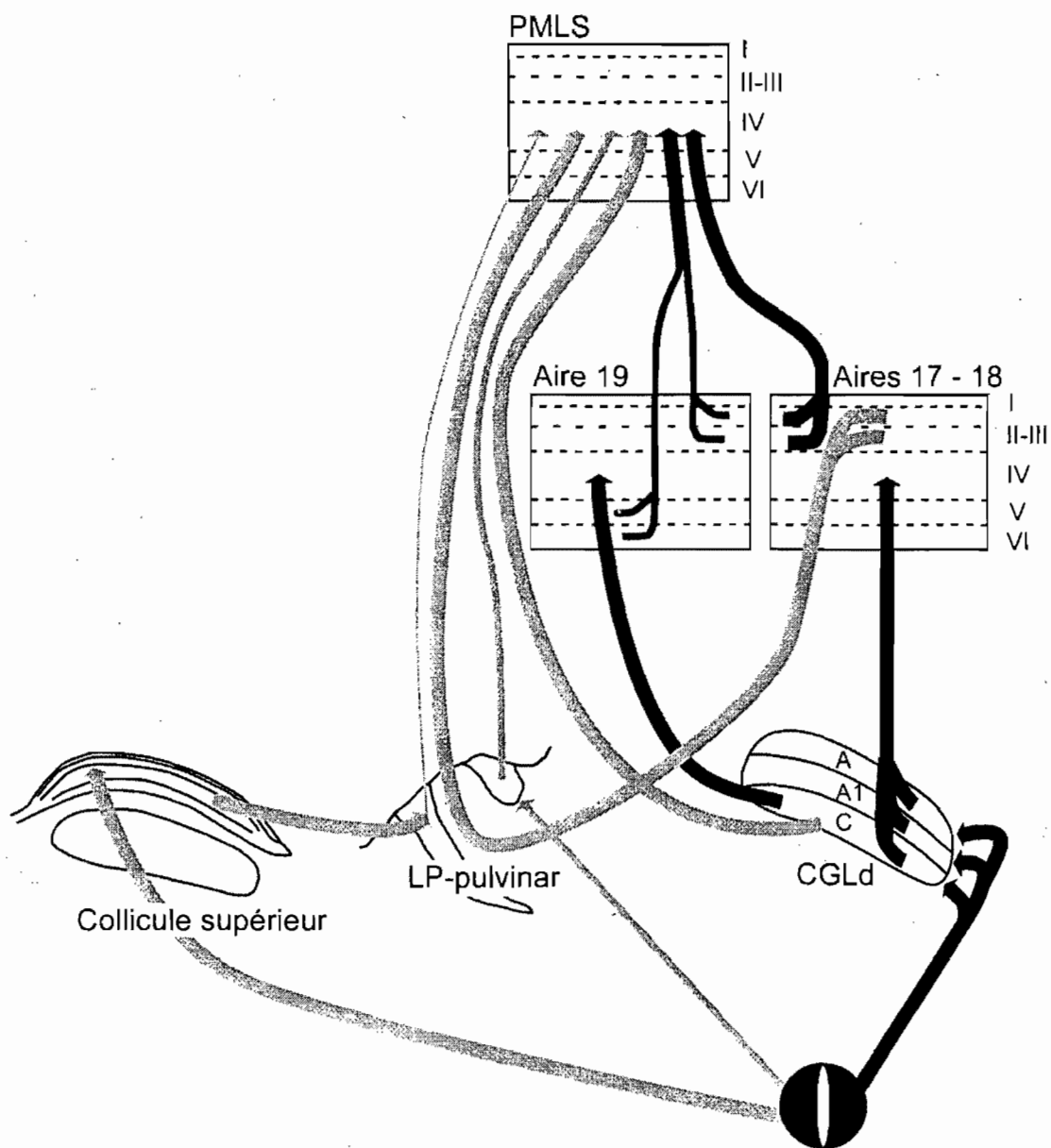


**Figure 1**

Représentation des projections géniculo-aire visuelle primaire. Les trois voies sont en noire, alors que les projections que nous verrons subséquentement sont en gris.

Une schématisation d'une des hiérarchies proposées est présentée à la Figure 2. La position verticale de chaque région représente son niveau présumé dans la hiérarchie. Les aires 17 et 18 (en gris), qui ont été décrites comme projetant essentiellement au PMLS à partir des couches supragranulaires, sont placées en dessous du PMLS. Alors que l'aire 19 (en gris), qui projette au PMLS à partir des couches supragranulaires et infragranulaires, est placée au même niveau que le PMLS (en gris). Pour ce qui est de la projection du PMLS vers les aires 17 et 18, celle-ci provient surtout des couches infragranulaires, essentiellement de la couche VI (Symonds & Rosenquist, 1984b; Shipp & Grant, 1991) et les terminaisons se retrouvent généralement dans la couche I. Ainsi les projections des aires 17 et 18 vers le PMLS seraient de type *feedforward*, la projection de l'aire 19 vers le PMLS serait de type horizontal, et la projection du PMLS vers 17 et 18 serait rétroactive (*feedback*). Il est donc possible d'établir la position relative d'une aire corticale dans la hiérarchie dès que des données anatomiques suffisantes sont disponibles.



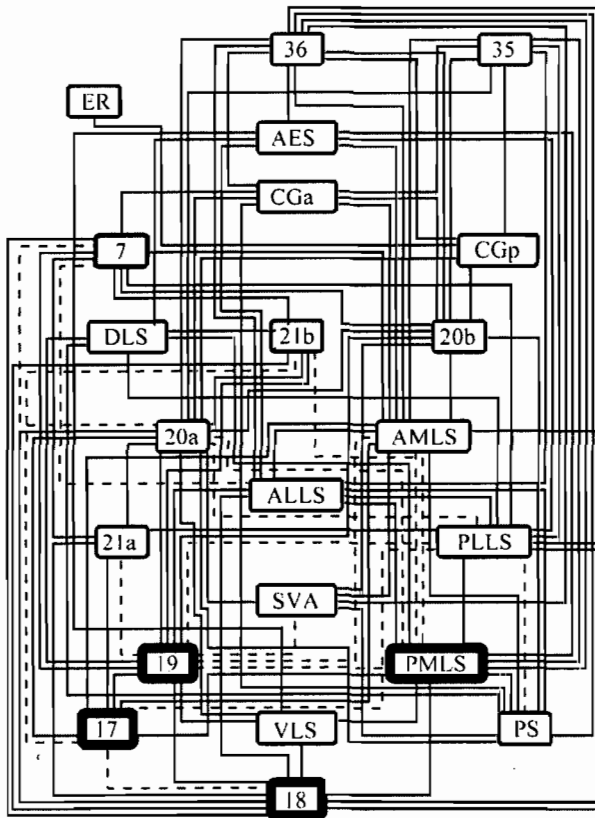


**Figure 2**

Version schématisée de la hiérarchie corticale basée sur les couches d'origines et d'aboutissement des projections. Les quatre régions d'intérêt sont présentées en gris. La figure est adaptée de Hilgetag *et al.* (2000b).

### 2.1.2 La voie cortico-thalamo-corticale

Quoique discutable comme catégorisation, dans le présent ouvrage la projection de la partie latérale du noyau thalamique latéral postérieur (LPI : Figure 3) vers le PMLS (Maciewicz, 1974; Berson & Graybiel, 1978; Tong *et al.*, 1982; Berson & Graybiel, 1983b; Raczkowski & Rosenquist, 1983; Miceli *et al.*, 1991; Norita *et al.*, 1996; MacNeil *et al.*, 1997) sera considérée comme faisant partie de la voie géniculaires 17, 18 et 19. La présente catégorisation est fondée sur la contribution principalement corticale au LPI, et non rétinienne (Berson & Graybiel, 1978; Graybiel & Berson, 1980; Raczkowski & Rosenquist, 1983; Miceli *et al.*, 1991). Parmi les projections thalamiques vers le PMLS, celle du LPI est la plus importante en nombre (Tong *et al.*, 1982; Norita *et al.*, 1996).

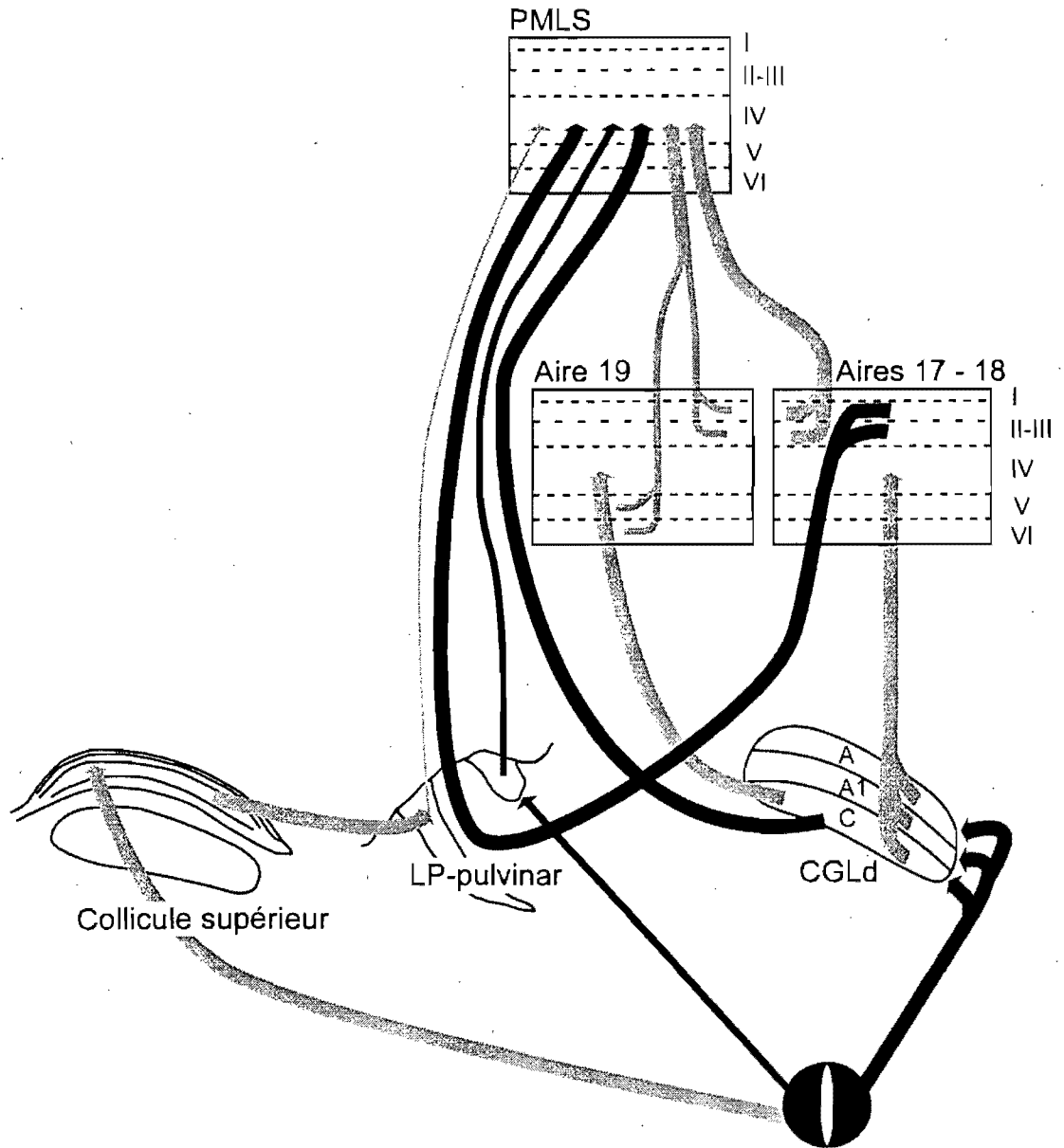


**Figure 3**

Représentation des projections rétino-thalamo-corticales. Le code couleur est le même que celui de la Figure 1.

### 2.1.3 La voie cortico-corticale

Tel que mentionné ci-dessus, une fois que l'information visuelle atteint l'aire 17, celle-ci est re-distribuée vers un grand nombre d'aires visuelles. Parmi celles-ci, plusieurs projettent vers le PMLS. Brièvement, ces aires corticales sont la partie postéro-latérale du sulcus suprasylvien latéral (PLLS), ainsi que la partie antéro-médiane (AMLS) et la partie ventro-latérale (VLS) de ce même sulcus, les aires 20a et b, les aires 21a et b, la partie visuelle du sulcus ectosylvien antérieur (AEV), et l'aire 7 (Symonds & Rosenquist, 1984b; Miceli *et al.*, 1985; Norita *et al.*, 1996). Il est à noter que la plupart de ces aires sont soit au même niveau de la hiérarchie visuelle ou à une position supérieure. Ainsi, il est peu probable que ces aires contribuent de façon significative à l'élaboration des propriétés du PMLS, elles contribueraient plutôt à la modulation de leur activité.

### 2.2 La voie rétino-thalamo-corticale

Il existe une projection de la rétine vers le PMLS qui n'est qu'à deux synapses. L'information visuelle passe alors soit par le CGLd, soit par le pulvinar (Figure 3). Dans le cas du CGLd, il y a de nombreuses études qui ont su mettre en évidence cette projection, notamment à partir de la couche C (Raczkowski & Rosenquist, 1980; Tong *et al.*, 1982; Raczkowski & Rosenquist, 1983; Norita *et al.*, 1996; MacNeil *et al.*, 1997; Payne & Lomber, 1998b). De plus, des études électrophysiologiques ont non seulement confirmées cette

projection, mais ont également démontré que ces synapses peuvent avoir un effet qui va au-delà d'un rôle de modulation (Berson, 1985; Rauschecker *et al.*, 1987b).

Enfin une autre projection de la rétine aboutie au niveau du PMLS en passant directement par le thalamus, celui-ci implique le noyau du pulvinar tel que représenté dans la Figure 3 (Tekian & Afifi, 1981; Naito & Kawamura, 1982; Tong *et al.*, 1982; Norita *et al.*, 1996). Il est important de noter cependant que l'importance fonctionnelle de cette projection est incertaine car le nombre de fibres est limité tant pour les projections de la rétine vers le pulvinar que pour celles du pulvinar vers le cortex (Labar *et al.*, 1981; Tong *et al.*, 1982; Norita *et al.*, 1996; Payne & Lomber, 1998b; Boire *et al.*, 2004). Enfin, il existe plusieurs autres noyaux thalamiques visuels qui projettent vers le PMLS, notamment le noyau intralaminaire et l'aile géniculée (tous deux font partie du complexe géniculé), le noyau centro-latéral, ainsi que le noyau postérieur (Tong *et al.*, 1982; Norita *et al.*, 1996). Ces projections sont encore moins importantes en nombre que celles provenant du pulvinar.

### 2.3 La voie tecto-thalamo-corticale

Une dernière voie projette vers le PMLS, soit la voie tecto-thalamo-corticale (Figure 4). Cette voie est probablement moins importante fonctionnellement que la voie géniculo-aies 17, 18 et 19 car le collicule supérieur (CS) projette vers la partie médiane du noyau latéral postérieur (LPm)

du thalamus (Berson & Graybiel, 1978; Graybiel & Berson, 1980; Kelly *et al.*, 2003), alors que le PMLS reçoit la grande majorité de ces afférences de la partie latérale du noyau latéral postérieur (LPI: Berson & Graybiel, 1978; Tong *et al.*, 1982; Raczkowski & Rosenquist, 1983; Tong & Spear, 1986; Norita *et al.*, 1996; MacNeil *et al.*, 1997). Il est néanmoins important de noter qu'une projection moins importante du LPm atteint également le PMLS. Ainsi, la contribution de cette voie n'est pas claire et devrait être élucidée dans l'avenir.

Une voie qui est souvent passée sous silence mais qui pourraient avoir une influence importante est également d'origine tectale. Cette voie est tecto-geniculo-extrastrée. Il est connu depuis longtemps que le collicule supérieur projette vers la couche C du CGL, en particulier les couches C<sub>2-3</sub> (Harting *et al.*, 1991). De plus, avec une étude d'inactivation au muscimol, il a été démontré que cette projection module sur l'amplitude de la réponse visuelle des neurones dans le CGL (Xue *et al.*, 1994). En particulier, cette voie semblerait impliquée dans une modulation qui augmenterait la saillance des objets périphériques et diminuerait la saillance des objets dans le centre du champ visuel. Étant donné la projection du CGL vers les aires 17, 18, et 19 ainsi que la projection directe vers le PMLS, il est clair que cette voie tecto-geniculo-extrastrée est bien placée pour moduler l'activité de cette région corticale.

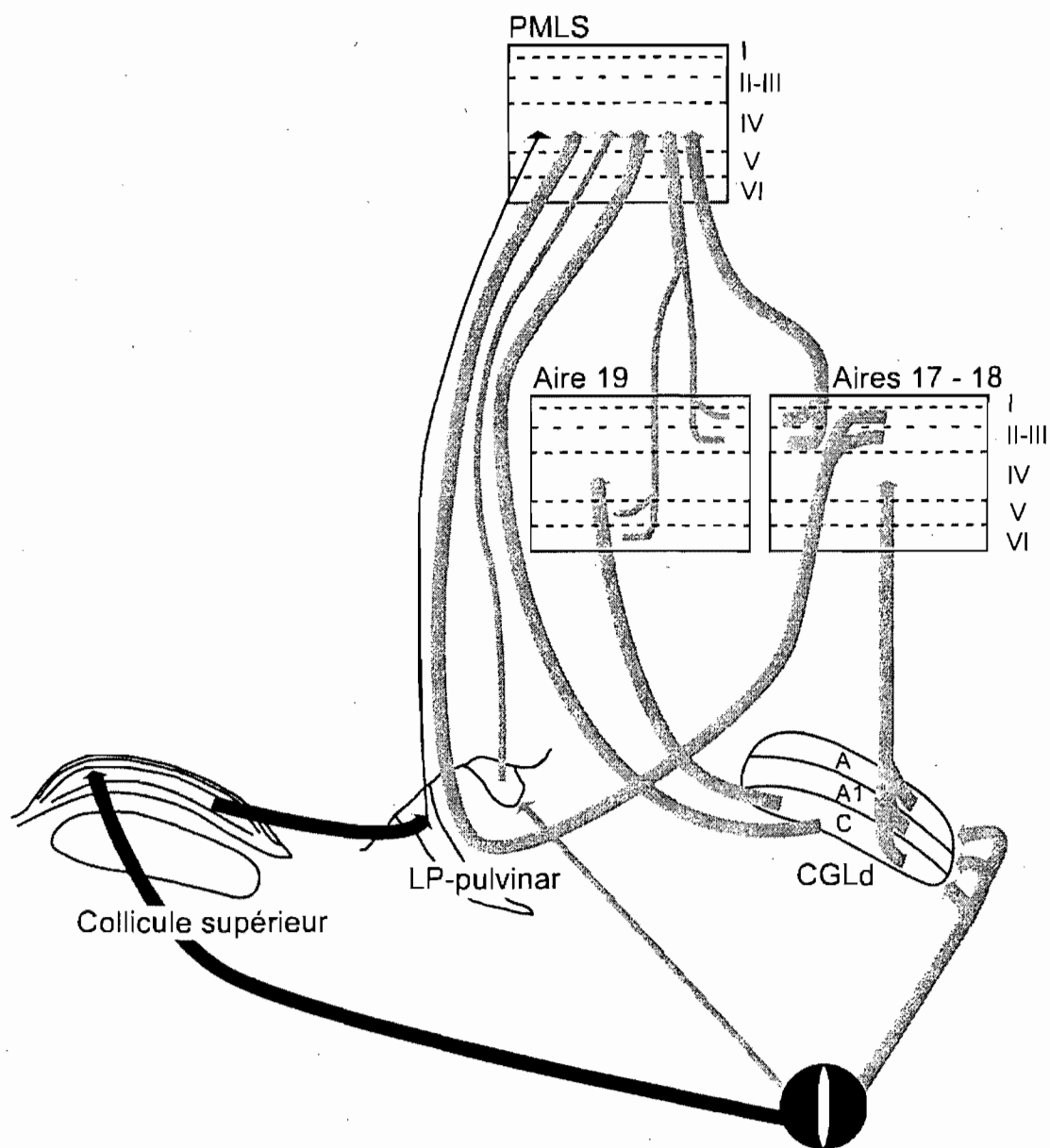


**Figure 4**

Représentation des projections tecto-thalamo-corticales. Le code couleur est tel qu'à la Figure 1.

### 3. Physiologie des neurones du PMLS

#### 3.1 Données électrophysiologiques

Maintenant que nous connaissons les régions qui projettent vers le PMLS, tournons nous vers les propriétés des neurones de cette région. La raison pour laquelle cette région est le point central de la présente thèse est qu'elle est la plus étudiée des aires extrastriées visuelles chez le chat. Un consensus clair ressort des études sur le PMLS concernant les propriétés visuelles des neurones du PMLS, soit que les cellules de cette aire corticale sont sélectives à la direction des stimuli (Rauschecker, 1988; Spear, 1991). La question qui demeure cependant, concerne le rôle de cette aire dans l'élaboration des comportements. Les cellules du PMLS sont sélectives à une diversité de stimuli contenant du mouvement dans l'axe fronto-parallèle (Camarda & Rizzolatti, 1976; von Grunau & Frost, 1983; Movshon *et al.*, 1985; Zumbroich & Blakemore, 1987; Dreher *et al.*, 1996b; Merabet *et al.*, 2000; Borghuis *et al.*, 2003; Vajda *et al.*, 2004; Vajda *et al.*, 2005; Vajda *et al.*, 2006; Villeneuve *et al.*, 2006a) mais également ceux qui simulent un déplacement du chat vers l'avant ou l'arrière dans l'environnement, soit le flux optique (Camarda & Rizzolatti, 1976; Toyama *et al.*, 1985; Toyama *et al.*, 1986a; Toyama *et al.*, 1986b; Rauschecker *et al.*, 1987a; Brenner & Rauschecker, 1990; Toyama *et al.*, 1990; Sherk *et al.*, 1995; Kim *et al.*, 1997; Mulligan *et al.*, 1997; Sherk *et al.*, 1997; Akase *et al.*, 1998; Brosseau-Lachaine *et al.*, 2001; Sherk & Kim, 2002). Ainsi, l'aire PMLS est impliquée dans l'analyse du mouvement, cependant la grande diversité des mouvements auxquels ses neurones répondent ne permet pas de



déterminer son rôle spécifique. Ni d'ailleurs de savoir si cette aire a un rôle spécifique ou général dans l'analyse du mouvement.

Le rôle du PMLS dans l'analyse du mouvement a de plus été confirmé par la méthode d'imagerie optique des signaux intrinsèques. En inactivant le PMLS, il est possible de constater que les cartes de sélectivités à la direction des aires 17 et 18 disparaissent, alors que les cartes de sélectivités à l'orientation demeurent (Galuske *et al.*, 2002; Shen *et al.*, 2006a). Bien qu'indirecte, ces deux études démontrent que le PMLS joue un rôle important dans l'analyse du mouvement. Il est à noter par contre que dans l'étude de Galuske *et al.* (2002) à cause de la méthode d'inactivation choisie (cryoprobés), il n'est pas clair que l'effet provienne uniquement de l'inactivation du PMLS, mais pourrait également être attribuable au PLLS.

### 3.2 Données comportementales

Les conclusions tirées des données électrophysiologiques sont confirmées par des travaux comportementaux. Ces travaux, via des désactivations ou lésions du PMLS, ont pu démontrer le rôle du PMLS dans l'analyse du mouvement fronto-parallèle (Pasternak *et al.*, 1989; Kruger *et al.*, 1993b; Rudolph & Pasternak, 1996; Lomber, 2001; Huxlin & Pasternak, 2004). Le point commun entre toutes ces études est que sans l'apport du PMLS le taux de réussite à des tâches de discrimination de stimuli en mouvement avoisine celui du hasard. Des déficits sont également observés après de telles manipulations

dans des tâches de déplacement dans l'environnement (Kruger *et al.*, 1993a; Sherk & Fowler, 2002). Des atteintes sont aussi observables dans des tâches d'attention spatiale reliées à la détection de nouveau stimuli (Lomber & Payne, 1996), quoiqu'avec une tâche très similaire aucun effet ai été observé par un autre groupe (Spear *et al.*, 1983). Supportant les études de lésions, une augmentation du métabolisme dans le PMLS a été notée suite à une tâche de détection (Vanduffel *et al.*, 1997b). Toutes ces données appuient l'idée selon laquelle le PMLS fait parti de la voie dorsale du système visuel. Il est intéressant de noter qu'une seule aire puisse avoir des fonctions aussi variées.

### 3.3 Modèle d'analyse du mouvement

Puisque les neurones du PMLS sont impliqués dans l'analyse du mouvement, tant par les résultats d'études électrophysiologiques que comportementales, il serait approprié de décrire deux modèles d'analyse du mouvement. Le modèle d'énergie de Adelson et Bergen (1985) sera présenté en premier, car il a grandement influencé la recherche dans le domaine de l'analyse du mouvement visuel. Ensuite le modèle de Nowlan et Sejnowski (1995) sera abordé car il est probablement une meilleure description du type d'analyse effectuée par les neurones du PMLS, et son premier niveau de traitement est basé sur l'analyse du modèle d'énergie.

### 3.3.1 Modèle d'énergie

Ce modèle fût élaboré afin d'expliquer comment des signaux de mouvement pouvaient être extraits par des neurones. Afin de comprendre ce modèle, commençons par une cellule du CGL qui est de type ON (Figure 5A). Il va de soit qu'un tel champ récepteur ne peut non seulement pas être sélectif à la direction, mais aussi que l'encodage de l'orientation est impossible. Une cellule de type simple, que l'on retrouve dans l'aire visuelle primaire (Figure 5B) est en mesure d'encoder l'orientation d'un stimulus, ainsi que son axe de déplacement mais pas sa direction. Cependant avec un stimulus qui est plus grand que le champ récepteur, dont la luminance varie spatialement dans une seule dimension comme une modulation sinusoïdale de la luminance (ci-après réseau), l'encodage de l'axe de déplacement risque d'être erroné (Movshon *et al.*, 1985). Ainsi, des cellules de type simple ne sont pas efficaces dans l'analyse du mouvement.

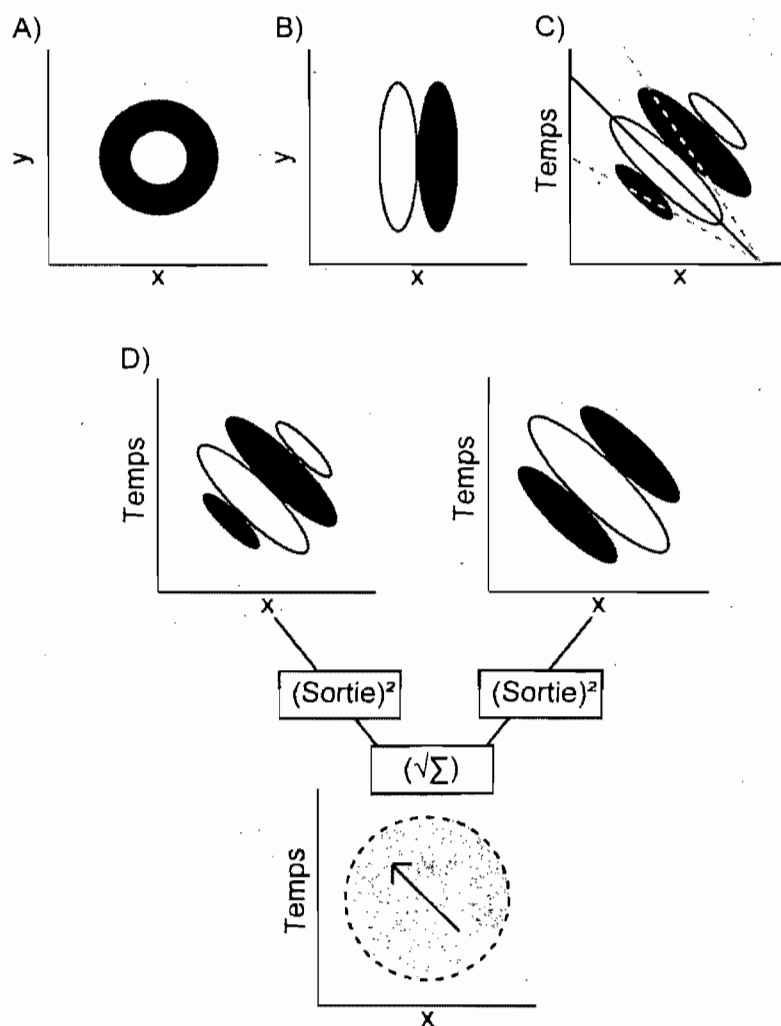


**Figure 5**

Schématisation du modèle d'énergie. Représentation d'un champ récepteur A) du CGL et B) de type simple. Les zones blanches et noires sont excitatrices et inhibitrices respectivement. C) Représentation espace-temps d'un champ récepteur simple. D) Une unité (bas) qui intègre l'information provenant de deux cellules simple (panneau C et haut). Le gris représente la perte de la dépendance au contraste. Adaptés de Adelson et Bergen (1985).

L'idée d'Adelson et Bergen (1985) était que le champ récepteur simple, présenté à la Figure 5B, pouvait se déplacer dans l'espace en fonction du temps. Nous nous retrouvons alors avec un filtre spatio-temporel, tel que celui à la Figure 5C. Afin de bien comprendre cette figure, notez que l'ordonnée représente maintenant la dimension temporelle, donc une seule dimension spatiale est présente. Ainsi, le filtre de la Figure 5C serait sélectif à un déplacement vers la gauche, puisque la partie excitatrice est orientée vers la gauche dans l'espace-temps. De plus, ce filtre répondrait de façon optimale pour une vitesse qui est équivalente à la pente des sous-unités (la ligne noire continue). Cette sélectivité provient du fait qu'une vitesse différente (les lignes grises pointillées) de l'optimale causerai une stimulation de la partie inhibitrice du champ récepteur.

Nous nous retrouvons donc avec un filtre qui est sélectif à la direction et la vitesse. Cependant, suite à l'observation de la Figure 5C, il est possible de remarquer qu'un tel mécanisme est dépendant du contraste du stimulus. Ceci n'est pas une propriété souhaitable pour un mécanisme de sélectivité à la direction. La proposition et solution de Adelson et Bergen (Adelson & Bergen, 1985) est de prendre la somme des carrés de la sortie de deux filtres, et que ces derniers diffèrent quant à leur phase de 90 degrés (Figure 5D). L'unité qui effectuerait une telle opération serait alors sélective à la direction et la vitesse sans être sensible au contraste du stimulus. En résumé, la sélectivité à la direction peut être expliquée par une somme des sorties rectifiée d'aussi peu que deux filtres spatio-temporels. Le résultat (la sortie du modèle) est similaire

à ce qui peut être observé lors de l'enregistrement d'une cellule complexe de l'aire visuelle primaire (Emerson *et al.*, 1992).

### 3.3.2 Modèle de sélection

Puisque la présente thèse porte sur une aire extrastrée, le modèle présenté ci-haut n'est pas suffisant afin de bien décrire les propriétés neuronales dans une aire telle que le PMLS. Le modèle de Nowlan et Sejnowski (1995) utilise le modèle d'énergie mentionné ci-haut et y ajoute un niveau de traitement. Le but du modèle est d'expliquer la sélectivité à la direction telle que nous la voyons dans MT chez le primate, et par le fait même il nous donne un aperçu quant aux mécanismes sous-jacents à la perception. La mise en évidence d'un lien entre MT et la perception provient d'une série d'études élégantes du laboratoire de William Newsome démontrant que cette région est à la fois nécessaire et suffisante pour la perception du mouvement chez le primate (Newsome & Pare, 1988; Newsome *et al.*, 1990; Britten *et al.*, 1996; Nichols & Newsome, 2002).

#### 3.3.2.1 La rétine

L'entrée du modèle est une matrice (64 X 64) bidimensionnelles qui simule la rétine (Figure 6D). Notons tout d'abord, qu'au premier niveau de ce modèle le nombre absolu d'unités est choisit de façon arbitraire, les proportions entre

les niveaux étant importantes, cela dicte le nombre d'unités dans les autres niveaux. Le nombre absolu d'unités à chaque niveau sera mentionné uniquement afin de mettre en évidence une intégration spatiale qui se produit à chaque étape du modèle. Cette intégration spatiale par les champs récepteurs est également présente dans le système visuel tel que nous le verrons à la section 4.2.1. Dans la représentation du modèle de la Figure 6, chaque niveau a une zone grise qui indique les unités qui seraient excitées par une stimulation visuelle hypothétique.

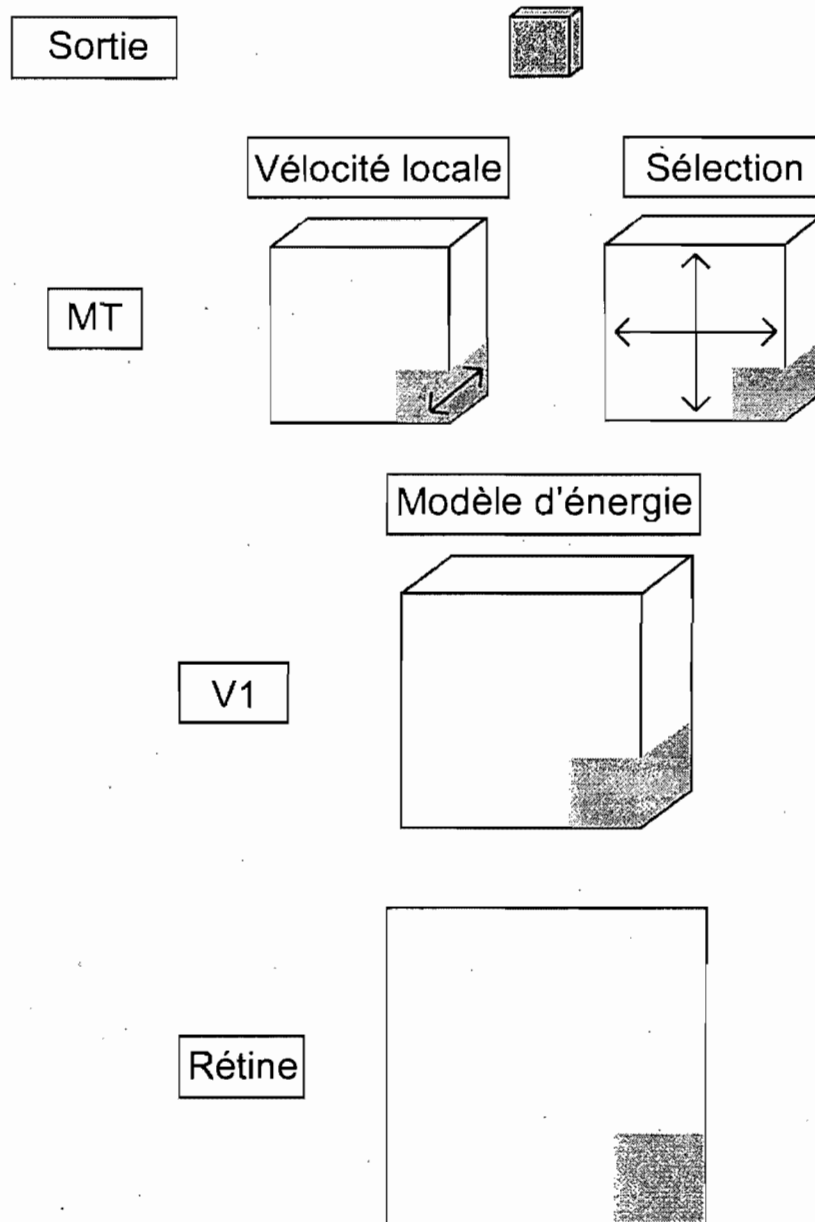


**Figure 6**

Schématisation du modèle de sélection. Au niveau de MT les flèches représentent la dimension sur laquelle la normalisation ce fait.



### 3.3.2.2 Le cortex visuel primaire

Le modèle passe alors l'information de la rétine vers le cortex visuel primaire (le CGL n'est pas mentionné que pour des raisons de simplification computationnelle, et cela ne représente en aucun cas une suggestion de projection directe entre la rétine et le cortex). Nous nous retrouvons avec 49X49 unités pour représenter le champ visuel. Rappelons qu'il y a moins d'unités à cause de l'intégration spatiale mentionnée ci-haut. Ce niveau du modèle est exactement le modèle d'énergie décrit à la section précédente (3.3.1). Il va de soit qu'une simple représentation bidimensionnelle de l'espace ne suffit plus, car comme nous l'avons vue les unités de ce niveau sont des filtres spatio-temporels. Pour être en mesure d'encoder plusieurs directions et fréquences, une représentation en trois dimensions est nécessaire tel que reproduit dans le panneau C de cette figure. Nous nous retrouvons donc avec 36 unités par position dans le champ visuel pour représenter les différentes possibilités de direction et de fréquence. Ceci est donc similaire à la notion d'hypercolonne retrouvée dans l'aire visuelle primaire.

### 3.3.2.3 L'aire MT

La sortie de ce niveau est transmise aux unités sensées être similaires à ce que nous pourrions retrouver dans MT. Mentionnons qu'il y a encore une intégration spatiale de l'information, ce qui donne alors une matrice de 8X8. Deux types de mécanismes parallèles sont alors proposés: d'une part des

unités dont la sortie varie en fonction des évidences indiquant la présence d'un déplacement dans leur direction optimale (vélocité locale) et d'autre part des unités avec des informations reliées à la fiabilité spatiale des évidences relatives à la direction (sélection). La question qui se pose alors est comment arriver à deux sorties différentes (vélocité locale et sélection) à partir d'une même entrée qui est celle du modèle d'énergie? La réponse est fort simple, il suffit de normaliser les sorties selon des dimensions différentes (représentées par les flèches). Pour le mécanisme de la vélocité locale la normalisation se fait dans chacune des hypercolonnes indépendamment. Nous nous retrouvons donc avec un estimé de la combinaison direction-fréquence pour chaque point du champ visuel. Pour ce qui est du mécanisme de sélection, la normalisation ce fait plutôt selon les dimensions spatiales, les combinaisons de direction-fréquence sont donc indépendantes les unes des autres. Il en résulte donc un estimé de la fiabilité du signal pour chaque combinaison direction-fréquence sur la totalité du champ visuel. Bien que ce mécanisme puisse paraître surprenant à première vue, il est critique pour le bon fonctionnement du modèle avec des stimuli dont les vecteurs de mouvement locaux ne correspondent pas au mouvement global (pour l'exemple classique voir: Adelson & Movshon, 1982).

Le lecteur aura sûrement noté qu'une simple normalisation est complètement inutile afin d'extraire l'information voulue. Dans le modèle de Nowlan et Sejnowski (1995), la normalisation ce fait avec ce qu'ils appellent la fonction *soft-max*, qui n'est pas une fonction linéaire. En fait, elle donne une plus grande pondération aux valeurs les plus élevées (présument les plus

fiables) au détriment des autres, ce qui facilite l'extraction des paramètres du stimulus qui est le plus probable d'avoir été présenté.

#### 3.3.2.4 La sortie

Enfin, le dernier niveau ne correspond pas à une région corticale à proprement dit mais serait plutôt une représentation du percept ou la sortie du système. Il y a donc une intégration spatiale qui couvre tout le champ visuel (panneau 6A), nous avons donc une matrice de  $1 \times 1$ . Cependant, le modèle conserve une représentation de toutes les combinaisons de direction-fréquence (d'où la profondeur). Ceci permet donc d'extraire un estimé de la combinaison de direction-fréquence basé sur l'amplitude de la sortie. Ce qui mène à une perception du mouvement global sans égard à des vecteurs locaux.

Il est vraie que le modèle reproduit de façon relativement fidèle les réponses neuronales de MT et des courbes psychophysiques (Nowlan & Sejnowski, 1995). Le modèle est également intéressant car c'est la démonstration que l'extraction de la direction globale peut être obtenue de façon relativement simple et physiologiquement plausible. Ceci permet donc de poser des questions à partir de ce modèle et de l'utiliser comme cadre afin d'interpréter des données physiologiques.

## 4. L'aspect parallèle du système

### 4.1 Lésion de l'aire visuelle primaire

#### 4.1.1 Lésion chez l'adulte

Tel que mentionné dans la section sur l'anatomie de la voie dorsale, il y a plusieurs régions visuelles qui projettent vers le PMLS. Ces voies sont très importantes afin d'expliquer la littérature concernant les effets des lésions de l'aire visuelle primaire chez le chat. Résumons rapidement les résultats obtenus lors d'une lésion effectuée chez l'adulte. Bien que l'aire visuelle primaire soit la principale afférence corticale du PMLS, une lésion de celle-ci modifie peu les propriétés neuronales du PMLS. Le changement le plus notable est une réduction de la proportion de cellules sélectives à la direction (Spear & Baumann, 1979; Spear, 1988; Guido *et al.*, 1990b). Dans une moindre mesure, il y a aussi une réduction de l'amplitude de la réponse (en potentiel d'action par seconde) et de la sensibilité au contraste. Cependant, la sélectivité aux fréquences spatiale et temporelle n'est essentiellement pas modifiée, tout comme l'organisation rétinotopique, et l'intégration spatiale. En résumé donc, les propriétés du PMLS sont peu modifiées si l'on considère que l'aire visuelle primaire est sa principale source d'afférences. Ceci suggère donc que d'autres voies sont suffisantes pour évoquer des réponses quasi-normales de la part des neurones du PMLS. Soit parce que ces afférences sont en mesure de prendre le relais des neurones de l'aire visuelle primaire, soit parce que ces voies alternatives sont déjà responsables des réponses dans le PMLS chez l'animal normal.

#### 4.1.2 Lésion chez le chaton

Étant donné la grande plasticité du jeune cerveau, il n'est pas surprenant que les études dans lesquelles une lésion a été effectuée très tôt démontre un effet encore moins important sur les propriétés des neurones du PMLS (Tong *et al.*, 1984; Guido *et al.*, 1990a, 1992). Lors de telles lésions, le changement principal se situe encore une fois au niveau de la sélectivité à la direction. Tout comme chez l'adulte, il y a une réduction de la proportion de neurones qui sont sélectifs à la direction. Cependant la proportion de neurones qui sont encore sélectifs est nettement plus élevée que lors d'une lésion chez l'adulte (Tong *et al.*, 1984).

##### 4.1.2.1 Nature des stimuli

Dans le contexte de la présente thèse il est important de considérer le stimulus utilisé lors des études ci-haut, et ce tant lors de lésions chez l'adulte que chez le chaton. Deux catégories de stimuli sont généralement utilisées lors de ces études. La première catégorie étant des stimuli lumineux d'une forme donnée, souvent un rectangle ou un cercle, déplacé manuellement. La deuxième étant le réseau dynamique décrit ci-haut (section 3.3.2.1). Pour ces deux types de stimuli, la direction peut être extraite par un mécanisme qui n'utilise que des informations locales (exception faite de *l'aperture problem* :

Movshon *et al.*, 1985). Ainsi, la direction de tels stimuli peut être encodée par un mécanisme relativement simple.

Comme nous l'avons vu dans la section sur le modèle d'énergie, les cellules complexes de l'aire visuelle primaire sont en mesure d'encoder la direction de ces stimuli. Il s'en suit, que ces stimuli ne représentent pas nécessairement le choix le plus judicieux pour élucider les effets des lésions de l'aire visuelle primaire sur les neurones du PMLS. Surtout dans la mesure où nous avons vu (voir la section : Physiologie des neurones du PMLS) que les neurones du PMLS chez l'adulte normal encodent une diversité de stimuli, dont plusieurs ne pourraient être analysés par des neurones d'aires corticales de plus bas niveau. Donc, il est possible qu'un effet important soit présent lors de lésions chez le chaton mais que les stimuli utilisés jusqu'à présent soient incapables de le révéler.

#### 4.1.2.2 Fondement anatomique

Parmi les études électrophysiologiques mentionnées ci-dessus, aucune ne fournit des indices suggérant quelle(s) afférence(s) du PMLS pourraient prendre le relais de l'aire visuelle primaire. Par contre, plusieurs études de traçage de voies anatomiques suggèrent que l'apport visuel principal (suite à une lésion) au PMLS provient du CGLd. En effet, il a été démontré que la projection de la couche C du CGLd vers le PMLS est supérieure à la normale suite à une lésion de l'aire visuelle primaire chez le chaton (Tong *et al.*, 1984;

Kalil *et al.*, 1991; Tong *et al.*, 1991; Payne & Cornwell, 1994; Spear, 1995; Payne & Lomber, 1998b).

Ceci étant dit, la projection qui existe du LP-pulvinar vers le PMLS chez l'animal normal (Maciewicz, 1974; Berson & Graybiel, 1978; Tong *et al.*, 1982; Berson & Graybiel, 1983b; Raczkowski & Rosenquist, 1983; Miceli *et al.*, 1991; Norita *et al.*, 1996; MacNeil *et al.*, 1997) pourrait également permettre la sélectivité résiduelle. En effet, les afférences de la rétine vers le LP-pulvinar augmentent suite à une lésion (Labar *et al.*, 1981; Payne *et al.*, 1993; Boire *et al.*, 2004), cependant la projection du LP-pulvinar vers le PMLS n'augmente pas ou peu suite à une telle lésion (Kalil *et al.*, 1991). Enfin, la projection tecto-thalamo-corticale mentionnée dans la section 2.3 pourrait également être impliquée. Cette dernière possibilité semble moins probable car la proportion de cellules sélectives à la direction diminue de beaucoup suite à une lésion de l'aire visuelle primaire (Mize & Murphy, 1976). Il est alors peu probable que la sélectivité à la direction observée dans le PMLS provient de cette voie. En résumé, bien que plusieurs possibilités existent afin d'expliquer la sélectivité résiduelle aux stimuli en mouvement, l'importance fonctionnelle de chacune des ces voies est encore peu connue.

## 4.2 Profil temporel des réponses

### 4.2.1 Les latences neuronales

Revenons rapidement à la notion de hiérarchie présentée dans la section 2.1.1, ainsi qu'une de ses implications. Nous avons vu qu'en considérant les couches corticales d'origine et de terminaison des projections, il est possible d'établir une hiérarchie des aires corticales. La notion de hiérarchie, dans le contexte d'un système qui traite l'information, implique qu'une aire au troisième niveau (par exemple) de la hiérarchie est directement dépendante d'une aire au deuxième niveau avec laquelle elle est connectée, et indirectement dépendante des aires de premier niveau. Ainsi, il devrait y avoir une progression des propriétés des neurones qui suit l'emplacement dans la hiérarchie de l'aire sous étude.

Lorsque nous observons les propriétés des champs récepteurs dans différentes aires corticales, nous remarquons justement une progression qui concorde avec la position de chaque aire dans la hiérarchie. Prenons comme exemple l'aire 17 et le PMLS, ce dernier étant de plus haut niveau que le premier. La taille des champs récepteurs du PMLS est nettement supérieure à celle de l'aire 17 (Hubel & Wiesel, 1969; Camarda & Rizzolatti, 1976; Movshon *et al.*, 1978a, b; Sherk & Mulligan, 1992; Brosseau-Lachaine *et al.*, 2001). De même, les neurones du PMLS sont sélectifs à des stimuli en mouvements qui ne peuvent être encodés par les neurones de l'aire 17 (par exemple : Kim *et al.*, 1997; Villeneuve *et al.*, 2006a).



Bien que ces données soient compatibles avec le traitement de l'information dans une hiérarchie bien établie, elles ne sont en rien la preuve de l'existence d'une telle organisation. Le lien de causalité entre les patrons de projection et l'évolution des propriétés des champs récepteurs n'a pas été démontré. Il est donc plausible d'avoir une telle évolution dans un système parallèle. Nous pouvons tenter de résoudre la question en nous basant sur une autre notion qui émane du concept d'un traitement sériel de l'information : les latences neuronales dans les différentes aires de la hiérarchie devraient refléter la position de chaque aire. Cependant les résultats des études de latences, tant chez le primate que chez le chat, suggèrent qu'il y ait, dans la voie dorsale, un traitement parallèle de l'information visuelle (Robinson & Rugg, 1988; Maunsell & Gibson, 1992; Dinse & Kruger, 1994; Nowak *et al.*, 1995; Schmolesky *et al.*, 1998; Schroeder *et al.*, 1998; Raiguel *et al.*, 1999; Lamme & Roelfsema, 2000; Bullier, 2001; Azzopardi *et al.*, 2003; Bullier, 2004a). Ceci étant dit, quelques unes de ces études soutiennent plutôt l'hypothèse d'un traitement sériel.

Il est à noter néanmoins que dans ces études, trois problèmes méthodologiques remettent en question les conclusions. Dans un premier temps, plusieurs de ces études n'ont été effectuées que dans une ou deux aires à la fois. Il devient alors difficile d'obtenir une vue d'ensemble du décours temporel du traitement dans les aires corticales. Il est, par ailleurs, difficile de comparer les divers études pour obtenir le décours temporel du système au complet car les paramètres des stimuli utilisés pour évoquer la réponse neuronale modifient les latences mesurées (Creutzfeldt & Ito, 1968; Lennie,

1981). Deuxièmement, dans la quasi-totalité des études les stimuli utilisés sont stationnaires. Il est clair que de tels stimuli ne sont pas idéaux pour évoquer des réponses dans une aire comme le PMLS, et la voie dorsale de façon générale. Les latences ainsi mesurées étaient donc pour un stimulus sous-optimal, ce qui pourrait biaiser les résultats. Enfin, dans les études qui rapportent des différences significatives les auteurs ont comparé les latences moyennes. Hors, les latences n'étant pas distribuées de façon normales, il s'en suit que la médiane est une mesure plus fiable. Ainsi, des problèmes méthodologiques limitent la portée des conclusions des différentes études de latences.

Les latences, comme outil pour établir la position hiérarchique d'une région, ont un intérêt particulier et complémentaire à l'anatomie. Nous avons vu que la hiérarchie est établie en fonction de la position laminaire des origines et des terminaisons des projections. Ceci pose un problème majeur pour des régions telles que le LP-pulvinar, qui n'ont aucune organisation laminaire. Dans de tels cas l'anatomie nous renseigne peu, mais les latences pourraient être un outil tout indiqué pour ces régions.

#### 4.2.2 D'autres mesures temporelles

D'autres mesures permettent également de croire que l'organisation hiérarchique ne se reflète pas par un traitement sériel de l'information. Des enregistrements unitaires simultanés dans l'aire 17 et le PMLS ont été effectués

par Katsuyama *et al.* (1996). Avec cette technique, les auteurs ont démontré qu'il y avait soit une réponse synchrone entre les deux aires ou les réponses des neurones du PMLS précédaient ceux de l'aire 17. Il y avait peu de paires de neurones qui correspondaient à une prédiction basée sur la hiérarchie, soit qu'une réponse de l'aire 17 précéderait celle du PMLS. De plus, en utilisant une stimulation orthodromique il a été démontré que la projection monosynaptique du CGL vers le PMLS est suffisamment forte pour évoquer une réponse à elle seule et que la latence de la transmission du potentiel d'action est similaire à celle du CGL vers l'aire 17 (Rauschecker *et al.*, 1987b). Ces deux techniques semblent donc confirmer les conclusions des études de latence mentionnées ci-haut, c'est-à-dire que la hiérarchie anatomique ne se reflète pas au niveau fonctionnel.

#### 4.3 Profile spatio-temporel des champs récepteurs

Un outil méthodologique fort intéressant afin de mieux comprendre l'intégration de l'information visuelle par les neurones, est la description du profile spatio-temporel du champ récepteur en utilisant la technique de la corrélation rétrograde (*reverse correlation*). Cette technique permet d'obtenir une description du champ récepteur dans l'espace-temps, similaire à ce que nous avons vue à la Figure 5B-C. Puisque cette technique est peu commune et qu'elle est un outil important dans une des trois études décrites dans cette thèse, commençons d'abord par une explication de ce qu'est cette technique.

#### 4.3.1 La corrélation rétrograde

D'abord, la corrélation rétrograde n'est en fait que la moitié d'une corrélation croisée, dont seule la partie négative est utilisée. Abordons le sujet par un exemple simplifié (représenté à la figure 7), soit une entrée binaire qui provoque une sortie également binaire (sortie 1) suite à un délai de 2 unités temporelles (en unité arbitraire). Dans le cross-corrélogramme résultant nous pouvons observer un pic unitaire au temps -2, qui résulte du fait que l'entrée s'est produite deux unités temporelles avant la sortie. Dans le cas d'un neurone, il va de soit que nous nous n'intéresserons pas aux situations où la sortie précède l'entrée, ainsi toutes les valeurs positives (partie en gris) dans le cross-corrélogramme peuvent être ignorées. Le fait de n'observer que les valeurs négatives du cross-corrélogramme explique donc le nom de cette technique ; nous procédons de reculons dans le temps à partir du moment de l'occurrence de la sortie afin d'identifier l'entrée la plus probable d'avoir provoqué la sortie.

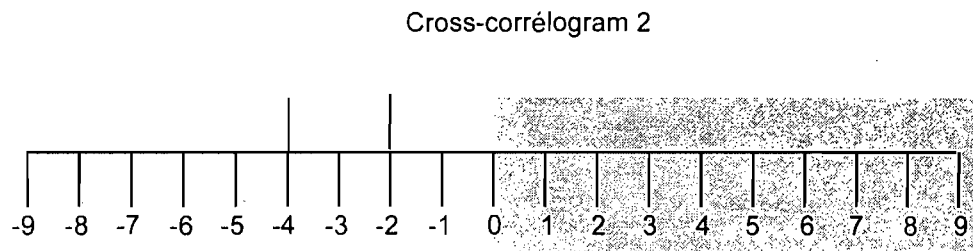
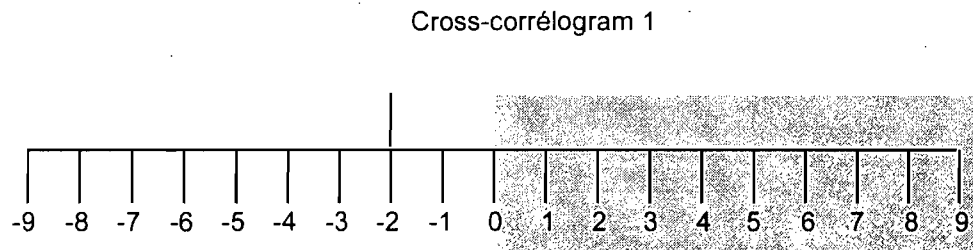
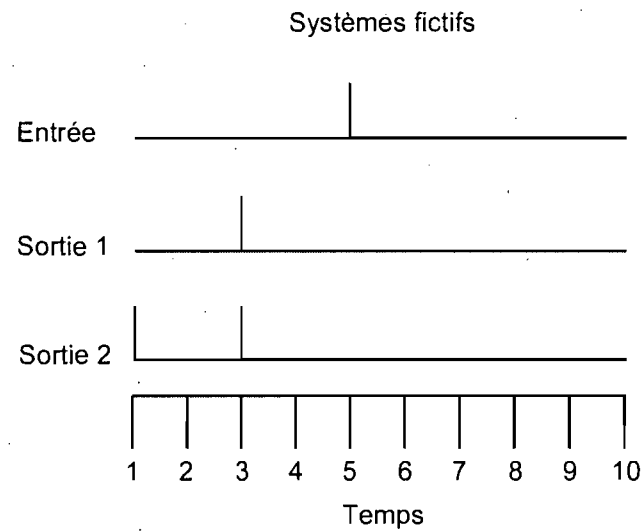


**Figure 7**

Schématisation d'une version simplifiée de la corrélation rétrograde. Le temps est représenté en unité arbitraire. La partie grise est ignorée car elle représente un lien non-causal entre l'entrée et la sortie.

Approchons nous maintenant d'une situation plus réaliste, soit un système avec la même fonction entrée-sortie que le précédent exemple mais avec du bruit (sortie 2). En observant maintenant le cross-corrélogramme qui en résulte, il est possible de voir que deux incidences sont présentes. Ne connaissant pas *a priori* la fonction entrée-sortie d'un neurone (le but de l'exercice étant d'identifier cette fonction) il est impossible de savoir si c'est l'incidence à -2 ou -4 qui a été provoquée par l'entrée. Ce problème est facile à contourner en utilisant plusieurs répétitions de l'entrée (stimulus). Ainsi, la nature aléatoire du bruit devrait se refléter par des incidences réparties de façon égale dans le cross-corrélogramme, alors que la fonction entrée-sortie devrait être visible en tant qu'un pic significatif. C'est ce que nous pouvons voir à la Figure 8, qui est basé sur 100 répétitions d'un stimulus présenté à un système bruité. Bien qu'il y ait des incidences à tous les délais à cause du bruit, il y a seulement un pic clair à -2. Dans le cas où nous ne connaissons pas la fonction entrée-sortie, cette figure nous permettrait d'en déduire le délai.

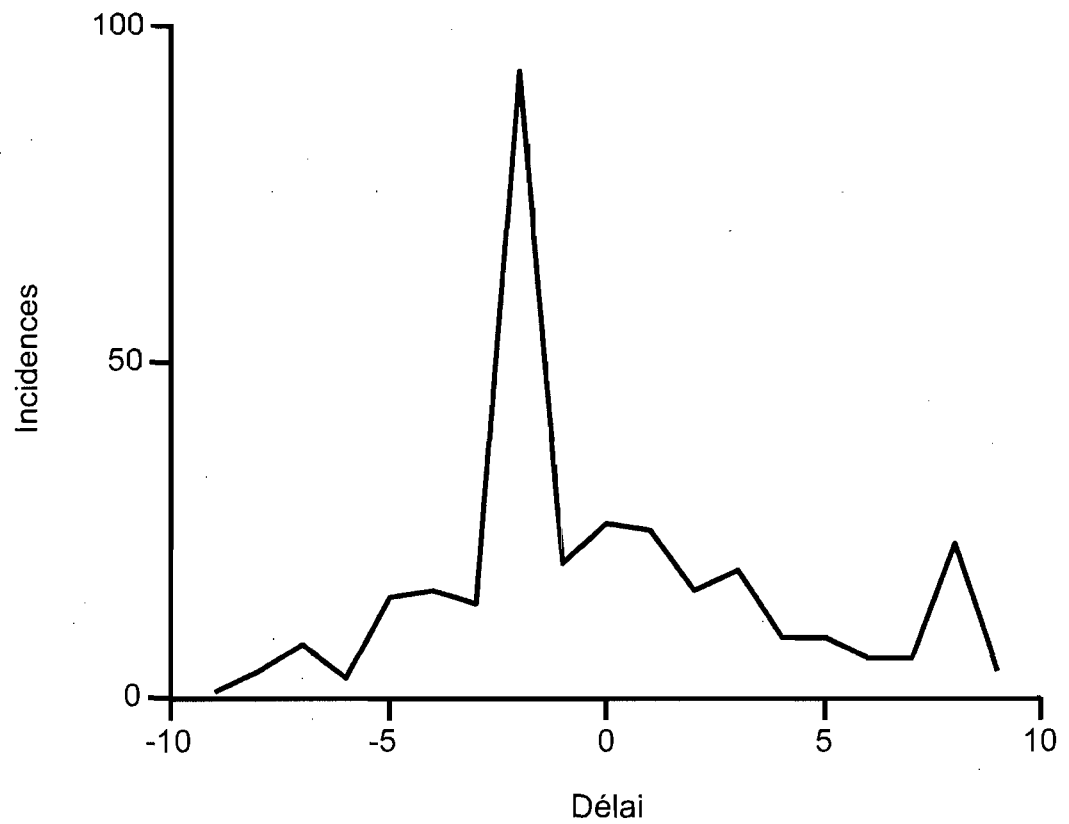


**Figure 8**

Cross-corrélogram suite à cent répétitions. Le système est le même que celui à la Figure 7, mais avec du bruit ajouté. Il est clair que malgré le bruit il est possible d'identifier un pic unique grâce à la répétition du stimulus.

Enfin, pour utiliser cette technique de façon efficace pour cartographier un champ récepteur visuel nous devons ajouter deux dimensions spatiales. Il n'est alors pas uniquement question de déterminer le délai qui sépare l'entrée et la sortie, mais aussi d'identifier quel stimulus (en occurrence sa position) a évoqué un pic significatif. Dans la figure 9A, nous voyons un exemple simplifié dans la mesure où le champ visuel a été divisé en 4 X 4 sections et qu'il y a un seul contraste de stimulus. Dans la rangée du haut nous avons une représentation du champ visuel, et la position du stimulus est représentée par le carré noir. En dessous, nous voyons une représentation binaire d'un potentiel d'action évoqué par une de ces positions. Il est impossible de déterminer la position stimulée qui a évoqué le potentiel d'action, à moins de connaître la latence précise du neurone à ce stimulus spécifique. Afin d'estimer cette latence, nous devons alors incrémenter chacune des positions où un stimulus a été présenté précédemment. Il va sans dire que ce type d'analyse s'effectue dans une fenêtre temporelle très courte (généralement 250-300ms), qui reflète le temps nécessaire pour que le signal se rende à la cellule, le temps d'intégration de cette dernière, ainsi qu'un temps tampon.



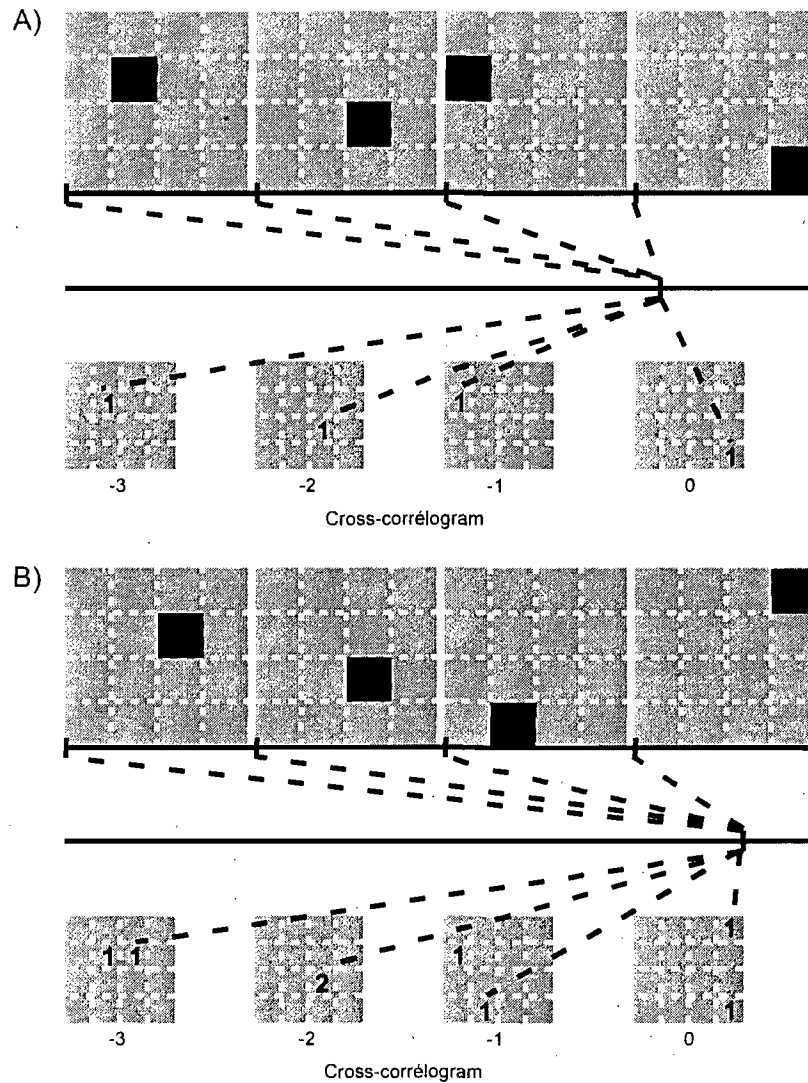


**Figure 9**

Schématisation de la corrélation rétrograde. La rangée du haut représente l'emplacement spatial du stimulus. La deuxième ligne montre l'emplacement temporel du potentiel d'action relatif au temps de présentation des stimuli. La troisième rangée est la matrice bidimensionnelle qui représente l'emplacement spatial le plus probable d'avoir évoqué le potentiel d'action, et ce pour chaque ms pré-potentiel d'action. Les rangées 4-6 sont identiques mais lors d'une apparition subséquente du potentiel d'action.

Pour déterminer laquelle des quatre positions a évoqué le potentiel d'action, il est nécessaire de présenter une autre séquence aléatoire de positions pour le stimulus. Lors du prochain potentiel d'action (Figure 9B), nous effectuons à nouveau des incréments aux positions stimulées. Nous pouvons maintenant observer une tendance, bien que loin d'être significative, qui suggère que l'endroit où il y a déjà deux incidences soit la partie du champ visuel qui évoque une réponse de notre neurone.

À la fin du processus, nous nous retrouvons donc avec une matrice en deux dimensions, et ce pour chaque période de temps  $< 0$  ms (la partie négative du cross-corrélogram). Autrement dit, une matrice tridimensionnelle, dont la troisième dimension est le temps. Nous nous retrouvons donc avec une estimation de la fonction entrée-sortie du neurone dans l'espace-temps (pour des traités exhaustifs sur les présomptions et les fondements statistiques de la méthode voir : de Boer & Kuyper, 1968; Eggermont *et al.*, 1983; Marmarelis *et al.*, 1986).

#### 4.3.2 Les profils de l'aire 17

Jusqu'à présent la quasi-totalité des études portant sur les profils spatio-temporels neuronaux, qu'elles soient effectuées avec des corrélations rétrogrades ou des techniques similaires, ont été des descriptions des champs récepteurs des neurones de l'aire 17 (Movshon *et al.*, 1978b, a; Palmer & Davis, 1981b, a; Citron & Emerson, 1983; Emerson *et al.*, 1987; Jones & Palmer, 1987;

Ohzawa *et al.*, 1990; Szulborski & Palmer, 1990; DeAngelis *et al.*, 1993; McLean *et al.*, 1994; DeAngelis *et al.*, 1995a, b; Ohzawa *et al.*, 1997; Ringach *et al.*, 1997b). De façon générale, nous pouvons dire que ces profils ont permis de confirmer de façon quantitative les descriptions jusqu'alors qualitatives des champs récepteurs de cette région. C'est-à-dire la présence de champs récepteurs de type simple et complexe. De plus, les profils spatio-temporels de certains neurones évoluent dans le temps (tel que dans le modèle d'énergie), et ce changement permet de prédire la direction préférée d'une cellule. En effectuant une analyse de Fourier sur ces mêmes profils, il est possible de prédire les sélectivités aux fréquences spatiale et temporelle des neurones (DeAngelis *et al.*, 1993). Cette technique a également permis une meilleure compréhension de la sélectivité à la disparité binoculaire (Ohzawa *et al.*, 1990; DeAngelis *et al.*, 1995a; Ohzawa *et al.*, 1997). De plus, ces données permettent de spéculer quant aux afférences des neurones sous étude. Par exemple, dans les travaux de Movshon *et al.* (1978a) il a été démontré que les champs récepteurs des cellules complexes sont formés à partir de sous-unités qui intègrent l'information de façon linéaire. Ce n'est que l'interaction et l'intégration de plusieurs sous-unités qui provoquent une réponse non-linéaire caractéristique des cellules complexes.

#### 4.3.3 Les profils du PMLS

Il y a eu beaucoup moins d'étude de corrélations rétrogrades dans le PMLS (Borghuis *et al.*, 2003; Vajda *et al.*, 2004; Vajda *et al.*, 2005; Vajda *et al.*,

2006), et toutes celles qui existent proviennent du même laboratoire. La technique de ce groupe de recherche est utile afin de déterminer jusqu'à quel point le champ récepteur d'une cellule est spatialement homogène quant à sa direction préférée. Elle est aussi utile pour déterminer des interactions temporelles entre des stimuli directionnels. Le résultat le plus intéressant, car il va à l'encontre de ce que nous pourrions prédire à partir de la littérature, est que les interactions temporelles dans le PMLS sont très rares (Vajda *et al.*, 2006). Alors que de telles interactions sont plutôt communes dans l'aire 18 (testé par le même groupe dans la même étude). Si nous nous référons à la représentation de la hiérarchie des aires visuelles (Figure 2), nous constatons que l'aire 18 est en dessous du PMLS, ce qui correspond à une projection *feedforward*. Ainsi, les neurones du PMLS devraient refléter, au moins partiellement, les propriétés des neurones de l'aire 18. En d'autres termes, il y a donc une inversion de ce qui pourrait être attendu quant à la présence ou non de traitement temporel non-linéaire (interaction) de l'information visuelle dans l'aire 18 et le PMLS.

Bien que fort intéressant, les résultats de Vajda *et al.* (2006) ne peuvent être comparés avec ceux obtenues dans l'aire 17 car les deux techniques utilisées ne donnent pas les mêmes informations. Les études sur les profils spatio-temporels, telles que celles mentionnées pour l'aire 17 n'ont pas été effectuées sur des cellules du PMLS en partie pour des raisons méthodologiques (voir discussion). Nous ne connaissons donc pas la fonction entrée-sortie linéaire des neurones du PMLS. C'est-à-dire comment ces neurones intègrent l'information visuelle à partir leurs afférences.

## 5. Objectif et hypothèse

Suite à la section 2, il devrait être clair qu'une investigation du rôle fonctionnel des régions afférentes du PMLS est nécessaire. Ceci découle du fait que seul l'apport de l'aire visuelle primaire est abordé dans la plupart des travaux. Les trois études qui forment la présente thèse abordent cette question de différentes façons.

### 5.1 Première étude

Dans la première étude, le but était de savoir si les afférences autres que l'aire visuelle primaire étaient suffisantes pour permettre une sélectivité à la direction dans les neurones du PMLS, et ce suite à une lésion chez le nouveau né. Le lecteur notera que selon les informations fournies dans la section 4.1, de telles études ont déjà été effectuées. Cependant, tel que mentionné dans la même section, ces études utilisaient des stimuli qui requièrent très peu d'intégration spatio-temporelle. Il est donc envisageable que les neurones du PMLS démontrent des déficits dans la sélectivité à la direction mais que cela ait été masqué par le type de stimuli. Cette sélectivité amoindrie pourrait provenir du fait qu'une analyse initiale effectuée par l'aire visuelle primaire n'est plus lieu, ce qui pourrait entraver l'intégration du mouvement dans le PMLS. L'hypothèse veut donc que la sélectivité à la direction des neurones du PMLS ne devrait plus

être présente lors de la présentation de stimuli qui requièrent une intégration spatio-temporelle importante.

Cependant, une deuxième hypothèse contradictoire peut également être formulée. Une étude de Pasternak *et al.* (1995) a démontré que lorsqu'une lésion de l'aire 17 est effectuée chez l'adulte, la capacité de discriminer la direction augmente pour des stimuli qui requièrent une intégration spatio-temporelle. Si cette augmentation est attribuable aux neurones du PMLS, alors leur sélectivité à la direction devrait être plus prononcée.

## 5.2 Deuxième étude

La question des afférences a été abordée d'une autre façon dans la deuxième étude. Rappelons qu'un des postulats d'une hiérarchie telle que décrite dans la section 2.1.1 est le traitement sériel de l'information. Il s'en suit que les latences des aires les plus élevées devraient être supérieures à celles des niveaux inférieurs, puisque l'analyse effectuée dans le premier dépend de l'apport du deuxième. L'hypothèse est donc qu'il devrait y avoir une relation entre les latences obtenues dans les diverses aires corticales et leur niveau dans la hiérarchie. Nous avons donc étudié les latences dans quatre aires corticales, mais également dans le thalamus extra-géniculé. L'intérêt de ce dernier est que cette structure n'a pas d'organisation laminaire et il est donc impossible d'en déduire sa position dans la hiérarchie en utilisant des

informations anatomiques. Pour les aires corticales, les latences devraient croître en passant de l'aire 17, au PMLS, à l'AMLS et finalement l'AEV.

### 5.3 Troisième étude

Dans la troisième étude, la corrélation rétrograde a été utilisée afin de décrire les champs récepteurs spatio-temporels et de mieux identifier les afférences impliquées lors de la réponse initiale dans le PMLS. Si les principaux apports du PMLS sont les aires 17 et 18, alors les champs récepteurs du PMLS devraient refléter ces apports. Donc pour cette étude, l'hypothèse est que les champs récepteurs du PMLS seraient presque entièrement de type complexe étant donné qu'ils reçoivent des projections surtout des couches supra-granulaires (Symonds & Rosenquist, 1984b; Einstein & Fitzpatrick, 1991; Norita *et al.*, 1996). Si d'autres afférences ont un rôle important dans l'élaboration des champs récepteurs du PMLS, alors ceci devrait se refléter dans le profil spatio-temporel.

### 5.4 Résumé de l'objectif

Comme nous l'avons vu plutôt dans ce texte, le système visuel du chat est hautement parallèle. Des aires extrastriées telles que le PMLS reçoivent des afférences de plusieurs régions corticales et sous-corticales. L'apport fonctionnel au PMLS de chacune de ces afférences est peu connu. Les travaux

de la présente thèse cherchent donc à déterminer, en utilisant trois méthodes différentes, le rôle fonctionnel des multiples afférences du PMLS mentionnées ci-haut. Spécifiquement, les afférences autres que les aires 17 et 18.



Article 1

**Complex motion selectivity in PMLS cortex following early lesions of primary visual cortex in the cat.**

B.G. Ouellette<sup>1,2</sup>, K. Minville<sup>1</sup>, D. Boire, M. Ptito, C. Casanova<sup>1,3</sup>

<sup>1</sup> École d'optométrie, Université de Montréal

<sup>2</sup> Département de Psychologie, Université de Montréal

<sup>3</sup> Corresponding author

Published in Visual Neuroscience (2007), 24, 53-64.

Copyright © 2007 Cambridge University Press. All rights reserved. No part of this publication may be reproduced, in any form or by any means, electronic, photocopy, or otherwise, without permission in writing from Cambridge University Press.

Reprinted with the permission of Cambridge University Press

## Abstract

In the cat, the analysis of visual motion cues has generally been attributed to the posteromedial lateral suprasylvian cortex (PMLS) (Toyama *et al.*, 1985; Rauschecker *et al.*, 1987a; Rauschecker, 1988; Kim *et al.*, 1997). The responses of neurons in this area are not critically dependent upon inputs from the primary visual cortex (VC), as lesions of VC leave neuronal response properties in PMLS relatively unchanged (Spear & Baumann, 1979; Spear, 1988; Guido *et al.*, 1990b). However, previous studies have used a limited range of visual stimuli. In the present study, we assessed whether neurons in PMLS cortex remained direction selective to complex motion stimuli following a lesion of VC, particularly to complex random dot kinematograms (RDKs). Unilateral aspiration of VC was performed on post-natal days 7-9. Single unit extracellular recordings were performed one year later in the ipsilateral PMLS cortex. As in previous studies, a reduction in the percentage of direction selective neurons was observed with drifting sinewave gratings. We report a previously unobserved phenomenon with sinewave gratings, in which there is a greater modulation of firing rate at the temporal frequency of the stimulus in animals with a lesion of VC, suggesting an increased segregation of ON and OFF sub-regions. A significant portion of neurons in PMLS cortex were direction selective to simple (16/18) and complex (11/16) RDKs. However, the strength of direction selectivity to both stimuli was reduced as compared to normals. The data suggest that complex motion processing is still present, albeit reduced, in PMLS cortex despite the removal of VC input. The complex RDK motion selectivity is

consistent with both geniculo-cortical and extra-geniculate thalamo-cortical pathways in residual direction encoding.

## Introduction

In the cat, the analysis of visual motion cues has generally been attributed to the areas surrounding the lateral suprasylvian sulcus, specifically the cortex of the posteromedial lateral suprasylvian sulcus (PMLS: von Grunau & Frost, 1983; Toyama *et al.*, 1985; Rauschecker *et al.*, 1987a; Rauschecker, 1988). Neurons in PMLS cortex are known to respond to simple and complex motion cues (Kim *et al.*, 1997; Villeneuve *et al.*, 2006a) and their destruction yields direction discrimination deficits (Rudolph & Pasternak, 1996). In kittens, lesions of primary visual cortex (VC) lead to minor deficits in direction processing in PMLS cortex as assessed by neuronal response properties (Tong *et al.*, 1984; Guido *et al.*, 1990a, 1992) and behavioral testing (Wetzel *et al.*, 1965; Tucker *et al.*, 1968; Murphy *et al.*, 1975; Cornwell & Payne, 1989). This sparing may be due to an increase of and/or novel projections to PMLS cortex from the lateral geniculate nucleus (LGN) and the lateral posterior-pulvinar complex (LP-pulvinar: Labar *et al.*, 1981; Tong *et al.*, 1984; Kalil *et al.*, 1991; Payne *et al.*, 1993; Spear, 1995; Payne & Lomber, 1998a).

To date, the effects of early VC lesions on the motion processing capabilities of neurons in PMLS cortex have been determined with simple motion stimuli (Spear & Baumann, 1979; Tong *et al.*, 1984; Spear, 1988; Guido *et al.*, 1990a; Guido *et al.*, 1990b; Guido *et al.*, 1992), but not complex motion stimuli. Two contradictory hypotheses regarding complex motion sensitivity motivated this study; 1- Following an early lesion of VC, PMLS neurons no longer receive projections relaying local direction signals. This may hinder

complex motion integration in PMLS cortex, since these local signals may be necessary for global motion processing. 2- Following a lesion of area 17 in adult cats, Pasternak *et al.* (1995) demonstrated that complex motion processing is increased in a discrimination task. This suggests that area 17 impedes processing carried out in motion sensitive areas. Hence, a lesion of VC may actually increase complex motion processing in PMLS cortex. The aim of the present study was to determine if complex motion selectivity is present among PMLS neurons following early VC lesions.

## Methods

### Lesion protocol

All procedures were in accordance with the directives of the Canadian Council for the Protection of Animals and the ethics review board of the Université de Montréal. Seven kittens (post-natal days 7-9) received injections of Atropine (0.04mg/kg) and Atravet (0.5mg/kg) and were anesthetized with Halothane (5%), in a 50:50 mixture of O<sub>2</sub> and N<sub>2</sub>O. Anesthesia was reduced to 2% Halothane during the operation. Heart rate and blood O<sub>2</sub> saturation levels were monitored with an oxymeter. A craniotomy exposed the marginal and posterolateral gyri, allowing unilateral lesions of areas 17 and 18 by subpial aspiration. Sterile gelfoam was placed in the lesion site and covered with Surgicell before the bone flap was replaced. Kittens received Buprenex (0.001mg/kg) for two to three days and Tribissen (15mg/kg) for 10 days. For the

purposes of comparison, raw data for PMLS cortex in normal animals came from work presented in Villeneuve *et al.* (2006a).

### Animal preparation

Recordings were performed one year after the lesions. Animals were pre-anesthetized and anesthetized as described above. Pressure points and incisions were treated with a local anesthetic (Lidocaine Hydrochloride 2%). Cannulation of the cephalic vein allowed for muscle relaxation of the animal with gallamine triethiodide (10mg/kg/hr) in lactated ringers solution. The animal was artificially ventilated, via a tracheal adaptor, with N<sub>2</sub>O/O<sub>2</sub> (70/30%) and Halothane (0.5-1%). Levels of CO<sub>2</sub> were maintained between 28 and 32 mmHg by adjusting stroke volume and respiratory rate. The EKG and EEG were monitored and rectal temperature was maintained at  $\pm 37.5$  C°. Atropine (1%) and phenylephrine hydrochloride (2.5%) were applied to dilate the pupils and retract nictitating membranes respectively. Contact lenses with appropriate refractive power were applied. Unilateral craniotomies were performed over PMLS cortex, as defined by Palmer *et al.* (1978), ipsilateral to the lesioned cortex. The dura was reflected to expose the cortex. Varnished tungsten microelectrodes (A&M systems, Carlsborg, WA) were angled at  $\sim 40$ deg.

## Recordings and visual stimulation

Single unit recordings were isolated from the signal with a window discriminator. Using an analogue digital interface (CED 1401 plus), signals were fed to a PC running acquisition software (Spike 2, CED, Cambridge UK). Peristimulus time histograms (PSTH) with a binwidth of 10 ms were created and saved for further analysis.

An ophthalmoscope and a hand held projector were used to map receptive fields on a screen covering 80deg X 107deg placed 57cm in front of the animal. Computer generated stimuli subtending 75° x 92° of visual angle were back projected onto the screen, at a mean luminance of 25cd/m<sup>2</sup>. Stimuli were generated, at 67Hz, by a G3 Macintosh computer running VPixx 1.5 (Sentinel Medical Research, Ste-Julie, Quebec, Canada). Each condition was presented at least 4 times in a random order for a duration of 4 seconds per presentation and separated by a one second interval.

## Receptive field properties

The size and location of receptive fields and ocular dominance were first assessed *qualitatively*. *Quantitative assessment of receptive field properties* was performed using 60% contrast drifting sinusoidal gratings. Preferred direction, spatial and temporal frequencies were determined.



### Plaid patterns

Two identical (differing only by 120deg) superimposed drifting sinewave gratings were presented at their previously determined preferred spatial and temporal frequency. The contrast of each grating was set to 30%, so that the contrast of the plaid was equal to that of a single grating.

### Random dot kinematograms

Two types of RDKs were presented, simple and complex. Detailed descriptions of these stimuli have previously been published (Dumbrava *et al.*, 2001; Ouellette *et al.*, 2004b; Villeneuve *et al.*, 2006a). Briefly, RDKs were 1deg white dots on a black background (100% contrast). Simple RDKs were a rigidly translating random dot field. For complex RDKs, the dots had a lifetime of two-frames, that is, they moved only once before being randomly repositioned. At any one time, half the dots were displaced in the coherent motion direction while the other half was repositioned randomly. Complex RDKs require the temporal integration of many dots over a large spatial extent in order to extract the veridical direction of the stimulus. Supporting the complex nature of this stimulus, almost all simple RDK direction selective neurons in area 17 were unable to code the direction of complex motion RDKs (Dumbrava *et al.*, 2001; Villeneuve *et al.*, 2006a).

## Data analysis

A detailed description of data analysis has previously been published (Ouellette *et al.*, 2004b). A modulation index (MI), traditionally used to discriminate simple from complex cells (Skottun *et al.*, 1991b), was computed for sinewave gratings presented at the preferred direction at optimal spatial and temporal frequencies. Cells with an MI above 1.0 exhibited a high modulation of their response amplitude to the temporal frequency of the grating (i.e. distinct ON and OFF sub regions), while cells with an MI below 1.0 show a less pronounced modulation of their discharge rate. Direction selectivity among PMLS neurons was determined with a direction index (DI). Neurons with a DI value above 0.5 were considered to be direction selective. Direction bandwidth was calculated as the half-width at half-height at the preferred direction. Neurons were classified as either pattern or component motion selective, according to the method of Movshon *et al.* (1986, corrected). The resulting partial correlation coefficients were converted to Z scores using a modified version of Fisher's transform (Majaj *et al.*, 1999; Ouellette *et al.*, 2004b; Smith *et al.*, 2005). Comparisons of lesioned and normal animals were carried out using student's t test or a chi-square test ( $\alpha = 0.05$ ).

## Histology

Animals were intravenously administered pentobarbital sodium (Euthanyl: 240 mg/ml, 110mg/kg) and then perfused transcardially with phosphate buffer

solution and fixative (3% paraformaldehyde and 0.1% glutaraldehyde). Using a cryostat, coronal serial sections (40 $\mu$ m) of the lateral geniculate nucleus (LGN) were cut, stained with cresyl violet. The degeneration of the LGN was compared to the retinotopic maps of Sanderson (1971) to determine the extent of the visual field affected by the lesion. It has previously been reported that neurons with receptive fields entirely outside the lesioned part of the visual field exhibit response properties which differ from normals (Tong *et al.*, 1984). Despite this result we limited our analysis to receptive fields which had an overlap of at least 75% with the lesioned part of the visual field. This criterion seems reasonable as the stimulus of interest, complex RDKs, require a large scale spatial integration of motion cues.

## Results

### Extent of the lesions

All primary visual cortex lesions presented here caused cellular degeneration throughout most of the visual field representation in the LGN as can be seen for one animal in Figure 1. For the case presented, the degeneration in the LGN ipsilateral to the lesion makes it difficult to establish both the layers and borders of the nucleus. The bottom panel shows that the receptive fields were predominantly situated within the part of the visual field that was affected by the lesion. Six of the seven animals had lesions that clearly covered all the visual field up to an azimuth and elevation of at least 40 degrees

eccentricity, while in the seventh animal the preserved visual field representation began at an azimuth greater than 30 degrees.

Schematic representations of degeneration are shown in Figure 2 for all seven animals. The mapping of the degeneration has been superimposed on standardised retinotopic maps (Sanderson, 1971) in order to estimate the visual field representation affected by the lesions. Due to the non-uniform nature of VC lesions on the LGN, the degeneration has been divided into three sub-categories: normal (white), degenerated (light gray), and severely degenerated (dark gray). An example of the degenerated and severely degenerated nomenclatures may be observed for case GBK0506 (third row) which is the animal for which photomicrographs were presented in Figure 1. The second map from the left (dark gray) and the rightmost map (light gray) are approximately at the same antero-posterior positions as the photomicrographs in the second and third rows of Figure 1 respectively.

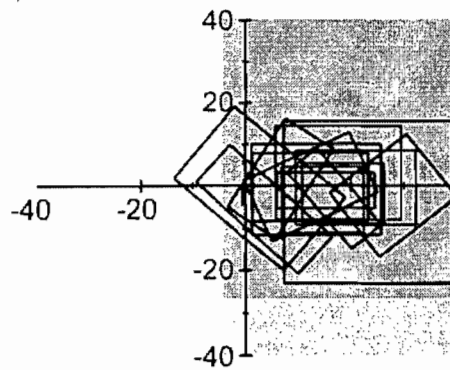
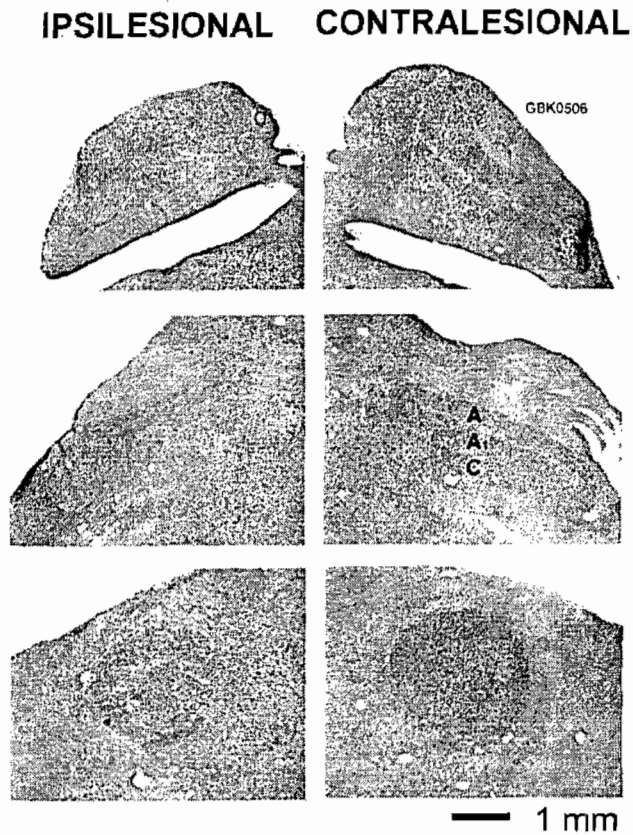


**Figure 1**

Example of degeneration of the LGN in one animal. Cresyl violet staining was heavier and the definition of the three cellular layers was clearer in the thalamus contralateral to the lesion. The bottom panel represents the extent of visual field representation (out to 40 degrees) that was affected by the lesion. The gray shading represents the extent and the saturation represents the magnitude of degeneration in the LGN. Note that the photomicrographs in the left and right panel were taken from the same coronal slice.

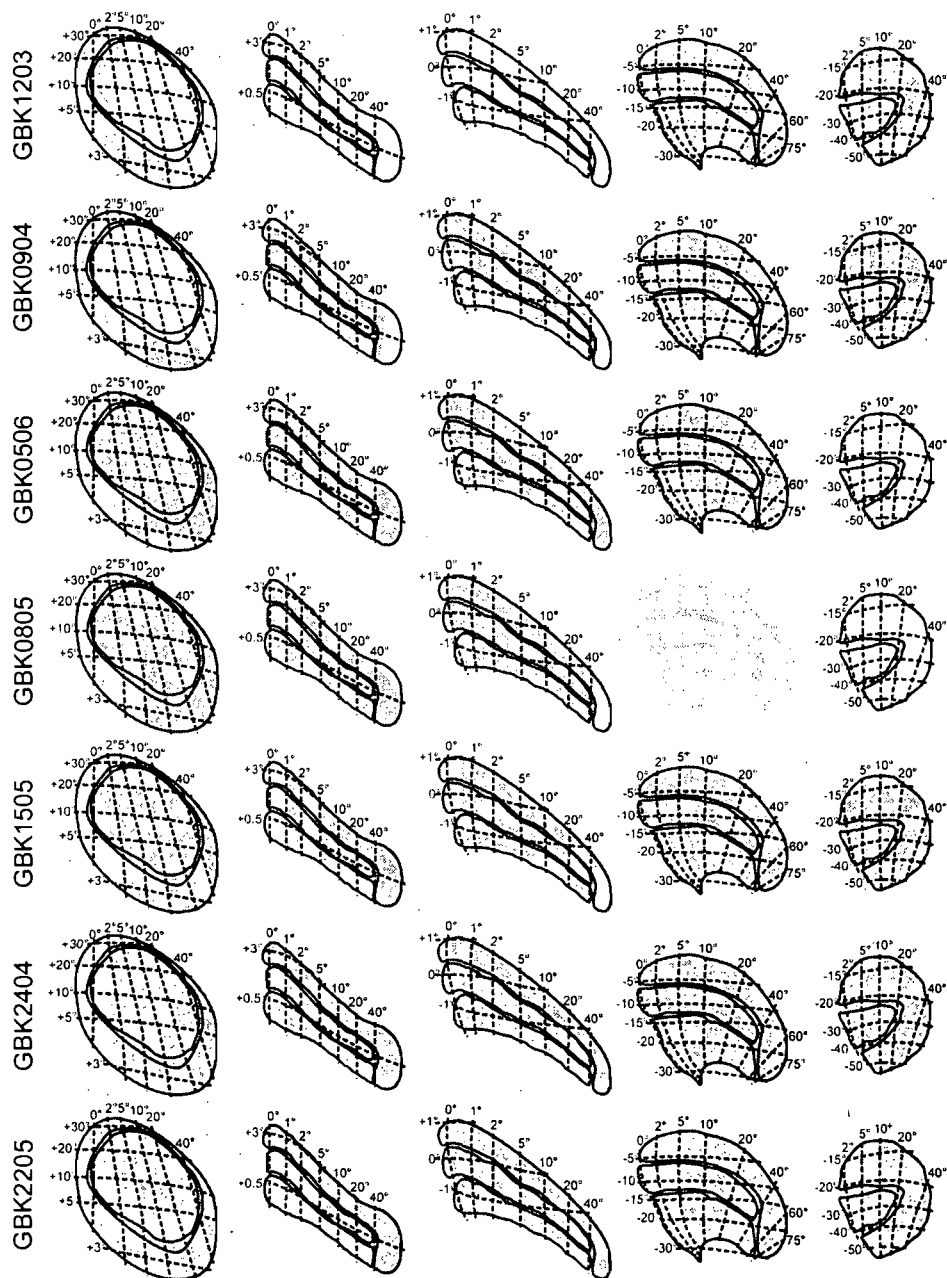


**Figure 2**

Representation of degeneration of the LGN following the cortical lesions. The cases shown are from the least to the most severely degenerated. Intact, degenerated and heavily degenerated sections of the LGN are represented by white, light gray, and dark gray respectively. The sole representation of the LGN where the outline is light gray is a case where no stained sections exhibited a form similar to that represented, likely due to distortion attributable to the lesion.

### Basic receptive field properties

Testing was carried out in the PMLS cortex of seven cats and only data obtained from neurons with more than 75% of their receptive fields within the lesioned part of the visual field are presented here (45 neurons). The mean ( $\pm$  S.D.) maximum response amplitude to optimized sinewave gratings did not significantly differ from normal animals (lesioned:  $25.4 \pm 24$  spikes/s,  $n = 41$ ; normal:  $26.1 \pm 19.6$ ,  $n = 48$ ;  $t = 0.15$ ,  $p = 0.88$ ). Spontaneous activity was weak, as in normal cats, and no significant difference was observed (lesioned:  $5.8 \pm 7.9$  spikes/s,  $n = 41$ ; normal:  $5.5 \pm 11.9$ ,  $n = 48$ ;  $t = 0.17$ ,  $p = 0.87$ ). Among neurons whose receptive fields could clearly be mapped, the mean receptive field areas were comparable (lesioned:  $363.2 \pm 272.7$  deg<sup>2</sup>,  $n = 29$ ; normal:  $334.0 \pm 262.5$  deg<sup>2</sup>,  $n = 47$ ;  $t = 0.46$ ,  $p = 0.644$ ).

### Sinewave gratings

In animals with and without a lesion, the spatio-temporal response characteristics to sinewave gratings were similar. No significant difference was observed for mean optimal spatial frequencies (lesioned:  $0.15 \pm 0.22$  c/deg,  $n = 41$ ; normal:  $0.16 \pm 0.17$  c/deg,  $n = 30$ ;  $t = 0.21$ ,  $p = 0.84$ ). Mean optimal temporal frequencies were not significantly different either (lesion:  $3.9 \pm 2.3$  Hz,  $n = 29$ ; normal:  $3.6 \pm 1.2$ ,  $n = 23$ ;  $t = 0.46$ ,  $p = 0.65$ ).

Although there was a lack of effect of lesion on spatial and temporal frequencies this was not the case for direction selectivity. The proportion of

direction selective neurons was smaller in lesioned versus normal animals (lesion: 25/41 or 61%; normal: 39/45 or 87%), this was a statistically significant reduction ( $\chi^2 = 7.44$ ,  $p < 0.01$ ). Accordingly, the mean DI was significantly lower in animals with lesions (lesion:  $0.61 \pm 0.32$ ,  $n = 41$ ; normal:  $0.86 \pm 0.21$ ,  $n = 45$ ;  $t = 4.1$ ,  $p < 0.001$ ;

A yet undescribed difference in the response to sinewave gratings was observed. In animals with a lesion, neurons exhibited a greater modulation of their discharge rate as evidenced by the MI (lesion:  $0.80 \pm 0.55$ ,  $n = 38$ ; normal:  $0.54 \pm 0.35$ ,  $n = 28$ ;  $t = 2.19$ ,  $p = 0.03$ ). A distribution of MIs in normal and lesioned cats is presented in Figure 3. Note that the MI distribution is skewed to the left among neurons recorded in normal animals (only 3/28 neurons have a  $MI > 1$ ), while this asymmetry is less pronounced for animals with lesions (12/38 neurons had a  $MI > 1$ ), however this shift in the distribution is not significantly different ( $\chi^2 = 2.4374$ ,  $p > 0.05$ ).



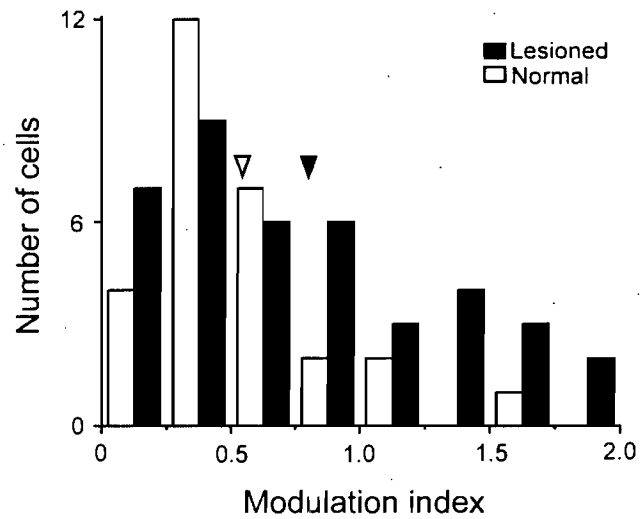


**Figure 3**

The distribution of modulation indices for neurons in normal (white bars) and lesioned (black bars) animals. Note that the distribution for normal animals was skewed to the left, while it was more homogeneous for animals with a lesion. The mean MI for the lesioned and normal groups are presented as filled and open triangles respectively.

## Plaid patterns

Plaid pattern selectivity was assessed among the 24 neurons that were direction selective to sinewave gratings. All cells that were clearly responsive to plaid patterns were component motion selective. The response profile of such a neuron is presented in Figure 4A and is similar to what is found in animals without a lesion. The distribution of response profiles for the sample of neurons is presented in panel B. Among the 24 sinewave grating direction selective cells tested, 15 were component motion selective, six were unclassified, while an additional three neurons were non-responsive (not shown). The ratio of unclassified and component motion cells was not significantly different in the PMLS cortex of animals with (6/15) and without (3/26) a lesion ( $\chi^2 = 2.74$ ,  $p > 0.05$ ). The three non-responsive neurons did not discharge above spontaneous activity levels (panel C) to plaid patterns, de(Villeneuve *et al.*, 2006a) despite being direction selective to drifting sinewave gratings (panel D) before and after tests with plaid patterns. Note the very narrow direction tuning bandwidth in panel D, which was present in the three cells. The mean bandwidth for these three cells was 10.47 deg as compared to 22.96 deg for the whole sample.

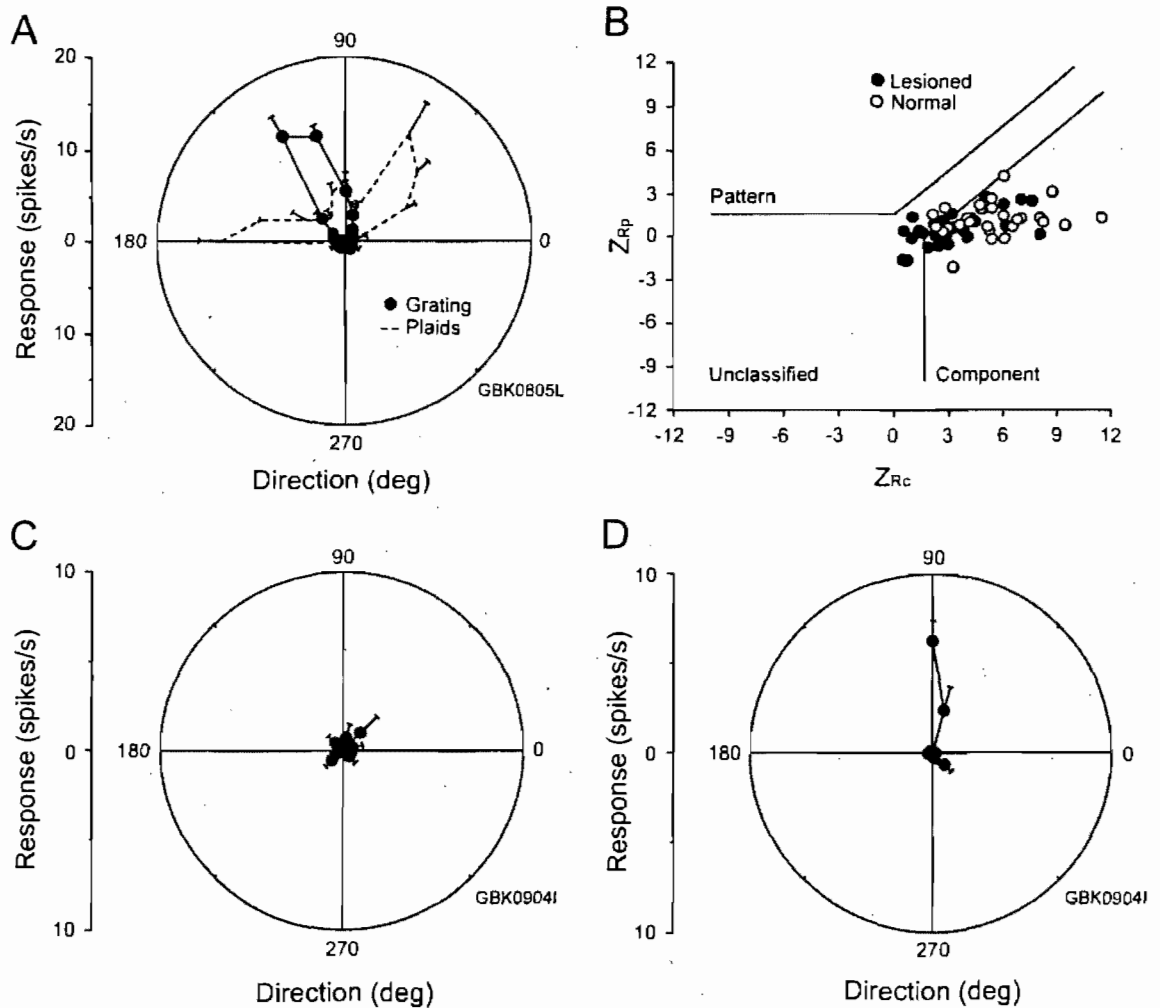


**Figure 4**

Response to plaid patterns. **A**) Typical sinewave grating (dashed lines) and plaid pattern (black circles) response profiles. **B**) The distribution of response profiles for plaids was presented for animals with (black circles) and without lesions (white circles). **C & D**) An example of a neuron that was non-responsive to a plaid pattern (panel C) despite being direction selective to a sinewave grating (panel D). This type of cell was not included as an unclassified neuron in panel B. Full lines represent response amplitude, spontaneous activity is too low to be seen.

## RDKs

Direction selectivity for simple RDKs was present in 16 out of 18 neurons that had previously been assessed to be direction selective for sinewave gratings. A tuning curve of a typical direction selective neuron is presented in panel A of Figure 5. Generally, neurons were not as direction selective as in normal animals (a 21% decrease in mean DI) as revealed by a significantly lower mean DI for lesioned animals (lesion:  $0.79 \pm 0.31$ ,  $n = 18$ ; normal:  $1.0 \pm 0.23$ ,  $n = 35$ ;  $t = 2.79$ ,  $p = 0.007$ ). In panel B, the decreased direction selectivity is reflected as a leftward shift of the DI distribution, however a majority (89%) of neurons nonetheless remained direction selective with a criterion of 0.5. Mean direction bandwidths for simple RDKs were similar between both groups (lesion:  $64 \pm 23.7$  deg,  $n = 10$ ; normal:  $50.9 \pm 21.2$  deg,  $n = 37$ ;  $t = 1.69$ ,  $p = 0.097$ ). The mean optimal speed was  $131.3 \pm 74.2$  deg/s ( $n = 8$ ) and  $106.1 \pm 59.4$  deg/s ( $n = 33$ ) for lesioned and normal animals respectively, these means were not significantly different ( $t = 1.02$ ,  $p = 0.311$ ).

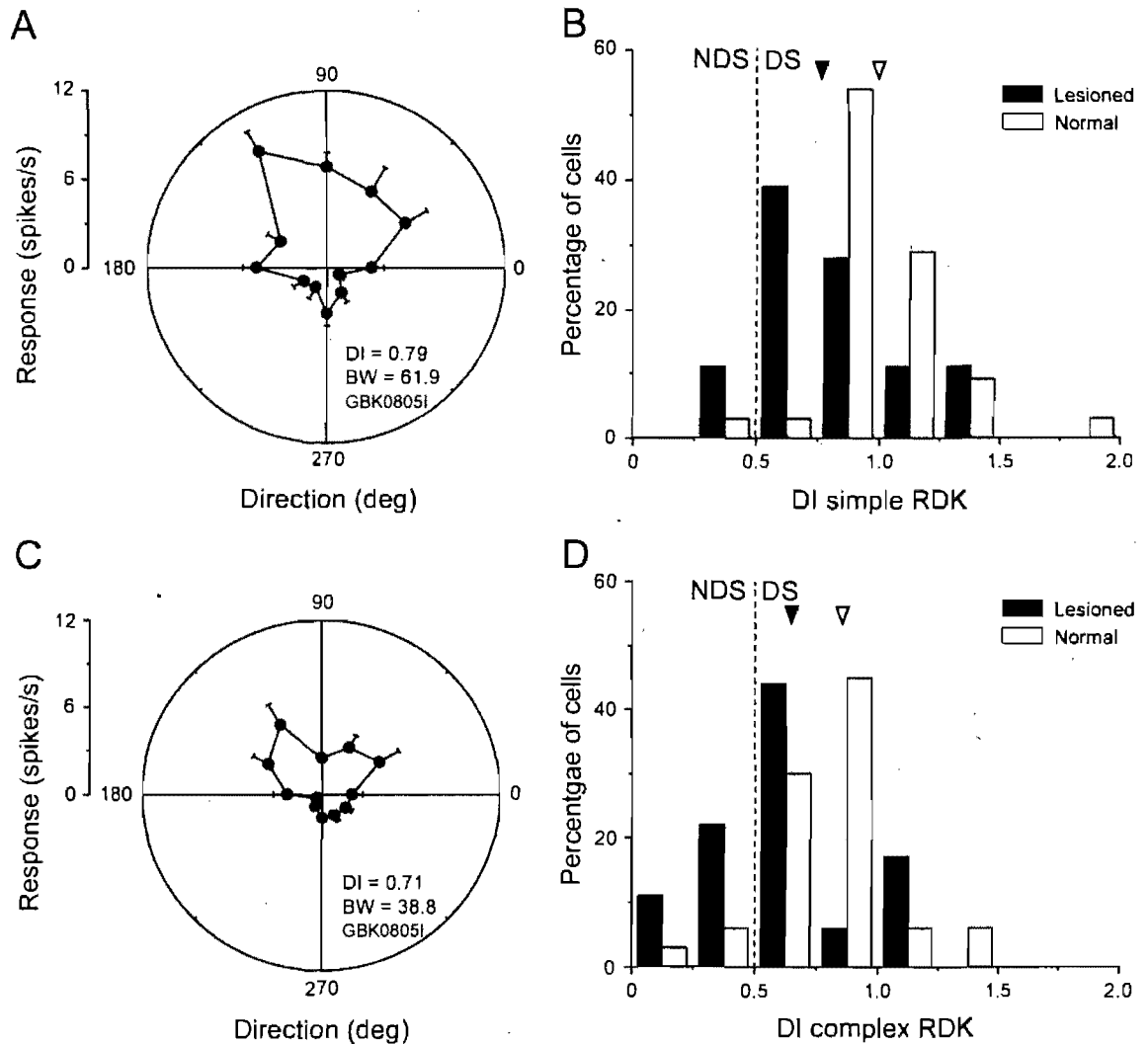


**Figure 5**

Direction selectivity for RDKs. **A)** A typical response curve for different directions of a simple RDK stimulus. The full line represents the response amplitude, spontaneous activity was too weak to be represented. **B)** Histogram of simple RDK direction indices measured in PMLS following a lesion of VC (black bars) and in normals (white bars). **C)** Typical response of a complex RDK selective neuron. This is the same cell as in panel A. **D)** Histogram of direction indices for complex RDKs in lesioned (black bars) and normal (white bars) animals. The vertical and horizontal dashed lines represent the cutoff between non-direction selective (NDS) and direction selective (DS) neurons. The means for lesioned and normal groups are presented as filled and open triangles respectively.

Among the 16 neurons that were direction selective to simple RDKs, 11 also signaled complex RDK direction. The direction tuning curve for a complex RDK selective cell is presented in Figure 5C (same cell as in panel A). Complex RDK direction selectivity was significantly lower among lesioned cats (lesioned:  $DI = 0.64 \pm 0.27$ ,  $n = 16$ ; normals:  $DI = 0.83 \pm 0.34$ ,  $n = 33$ ;  $t = 2.04$ ,  $p = 0.047$ ). This is a 33% reduction in mean DI and can be seen as a leftward shift in the distribution of DI values in panel D. The majority (69%) of neurons however, are direction selective to complex motion RDKs ( $DI > 0.5$ ). Complex RDK direction bandwidth did not significantly differ ( $t = 0.76$ ,  $p = 0.453$ ), the means were  $62.8 \pm 44.9$  deg ( $n=8$ ) for lesioned and  $72.8 \pm 28.9$  deg ( $n=28$ ) for normal animals. The optimal speed for complex RDKs did significantly differ ( $t = 2.05$ ,  $p = 0.048$ ), with means of  $79.3 \pm 57.1$  deg/s ( $n=7$ ) and  $178.3 \pm 123.9$  deg/s ( $n=31$ ) for lesioned and normal animals respectively.

#### Stimulus dependent direction selectivity

Direction selectivity was significantly reduced for sinewave gratings, simple and complex RDKs in lesioned animals. When observing the behavior of a single neuron, this reduction of direction selectivity could either be stimulus dependent or independent. To distinguish between these two possibilities, three correlations were calculated between DIs for different stimuli (Bonferroni corrected familywise error of 0.05). There was no significant correlation of sinewave grating DIs with those of simple ( $r = 0.33$ ,  $p = 0.19$ ) or complex RDKs ( $r = 0.21$ ,  $p = 0.41$ ). Direction selectivity was significantly correlated ( $r = 0.61$ ,  $p =$

0.01) between simple and complex RDKs. The same pattern was observed in normal animals, for which there was no significant correlation between sinewave gratings and simple ( $r = 0.06$ ,  $p = 0.81$ ) or complex RDKs ( $r = -0.12$ ,  $p = 0.61$ ), while DIs for simple and complex RDKs were significantly correlated ( $r = 0.55$ ,  $p = 0.01$ ). Thus direction selectivity, at the single cell level, is stimulus dependent both in lesioned and normal animals.

## Discussion

### General observations

Following neonatal lesions of VC few functional properties were altered among neurons in PMLS cortex. Basic response properties were unchanged except for an increased MI and a reduction in direction selectivity; the latter finding is similar to that of previous investigators (Tong *et al.*, 1984; Guido *et al.*, 1990a; Guido *et al.*, 1990b; Guido *et al.*, 1992). Regardless of stimulus type there was a reduction of the strength of direction selectivity among PMLS neurons. However, the direction selectivity of a single neuron to one stimulus was not a good predictor of selectivity to another stimulus. The main finding of the present study is that complex motion processing persists in PMLS cortex despite early lesions of VC.

### Unilateral nature of the lesions

One could suggest that the incomplete reduction of direction selectivity is attributable to the unilateral nature of the lesions. This seems improbable as unilateral and bilateral lesions have similar effects on response properties (Guido *et al.*, 1990a). Similarly a lesion of the corpus callosum has little effect on the modification of response properties following a VC lesion when performed in very young kittens (Tong *et al.*, 1987). It is therefore unlikely that the intact contralateral VC played a role in the residual direction selectivity of PMLS neurons.

### Proportion of direction selective cells

A general reduction in direction selectivity for all stimuli was observed. Of particular interest is the decrease in direction selectivity for complex RDKs. This is in keeping with the first hypothesis that motivated this study, in which the elimination of local motion processing in the VC hampers complex motion integration in PMLS cortex. It is important to note however, that the decrease is not as severe as what could be expected based on the first hypothesis. The decrease in complex motion selectivity suggests that the increase in discriminability observed by Pasternak *et al.* (1995) is attributable to visual areas that are higher up in the hierarchy relative to PMLS. A direct comparison with the work of Pasternak *et al.* (1995) is difficult as the lesions were not carried out at the same ages. We reasoned that increased complex motion selectivity would



be more likely following a long standing early lesion, due to neuronal plasticity. A study similar to the present one would be necessary to definitively eliminate the possibility that PMLS was responsible for the increased discriminability of complex motion selectivity in animals with lesions in adulthood.

### Possible pathways

Despite the aforementioned reduction in the strength of direction selectivity, a majority of PMLS neurons were nonetheless direction selective for simple, and to a lesser extent complex motion (i.e. complex RDKs). Previous authors have suggested that the relatively normal response properties observed in PMLS cortex are due to increased and/or novel projections from either the A or C layers of the LGN (Figure 6Aa), a tecto-thalamo-cortical circuit (Ab), a retino-thalamo-cortical pathway (6Ac), or novel computations that occur within PMLS (Labar *et al.*, 1981; Tong *et al.*, 1984; Spear, 1988; Kalil *et al.*, 1991; Tong *et al.*, 1991; Guido *et al.*, 1992; Payne *et al.*, 1993; Spear, 1995; Long *et al.*, 1996; Payne & Lomber, 1998a; Moore *et al.*, 2001; Boire *et al.*, 2004). All of these mechanisms are likely to be involved in residual direction selectivity in PMLS. However the present results, in conjunction with previous studies, suggest that the LGN has a central role in the transfer of information to PMLS, at least for the initial response of the latter neurons.

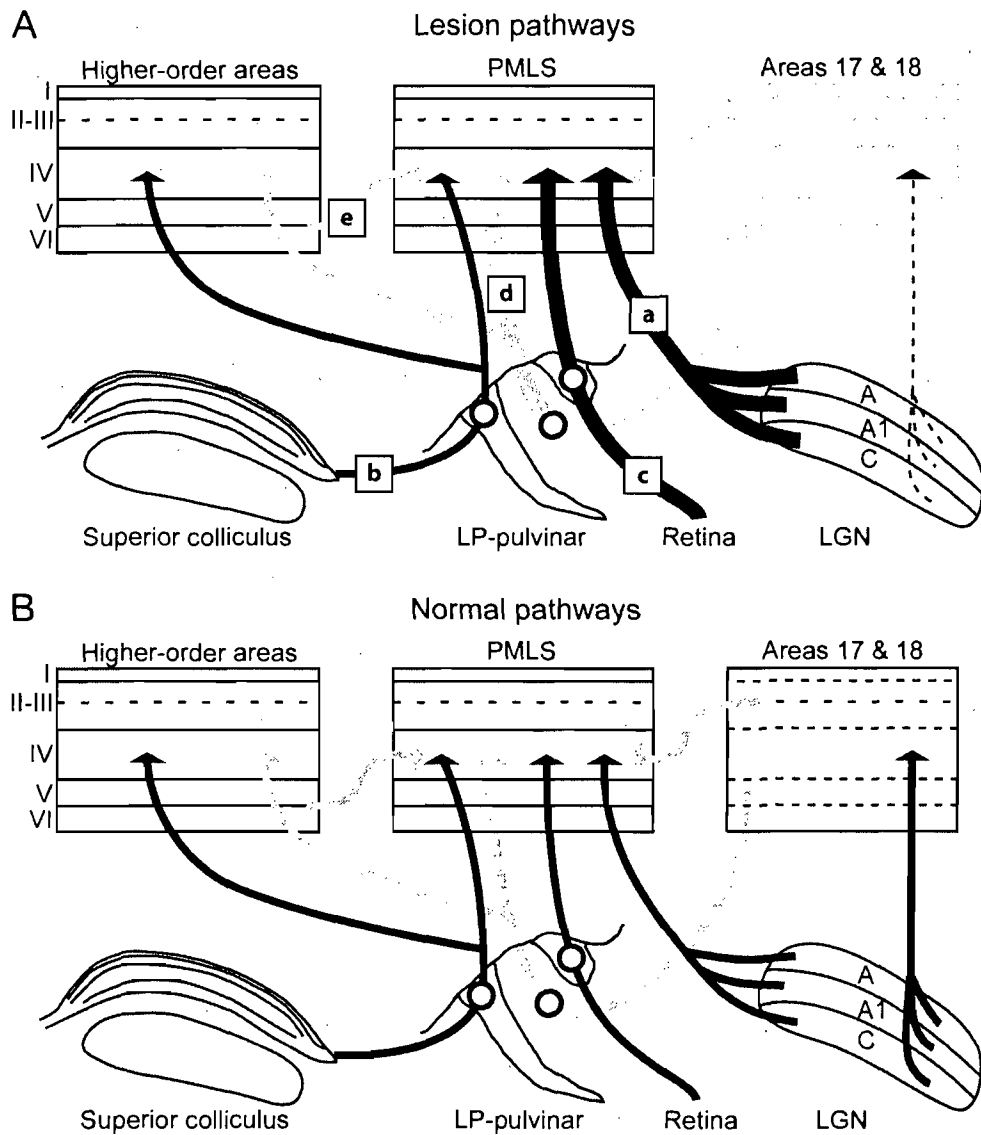


**Figure 6**

Simplified schematic representation of pathways in neonatal lesioned animals (A), equivalent pathways in normal animals are presented in B for comparison. For ease of viewing, subcortical pathways that project to cortex are represented by black lines, while pathways emanating from cortex are in gray. In panel A, the thickness of the lines represents the relative importance of the pathway as compared to normals. Dashed lines represent pathways which are no longer present and empty circles signify pathways with at least one synapse.

A geniculo-cortical route could potentially explain the increase in spatial segregation of ON and OFF sub-regions among PMLS neurons, which would arise from clearly segregated ON-OFF LGN receptive fields. The latter are known to augment their projections to PMLS cortex following early VC lesions (Kalil *et al.*, 1991; Spear, 1995; Payne & Lomber, 1998a). In the present experiments, occasional sampling of data from AMLS was carried out and an increase in MI was also observed (lesion:  $1.80 \pm 1.59$ ,  $n = 12$ ; normal:  $0.84 \pm 0.49$ ,  $n = 116$ ), despite the fact that projections from the LGN to AMLS do not increase following VC lesions (Payne & Lomber, 1998a). A similar increase in MI has been reported in the LP-pulvinar (Desautels & Casanova, 2001). This increased segregation of ON and OFF sub-regions in both areas could be inherited from PMLS, as the latter sends driver inputs to the LP-pulvinar (Huppé-Gourgue *et al.*, 2006b), and feedforward projections to AMLS cortex (Symonds & Rosenquist, 1984b; Grant & Hilgetag, 2005).

Similarly, LGN projections may explain the residual complex motion selectivity observed in the present study for two reasons. 1- LGN neurons have been shown to acquire non-linear response characteristics (Tumosa *et al.*, 1989) following VC lesions, which may partially compensate for the removed cortex. 2- Although area 17 neurons, which receive their major excitatory input from the LGN, do not signal complex RDK direction (Dumbrava *et al.*, 2001; Villeneuve *et al.*, 2006a), PMLS neurons could use this input to create direction selectivity *de novo*. Work by Thiele *et al.* (2004), suggests that the initial part of the directional response in MT (a possible homolog of PMLS) is attributable to intra-cortical

inhibitory processes which tune non-direction selective inputs. Moreover, response timing is not compatible with an initial PMLS response driven by area 17 neurons (Dinse & Kruger, 1994; Katsuyama *et al.*, 1996; Ouellette & Casanova, 2006b). An initial LGN based response of PMLS neurons may lead to directional responses via intra-cortical processes. It seems reasonable that inhibitory processing, as proposed by Thiele *et al.* (2004), could occur as Huxlin and Pasternak (2001) have demonstrated that GABAergic neurons are maintained in PMLS following a VC lesion (lesions in adults). Thus even in normal animals, the initial PMLS response may be inherited from the LGN (Figure 6Ba). Furthermore, a lesion of the LGN subsequent to a neonatal VC lesion temporarily eliminates orienting behavior in cats (Payne, 2004), arguing for the importance of geniculo-cortical pathways after cortical lesions.

It could be argued however, that if the LGN were responsible for the residual selectivity in PMLS, the receptive fields of the latter should be smaller than that observed in normals. This need not be the case for two reasons. Firstly, following lesions of VC the remaining neurons in the LGN have larger than average receptive fields (Murphy & Kalil, 1979; Tumosa *et al.*, 1989). Secondly, the size of receptive fields in PMLS have been shown to be independent of their input (Illig *et al.*, 2000), which suggests that large receptive fields are an intrinsic property of PMLS neurons.

The above argument for LGN input to PMLS has focused on the initial response. The subsequent direction selective response in PMLS may remain dependent upon the LGN, but may also use retino-thalamo-cortical (implicating

the LP-pulvinar complex) and/or tecto-thalamo-cortical input. This possibility does not require the assumption of any supplemental novel intra-cortical computations. Anatomically, the known reorganization of the visual system could permit such pathways to contribute to spared response properties observed in PMLS. In normal animals, PMLS neurons receive projections from the LP-pulvinar (Figure 6Bb,c&d: Updyke, 1981; Tong *et al.*, 1982), and this input increases following a VC lesion (Figure 6Ab,c&d: Labar *et al.*, 1981; Tong *et al.*, 1984; Payne *et al.*, 1993; but see Boire *et al.*, 2004 who have shown that retino-LP-pulvinar projections may be present even in normals). Although less conclusive, the results of physiological studies also suggest that information passing via the LP-pulvinar is involved in PMLS responses. For example, complex RDK selectivity is present in the LP-pulvinar of normal animals (Dumbrava *et al.*, 2001; Villeneuve *et al.*, 2006a). While this has yet to be assessed in early VC lesioned animals, encoding of simple motion is preserved (Desautels & Casanova, 2001) in the LP-pulvinar following such a lesion. Destruction of the tectum changes the response properties of neurons in PMLS cortex (Smith & Spear, 1979), specifically there is an increased responsiveness to stationary and slowly moving stimuli which does not occur for stimuli moving at higher velocities. Taken together these data suggest that past the initial response, residual direction selectivity in PMLS cortex may be partially attributable to an extra-geniculate thalamo-cortical pathway involving the LP-pulvinar complex. It remains to be determined whether the input to this thalamo-cortical route is preponderantly a retinal and/or retino-tectal in nature.

Regardless, the mechanisms necessary for motion processing in lesioned animals may already be present in normal animals (Figure 6B).

#### Role of feedback connections

It seems unlikely that feedback connections could, on their own, evoke robust responses in PMLS due to their multisynaptic nature. However, they could account for the residual direction selectivity in PMLS by imposing a directional map in the absence of highly organized VC input. The importance of feedback connections from PMLS for the emergence of direction selectivity maps in areas 17 and 18 has been previously demonstrated (Galuske *et al.*, 2002; Shen *et al.*, 2006b), however both areas remain visually responsive despite the loss of direction selectivity. Similarly, the direction selective maps in PMLS may arise from feedback projections from higher-order areas (Figure 6Ae) that are not as dependent upon VC input. For example, the tecto-thalamo-cortical route to the lateral bank of the posterior lateral suprasylvian sulcus (PLLS: Naito & Kawamura, 1982) could impose direction selectivity to residual responses in PMLS via feedback connections (Grant & Hilgetag, 2005). Visual response latencies also suggest a role for feedback connections, as the profile of onset latencies in PMLS following a lesion bear a greater resemblance to those seen in AMLS and AEV than in normal PMLS (Ouellette & Casanova, 2006b).

### Comparison with primate

A direct comparison of the present data with previous work in the primate is difficult due to the paucity of studies in which lesions were conducted at a young age in primates (Moore *et al.*, 1996). The few existing studies do suggest certain similarities with the literature in cats. Early lesions of VC lead to lesser behavioral deficits than when conducted in adulthood (Moore *et al.*, 1996) and there is selective survival of larger caliber LGN neurons than that found in normal animals (Hendrickson & Dineen, 1982). In the adult, the effect of elimination of VC input on MT neurons is controversial, with reports ranging from quasi-normal to non-existent visual responses (Rodman *et al.*, 1989, 1990; Girard *et al.*, 1992; Kaas & Krubitzer, 1992; Rosa *et al.*, 2000; Azzopardi *et al.*, 2003; Collins *et al.*, 2003). Interestingly, neither the VC nor the superior colliculus are necessary for direction selective responses in MT (Rodman *et al.*, 1990), while the elimination of both abolishes neuronal activity in MT. It is thus tempting to attribute residual responses in MT following VC lesions to a tecto-thalamo-cortical route. However a direct transfer of information from the superior colliculus to MT via the pulvinar must be discarded (Bender, 1983; Stepniewska *et al.*, 1999) since the main tecto-recipient portion of the pulvinar does not project to MT. Moreover, removal of VC silences the pulvinar (Bender, 1983) making it an unlikely candidate for the transmission of information from the tectum to cortex in primates. Alternatively, a direct projection from the LGN to MT is scarce to non-existent (Benevento & Yoshida, 1981; Fries, 1981;

Benevento & Standage, 1982; Sorenson & Rodman, 1999; Stepniewska *et al.*, 1999), and hence unlikely to explain residual responsiveness. The most likely explanation is that connections from other cortical areas which receive input from the tecto-recipient koniocellular layers of the LGN are responsible for the observed responsiveness in MT (Stepniewska *et al.*, 1999). Supporting this, deactivation of the LGN eliminates responses in MT (Maunsell *et al.*, 1990), an effect that cannot be attributed solely to the silencing of VC (see above). Hence, feedforward and feedback projections between cortical areas may play an instrumental role in residual responses in MT.

#### Implications for motion processing

Multi-stage models of motion processing have proposed an initial analysis of local motion cues and a subsequent stage that uses the extracted information to detect the real motion of a stimulus (Adelson & Bergen, 1985; Nowlan & Sejnowski, 1995). The first stage has usually been attributed to primary visual cortex and the second to MT or PMLS in the primate and cat respectively. The reduction in the direction selectivity of neurons in the present study (i.e. decreased mean DI) suggests that the removal of a preliminary stage does indeed hinder motion processing in PMLS cortex. On the other hand, the mere presence of residual direction selectivity to complex stimuli in PMLS suggests that the first stage is not an absolute necessity. The normal visual system probably operates according to the principles of multi-stage models, while this is not the only functionally viable organisational principle for motion processing.



Similar to what was proposed by Illig *et al.* (2000) for receptive field size, motion selective responses observed in PMLS may be relatively independent of the afferents giving rise to them.

Within the framework of PMLS neurons receiving inputs from a relatively fixed area of the visual field regardless of the origin of inputs (Illig *et al.*, 2000), the large receptive fields in PMLS would remain ideally suited to extract the motion cues even from complex motion stimuli. A simple Reichardt type model (Reichardt, 1961b) may be sufficient to explain the residual direction selectivity in PMLS based on LGN inputs. This less efficient form of motion analysis provided by a Reichardt model may partially explain the decrease in direction selectivity (i.e. DI) of PMLS neurons. A Reichardt type model was created to determine whether such a mechanism could explain the observed direction selectivity. The direction and velocity tuning curves presented in Figure 7 (panels A&B) clearly show that such a model is capable of extracting directional information, suggesting that PMLS neurons could use LGN input to extract complex RDK direction.

Alternatively, the first stage analysis may simply be taken over by another region. Note that this first stage analysis may partially be taken over by the LGN itself, as some LGN neurons take on non-linear response properties following VC lesions (Tumosa *et al.*, 1989). A study of PMLS cortex in VC lesioned animals during deactivation of the LGN would be necessary to determine which of these two possibilities is correct.

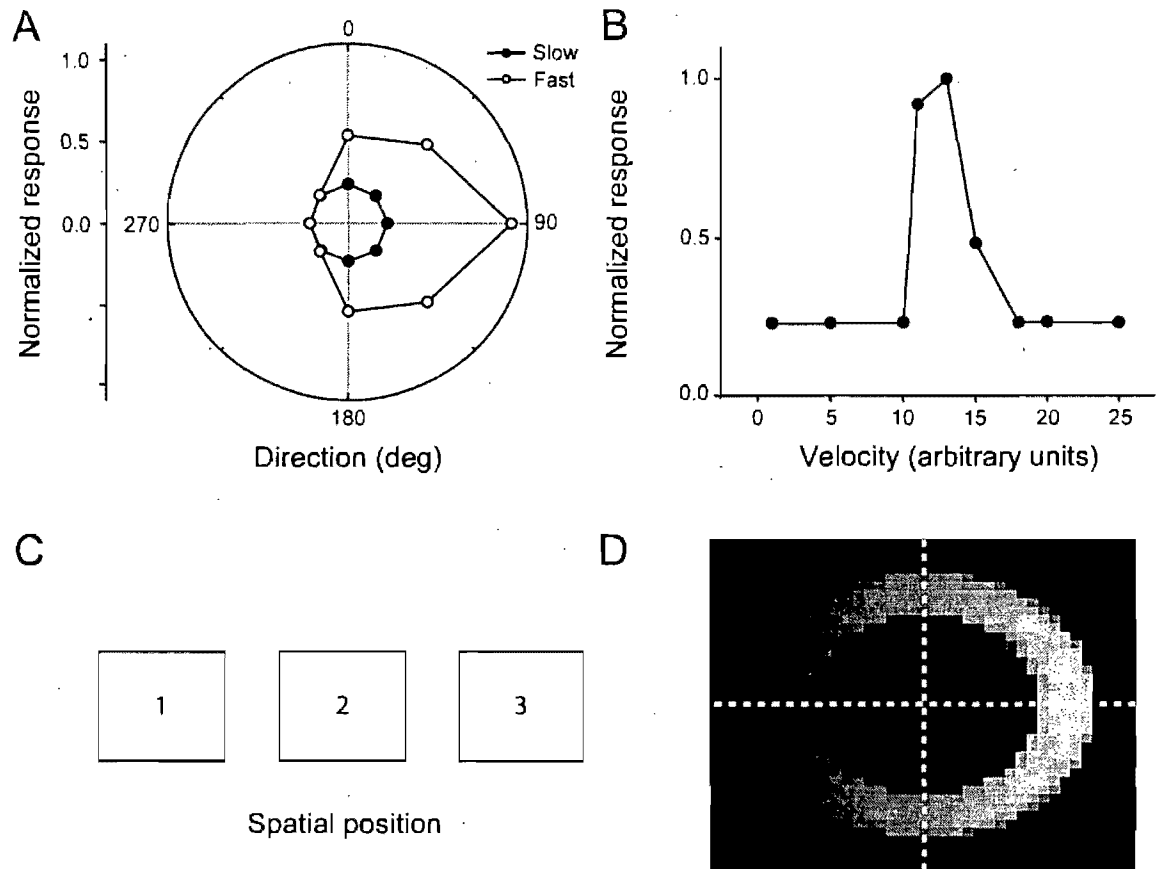


**Figure 7**

Direction (A) and velocity (B) selectivity of the Reichardt model. The model consisted of inputs which mimicked ON and OFF LGN responses to complex RDKs. A frame by frame 2-D cross-correlation of the image was then carried out. Such a model would produce approximately equal output values regardless of direction or velocity. In order to impose selectivity on the model, certain regions of the temporally summed cross-correlogram were filtered. This is computationally equivalent to giving greater synaptic weight to certain spatial shift amplitudes (i.e. a displacement 1-2 versus 1-3 in panel C) and directions (i.e. 1-3 versus 3-1). The imposed filter can be seen in panel D. It is composed of an annulus whose intensity has a Gaussian distribution along radial lines extending from the center, multiplied by a uni-dimensional exponentially increasing function. The position of the peak of the Gaussian equals the preferred spatial shift (i.e. velocity, if interframe interval is kept constant), while velocity bandwidth increases with the width of the Gaussian. In other words, if the filter were a single central point, the neuron would respond maximally to static stimuli. As the annulus moves away from the center, the preferred velocity increases proportionally. The exponent of the uni-dimensional function controls the direction selectivity, while the orientation of the latter function determines the preferred direction of the neuron.

## Conclusions

The present data demonstrates that complex motion selectivity is still present, albeit reduced, among PMLS neurons following neonatal lesions of VC. Previously observed increases in direction discrimination (Pasternak *et al.*, 1995) are not likely attributable to changes in response properties in PMLS cortex. This improvement in discrimination likely rest on changes higher up in the cortical hierarchy. Although the data do not offer a definitive answer, the presence of complex RDK selectivity supports the role of both geniculo-cortical and extra-geniculate thalamo-cortical pathways in maintaining near normal response properties in PMLS cortex, coupled with intracortical processing.

## Acknowledgements

The authors wish to thank the two anonymous reviewers for the numerous constructive comments. This work was supported by a CIHR grant to C.C. and part of C.C.'s salary was provided by FRSQ (chercheur National). B.G.O. was supported by FRSQ and NSERC scholarships.

## References

- ADELSON, E. H. & BERGEN, J. R. (1985). Spatiotemporal energy models for the perception of motion. *J Opt Soc Am A* **2**, 284-299.
- AZZOPARDI, P., FALLAH, M., GROSS, C. G. & RODMAN, H. R. (2003). Response latencies of neurons in visual areas MT and MST of monkeys with striate cortex lesions. *Neuropsychologia* **41**, 1738-1756.
- BENDER, D. B. (1983). Visual activation of neurons in the primate pulvinar depends on cortex but not colliculus. *Brain Res* **279**, 258-261.
- BENEVENTO, L. A. & STANDAGE, G. P. (1982). Demonstration of lack of dorsal lateral geniculate nucleus input to extrastriate areas MT and visual 2 in the macaque monkey. *Brain Res* **252**, 161-166.
- BENEVENTO, L. A. & YOSHIDA, K. (1981). The afferent and efferent organization of the lateral geniculo-prestriate pathways in the macaque monkey. *J Comp Neurol* **203**, 455-474.
- BOIRE, D., MATTEAU, I., CASANOVA, C. & PTITO, M. (2004). Retinal projections to the lateral posterior-pulvinar complex in intact and early visual cortex lesioned cats. *Exp Brain Res* **159**, 185-196.
- COLLINS, C. E., LYON, D. C. & KAAS, J. H. (2003). Responses of neurons in the middle temporal visual area after long-standing lesions of the primary visual cortex in adult new world monkeys. *J Neurosci* **23**, 2251-2264.
- CORNWELL, P. & PAYNE, B. (1989). Visual discrimination by cats given lesions of visual cortex in one or two stages in infancy or in one stage in adulthood. *Behav Neurosci* **103**, 1191-1199.
- DESAUTELS, A. & CASANOVA, C. (2001). Response properties in the pulvinar complex after neonatal ablation of the primary visual cortex. *Prog Brain Res* **134**, 83-95.
- DINSE, H. R. & KRUGER, K. (1994). The timing of processing along the visual pathway in the cat. *Neuroreport* **5**, 893-897.
- DUMBRAVA, D., FAUBERT, J. & CASANOVA, C. (2001). Global motion integration in the cat's lateral posterior-pulvinar complex. *Eur J Neurosci* **13**, 2218-2226.
- FRIES, W. (1981). The projection from the lateral geniculate nucleus to the prestriate cortex of the macaque monkey. *Proc R Soc Lond B Biol Sci* **213**, 73-86.

- GALUSKE, R. A., SCHMIDT, K. E., GOEBEL, R., LOMBER, S. G. & PAYNE, B. R. (2002). The role of feedback in shaping neural representations in cat visual cortex. *Proc Natl Acad Sci U S A* **99**, 17083-17088.
- GIRARD, P., SALIN, P. A. & BULLIER, J. (1992). Response selectivity of neurons in area MT of the macaque monkey during reversible inactivation of area V1. *J Neurophysiol* **67**, 1437-1446.
- GRANT, S. & HILGETAG, C. C. (2005). Graded classes of cortical connections: quantitative analyses of laminar-projections to motion areas of cat extrastriate cortex. *Eur J Neurosci* **22**, 681-696.
- GUIDO, W., SPEAR, P. D. & TONG, L. (1990a). Functional compensation in the lateral suprasylvian visual area following bilateral visual cortex damage in kittens. *Exp Brain Res* **83**, 219-224.
- GUIDO, W., SPEAR, P. D. & TONG, L. (1992). How complete is physiological compensation in extrastriate cortex after visual cortex damage in kittens? *Exp Brain Res* **91**, 455-466.
- GUIDO, W., TONG, L. & SPEAR, P. D. (1990b). Afferent bases of spatial- and temporal-frequency processing by neurons in the cat's posteromedial lateral suprasylvian cortex: effects of removing areas 17, 18, and 19. *J Neurophysiol* **64**, 1636-1651.
- HENDRICKSON, A. & DINEEN, J. T. (1982). Hypertrophy of neurons in dorsal lateral geniculate nucleus following striate cortex lesions in infant monkeys. *Neurosci Lett* **30**, 217-222.
- HUPPÉ-GOURGUE, F., BICKFORD, M. E., BOIRE, D., PTITO, M. & CASANOVA, C. (2006). Distribution, morphology and synaptic targets of corticothalamic terminals in the cat lateral posterior-pulvinar complex that originates from the posteromedial lateral suprasylvian cortex. *J Comp Neurol* **45**, 137-145.
- HUXLIN, K. R. & PASTERNAK, T. (2001). Long-term neurochemical changes after visual cortical lesions in the adult cat. *J Comp Neurol* **429**, 221-241.
- ILLIG, K. R., DANILOV, Y. P., AHMAD, A., KIM, C. B. & SPEAR, P. D. (2000). Functional plasticity in extrastriate visual cortex following neonatal visual cortex damage and monocular enucleation. *Brain Res* **882**, 241-250.
- KAAS, J. H. & KRUBITZER, L. A. (1992). Area 17 lesions deactivate area MT in owl monkeys. *Vis Neurosci* **9**, 399-407.
- KALIL, R. E., TONG, L. L. & SPEAR, P. D. (1991). Thalamic projections to the lateral suprasylvian visual area in cats with neonatal or adult visual cortex damage. *J Comp Neurol* **314**, 512-525.

- KATSUYAMA, N., TSUMOTO, T., SATO, H., FUKUDA, M. & HATA, Y. (1996). Lateral suprasylvian visual cortex is activated earlier than or synchronously with primary visual cortex in the cat. *Neurosci Res* **24**, 431-435.
- KIM, J. N., MULLIGAN, K. & SHERK, H. (1997). Simulated optic flow and extrastriate cortex. I. Optic flow versus texture. *J Neurophysiol* **77**, 554-561.
- LABAR, D. R., BERMAN, N. E. & MURPHY, E. H. (1981). Short- and long-term effects of neonatal and adult visual cortex lesions on the retinal projection to the pulvinar in cats. *J Comp Neurol* **197**, 639-659.
- LONG, K. D., LOMBER, S. G. & PAYNE, B. R. (1996). Increased oxidative metabolism in middle suprasylvian cortex following removal of areas 17 and 18 from newborn cats. *Exp Brain Res* **110**, 335-346.
- MAJAJ, N., CARANDINI, M., SMITH, M. A. & MOVSHON, J. A. (1999). Local integration of features for the computation of pattern direction by neurons in macaque area MT. *Society for Neuroscience Abstracts* **25**, 674.
- MAUNSELL, J. H., NEALEY, T. A. & DEPRIEST, D. D. (1990). Magnocellular and parvocellular contributions to responses in the middle temporal visual area (MT) of the macaque monkey. *J Neurosci* **10**, 3323-3334.
- MOORE, T., RODMAN, H. R. & GROSS, C. G. (2001). Direction of motion discrimination after early lesions of striate cortex (V1) of the macaque monkey. *Proc Natl Acad Sci U S A* **98**, 325-330.
- MOORE, T., RODMAN, H. R., REPP, A. B., GROSS, C. G. & MEZRICH, R. S. (1996). Greater residual vision in monkeys after striate cortex damage in infancy. *J Neurophysiol* **76**, 3928-3933.
- MOVSHON, J. A., ADELSON, E. H., GIZZI, M. S. & NEWSOME, W. T. (1986). The analysis of moving visual patterns. In *Pattern recognition mechanisms*. ed. CHAGAS, C., GATTAS, R. & GROSS, C., pp. 148-164. Springer Verlag, New York.
- MURPHY, E. H. & KALIL, R. (1979). Functional organization of lateral geniculate cells following removal of visual cortex in the newborn kitten. *Science* **206**, 713-716.
- MURPHY, E. H., MIZE, R. R. & SCHECHTER, P. B. (1975). Visual discrimination following infant and adult ablation of cortical areas 17, 18, and 19 in the cat. *Exp Neurol* **49**, 386-405.
- NAITO, J. & KAWAMURA, K. (1982). Thalamocortical neurons projecting to the areas surrounding the anterior and middle suprasylvian sulci in the cat. A horseradish peroxidase study. *Exp Brain Res* **45**, 59-70.

- NOWLAN, S. J. & SEJNOWSKI, T. J. (1995). A selection model for motion processing in area MT of primates. *J Neurosci* **15**, 1195-1214.
- OUELLETTE, B. G. & CASANOVA, C. (2006). Overlapping visual response latency distributions in visual cortices and LP-pulvinar complex of the cat. *Exp Brain Res* **175**, 332-341.
- OUELLETTE, B. G., MINVILLE, K., FAUBERT, J. & CASANOVA, C. (2004). Simple and complex visual motion response properties in the anterior medial bank of the lateral suprasylvian cortex. *Neuroscience* **123**, 231-245.
- PALMER, L. A., ROSENQUIST, A. C. & TUSA, R. J. (1978). The retinotopic organization of lateral suprasylvian visual areas in the cat. *J Comp Neurol* **177**, 237-256.
- PASTERNAK, T., TOMPKINS, J. & OLSON, C. R. (1995). The role of striate cortex in visual function of the cat. *J Neurosci* **15**, 1940-1950.
- PAYNE, B. R. (2004). Neuroplasticity in the cat's visual system: test of the role of the expanded retino-geniculo-parietal pathway in behavioral sparing following early lesions of visual cortex. *Exp Brain Res* **155**, 69-80.
- PAYNE, B. R., FOLEY, H. A. & LOMBER, S. G. (1993). Visual cortex damage-induced growth of retinal axons into the lateral posterior nucleus of the cat. *Vis Neurosci* **10**, 747-752.
- PAYNE, B. R. & LOMBER, S. G. (1998). Neuroplasticity in the cat's visual system. *Exp Brain Res* **12**, 334-349.
- RAUSCHECKER, J. P. (1988). Visual function of the cat's LP/LS subsystem in global motion processing. *Prog Brain Res* **75**, 95-108.
- RAUSCHECKER, J. P., VON GRUNAU, M. W. & POULIN, C. (1987). Centrifugal organization of direction preferences in the cat's lateral suprasylvian visual cortex and its relation to flow field processing. *J Neurosci* **7**, 943-958.
- REICHARDT, W. (1961). Autocorrelation, a principle for the evaluation of sensory information by the central nervous system. In *Sensory Communication*. ed. ROSEMBLICH, W., pp. 303-317. MIT Press, New York.
- RODMAN, H. R., GROSS, C. G. & ALBRIGHT, T. D. (1989). Afferent basis of visual response properties in area MT of the macaque. I. Effects of striate cortex removal. *J Neurosci* **9**, 2033-2050.
- RODMAN, H. R., GROSS, C. G. & ALBRIGHT, T. D. (1990). Afferent basis of visual response properties in area MT of the macaque. II. Effects of superior colliculus removal. *J Neurosci* **10**, 1154-1164.



- ROSA, M. G., TWEEDALE, R. & ELSTON, G. N. (2000). Visual responses of neurons in the middle temporal area of new world monkeys after lesions of striate cortex. *J Neurosci* **20**, 5552-5563.
- RUDOLPH, K. K. & PASTERNAK, T. (1996). Lesions in cat lateral suprasylvian cortex affect the perception of complex motion. *Cereb Cortex* **6**, 814-822.
- SANDERSON, K. J. (1971). The projection of the visual field to the lateral geniculate and medial interlaminar nuclei in the cat. *J Comp Neurol* **143**, 101-108.
- SHEN, W., LIANG, Z., CHEN, X. & SHOU, T. (2006). Posteromedial lateral suprasylvian motion area modulates direction but not orientation preference in area 17 of cats. *Neuroscience* **142**, 905-916.
- SKOTTUN, B. C., GROSOF, D. H. & DE VALOIS, R. L. (1991). On the responses of simple and complex cells to random dot patterns. *Vision Res* **31**, 43-46.
- SMITH, D. C. & SPEAR, P. D. (1979). Effects of superior colliculus removal on receptive-field properties of neurons in lateral suprasylvian visual area of the cat. *J Neurophysiol* **42**, 57-75.
- SMITH, M. A., MAJAJ, N. J. & MOVSHON, J. A. (2005). Dynamics of motion signaling by neurons in macaque area MT. *Nat Neurosci* **8**, 220-228.
- SORENSEN, K. M. & RODMAN, H. R. (1999). A transient geniculo-extrastriate pathway in macaques? Implications for 'blindsight'. *Neuroreport* **10**, 3295-3299.
- SPEAR, P. D. (1988). Influence of areas 17, 18, and 19 on receptive-field properties of neurons in the cat's posteromedial lateral suprasylvian visual cortex. *Prog Brain Res* **75**, 197-210.
- SPEAR, P. D. (1995). Plasticity following neonatal visual cortex damage in cats. *Can J Physiol Pharmacol* **73**, 1389-1397.
- SPEAR, P. D. & BAUMANN, T. P. (1979). Effects of visual cortex removal on receptive-field properties of neurons in lateral suprasylvian visual area of the cat. *J Neurophysiol* **42**, 31-56.
- STEPNIEWSKA, I., QI, H. X. & KAAS, J. H. (1999). Do superior colliculus projection zones in the inferior pulvinar project to MT in primates? *Eur J Neurosci* **11**, 469-480.
- SYMONDS, L. L. & ROSENQUIST, A. C. (1984). Laminar origins of visual corticocortical connections in the cat. *J Comp Neurol* **229**, 39-47.
- THIELE, A., DISTLER, C., KORBMACHER, H. & HOFFMANN, K. P. (2004). Contribution of inhibitory mechanisms to direction selectivity and response

- normalization in macaque middle temporal area. *Proc Natl Acad Sci U S A* **101**, 9810-9815.
- TONG, L., KALIL, R. E. & SPEAR, P. D. (1982). Thalamic projections to visual areas of the middle suprasylvian sulcus in the cat. *J Comp Neurol* **212**, 103-117.
- TONG, L., KALIL, R. E. & SPEAR, P. D. (1984). Critical periods for functional and anatomical compensation in lateral suprasylvian visual area following removal of visual cortex in cats. *J Neurophysiol* **52**, 941-960.
- TONG, L., SPEAR, P. D. & KALIL, R. E. (1987). Effects of corpus callosum section on functional compensation in the posteromedial lateral suprasylvian visual area after early visual cortex damage in cats. *J Comp Neurol* **256**, 128-136.
- TONG, L. L., KALIL, R. E. & SPEAR, P. D. (1991). Development of the projections from the dorsal lateral geniculate nucleus to the lateral suprasylvian visual area of cortex in the cat. *J Comp Neurol* **314**, 526-533.
- TOYAMA, K., KOMATSU, Y., KASAI, H., FUJII, K. & UMETANI, K. (1985). Responsiveness of Clare-Bishop neurons to visual cues associated with motion of a visual stimulus in three-dimensional space. *Vision Res* **25**, 407-414.
- TUCKER, T. J., KLING, A. & SCHARLOCK, D. P. (1968). Sparring of photic frequency and brightness discriminations after striatectomy in neonatal cats. *J Neurophysiol* **31**, 818-832.
- TUMOSA, N., MCCALL, M. A., GUIDO, W. & SPEAR, P. D. (1989). Responses of lateral geniculate neurons that survive long-term visual cortex damage in kittens and adult cats. *J Neurosci* **9**, 280-298.
- UPDYKE, B. V. (1981). Projections from visual areas of the middle suprasylvian sulcus onto the lateral posterior complex and adjacent thalamic nuclei in cat. *J Comp Neurol* **201**, 477-506.
- VILLENEUVE, M. Y., PTITO, M. & CASANOVA, C. (2006). Global motion integration in the postero-medial part of the lateral suprasylvian cortex in the cat. *Exp Brain Res* **172**, 485-497.
- VON GRUNAU, M. & FROST, B. J. (1983). Double-opponent-process mechanism underlying RF-structure of directionally specific cells of cat lateral suprasylvian visual area. *Exp Brain Res* **49**, 84-92.
- WETZEL, A. B., THOMPSON, V. E., HOREL, J. A. & MEYER, P. M. (1965). Some consequences of perinatal lesions of the visual cortex in the cat. *Psychon Sci* **3**, 381-382.

Article 2

***Overlapping visual response latency distributions in visual cortices  
and LP-pulvinar complex of the cat.***

**Brian G. Ouellette<sup>1,2</sup>, Christian Casanova<sup>1,3</sup>**

<sup>1</sup> École d'optométrie, Université de Montréal

<sup>2</sup> Département de Psychologie, Université de Montréal

<sup>3</sup> Corresponding author

Springer and Experimental Brain Research, 175, 2006, 332-341, Ouellette,  
B.G., Casanova, C.; with kind permission from Springer Science and  
Business Media.

## Abstract

The visual system of the cat is considered to be organized in both a serial and parallel manner. Studies of visual onset latencies generally suggest that parallel processing occurs throughout the dorsal stream. These studies are at odds with the proposed hierarchies of visual areas based on termination patterns of cortico-cortical projections. In previous studies a variety of stimuli have been used to compute latencies, and this is problematic as latencies are known to depend on stimulus parameters. This could explain the discrepancy between latency and neuroanatomical based studies. Therefore, the first aim of the present study was to determine, whether latencies increased along the hierarchy of visual areas when the same stimuli are used. In addition, the effect of stimulus complexity was assessed. Visual onset latencies were calculated for area 17, PMLS, AMLS, AEV, and PMLS neurons following lesions of primary visual cortex. Latencies were also computed from neurons in the LP-pulvinar complex given the importance of this extrageniculate complex in cortical intercommunication. Latency distributions from all regions overlapped substantially, and no significant difference was present, regardless of the type of stimulus used. The onset latencies in the LP-pulvinar complex were comparable to those seen in cortical areas. The data suggest that the initial processing of information in the visual system is parallel, despite the presence of a neuroanatomical hierarchy. Simultaneous response onsets among cortical areas and the LP-pulvinar suggest that the latter is more than a simple relay station for information headed to cortex. The data are consistent with proposals of the LP-

pulvinar as a center for the integration and distribution of information from/to multiple cortical areas.

## Introduction

A large number of visual cortical areas have been identified in both cat and monkey. Despite known parallel processing pathways (Stone *et al.*, 1979; Lennie, 1980; Mishkin *et al.*, 1983), there is ample evidence that visual information is processed in a hierarchal manner across these areas. Neuroanatomical studies have revealed a repetitive axonal termination pattern between cortical areas (Rockland & Pandya, 1979; Symonds & Rosenquist, 1984b) that has allowed the establishment of hierarchical organizations of these visual areas (Maunsell & van Essen, 1983; Felleman & Van Essen, 1991; Scannell *et al.*, 1995; Scannell *et al.*, 1999; Hilgetag *et al.*, 2000b). Evidence of hierarchical processing also comes from single unit recordings, which revealed that the receptive field properties of neurons vary in a predictable manner along the hierarchy. For example, receptive field size gets progressively larger at increasing levels of the hierarchy (Lamme & Roelfsema, 2000; Bair & Movshon, 2004) and there is an increase in complex motion selectivity from lower to higher-order areas (Movshon *et al.*, 1986; Scannell *et al.*, 1996; Villeneuve *et al.*, 2006b).

Implicit in the proposed hierarchy model, is the notion that each subsequent level inherits processed visual information from lower areas and is involved in additional processing of its own. It follows that neuronal response latencies should increase at higher echelons of the visual system. A comparison of latency distributions in dorsal stream cortical areas reveals a substantial overlap in both monkey (Robinson & Rugg, 1988; Raiguel *et al.*, 1989; Nowak *et*

*al.*, 1995; Schmolesky *et al.*, 1998; Schroeder *et al.*, 1998; Lamme & Roelfsema, 2000; Bullier, 2001, 2004b) and cat (Dinse & Kruger, 1994; Bullier, 2004b), inconsistent with a strictly organized hierarchy. Moreover, based on the analysis of cross-correlograms it has been suggested that, in cats, some postero-medial lateral suprasylvian sulcus (PMLS) neurons may drive area 17 neurons (Katsuyama *et al.*, 1996). Thus there is an apparent contradiction between neuroanatomically based hierarchies and neurophysiological data.

This contradiction may be attributable to a limitation of previous work. Studies of response latencies have rarely involved more than two or three areas. To get a glimpse of the temporal order of visual information processing across the dorsal stream, latencies from different studies must be compared. Thus the data originates from different laboratories, each using a unique set of stimulus parameters. This is problematic as visual latencies are known to vary considerably with stimulus parameters (Creutzfeldt & Ito, 1968; Lennie, 1981). Furthermore, visual stimuli have generally been limited to flashes and static contrast gratings, which are not likely to evoke a strong response in areas known to be strongly motion sensitive such as area MT in primates and PMLS cortex in cats. Until latencies are calculated from responses to motion stimuli, it will be difficult to determine if neuroanatomical data and visual latencies truly are contradictory.

The above mentioned latency studies have all focused on the timing of information processing across cortical visual areas. Although informative, these studies have neglected the extra-geniculate thalamus. Theoretical papers have emphasized the functional importance of reciprocal connections between the



cortex and extra-geniculate thalamus (Mumford, 1992; Miller, 1996; Sherman & Guillery, 1998). Within the context of motion processing mentioned above, the cat's thalamic lateral posterior-pulvinar nucleus (LP-pulvinar complex) has been shown to contribute to complex motion analysis (Merabet *et al.*, 1998; Dumbrava *et al.*, 2001). Yet how response onsets in extra-geniculate nuclei compare to reciprocally connected cortical areas is unknown. Estimating the hierarchical position of a region that does not have the prototypical laminar organization found in cortex is difficult based solely on neuroanatomical data (Scannell & Young, 1993).

The present study had the following goals; 1- to ascertain whether onset latencies across visual areas reflect the anatomically based hierarchy when measured under identical physical conditions (luminance and contrast) using motion stimuli. 2- to determine if, within a single visual area, complex motion stimuli would evoke responses with longer latencies than simple stimuli, reflecting a greater level of processing. 3- to seek where the LP-pulvinar complex is situated, according to onset latencies, as compared to cortical areas. Parts of these findings have been presented elsewhere in abstract form (Ouellette *et al.*, 2004a).

## Methods

### Single unit recordings

Single unit recording data was obtained from previously published data in our laboratory (Dumbrava *et al.*, 2001; Ouellette *et al.*, 2002; Zabouri *et al.*, 2003; Ouellette *et al.*, 2004b; Villeneuve *et al.*, 2006b). Methodological details concerning the recordings can be found in the above cited work.

### Stimuli

Visual onset latencies were calculated at each cells preferred direction for four different motion stimuli, namely drifting sinewave gratings, plaid patterns, simple and complex random dot kinematograms (RDKs). Drifting sinewave gratings were presented with optimal (eliciting a maximal response) spatial and temporal frequencies, determined for each cell. Plaid patterns consisted of two sinewave gratings differing only in orientation ( $120^\circ$  separation), the total contrast (60%) was equivalent to that of the lone sinewave grating. Simple RDKs consisted of a rigidly translating field of white dots on a black background (100% contrast). Complex RDKs differed in that each dot was displaced only once before being randomly repositioned. For stimulus details see Dumbrava *et al.* (2001). For both simple and complex RDKs, the latencies were computed from test in which the optimal dot speed and density were used. Stimuli were presented at least four times, each presentation lasting 4 seconds.

A pre-stimulus blank screen of equal mean luminance to that of the stimulus was presented for 1 second. Although similar to the spontaneous activity (SA) condition (blank screen lasting 4 seconds, as per the stimuli), the pre-stimulus blank was separate, and its level of activity was not used for analysis purposes. The pre-stimulus blank avoided an initial onset response evoked by a rapid change in luminance upon stimulus appearance.

### Visual onset latencies

Visual onset latencies were calculated using the cumulative sum technique (Ellaway, 1978; Vogels & Orban, 1990; Raiguel *et al.*, 1999). As mentioned above, analyses were carried out on the preferred direction (Figure 1A). The peri-stimulus time histograms (PSTH) for the preferred direction and that for the SA were calculated over the four second trials with a bin width of 1ms (Figure 1B). Although previous studies using the cumulative sum technique have employed longer bin widths (10-25ms), the choice of 1ms allowed for a greater temporal resolution. This choice is even more appropriate given that Raiguel *et al.* (1999) have demonstrated that varying bin width does not greatly modify the reliability of the computed values. The standard error of the mean for the SA condition was then calculated. Thereafter, the temporally corresponding bin of the SA condition PSTH (bottom panel) was subtracted from that of the preferred direction (top panel). At each millisecond post-stimulus onset, a cumulative sum of the above mentioned subtraction was then calculated (Figure 1C<sub>1</sub>). Positive and negative values indicate that the preferred direction stimulus

evoked respectively more or less of a response than the SA condition. The time at which the cumulative sum went above a preset threshold was considered to be the onset latency (Figure 1C<sub>2</sub>). The threshold was defined as 1 standard error of the mean above the SA condition. This value is below that chosen by previous authors (Vogels & Orban, 1990, 1994; Raiguel *et al.*, 1999) as fewer repetitions were carried out in the current study, increasing measures of variability. Thus using the same threshold as previous authors would have led to unrealistically long latencies. Preliminary analysis using a threshold of 2 standard deviations indeed revealed late response onsets. Moreover, absolute latency values should not be compared as they are known to be dependent upon stimulus parameters (Lennie, 1981), rather the difference in latencies between visual areas should be considered (Raiguel *et al.*, 1989).

Latencies were calculated for 28 neurons in area 17, 51 in the PMLS cortex of normal animals, 34 in the anteromedial lateral suprasylvian cortex (AMLS), 43 in the anterior ectosylvian visual cortex (AEV), and 39 in the lateral subdivision of the LP-pulvinar complex (LPI). In addition, latencies for 40 PMLS neurons in animals with a neonatal lesion of primary visual cortex (PMLS-lesion) were computed. Note that as almost all area 17 neurons were not direction selective to complex RDKs (Dumbrava *et al.*, 2001; Villeneuve *et al.*, 2006b), these latencies were calculated on the direction that evoked the strongest response (as if they were direction selective). Visual onset latencies were not normally distributed, comparisons were thus carried out using Mann-Whitney and Kruskal-Wallis tests and a 0.05 significance level was used.

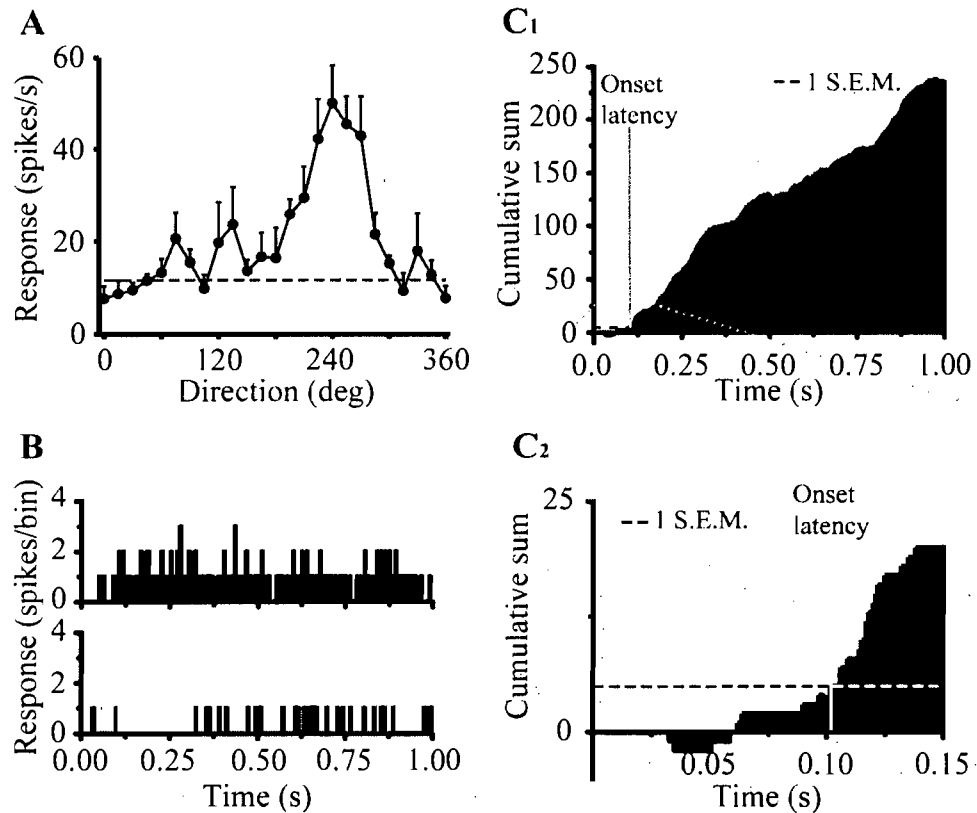


**Figure 1**

Cumulative sum technique. **A)** An example direction tuning curve. Latencies were calculated using the direction evoking the highest response rate, regardless of stimulus type. The dashed line is spontaneous activity. **B)** The PSTH over a one second period for the preferred direction (top) and spontaneous activity (bottom) are shown. The bin width is of 1 ms. **C<sub>1</sub>)** The spontaneous activity PSTH was subtracted from that of the preferred direction. A cumulative sum of the result was then calculated. The shaded grey box is expanded in C<sub>2</sub>, the white dashed line is the threshold. **C<sub>2</sub>)** Expanded view of C<sub>1</sub>. The dashed line is the threshold for calculating latency, the point at which the cumulative sum crosses this line corresponds to the onset latency.

## Results

### Differences across areas

Latencies were compared for all regions, separated according to the type of stimulus presented (Figure 2A-D). The general result is that response onset latency was similar across regions. This is reflected in the considerable degree of overlap between the distributions in panels A-C (except PMLS-lesion data in panel C, see the appropriate section below). This overlap is even present between area 17 and AEV data, the two areas which would be expected to have the greatest difference in latencies based on the neuroanatomical hierarchy. The similarity between the data from these two regions is present regardless of the stimulus under study. Visually, there does appear to be a difference in panel D, where complex RDKs evoke longer latencies in AMLS and AEV cortex. However, both of these regions only distinguish themselves from the other areas once 70-75% (approximately) of neurons have already responded. When data was collapsed over stimulus type, no significant difference in latency was present across regions ( $H = 5.366$ ,  $p = 0.252$ ). Note that this test was carried out without the PMLS-lesion data, as were subsequent test. Measures of central tendency are given in Table 1. To aid in the visualisation of the quasi-simultaneous responses across areas, the values from Table 1 are reproduced in Figure 3A as histograms.

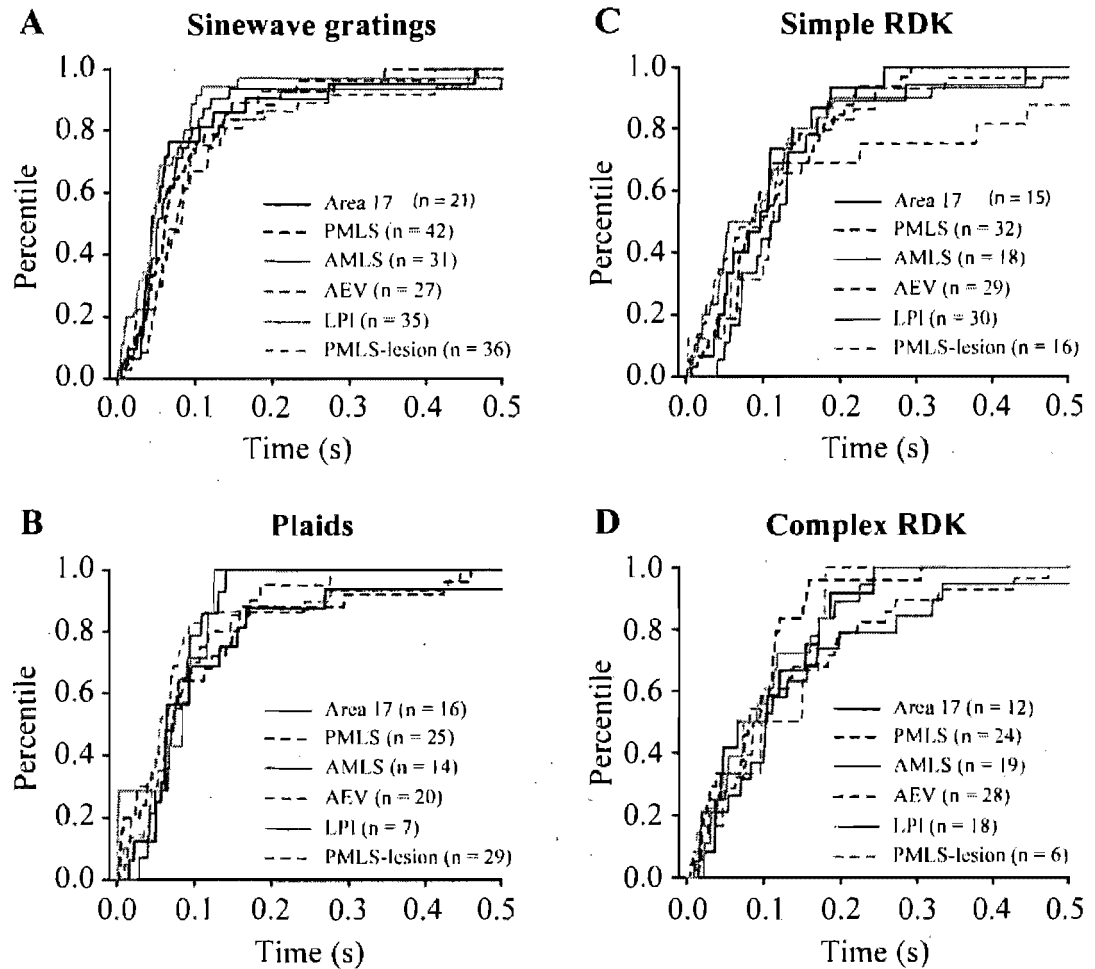


**Figure 2**

Latencies in different areas, separated according to stimulus. **A-D)** Shown is the cumulative percentage of latencies. For all types of stimuli, there is a clear overlap of onset latencies in different areas until approximately 70% of neurons have responded, at which point a slight distinction can be observed with RDKs (panels C and D).

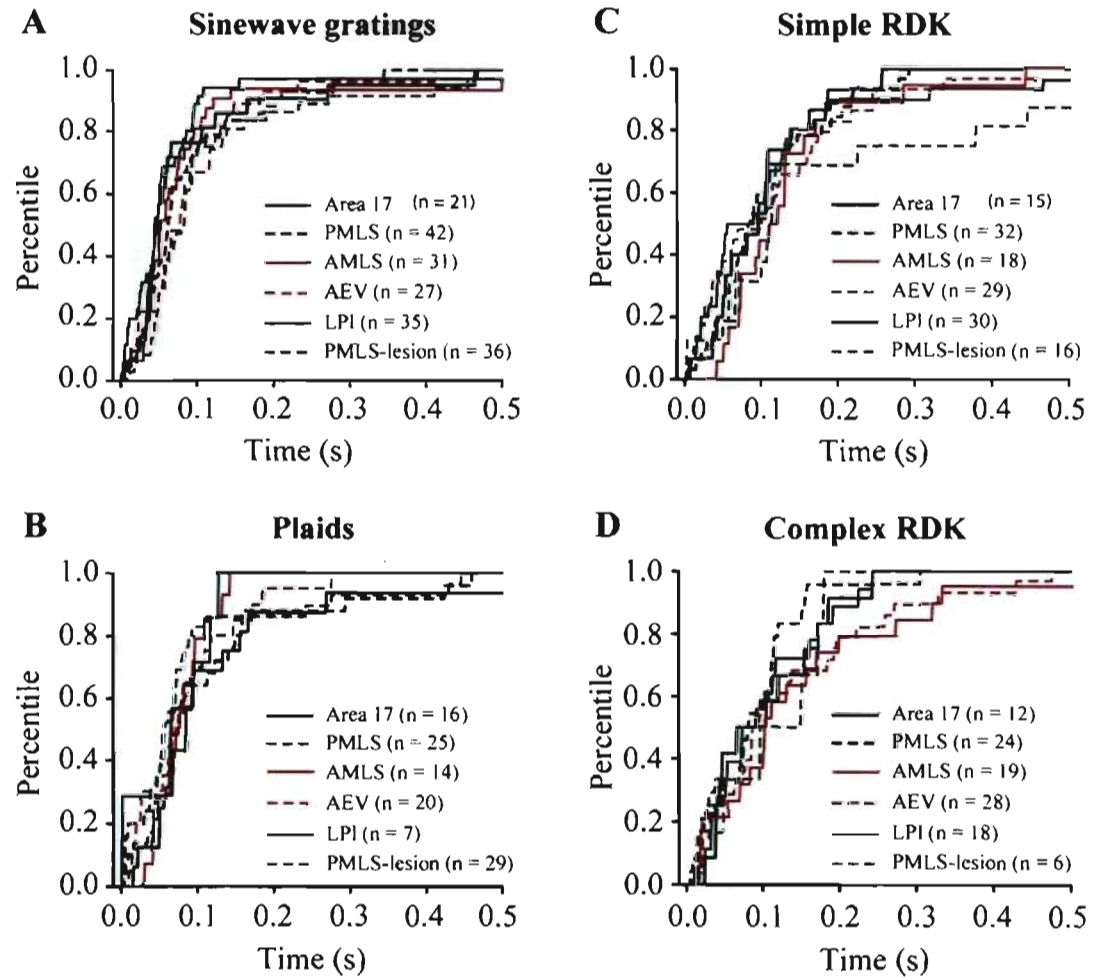


**Figure 2**

Latencies in different areas, separated according to stimulus. **A-D)** Shown is the cumulative percentage of latencies. For all types of stimuli, there is a clear overlap of onset latencies in different areas until approximately 70% of neurons have responded, at which point a slight distinction can be observed with RDKs (panels C and D).



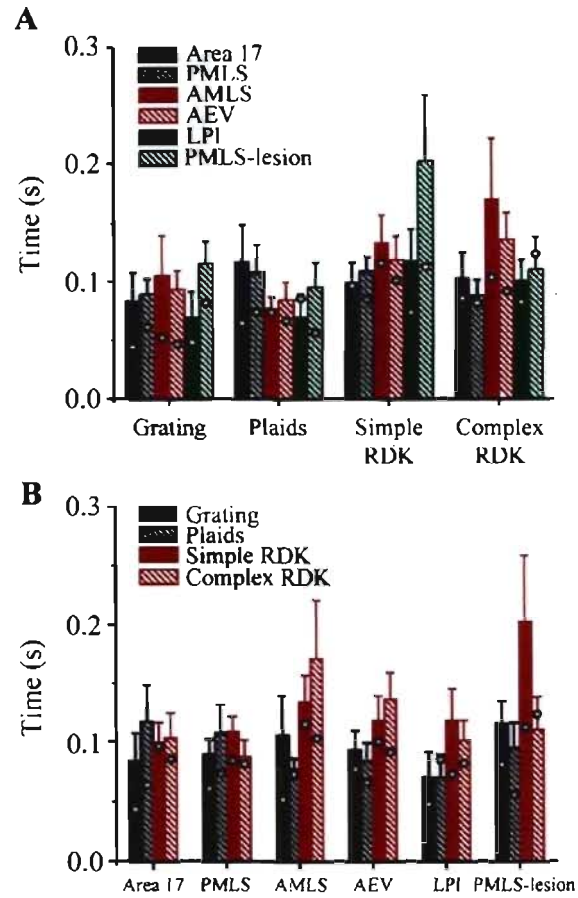


**Figure 3**

Mean and median latencies; in A) data are grouped according to stimulus condition for different areas, in B) they are grouped according to area for all stimulus conditions. Each bar shows mean values ( $\pm$  S.D.) that are presented in Table 1. Similarly each empty circle corresponds to median latencies given in Table 1.

Table 1

## Measures of central tendency

Region	Grating	Plaids	Simple RDK	Complex RDK
Area 17				
Mean	0.084	0.117	0.099	0.103
(± S.E.M.)	(0.023)	(0.031)	(0.017)	(0.021)
Median	0.044	0.064	0.096	0.085
N	21	16	15	12
PMLS				
Mean	0.089	0.107	0.108	0.087
(± S.E.M.)	(0.013)	(0.024)	(0.013)	(0.014)
Median	0.061	0.073	0.084	0.081
N	42	25	32	24
PMLS-lesion				
Mean	0.115	0.095	0.202	0.110
(± S.E.M.)	(0.019)	(0.021)	(0.056)	(0.028)
Median	0.081	0.056	0.112	0.123
n	36	29	16	6
AMLS				
Mean	0.105	0.077	0.134	0.171
(± S.E.M.)	(0.034)	(0.009)	(0.023)	(0.050)
Median	0.052	0.073	0.115	0.103
N	31	14	18	19
AEV				
Mean	0.093	0.084	0.118	0.136
(± S.E.M.)	(0.016)	(0.015)	(0.021)	(0.023)
Median	0.077	0.066	0.100	0.091
N	27	20	29	28
LP-Pulvinar				
Mean	0.070	0.070	0.118	0.101
(± S.E.M.)	(0.021)	(0.019)	(0.027)	(0.017)
Median	0.048	0.085	0.073	0.082
N	35	7	30	18

### Differences between stimuli

Onset latencies to different stimuli, regardless of region, are presented in Figure 4. The type of stimulus had a clear effect on the latency of the neuronal response, as revealed by a statistically significant difference ( $H = 19.233$ ,  $p < 0.001$ ). The neuronal responses can be divided into three distinct groups based on latencies; short latency responses to gratings, medium latencies to plaids and longer latencies to dot based stimuli. Post hoc analyses partially confirmed this observation, response latencies were shorter for gratings than simple ( $U = 7098$ ,  $p < 0.001$ ) and complex RDKs ( $U = 5946$ ,  $p = 0.001$ ) but not shorter than those of plaids ( $U = 5470.5$ ,  $p = 0.067$ ). Plaids did not evoke significantly shorter latencies than simple ( $U = 4349.5$ ,  $p = 0.079$ ) or complex RDKs ( $U = 3517$ ,  $p = 0.080$ ). Although the main effect of plaids versus RDK based stimuli was not significant, we took the liberty to test this separately for each region (see below). This seems justified as the very notion of a hierarchy suggests that different regions may analyse information differently, thus averaging data over regions may mask the effect of stimulus.

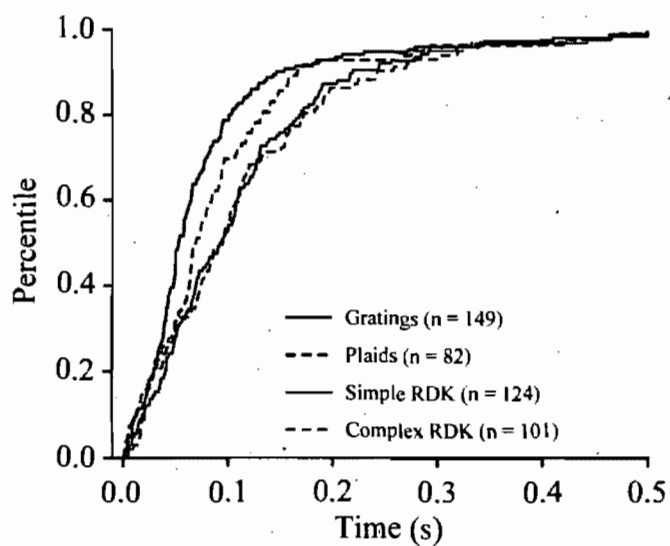


**Figure 4**

The cumulative percentage of latencies, separated according to stimulus regardless of area. The type of stimulus has a clear effect of the onset latency. The data for the PMLS-lesion neurons are not included in this figure.

When the region was taken into account, the neuronal response was still shorter for gratings than for RDK based stimuli, but this was not the case in all regions (Figure 5A-F). Upon visual inspection, three profiles can be seen in Figure 5. In area 17 and the LPI, gratings appear to evoke somewhat shorter responses than the three other stimuli. In the LPI, this was supported by a significant difference between gratings and simple ( $U = 360.5$ ,  $p = 0.030$ ) and complex RDKs ( $U = 187.5$ ,  $p = 0.017$ ). Other comparisons between gratings and RDKs were not significant in both area 17 and LPI. The second set of response profiles, were found in AMLS and AEV cortex, were both gratings and plaids appeared to have shorter latencies than RDKs. Significantly shorter latencies were observed in AMLS for gratings as compared to simple ( $U = 127.5$ ,  $p = 0.002$ ) and complex RDKs ( $U = 189.5$ ,  $p = 0.036$ ), plaids were also found to have shorter latencies than simple ( $U = 69.5$ ,  $p = 0.030$ ) but not complex RDKs ( $U = 91$ ,  $p = 0.126$ ). The same comparisons conducted in AEV revealed no significant differences. This may be due to the fact that the curves for grating and dot based stimuli diverge later than those seen in AMLS cortex. The final response profile was observed in PMLS cortex, where latency distributions to all stimuli appear to overlap throughout the time course of the response. However, statistical analysis revealed that gratings had shorter latencies than simple RDKs ( $U = 492.5$ ,  $p = 0.050$ ). Although slight, this difference in the latency distributions is consistent throughout the range of response onsets. In other comparisons, significant differences were not observed. Measures of central tendency are given in Table 1. These values have been reproduced in Figure 3B

as histograms to aid in distinguishing differential stimulus dependent response latency patterns among areas.

#### Effect of primary visual cortex lesions

Motion processing in PMLS neurons has been examined following neonatal lesions of primary visual cortex (ex: Tong *et al.*, 1984; Guido *et al.*, 1990a, 1992). These studies demonstrated that direction selectivity was relatively intact following such a lesion. One element that has not been considered is the response latency of PMLS neurons.

The latencies following lesions can be seen in panel F of Figure 5. The profiles of the curves bear more of a resemblance to AMLS and AEV rather than normal PMLS cortex. Specifically, a distinction between grating based and dot based stimuli seems present. This dichotomy was limited to latencies to plaid patterns, which occurred earlier than to simple RDKs ( $U = 138$ ,  $p = 0.026$ ). Other comparisons between the two stimulus types were not significant.

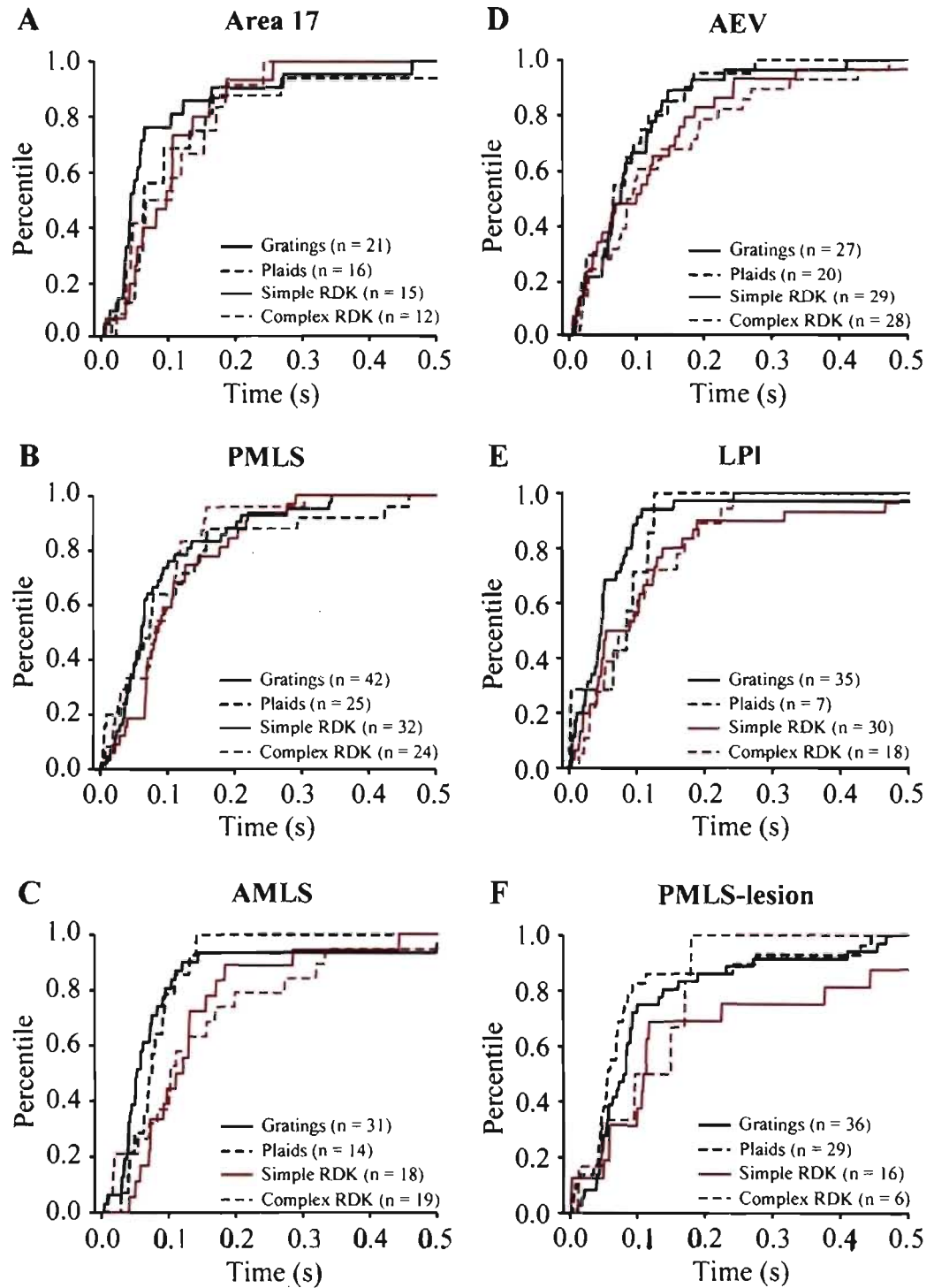


**Figure 5**

Latencies obtained when different stimuli are presented, separated according to area. **A-D)** Shown is the cumulative percentage of latencies.

Despite a lesion to primary visual cortex, PMLS-lesion neurons did not have significantly different onset latencies as compared to PMLS neurons in a normal cortex (Figure 2A-D). Although simple RDKs appear to have longer onset latencies in PMLS-lesion than normal PMLS (panel C), this was not confirmed statistically ( $U = 211$ ,  $p = 0.325$ ). The lack of significance may be explained by the fact that the curves begin to deviate only once approximately 70% of neurons have already responded. No significant differences between PMLS-lesion and normal PMLS were found for gratings ( $U = 635.5$ ,  $p = 0.227$ ), plaids ( $U = 345.5$ ,  $p = 0.768$ ), and complex RDKs ( $U = 54.5$ ,  $p = 0.364$ ).

## Discussion

### General findings

Overall, the data obtained with more appropriate stimuli for extra-striate neurons support previous findings that have demonstrated a substantial overlap of onset latencies between cortical visual areas in the dorsal stream, and this has been extended to the LPI. The overlap of cortical and thalamic onset latencies is consistent with the possibility that the LPI receives and integrates information from a large number of cortical areas and then relays this pre-processed information (Casanova *et al.*, 2001). Finally, the removal of primary visual cortex does not significantly alter the timing of information processing in extrastriate cortex (specifically PMLS), suggesting that the initial responses in



PMLS may not be entirely dependent upon projections from primary visual cortex.

#### Methodological considerations

Stimulus parameters are known to influence response onset latency (Creutzfeldt & Ito, 1968; Lennie, 1981). Although a number of parameters among our stimuli were identical when presented in different regions, some elements varied since the parameters (e.g. velocity) were set to elicit the strongest direction selective response for each cell, similar to a previous study (Raiguel *et al.*, 1999). While this variation of parameters is problematic, no feasible alternative seems available. For example, one less desirable option would have been to set all stimulus parameters to the preferred values for one of the regions. In such a case, the latency to the preferred stimulus for one region would be compared to that of a non-optimal stimulus for another region. This appears as a greater confound than using the optimal parameters for each cell. The present study measured the latency to the optimal stimulus for a cell, which should presumably produce the shortest possible latency to a particular class of stimuli. Knowing the shortest possible latency in turn allows the determination of degree of overlap between latency distributions for different areas.

It could be argued that the present study did not measure onset latencies to motion stimuli but rather to the initial appearance of the stimulus, before any integration could occur. This seems unlikely for four reasons. Firstly, a 1 second pre-stimulus blank of equal luminance to the stimulus was presented. This

avoided any mean increase in luminance upon stimulus onset which could evoke a non-motion induced response. Secondly, if the latencies measured were truly triggered by the flash of the stimulus one would expect area 17 neurons to respond sooner than extra-striate cortex neurons, no such difference was observed. Thirdly, previous studies using flashed stimuli in the cat have found onset latencies that were shorter than those measured here (Best *et al.*, 1986; Dinse & Kruger, 1994), suggesting that more processing was required in the present experiments. Finally, when averaged across regions onset latencies to gratings and plaids differed despite having the same mean luminance (Figure 3), which was also true when area 17 and LPI are considered separately. Such a difference should not exist if the initial response is purely stimulus onset driven.

Careful examination of Figures 2, 4, and 5 reveals that a small proportion (on average 5.8% of cells) of computed latencies were unexpectedly short (i.e < 10ms). It is unlikely that any cortical neurons can respond with such short latencies, as Levick (1973) has shown that retinal ganglion cells generally respond with latencies above 20ms, and cortical areas have rarely been reported to exhibit latencies below 30ms (Creutzfeldt & Ito, 1968; Ikeda & Wright, 1975; Best *et al.*, 1986; Eschweiler & Rauschecker, 1993; Dinse & Kruger, 1994). In all likelihood the shortest latencies here reflect 'measurement error' inherent to the method used. Although the data from these cells could be removed, the dilemma of subjectively choosing a cut-off latency arises. Such a cut-off would inherently bias the data. It seems more appropriate to admit a certain number of measurement errors, which should be equally distributed in all conditions, thus not affecting the relative latency-based position of each area.

Despite very short latencies, comparison of the overall data with previous findings reveals that mean and median latencies are consistently greater in the present study (Creutzfeldt & Ito, 1968; Ikeda & Wright, 1975; Best *et al.*, 1986; Eschweiler & Rauschecker, 1993; Dinse & Kruger, 1994). This discrepancy is not surprising given that the nature of the stimuli varies across studies and that stimulus parameters are known to greatly influence latency estimates (Creutzfeldt & Ito, 1968; Lennie, 1981). Comparing latencies obtained with identical stimulus parameters was indeed one of the initial motivations for this study in order to allow direct comparisons between areas.

#### Differences across areas

Visual information was found to be treated in a parallel manner along the established hierarchy of visual areas. The present data demonstrate a considerable overlap in response onset latencies between dorsal cortical areas, as well as the extra-geniculate thalamus, consistent with previous work (Eordegh *et al.*, 2005). However, the present study is at odds with the only study in cat reporting latencies from several cortical areas (Dinse & Kruger, 1994), which found significant differences among certain regions, including area 17 (mean of 52.7 ms) and PMLS cortex (66.7 ms). Their stimulus however was a flicker that was unlikely to elicit fast responses in PMLS, which could explain the differences they observed. Similar to the present study however, Dinse and Kruger (1994) found an important overlap of latency distributions and concluded that processing likely occurs simultaneously throughout the visual pathways.

This is further supported by the work of Katsuyama *et al.* (1996) who have demonstrated that among area 17 - PMLS cell pairs, a significant proportion of PMLS cells putatively drive the former.

The data from the present study resembles findings reported in monkeys, where overlapping latencies were commonly reported (for example mean latencies range from 53-72ms for V1 and from 58-87ms for MT: Robinson & Rugg, 1988; Raiguel *et al.*, 1989; Nowak *et al.*, 1995; Schmolesky *et al.*, 1998; Lamme & Roelfsema, 2000; Bullier, 2001, 2004b), at least for areas which may be considered homologous to those studied here. Parallel processing is not necessarily at odds with a hierarchically organized system, as demonstrated by a model based on neuroanatomical connections (Petroni *et al.*, 2001). Simultaneous responses could permit an early global analysis in higher-order areas which would modulate local analysis in lower-order areas (Bullier, 2001). This is supported by a variety of studies which have demonstrated the role of higher-order areas on motion analysis by lower order areas, even at the very earliest parts of the neuronal response (Hupe *et al.*, 2001; Pascual-Leone & Walsh, 2001; Galuske *et al.*, 2002), and cross-correlation data (Katsuyama *et al.*, 1996). Thus quasi-simultaneous response onsets, possibly reflecting parallel processing, occur within a neuroanatomical hierarchy in many cortical and sub-cortical areas (but see Lamme and Roelfsema (2000) for an alternate proposal, based on parallel pathways that successively follow the classical hierarchy).

Although no significant differences were found between areas, the profiles of the latency distributions seemed to show trends which could distinguish different regions. In Figure 5, it can be seen that the lowest area

along the hierarchy (area 17) responded rapidly to gratings, as did the LPI which receives direct driver input from area 17 (Vidnyanszky *et al.*, 1996; Huppé-Gourgue *et al.*, 2006a). In contrast, the two highest areas according to the neuroanatomical hierarchy (AMLS and AEV) differed in two ways. Firstly, the latency distributions to plaids in the latter two regions were identical to those for gratings. Secondly, the distinction between grating based and dot based stimuli was much stronger than in area 17. This suggests that although information is generally being treated simultaneously throughout the visual system, it may not be done in the same manner. The local nature of the analysis carried out by area 17 neurons (e.g. the above mentioned lack of selectivity to complex RDKs) is reflected in the stimulus independent latencies observed here. As opposed to area 17, neurons in AMLS and AEV are capable of global integration (Scannell *et al.*, 1996; Ouellette *et al.*, 2004b), which may be necessary in order to encode the direction of non-oriented sparse stimuli such as RDKs. This is reflected in the greater latencies observed for these stimuli, as compared to grating based stimuli. This suggests that future studies should concentrate on trends of latency distributions for multiple and distinct stimuli in order to better appreciate the differences in processing across cortical (and subcortical) areas.

#### Differences across stimuli

The initial hypothesis in regards to stimulus type was that simple stimuli would have shorter onset latencies than complex stimuli (in complex motion selective areas). This was not found to be the case, as stimuli composed of the

same underlying elements (sinewave gratings and plaids or simple and complex RDKs) evoked responses with latencies that did not significantly differ. Recent work (Smith *et al.*, 2005), may explain this counterintuitive finding. They demonstrated that the initial response of a pattern motion selective neuron was in fact component motion selective. In complex motion selective regions therefore, the latency measured with our complex stimuli (plaids and complex RDKs) may be attributable to an initial simple motion analysis.

It could be suggested that the similar simple and complex RDK latencies argue that the latter are not so complex. If this were the case, then the other complex stimulus (plaids) should have evoked longer latencies than sinewave gratings in higher-order areas where pattern motion selectivity has been observed. This was not the case, suggesting that the similarity between simple and complex RDK latencies is related to their underlying properties rather than the type of motion *per se*.

The largest difference was between latencies for sinewave gratings and RDK based stimuli, the former being shorter than the latter. This difference could be attributable to higher contrast levels for the RDK based stimuli, although this leads to the prediction of shorter latencies for RDKs than for gratings and plaids. The present results demonstrate the opposite. The longer RDK latencies may be a conservative estimate of the extra processing time required for RDK stimuli, perhaps due to their lack of oriented information or due to the greater spatial integration required. This conclusion should be taken lightly however, as the mean luminance of the sinewave grating stimuli was greater than that of the RDKs. It could thus be suggested that shorter latencies would be expected for

sinewave grating based stimuli, precisely the result found here. However, gratings in area 17 and the LPI tended to evoke shorter responses than plaids despite equal luminance.

#### Cortical versus thalamic latencies

The latencies measured for the LPI were found to occur at the same time as those in cortical areas. This precludes that the LPI could act as a relay station, simply passing information on to cortical areas. If this were the case, then onset latencies in the LPI should consistently precede those in cortical areas, especially compared to higher-order cortical areas. However, the LP-pulvinar is known to entertain reciprocal connections with a large number of cortical visual areas (e.g. Graybiel & Berson, 1980; Updyke, 1981; Berson & Graybiel, 1983a; Abramson & Chalupa, 1985; Norita *et al.*, 1986; Norita *et al.*, 1996), this has led to the proposition that it is ideally placed to integrate and continuously update information before redirecting the information back to cortex (Mumford, 1992). The overlapping latency distributions observed for the cortex and the LPI are consistent with this notion. It is interesting to note that Eordeghe *et al.* (2005) have found a similar latency overlap between suprageniculate nucleus and AEV responses, suggesting a general rule of functional connectivity between higher-order thalamic nuclei and cortical areas.

## PMLS-lesion

If responses in PMLS were heavily dependent upon classical feedforward channels, one would predict a change in latencies in PMLS following a lesion of primary visual cortex. Two conflicting predictions seem possible: 1- Due to a lack of processed information from primary visual cortex, neurons in PMLS may compensate by carrying out a greater level of processing to extract directional information, thereby increasing response latency. 2- Direct projections from the LGN to PMLS expand following these neonatal lesions (Tong *et al.*, 1984; Kalil *et al.*, 1991; Payne & Lomber, 1998b), which may decrease response latencies.

It is interesting that latencies in the PMLS-lesion condition were similar to normal PMLS cortex. This result does not fit either of the two predictions. The data lend further support to the notion of an initial global analysis prior to a local analysis in normal animals (Bullier, 2001). The initial response in normal PMLS not being dependent upon the lesioned cortex but rather the LGN, the removal of the former would not influence the early part of the response of the PMLS-lesion neurons.

## Conclusion

A substantial overlap between latency distributions in different areas was observed. This effect was present regardless of which of four stimuli was used to measure response onset latencies. More importantly however, the latencies measured in the LPI also overlapped with those in cortical areas. This suggests that simultaneous responses across regions are not limited to cortex. As



mentioned above, this supports the LP-pulvinar's role in integrating and updating information from a wide variety of cortical areas. Overall, the data demonstrate a dichotomy between the classical neuroanatomical hierarchy and the timing of response onset across visual areas. Thus parallel processing occurs within hierarchically organized neuroanatomical pathways. This suggest that the predictable progression of receptive field properties along the hierarchy may be attributable to intra-cortical processes rather than being successive modifications of feedforward input. The temporal evolution of these properties should be examined in greater detail to determine whether parallel processing is limited to the initial response or if it is maintained throughout the response period.

## Acknowledgements

This work was supported by a CIHR grant to C.C. and part of C.C.'s salary was provided by FRSQ (chercheur National). B.G.O. was supported by FRSQ and NSERC scholarships. We thank those who generously shared their data so as to allow the calculation of response onset latencies. The authors also wish to thank Annie-Hélène Samson and Barbara Lindsay with help in calculating the latencies.

## References

- Abramson BP, Chalupa LM (1985) The laminar distribution of cortical connections with the tecto- and cortico-recipient zones in the cat's lateral posterior nucleus. *Neuroscience* 15: 81-95
- Bair W, Movshon JA (2004) Adaptive temporal integration of motion in direction-selective neurons in macaque visual cortex. *J Neurosci* 24: 7305-7323
- Berson DM, Graybiel AM (1983) Organization of the striate-recipient zone of the cats lateralis posterior-pulvinar complex and its relations with the geniculostriate system. *Neuroscience* 9: 337-372
- Best J, Reuss S, Dinse HR (1986) Lamina-specific differences of visual latencies following photic stimulation in the cat striate cortex. *Brain Res* 385: 356-360
- Bullier J (2001) Integrated model of visual processing. *Brain Res Brain Res Rev* 36: 96-107
- Bullier J (2004) Communications between cortical areas of the visual system. In: *The visual neurosciences, vol 2*. Bradford Book, Cambridge, Massachusetts, pp 522-540
- Casanova C, Merabet L, Desautels A, Minville K (2001) Higher-order motion processing in the pulvinar. In: Casanova C, Ptito M (eds) *Progress in Brain Research, vol 134*, pp 71-82
- Creutzfeldt O, Ito M (1968) Functional synaptic organization of primary visual cortex neurones in the cat. *Exp Brain Res* 6: 324-352
- Dinse HR, Kruger K (1994) The timing of processing along the visual pathway in the cat. *Neuroreport* 5: 893-897
- Dumbrava D, Faubert J, Casanova C (2001) Global motion integration in the cat's lateral posterior-pulvinar complex. *Eur J Neurosci* 13: 2218-2226
- Ellaway PH (1978) Cumulative sum technique and its application to the analysis of peristimulus time histograms. *Electroencephalogr Clin Neurophysiol* 45: 302-304
- Eordeghe G, Nagy A, Berenyi A, Benedek G (2005) Processing of spatial visual information along the pathway between the suprageniculate nucleus and the anterior ectosylvian cortex. *Brain Res Bull* 67: 281-289
- Eschweiler GW, Rauschecker JP (1993) Temporal integration in visual cortex of cats with surgically induced strabismus. *Eur J Neurosci* 5: 1501-1509

- Felleman DJ, Van Essen DC (1991) Distributed hierarchical processing in the primate cerebral cortex. *Cereb Cortex* 1: 1-47
- Galuske RA, Schmidt KE, Goebel R, Lomber SG, Payne BR (2002) The role of feedback in shaping neural representations in cat visual cortex. *Proc Natl Acad Sci U S A* 99: 17083-17088
- Graybiel AM, Berson DM (1980) Histochemical identification and afferent connections of subdivisions in the lateralis posterior-pulvinar complex and related thalamic nuclei in the cat. *Neuroscience* 5: 1175-1238
- Guido W, Spear PD, Tong L (1990) Functional compensation in the lateral suprasylvian visual area following bilateral visual cortex damage in kittens. *Exp Brain Res* 83: 219-224
- Guido W, Spear PD, Tong L (1992) How complete is physiological compensation in extrastriate cortex after visual cortex damage in kittens? *Exp Brain Res* 91: 455-466
- Hilgetag CC, O'Neill MA, Young MP (2000) Hierarchical organization of macaque and cat cortical sensory systems explored with a novel network processor. *Philos Trans R Soc Lond B Biol Sci* 355: 71-89
- Hupe JM, James AC, Girard P, Lomber SG, Payne BR, Bullier J (2001) Feedback connections act on the early part of the responses in monkey visual cortex. *J Neurophysiol* 85: 134-145
- Huppé-Gourgue F, Bickford ME, Boire D, Ptito M, Casanova C (2006) Distribution, morphology and synaptic targets of corticothalamic terminals in the cat lateral posterior-pulvinar complex that originates from the posteromedial lateral suprasylvian cortex. *J Comp Neurol* In Press
- Ikeda H, Wright MJ (1975) Retinotopic distribution. Visual latency and orientation tuning of 'sustained' and 'transient' cortical neurones in area 17 of the cat. *Exp Brain Res* 22: 385-398
- Kalil RE, Tong LL, Spear PD (1991) Thalamic projections to the lateral suprasylvian visual area in cats with neonatal or adult visual cortex damage. *J Comp Neurol* 314: 512-525
- Katsuyama N, Tsumoto T, Sato H, Fukuda M, Hata Y (1996) Lateral suprasylvian visual cortex is activated earlier than or synchronously with primary visual cortex in the cat. *Neurosci Res* 24: 431-435
- Lamme VA, Roelfsema PR (2000) The distinct modes of vision offered by feedforward and recurrent processing. *Trends Neurosci* 23: 571-579
- Lennie P (1980) Parallel visual pathways: a review. *Vision Res* 20: 561-594

- Lennie P (1981) The physiological basis of variations in visual latency. *Vision Res* 21: 815-824
- Levick WR (1973) Variation in the response latency of cat retinal ganglion cells. *Vision Res* 13: 837-853
- Maunsell JH, van Essen DC (1983) The connections of the middle temporal visual area (MT) and their relationship to a cortical hierarchy in the macaque monkey. *J Neurosci* 3: 2563-2586
- Merabet L, Desautels A, Minville K, Casanova C (1998) Motion integration in a thalamic visual nucleus. *Nature* 396: 265-268
- Miller R (1996) Cortico-thalamic interplay and the security of operation of neural assemblies and temporal chains in the cerebral cortex. *Biol Cybern* 75: 263-275
- Mishkin M, Ungerleider LG, Macko KA (1983) Object vision and spatial vision: two cortical pathways. *Trends Neurosci* 6: 263-275
- Movshon JA, Adelson EH, Gizzi MS, Newsome WT (1986) The analysis of moving visual patterns. In: Chagas C, Gattas R, Gross C (eds) *Pattern recognition mechanisms*. Springer Verlag, New York, pp 148-164
- Mumford D (1992) On the computational architecture of the neocortex. II. The role of cortico-cortical loops. *Biol Cybern* 66: 241-251
- Norita M, Kase M, Hoshino K, Meguro R, Funaki S, Hirano S, McHaffie JG (1996) Extrinsic and intrinsic connections of the cat's lateral suprasylvian visual area. *Prog Brain Res* 112: 231-250
- Norita M, Mucke L, Benedek G, Albowitz B, Katoh Y, Creutzfeldt OD (1986) Connections of the anterior ectosylvian visual area (AEV). *Exp Brain Res* 62: 225-240
- Nowak LG, Munk MH, Girard P, Bullier J (1995) Visual latencies in areas V1 and V2 of the macaque monkey. *Vis Neurosci* 12: 371-384
- Ouellette BG, Lindsay B, Casanova C (2004a) Visual response latencies vary for different stimuli and across visual areas in cats. *Society for Neuroscience Abstracts*: 410.417
- Ouellette BG, Minville K, Boire D, Ptito M, Casanova C (2002) Simple and complex motion selectivity in PMLS cortex following early primary visual cortex lesions in the cat. *Society for Neuroscience Abstracts*: 657.655
- Ouellette BG, Minville K, Faubert J, Casanova C (2004b) Simple and complex visual motion response properties in the anterior medial bank of the lateral suprasylvian cortex. *Neuroscience* 123: 231-245

- Pascual-Leone A, Walsh V (2001) Fast backprojections from the motion to the primary visual area necessary for visual awareness. *Science* 292: 510-512
- Payne BR, Lomber SG (1998) Neuroplasticity in the cat's visual system. Origin, termination, expansion, and increased coupling of the retino-geniculo-middle suprasylvian visual pathway following early ablations of areas 17 and 18. *Exp Brain Res* 121: 334-349
- Petroni F, Panzeri S, Hilgetag CC, Kotter R, Young MP (2001) Simultaneity of responses in a hierarchical visual network. *Neuroreport* 12: 2753-2759
- Raiguel SE, Lagae L, Gulyas B, Orban GA (1989) Response latencies of visual cells in macaque areas V1, V2 and V5. *Brain Res* 493: 155-159
- Raiguel SE, Xiao DK, Marcar VL, Orban GA (1999) Response latency of macaque area MT/V5 neurons and its relationship to stimulus parameters. *J Neurophysiol* 82: 1944-1956
- Robinson DL, Rugg MD (1988) Latencies of visually responsive neurons in various regions of the rhesus monkey brain and their relation to human visual responses. *Biol Psychol* 26: 111-116
- Rockland KS, Pandya DN (1979) Laminar origins and terminations of cortical connections of the occipital lobe in the rhesus monkey. *Brain Res* 179: 3-20
- Scannell JW, Blakemore C, Young MP (1995) Analysis of connectivity in the cat cerebral cortex. *J Neurosci* 15: 1463-1483
- Scannell JW, Burns GA, Hilgetag CC, O'Neil MA, Young MP (1999) The connectional organization of the cortico-thalamic system of the cat. *Cereb Cortex* 9: 277-299
- Scannell JW, Sengpiel F, Tovee MJ, Benson PJ, Blakemore C, Young MP (1996) Visual motion processing in the anterior ectosylvian sulcus of the cat. *J Neurophysiol* 76: 895-907
- Scannell JW, Young MP (1993) The connectional organization of neural systems in the cat cerebral cortex. *Curr Biol* 3: 191-200
- Schmolesky MT, Wang Y, Hanes DP, Thompson KG, Leutgeb S, Schall JD, Leventhal AG (1998) Signal timing across the macaque visual system. *J Neurophysiol* 79: 3272-3278
- Schroeder CE, Mehta AD, Givre SJ (1998) A spatiotemporal profile of visual system activation revealed by current source density analysis in the awake macaque. *Cereb Cortex* 8: 575-592

- Sherman SM, Guillery RW (1998) On the actions that one nerve cell can have on another: distinguishing "drivers" from "modulators". *Proc Natl Acad Sci U S A* 95: 7121-7126
- Smith MA, Majaj NJ, Movshon JA (2005) Dynamics of motion signaling by neurons in macaque area MT. *Nat Neurosci* 8: 220-228
- Stone J, Dreher B, Leventhal A (1979) Hierarchical and parallel mechanisms in the organization of visual cortex. *Brain Res* 180: 345-394
- Symonds LL, Rosenquist AC (1984) Laminar origins of visual corticocortical connections in the cat. *J Comp Neurol* 229: 39-47
- Tong L, Kalil RE, Spear PD (1984) Critical periods for functional and anatomical compensation in lateral suprasylvian visual area following removal of visual cortex in cats. *J Neurophysiol* 52: 941-960
- Updyke BV (1981) Projections from visual areas of the middle suprasylvian sulcus onto the lateral posterior complex and adjacent thalamic nuclei in cat. *J Comp Neurol* 201: 477-506
- Vidnyanszky Z, Borostyankoi Z, Gorcs TJ, Hamori J (1996) Light and electron microscopic analysis of synaptic input from cortical area 17 to the lateral posterior nucleus in cats. *Exp Brain Res* 109: 63-70
- Villeneuve MY, Ptito M, Casanova C (2006) Global motion integration in the postero-medial part of the lateral suprasylvian cortex in the cat. *Exp Brain Res* In Press
- Vogels R, Orban GA (1990) How well do response changes of striate neurons signal differences in orientation: a study in the discriminating monkey. *J Neurosci* 10: 3543-3558
- Vogels R, Orban GA (1994) Activity of inferior temporal neurons during orientation discrimination with successively presented gratings. *J Neurophysiol* 71: 1428-1451
- Zabouri N, Ptito M, Casanova C (2003) Complex motion sensitivity of neurons in the visual part of the anterior ectosylvian cortex. *Society for Neuroscience Abstracts*: 179.174

Article 3



**Spatio-temporal profiles of receptive field structure among PMLS cortex neurons in the cat: presence of linear properties?**

B.G. Ouellette<sup>1,2</sup>, C. Casanova<sup>1,3</sup>

<sup>1</sup> École d'optométrie, Université de Montréal

<sup>2</sup> Département de Psychologie, Université de Montréal

<sup>3</sup> Corresponding author


Running head: PMLS spatio-temporal profiles

Corresponding author address:

Christian Casanova  
Visual Neuroscience Laboratory  
School of Optometry  
Université de Montréal  
CP 6128, succ. Centre-ville  
Montréal, Quebec,  
Canada, H3C 3J7.

Tel : 514-343-2407

Fax : 514-343-2382



Section editor: Dr Gregory DeAngelis

## Abstract

The cortex surrounding the lateral portion of the postero-medial suprasylvian sulcus (PMLS) receives major projections from area 17 and 18 neurons which exhibit complex receptive fields (RF). Based on this input, complex like receptive fields are also expected in PMLS cortex and this corresponds to hand mapping data. However a motion reverse correlation mapping paradigm (Vajda *et al.*, 2006) revealed that few neurons in PMLS exhibit any temporal interactions, suggesting linear integration. The present study sought to determine whether such linear properties were also present in the spatial domain. Single unit extracellular recordings were conducted in the PMLS cortex of anaesthetised adult cats. Coarse white noise stimuli were employed to elicit responses analysed using reverse correlation in order to obtain first-order spatio-temporal profiles. Profiles were successfully obtained for 72/107 neurons. Six of these cells responded to only one contrast. The majority of neurons (52/66) exhibited spatially overlapping receptive fields. However the size of the subfields was asymmetric to opposite contrast stimuli. Analysis of the temporal profile also revealed contrast dependent responses. The difference in peak latency between contrast differed by more than 10ms for 40/66 cells. The multiple contrast dependent measures suggest that afferents other than area 17 and 18 may drive responses in PMLS neurons, at least for stimuli evoking short responses such as in the present study. The data are consistent with a functionally important projection from the LGN and possibly other thalamic structures.

## Introduction

The processing of visual information across cortical areas is thought to be carried out in a serial manner, although parallel pathways exist within this serial system. This has been formalised by cortical hierarchies which have been established based mainly on neuroanatomical findings. Along the putative dorsal stream in cats, the posteromedial lateral suprasylvian cortex (PMLS) receives large projections from area 17 (Symonds & Rosenquist, 1984a). The majority of area 17 neurons projecting to PMLS originate in the supragranular layers and terminate in layer IV (Maciewicz, 1974; Symonds & Rosenquist, 1984b; Einstein & Fitzpatrick, 1991; Lowenstein & Somogyi, 1991; Shipp & Grant, 1991; Norita *et al.*, 1996). The vast majority of these supranular layer area 17 neurons are known to be complex (Gilbert, 1977; Martinez *et al.*, 2005). Similarly, area 18 supragranular neurons also project to layer IV of PMLS (Symonds & Rosenquist, 1984b; Norita *et al.*, 1996) and almost all neurons are complex (or so called hypercomplex), regardless of laminar position (Hubel & Wiesel, 1965).

Based on hierarchical positions, one would expect to find receptive field (RF) properties in PMLS that build upon those in areas 17 and 18. Physiological investigations of PMLS neurons support this, as larger RFs have been described in PMLS than in area 17 (Hubel & Wiesel, 1969; Spear & Baumann, 1975; Zumbroich & Blakemore, 1987). Similarly, global motion stimuli evoke direction selective responses in PMLS while this is not the case in area 17 (Toyama *et al.*, 1990; Kim *et al.*, 1997; Mulligan *et al.*, 1997; Brosseau-Lachaine *et al.*, 2001;

Villeneuve *et al.*, 2006a). However, motion reverse correlation has shown little difference between responses in area 18 and PMLS (Vajda *et al.*, 2004). Moreover, Vajda *et al.* (2006) found that few PMLS neurons exhibited non-linear temporal integration, while a large proportion of area 18 neurons did exhibit second-order kernels.

Although there need not be a strict relationship, the presence of linear temporal integration among PMLS neurons raises the question as to the existence of linear spatial integration among these same neurons. This would be surprising as linear spatial summation in cortex is exclusively found among simple cells in area 17 (Movshon *et al.*, 1978a, b), whereas PMLS RFs have been described as complex like based on hand mapping (Hubel & Wiesel, 1969; Spear & Baumann, 1975; Zumbroich & Blakemore, 1987; Danilov *et al.*, 1995). However, a number of PMLS neurons have been found to modulate their response to the F1 component of sinewave gratings, consistent with linear integration, and segregated ON and OFF regions (Zumbroich & Blakemore, 1987; Guido *et al.*, 1990b; Ouellette *et al.*, 2007).

While the response properties of neurons in PMLS have been extensively described (for a review: Spear, 1991; for more recent work: Sherk & Mulligan, 1992; Sherk *et al.*, 1995; Kim *et al.*, 1997; Mulligan *et al.*, 1997; Sherk *et al.*, 1997; Minville & Casanova, 1998; Merabet *et al.*, 2000; Brosseau-Lachaine *et al.*, 2001; Sherk & Kim, 2002; Villeneuve *et al.*, 2006a), the spatio-temporal structure underlying their RFs is relatively unknown (Borghuis *et al.*, 2003). Conversely, the structure of area 17 RFs has been studied repeatedly (among

others: Palmer & Davis, 1981a; Palmer & Davis, 1981b; Emerson *et al.*, 1987; Jones & Palmer, 1987; Szulborski & Palmer, 1990; DeAngelis *et al.*, 1993; McLean *et al.*, 1994; DeAngelis *et al.*, 1995b; Ringach *et al.*, 1997b; Martínez *et al.*, 2005; Rust *et al.*, 2005; Nishimoto *et al.*, 2006). The present study aimed to determine, whether the observed temporal linear integration of PMLS neurons could also be observed in the spatial domain. We sought to determine whether PMLS receptive fields are best described as simple- or complex-like based on spatio-temporal response profiles obtained with reverse correlation. Parts of these findings have been presented in abstract form (Ouellette *et al.*, 2005, 2006).

## Methods

### Animal preparation

All procedures were in accordance with the directives of the Canadian Council for the Protection of Animals and the ethics review board of the Université de Montréal. Adult cats weighing between 2.5 and 4.5kg were used in this study (data was also collected for other projects). Animals received injections of Atropine (0.1mg/kg) and Atravet (1mg/kg), 30 minutes thereafter animals were anesthetized with Isoflurane (5%), in a 50:50 mixture of O<sub>2</sub> and N<sub>2</sub>O. Anesthesia was reduced to 2% Isoflurane during surgical procedures. Heart rate and blood O<sub>2</sub> saturation levels were monitored with an oxymeter. A local anesthetic (lidocaine hydrochloride 2%) was applied to incision and

pressure points. A cannulation of the cephalic vein and a tracheotomy were performed prior to transferring the animal to the stereotaxic apparatus.

Following administration of gallamine triethiodide (10mg/kg/h) in lactated Ringers solution, the animal was artificially ventilated with Isoflurane (2%) in a mixture of N<sub>2</sub>O/O<sub>2</sub> (70:30). Expired levels of CO<sub>2</sub> were maintained between 28 and 32 mmHg by adjusting the stroke volume and respiratory rate. Rectal temperature was monitored and maintained at approximately 38.0°C. The ECG and EEG were continuously monitored. Pupils were dilated and nictitating membranes retracted with atropine (1%) and phenylephrine hydrochloride (2.5%) respectively. The eyes were then protected with contact lenses with the appropriate refractive power. A craniotomy (Horsley-Clarke coordinates AP:-3 to +4, ML: 10 to 15) exposed a portion of the medial lateral suprasylvian sulcus as defined by Palmer *et al.* (1978). Varnished tungsten microelectrodes (3-5MΩ, H-J Winston, Winston-Salem, North Carolina) were angled at approximately 40° in order to follow the slant of the sulcus. The craniotomy was filled with warm agar and covered with melted wax in order to create a sealed chamber. During recordings the anesthetic agent was changed to Halothane and administered at a concentration of 0.5-1%.

Electrolytic lesions were performed at several points along each successful penetration. Upon termination of the experiment, the animals were intravenously administered pentobarbital sodium (Euthanyl: 240mg/ml, 110mg/kg) and then perfused transcardially with phosphate buffer solution and fixative (4% paraformaldehyde). Using a cryostat, coronal serial sections

(40 $\mu$ m) of PMLS cortex were cut and Nissl stained. Under microscopic inspection, penetrations were verified to ensure that the electrode did not cross over into the lateral bank of the lateral suprasylvian sulcus.

### Recordings

Once amplified and bandpass filtered (300Hz-10kHz), a window discriminator (WPI 121) was used to isolate action potentials from the surrounding neuronal activity. The analogue signal, digitized action potentials, and stimulus presentation time stamps were fed into a CED 1401 plus and acquired with Spike2 v5 (CED, Cambridge, UK). Data sampling was performed at 25kHz and saved for later analysis, although online analysis was also carried out in order to direct further tests.

### Visual stimulation

Prior to stimulation, RFs and ocular dominance were qualitatively assessed with a hand held light source displaced on the screen. Subsequent stimulation was carried out monocularly. Stimuli were back projected onto a translucent screen placed 57cm in front of the animal and the stimulated area covered 75°X92° of visual angle (although the screen was sometimes advanced in order to increase spatial resolution). Hence, the reverse correlation stimulus was not limited to a small area in and around the RF, but rather covered a large

portion of the visual field. This had the advantage of not assuming that the hand plotted RF was sufficiently accurate to limit the area of stimulation. This is especially important as many PMLS neurons have large RFs which do not respond reliably, complicating hand mapping.

Stimuli were generated by custom software written under Python v2.3.4 ([www.python.org](http://www.python.org)), running on a Pentium III 930MHz with a NVIDIA GeForce2 GTS graphics card. Stimuli consisted of a 25cd/m<sup>2</sup> gray background, upon which single white (hereafter bright: 50cd/m<sup>2</sup>) or black (hereafter dark: ≈0cd/m<sup>2</sup>) squares were presented. Each neuron was tested with a series of stimuli in which the size and duration got progressively and independently smaller/shorter in successive stimulation blocks. Stimulation ceased when the neuron no longer responded to the stimulus in a robust manner (Mata & Ringach, 2005). Presentation duration varied in steps of 16ms from 16-48ms, while the size of the squares varied from 1.85 to 9.41° (test with smaller squares were conducted but these never elicited a robust and reproducible response). In extreme cases this lead to 1200 positions for each contrast. A minimum of 30 presentations at each position and of each contrast were carried out for each block. The position and contrast of the stimuli were presented in a completely randomized order so as to avoid that any specific sequence of stimuli was ever repeated within the range of finite presentations used in the present experiment.

A subset of neurons was also tested with drifting sinewave gratings (hereafter gratings). The gratings were projected in the same manner as described above, however the stimulus was generated by a Macintosh G3



computer using VPixx 1.8 (Sentinel Medical Research, Ste-Julie, Quebec, Canada). Gratings were presented at 60% contrast at a mean luminance of 25cd/m<sup>2</sup>. The optimal direction, spatial (SF) and temporal (TF) frequencies were determined for each cell.

## Data analysis

### Reverse correlation

A slightly modified version of a previously used reverse correlation technique was performed (Jones & Palmer, 1987; DeAngelis *et al.*, 1993). The difference between the present and prior methods is threefold. Firstly, a spatial linear interpolation was carried out in order to increase the spatial resolution of the estimates of RF boundaries. Linear interpolation, as opposed to a 2-D Gaussian (for example), was chosen since the underlying shape of PMLS RFs has not yet been described. We therefore wished to avoid biasing the data with non-linear interpolation methods. For future reference, different possible functions which could describe PMLS RFs were fit to the data (see subfield fits section in the results).

The second modification was the use of a 2-D adaptive pixelwise linear Wiener filter (Matlab Image Processing Toolbox, Mathworks, Natick, MA, USA) using a 3X3 window, applied to the pre-interpolated data. An example of the effect of this filter can be seen in Figure 1, where the pre-filter (upper left) and post-filter (upper-right) images of a RF are presented. Clearly, the filter leaves

the general profile of the RF intact, while eliminating the noise from the image. The lower panel shows the subtraction of both images. It can be seen that there is very little change occurring in the vicinity of the RF. In brief (for a detailed description see Lim, 1990), this is a low pass filter whose attenuation is inversely related to the local variance in the data. It is adaptive in the sense that the attenuation of the filter is adjusted for each pixel, according to the variance within a window surrounding that pixel. This has the advantage of only slightly modifying the high variance areas of the image (i.e. the part of the visual field which evoked a robust response) while eliminating noise from low variance parts of the image (i.e. parts of the visual field evoking little to no neuronal response).

The third modification was to ascribe a possible evoking stimulus to all pre-spike times, rather than to intervals which were multiples of the stimulus presentation frame rate (McLean *et al.*, 1994; Bair & Movshon, 2004). This is similar to temporally boxcar filtering the data, with the advantage that an estimate of the temporal time course of the neuronal response is possible with a 1 ms resolution.

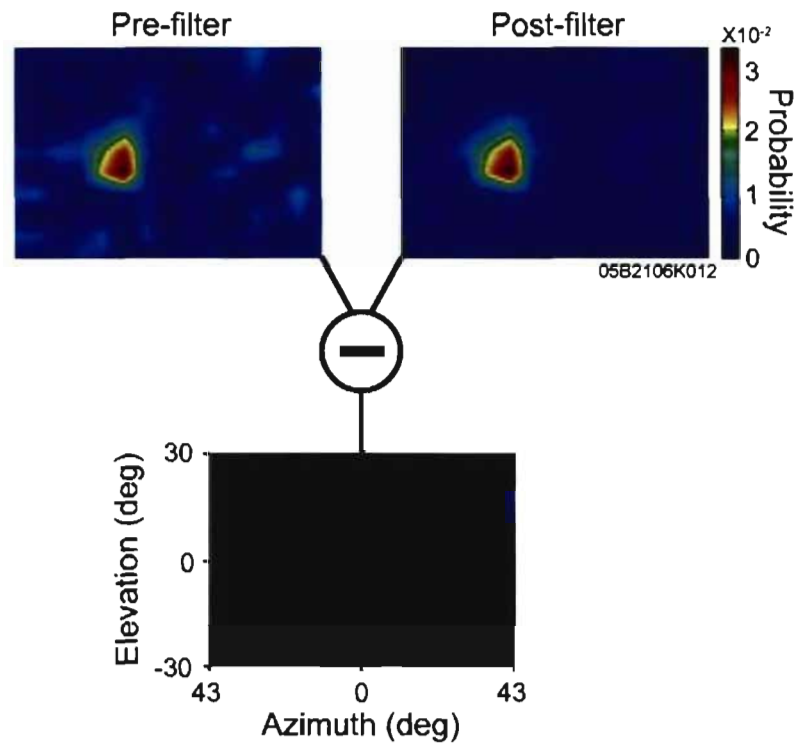


**Figure 1**

Adaptive pixel-wise Wiener filter. A non-filtered spatial map of a PMLS receptive RF (upper left) and the filtered result (upper right). Note that the robust response remains relatively unaltered, while the noise in the left hand image is no longer present. Bottom center: the subtraction of both images presented above. It can be seen that there is very little change due to the filter in the vicinity of the robust response.

Since PMLS neurons receive their main projection from complex cells in area 17, one would expect the former to exhibit complex RFs as well. Due to the non-linear spatial integration properties of complex cells (Movshon *et al.*, 1978a, b), bright and dark responsive subfields were analyzed separately. Carrying out a subtraction, as is usually done with simple cells (for example: Jones & Palmer, 1987; DeAngelis *et al.*, 1993), would have mutually canceled out the contribution of each subfield, while an addition would mask any differences between the subfields.

Different authors have expressed the output of reverse correlations in a variety of ways. In the present study, the spatio-temporal maps were visualized as probability surfaces. To obtain these maps, the number of spikes in each pixel of the map was divided by the total number of spikes recorded during the stimulus ensemble. Hence the reported probability is that of a specific stimulus (spatial position and contrast), at a specific pre-spike time to evoke an action potential. Note that this probability is dependent upon the number of positions used, and is therefore a relative measure.

Once the reverse correlation was carried out, the extent of the RF was defined as that part of the responsive area whose probability exceeded 1.96 S.D. above that expected by chance. Although chance level can be accurately calculated by  $1/\text{number of conditions}$ , it was estimated by taking the positive times (Borghuis *et al.*, 2003) from the cross-correlation, over a range equivalent to that for the reverse correlation (i.e. negative times). The former simply calculates the probability that a particular stimulus, which occurred after an

action potential, evoked that action potential. In such a case there is clearly no causal link. This had the advantage of allowing the calculation of a S.D. which could be used for the above mentioned threshold. The parameters of the RF (azimuth, elevation, width and height) were taken from the pre-spike time with peak probability. Latencies were measured as the first and last significant response, that is the time at which the probability exceeded chance plus 1.96 S.D. for at least 5 consecutive ms (i.e. the first or last of the five consecutive ms for the first and last significant responses respectively). The time of peak probability was also taken as a measure of latency. Wilcoxon's signed rank test was carried out on this data as the latencies were not normally distributed as determined by a Kolmogorov-Smirnov test. Occasionally, a neuron would exhibit more than one response peak. A response was considered as a secondary peak when the response fell below threshold for at least 5 consecutive ms and went back above the threshold for another 5 consecutive ms. The secondary peak was considered as the response with the lesser probability, regardless of the temporal order of the responses.

#### Assessment of overlap

In order to determine whether PMLS RFs exhibit simple-like RFs, an overlap index (OI) was calculated. In order to calculate this index, the pre-spike time of the responsive subfield was based on the peak probability, chosen independently for each contrast. The OI was defined as the total area of overlap of the responsive subfields to bright and dark stimuli divided by the total area of

the smaller of the two. As OI values progress from 0 to 1, the percentage of the area of the smaller of the two responsive subfields is increasingly overlapped by that of the larger responsive subfield. It could be argued that this OI is inappropriate as the peak response probability may not be the point at which maximal overlap occurs, and therefore biases the data towards lower OI values and therefore underestimates the complexity of PMLS RFs. As this is crucial to the question being asked, two alternate OIs were calculated. Details of these methods may be found in the appendix.

One may note that the OI is an incomplete measure, since a neuron which responds poorly to one of the two stimuli (say bright) will have an index of 1 if the smaller RF is centered within the larger. This is the case of the cell presented in Figure 2, which had an OI of 1. Clearly this value alone does not accurately capture how the cell responds to each contrast. To overcome this, an independence index was calculated (II). It was defined as the total non-overlapping area of both responsive subfields divided by the total non-overlapping and overlapping area (i.e. the overlapping area was only included once in the calculation). A value of 0 signifies that there is complete overlap, when the index is below 0.5 there is a greater proportion of the subfield areas which overlap, and as the value tends towards 1 there is a larger fraction of the area which is non-overlapping. For the cell presented in Figure 2, the II was 0.79 indicating that almost 80% of both subfields do not overlap with each other. Finally a subfield size index (SSI) was calculated, it was defined as the total area of the bright minus dark responsive subfields divided by their sum. When

the dark responsive subfield is larger, values vary from -1 to 0 and values range from 0 to 1 when the inverse occurs. The SSI for the cell in Figure 2 was -0.66.

### Cellular classification

Based on the three indices just described, the RFs of neurons could be divided into two classes; those with and without spatial overlap of their subfields. Those cells with overlapping subfields were further subdivided into three groups according to the following criteria. Superimposed cells had almost identical responses in the spatial domain to both contrasts, and were defined as having an  $OI > 0.9$ ,  $II < 0.3$ , and  $SSI < 0.3$ , a representative example is presented in Figure 7A. Partially overlapping cells exhibited a lesser degree of spatial register but their receptive fields nonetheless overlapped, as may be seen for the example cell in panel B. These cells were defined as having an  $OI > 0.2$ , an  $II$  and  $SSI$  of any value. Note that the criteria for superimposed and partially overlapping neurons are not mutually exclusive. Therefore a cell that met all the criteria for superimposed was considered as such, and not classified as partially overlapping. The third subgroup, spatially unbalanced cells had one subfield which was smaller than and entirely overlapped by the other subfield (Figure 7C). The criteria for this category was an  $OI = 1$ ,  $II > 0.3$ , and an absolute  $SSI > 0.3$ , with the extra constraint that the position along the azimuth and elevation of the subfield center must not differ by more than 10% of the width or height of the smaller subfield. Among the non-overlapping cells, juxtaposed cells exhibited minimal overlap however the subfields were in close proximity to

each other as per the cell in Figure 7D. The criteria for these cells were an  $OI < 0.2$ ,  $II > 0.9$ , an SSI of any value, and subfields separated by no more than 50% of the smaller of the two subfields along each axis. Finally, distant neurons had subfields which did not overlap at all such as in Figure 7E. The criteria for this subgroup was an  $OI = 0$ ,  $II = 1$ , SSI of any value, and subfields separated by more than 50% of the smaller subfields width or height.

#### Quantification of responses to gratings

For those cells that were tested with gratings, direction indices (DI) and modulation indices (MI) were calculated. The DI was defined as 1 minus the firing rate at the anti-preferred direction divided by that of the preferred direction (Minville & Casanova, 1998), following subtraction of spontaneous activity. Neurons with values below and above 0.5 were considered non-direction and direction selective respectively, while values above 1 signify that the neuron was direction selective and responded below spontaneous activity in the anti-preferred direction. The MI is classically employed to distinguish simple from complex cells (Skottun *et al.*, 1991a) based on the sinusoidal modulation of neuronal firing rate at the TF of the grating. This is an indirect measure of the overlap of ON and OFF sub-regions of the RF. Values below 1 are indicative of a cell which does not exhibit strong modulation of its response, while the opposite is true when the value is above 1.



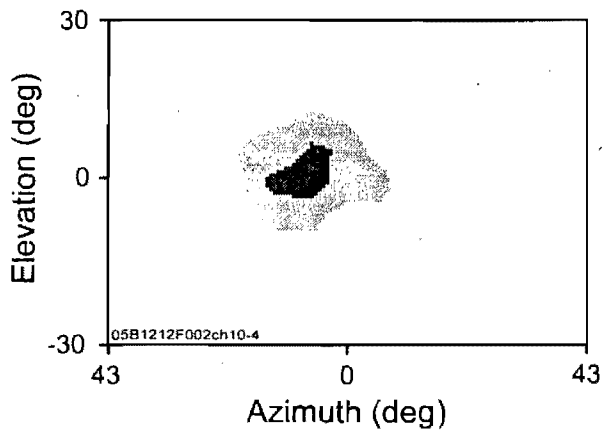


**Figure 2**

Overlap of subfields. Representation of the area of the visual field from which a significant response could be elicited from this cell. The black region represents parts of the visual field which responded to either contrast, while gray regions were uniquely responsive to dark stimuli, and white regions did not respond above threshold. The overlap index was 1, as can be seen however the response pattern is only partially described by this metric.

## Predicting RF parameters

If the RFs of PMLS neurons exhibit more linearity than previously thought one should be able to accurately predict the preferred SF of neurons based on the first order reverse correlation defined RFs (Movshon *et al.*, 1978a, b; Gaska *et al.*, 1994). This was assessed with three models. The first assumed that the width of a subfield would span half a cycle of the optimal SF, this is conceptually similar to the comparisons carried out by Movshon *et al.* (1978b). Hereafter this will be referred to as the subfield based model. The second method (hereafter product model) assumed that larger responses would be elicited from stimuli whose time varying spatial contrast profile corresponded to the spatio-temporal probability map of the neuron. The normalized luminance values of gratings with different parameters (direction, SF, TF, and phase) were multiplied by the spatial profile of the RF at each pre-spike  $t$ . Note that the RF profile had already passed the above mentioned threshold at this point and all values below threshold were set to zero. Thereby, those parts of the visual field which did not evoke a robust response did not contribute to the output of the model. The output was summed over spatial and temporal dimensions, as well as eight phases (to compensate for the short responses due to the impulse stimulation leading to the spatio-temporal maps). This provides, in arbitrary units, a prediction of the tuning curve for a given set of directions, SFs and TFs. Finally, a more flexible variation of the second method consisted of a 2-D correlation of the spatio-temporal profile and the normalized luminance of the grating, carried out at each pre-spike time. Again summation was carried out over the temporal

dimension and over phase. The use of correlation makes this method invariant to absolute luminance (in the case of a stationary process). For the product and correlation models the grating parameters used were identical to those presented to the cell during testing.

### Surface fitting

As a final rapid verification of the linear processing of visual information by PMLS neurons, the spatial map of the neuronal subfields at peak probability were fit with Gaussian and Gabor functions. The bright and dark subfields were either summed or subtracted from each other and then fit with a Gaussian or Gabor function respectively. In this case the use of addition and subtraction does not reflect an assumption of the precise integrative mechanisms at work in the neuron's RF, but rather it is used as a coarse test of the superposition of subfields and therefore of linearity. The fits were carried out using a least mean square (LMS) procedure using the Nelder-Mead method of unconstrained nonlinear optimization (Matlab Optimization Toolbox, Mathworks, Natick, MA, USA). The LMS of the best fit was then used to calculate an index  $I_{\text{linear}} = (E_{\text{Gabor}} - E_{\text{Gaussian}}) / (E_{\text{Gabor}} + E_{\text{Gaussian}})$ , where the variable E is the calculated LMS error of each fit. As  $I_{\text{linear}}$  approaches 1, the Gabor represents the best fit, while values close to zero indicate a better fit with the Gaussian.

## Results

Extracellular single unit recordings were carried out on 107 neurons in PMLS cortex. Neurons which were unresponsive to the sparse noise stimulus were further tested (gratings and/or random dot kinematograms) to determine whether the cells were non-responsive to this particular stimulus or to visual stimuli in general. Putative visually unresponsive neurons (25) were eliminated from further analysis, whereas an additional 10 visual neurons were not responsive to the sparse noise stimulus. The following analyses apply to the remaining 72 neurons, of which 6 responded to only one of the stimulus contrasts.

The two examples presented in Figures 3 & 4 are representative of the main response profiles observed. The cell in Figure 3 had bright (left) and dark (right) responsive subfields which overlapped in both the spatial and temporal domains. This is what one would expect of neurons that have a complex like RF. The other major observed profile was similar to the cell presented in Figure 4. For this type of neuron, the response to the dark (right) subfield occurred prior to the bright (left) subfield. The opposite temporal order was also observed. In this particular case, the response to the bright stimulus did not commence until the response to the dark stimulus had terminated. Note however that there was a spatial superposition of both subfields. Furthermore, in both cases (Figure 3 & 4) the response to the dark stimulus was of greater probability than that to the bright stimulus.

In both figures, no clear region of suppression was observable surrounding the excitatory region. In no case was significant suppression measured (i.e. random probability minus 1.96 S.D.), indicating that these neurons are best described by push-push mechanisms. Finally, these two neurons are representative of the sample in regards to their response duration, which is much shorter than what has been observed previously in area 17 (e.g. DeAngelis *et al.*, 1993).

### Spatial organization of the RF

#### Basic RF parameters

Based on the reverse correlation data, the geometric center of the RFs ranged from 3.7 to 37.7deg eccentricity, regardless of stimulus contrast. Thus the RFs were sampled from a large extent of the visual field and are likely representative of the region as a whole. The mean subfield size was significantly larger in response to dark as opposed to bright stimuli ( $t = 3.09$ ,  $p = 0.0029$ ,  $n = 66$ ), this can be observed in the number of points above the line of unity in panel A of Figure 5 (see overlap section below). There was nonetheless a significant correlation between the area of the subfields evoked by each contrast ( $r = 0.58$ ,  $p > 0.0001$ ,  $n = 66$ ).

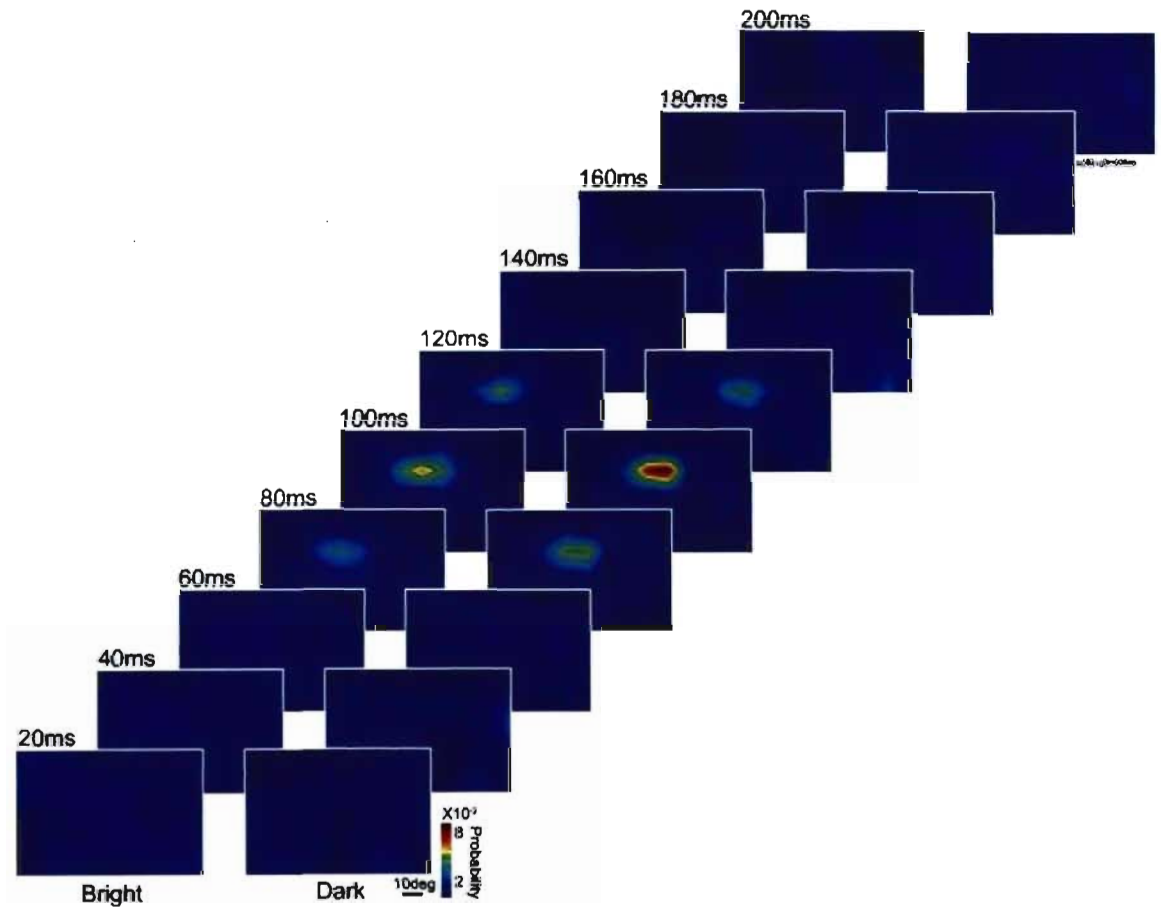


**Figure 3**

Spatio-temporal RF. Series of spatial probability maps taken from selected pre-spike times for temporally coincident responses for an example cell. Note that the response to one contrast was stronger than that to the other.

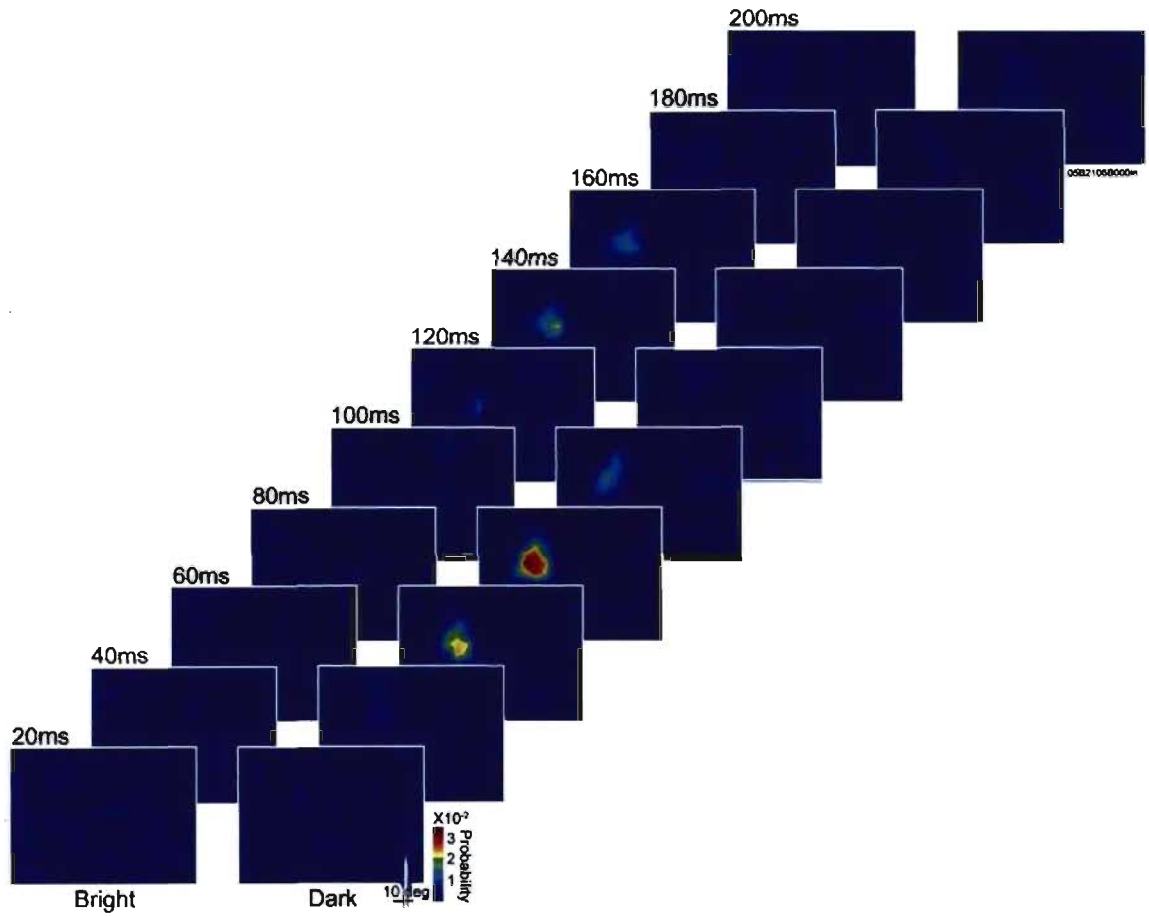


**Figure 4**

Spatio-temporal RF. Series of spatial probability maps taken from selected pre-spike times for temporally out of phase responses for an example cell. Note that as per the neuron in Figure 3, the response to one contrast was stronger than that to the other.

Panel B of Figure 5 shows the relationship between responsive subfield (i.e. same contrast) length and width. For both the bright and dark contrast conditions, the length is approximately one and a half times greater than the width of the RF (bright:  $1.66 \pm 0.49$ , dark:  $1.53 \pm 0.41$ ), and this difference was statistically significant ( $t_{\text{bright}} = 9.36$ ,  $p < 0.0001$ ;  $t_{\text{dark}} = 9.62$ ,  $p < 0.0001$ ,  $n = 66$  for both). Despite the preceding difference between length and width there was nonetheless a statistically significant correlation of these two values ( $r_{\text{bright}} = 0.83$ ,  $p < 0.0001$ ,  $n = 70$ ,  $r_{\text{dark}} = 0.85$ ,  $p < 0.0001$ ,  $n = 66$  for both).

### Overlap

In order to determine whether some PMLS neurons have simple-like RFs, a correlation between the eccentricities of the geometric centers of the responsive subfields to each contrast was carried out. This revealed a significant relationship between these two values ( $r = 0.99$ ,  $p < 0.0001$ ) suggesting that there may be a large amount of overlap between the subfields.



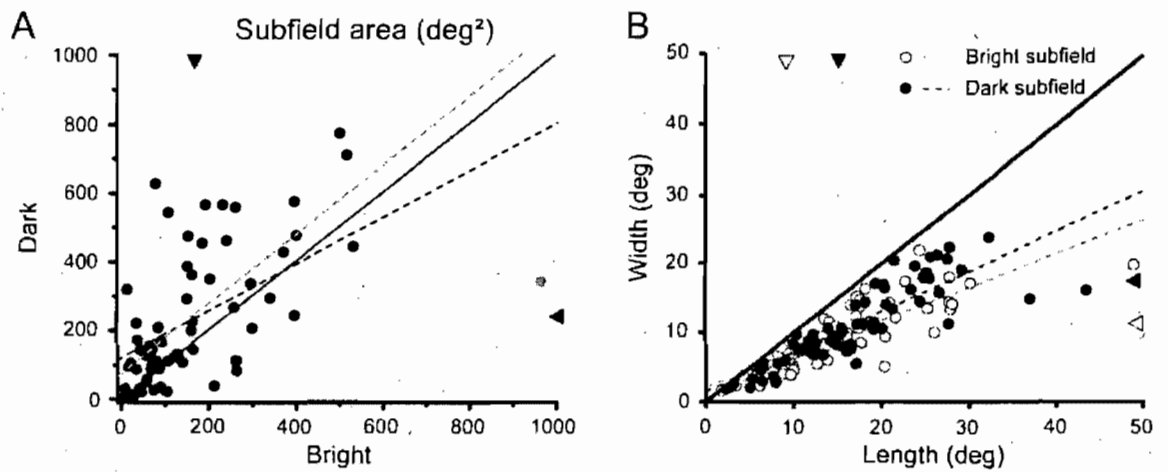


**Figure 5**

Receptive field parameters. **A)** The area of visual field that elicited a significant response when stimulated with bright and dark stimuli. The black dashed line is a linear regression and black arrows indicate mean area. The gray dashed line is with one outlier removed (gray dot at right), the correlation coefficient is then  $r = 0.68$ ,  $p < 0.0001$ ,  $n = 65$ . **B)** Comparison of the length and the width of PMLS RFs. Gray and black dashed lines represent the regression for bright and dark stimuli respectively. Empty and filled arrows represent means for bright and dark stimuli respectively.

In order to determine the extent of overlap between the responsive subfields for each contrast, an OI was calculated. The mean peak OI was  $0.63 \pm 0.40$  (mean  $\pm$  S.D.,  $n = 72$ ), this significantly differed from a value of 1 ( $t = 6.95$ ,  $p < 0.0001$ ), suggesting that there is a substantial portion of the RFs which do not overlap. However, the mean value is not representative of the sample. The distribution of the peak OIs can be seen in Figure 6A, where there were clearly two subsets of neurons, those with either substantial or no overlap. Among those with an OI of 0-0.2, it is important to note that there were 6 neurons which responded to only one stimulus contrast (gray). The remaining 14 neurons generally responded weakly to one of the two stimulus contrasts. Hence the majority (52/72) of neurons which responded to both stimulus contrasts could best be described as spatially overlapping (OI > 0.3), such as the two examples shown in Figures 3 & 4.

As mentioned in the methods section two other OI measures were calculated (see appendix). A significant correlation between these measures and the above mentioned peak latency OI revealed a good correspondence between these values ( $r_{2-D \text{ corr}} = 0.66$ ,  $p < 0.0001$  and  $r_{\text{summation}} = 0.55$ ,  $p < 0.0001$ ) despite the fundamentally different manner in which they were calculated. This suggests that the value of the index is not heavily dependent upon the method used to calculate the OI.

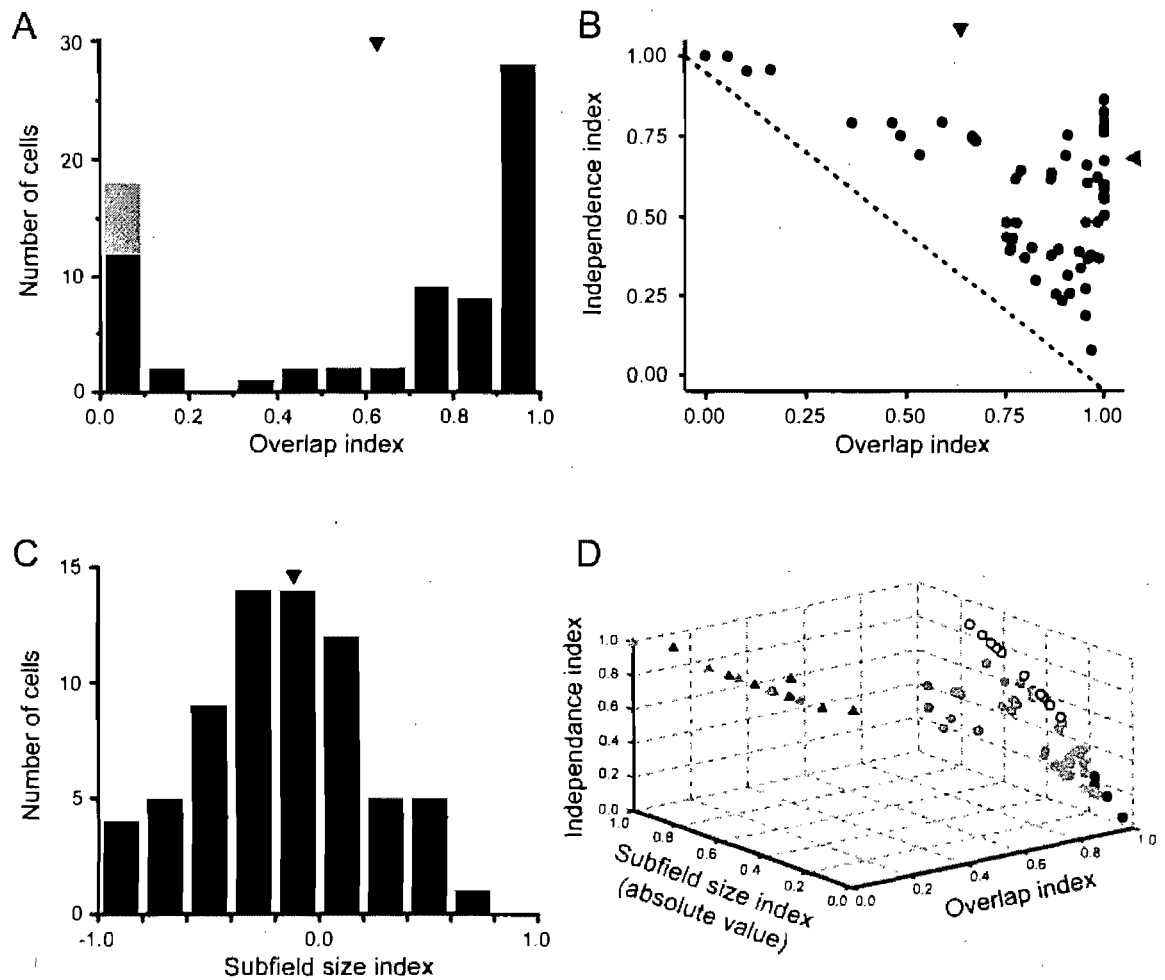


**Figure 6**

RF homogeneity. **A)** Distribution of the overlap index for the sample of neurons. The portion of the left most bar that in gray represents those neurons which responded uniquely to one contrast. **B)** Relationship between overlap and independence indices. Note that all neurons lie above the line of unity because the OI applies to the smaller subfield, while the II applies to the area of both subfields. **C)** Histogram of SSI which was biased towards negative values for the sample, however a large range of values were observed. **D)** Three dimensional plot of the indices presented in panels A-C. It can clearly be seen that the parameter with the greatest discriminating power is the overlap index. Cells tend to fall into two large groups. The juxtaposed and distant cells seem indistinguishable since the main discriminating characteristic is the distance between the centers of the subfields, which is not represented. Arrows represent mean values, and the dashed stroke in B is the line of unity.

As the response area to each stimulus contrast was not identical, which could bias the OI (see methods), an II was calculated which reflects the extent to which the percentage of subfield area does not overlap. As the scatter plot in Figure 6B reveals, these indices measure two different aspects of the superposition of the subfields. A subset of neurons present the profile expected, as the II increases the OI decreases. However, for another subset of cells no strict relationship exists between these two values. This is due to the fact that one subfield is much larger than the other. This was quantified using the SSI (see methods). The histogram in Figure 6C shows that for the majority of neurons, there is no large difference in the size of the subfields. This can be seen by the peak of the distribution which is centered close to 0, indicative of subfields of equal size. However, a non-negligible proportion (17/72) of neurons had one subfield that covered at least 50% more of the visual field than the other subfield. Moreover, the distribution was not centered at zero ( $t = 2.23$ ,  $p = 0.0289$ ), due to a bias towards larger dark responsive subfields (mean SSI of -0.12).

#### Cellular classification

When the three above indices are combined, as in Figure 6D, there are two subgroups which can clearly be distinguished. The OI is the metric which distinguishes these two groups of cells. As mentioned above (panel 6A), the vast majority of cells (52/66) demonstrate a substantial degree of overlap (circles), while the other cells (14/66) exhibit little to no overlap (triangles; note

that the 6 monocontrasts cells have been excluded from this panel). Three examples of neurons with overlapping RFs may be seen in the left panels of Figure 7, while two no-overlap examples are presented in the left panel. The two groups have been further divided into three and two subgroups respectively (see methods for criteria). In Figure 6D, the filled black circles represent neurons for which the subfields were superimposed and almost perfectly matched ( $n = 4$ ; see Figure 7A for a representative example). Filled gray circles in Figure 6D are cells that exhibited overlap however the match was not as good ( $n = 37$ ; example Figure 7B). Empty circles (Figure 6D) represent neurons for which one subfield was much smaller than the other, and which was centered within the larger subfield ( $n = 10$ ; example Figure 7C). Two subgroups were distinguished for the cells with little to no overlap, juxtaposed (dark triangles;  $n = 8$ ; example Figure 7D) and distant (empty triangles;  $n = 6$  example Figure 7E). Juxtaposed cells had subfields which minimally overlapped ( $OI < 0.2$ ) but which were in close proximity, while distant cells had non abutting subfields. Note that although the description of the juxtaposed neurons may *prima facie* seem like a simple cell, they are in fact different. A simple cell would show a push-pull mechanism, while the juxtaposed neurons exhibited push-push response profiles.

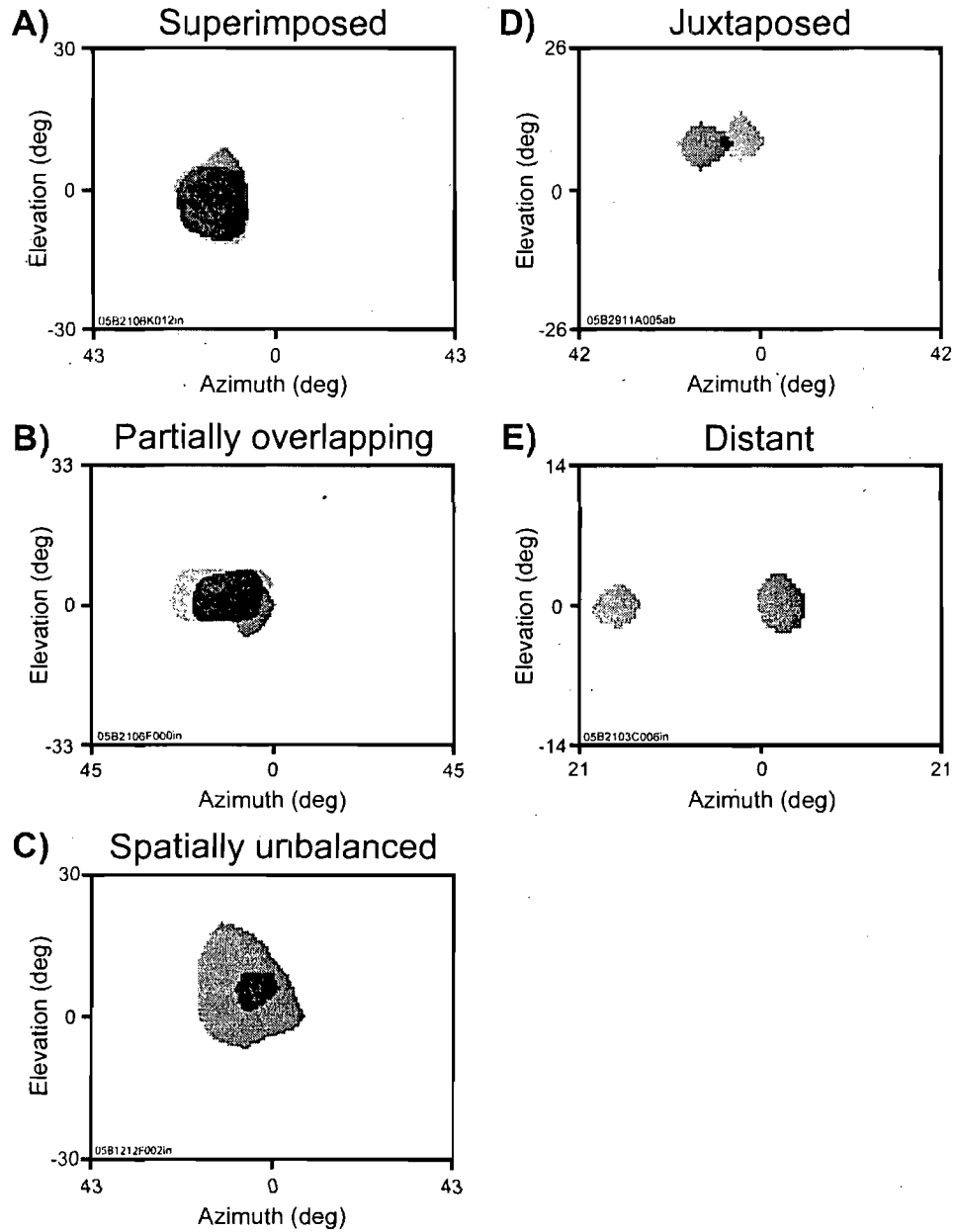


**Figure 7**

Examples of receptive field organization. A-C) Examples of RFs which exhibit varying levels of overlap, while examples in D & E) show little to no overlap. Presented are; A) superimposed, B) overlapping, C) spatially unbalanced, D) juxtaposed, and E) distant RF types. The lightest, mid-range and darkest regions are indicative of areas that responded to bright, dark and both contrast respectively.

## Temporal response profile

### Response latencies

The cumulative sum of response latencies is presented in Figure 8A for the first and last significant response, as well as the peak. Note that neurons that did not respond to one contrast have been excluded. It can be seen that the response to dark stimuli slightly precedes that to bright stimuli for the first and peak responses, while the opposite applies to the last significant response. Statistical analysis using a Wilcoxon signed rank test revealed that both the median peak (bright: 93ms, dark: 91.5ms) and last (bright: 133ms, dark: 135ms) latencies were not significantly different between contrasts ( $W = 4586.5$ ,  $p = 0.3699$ ,  $n = 66$ ,  $W = 4296$ ,  $p = 0.6737$ ,  $n = 66$ ). However, the median first latency was significantly shorter for dark stimuli (bright: 69.5ms, dark: 59ms;  $W = 4857$ ,  $p = 0.0333$ ,  $n = 66$ ), this is the only measure for which the difference was present from the first almost to the last neuron. Given these results one would expect most neurons to respond in a manner similar to that seen in Figures 3 and 9A, that is to say with identical temporal response profiles. However this was not the case.

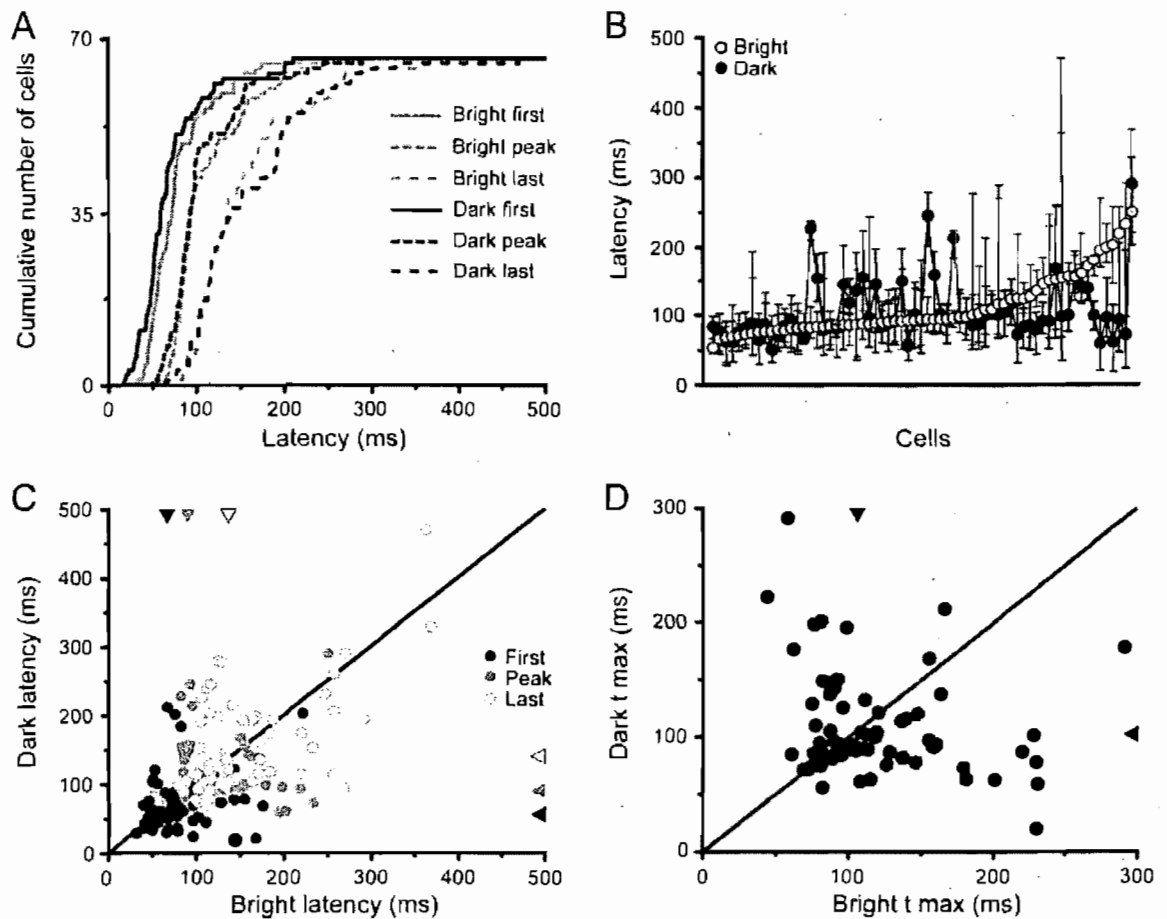


**Figure 8**

Response latencies. **A)** Cumulative sum of response latencies for both bright and dark stimuli. Note that for this and following panels the neurons with longer latencies may be responsive to stimulus offset rather than exhibiting a very long delay to stimulus onset. **B)** Peak latencies to bright stimuli (empty dots) arranged in ascending order, for which the bars represent first and last latencies. Each point along the abscissa is paired with its respective latencies to dark stimuli (filled dots). This demonstrates that a large proportion of neurons exhibit variability in peak response timing. Note that most neurons had peak responses to bright stimuli within a short time window (50% of cells had peak responses within a 44ms period). The same figure sorted according to peak dark responses had a similar profile (50% of cells peaked within a 35ms window). **C)** Scatter plot of the three latency measures demonstrating the variability mentioned in panel B. **D)** Distribution of  $t$  max values (see methods) which reveals that the observed variability cannot be attributed to the method used to access the latencies presented above. Arrows represent median values.



There is variability in the latencies between contrasts for each cell which is masked by the pooling of the data in 8A. This may be visualised in Figure 8B, where the peak latencies are presented in ascending order for the bright subfield, and the corresponding dark subfield latency is presented at the same position on the abscissa. It can be seen that a number of neurons had latencies which were stimulus contrast dependent. These are the non-overlapping data points. This may also be seen by the non negligible proportion of neurons which lie away from the line of unity in the scatter plot in panel C. Hence, despite the lack of significant differences described above (panel A), the response latencies of a single cell to different contrasts may be asynchronous, such as the cell in Figure 9B. Therefore the timing of the responses was compared once again, but maintaining the pairing of bright and dark latencies for each cell in order to determine whether the asynchronous responses significantly differed from zero. This was achieved by reflecting all data points that lie above the line of unity, in Figure 8C, below it (i.e. equivalent to reclassifying the data, on a neuron by neuron basis, according to the longest and shortest latency). This analysis revealed that the median response latency did indeed differ for first and last response, as well as peak latency between stimulus contrasts ( $W_{\text{first}} = 3166$ ,  $p < 0.0001$ ,  $W_{\text{last}} = 3455.5$ ,  $p = 0.0001$ ,  $W_{\text{peak}} = 3268.5$ ,  $p < 0.0001$ ,  $n = 66$  for all). This difference is reflected in the fact that a majority of neurons had a difference in response latency superior to 10ms for first (45/66), last (53/66) and peak (40/66) latencies. Median absolute differences were 18, 28, and 16ms respectively.

Although these latency measures differed in a contrast dependent manner for some cells, the relative timing of first, last, as well as peak responses may be irrelevant for the system. An alternative possibility could be that the subfields which exhibited maximal overlap would occur at the same pre-spike time. The time of maximum overlap ( $t_{max}$ ) for each subfield was therefore compared for each cell and is presented in Figure 8D. There is clearly a large degree of scatter in the data with no linear relationship. Although a number of neurons lie close to the line of unity, this is not the case for all cells. If a difference of 10ms (consistent with the value used above) either side of the line of unity is allotted to compensate for measurement error, there are only 13/66 neurons which have maximally overlapping RFs at similar pre-spike times. The median absolute difference in  $t_{max}$  was 31ms. This is consistent with the temporally asynchronous responses observed with the latency data above.

### Response phase

The preceding section demonstrated that some of the neurons exhibited temporal responses which were asynchronous, however the importance of a delay (say 15ms) between first responses to each contrast is dependent upon the duration of the response. We quantified the extent to which the response to both contrasts were phase shifted. To achieve this, the longer of the two response durations was considered as one cycle. The longer duration was chosen as it provides a more conservative estimate. Dividing the difference

between two contrast latencies (say first significant response) by response duration gives values between  $\pm \infty$ , for which negative values indicate that the dark stimuli evoked a response X phases earlier than the bright response, and the opposite holds for positive values. In order to help visualise the significance of this value two examples can be found in Figure 9A&B. The cell presented in panel A has a phase shift of approximately 0 for all three latencies (first: -0.13; peak: 0.02, last: -0.02), while the cell in panel B has a shift of approximately 1 (first: -1.13; peak: -0.93, last: -1.02). The distribution of neurons as a function of the phase shift between two responses is presented in the insert of Figure 10A. The mean phase shifts were close to zero (for first, peak and last responses they were -0.08, -0.02, and 0.03 respectively) and none of the measures significantly deviated from zero ( $t_{\text{first}} = 0.83$ ,  $p = 0.4121$ ,  $t_{\text{peak}} = 0.24$ ,  $p = 0.8132$ ,  $t_{\text{last}} = 0.27$ ,  $p = 0.7863$ ,  $n = 66$  for all three). In order to better appreciate the proportion of neurons which had phase shifted responses, the negative values have been reflected about the ordinate (Figure 10A). The phase shifts were similar across the three measures, as evidenced by the 1<sup>st</sup>, 2<sup>nd</sup> and 3<sup>rd</sup> quartiles for the first (0.08; 0.18; 0.59), peak (0.09/0.18/0.65) and last phase shifts (0.17/0.27/0.67). These values clearly demonstrate that an important proportion of neurons had a phase shifted response, regardless of how it was assessed (first/peak/last).

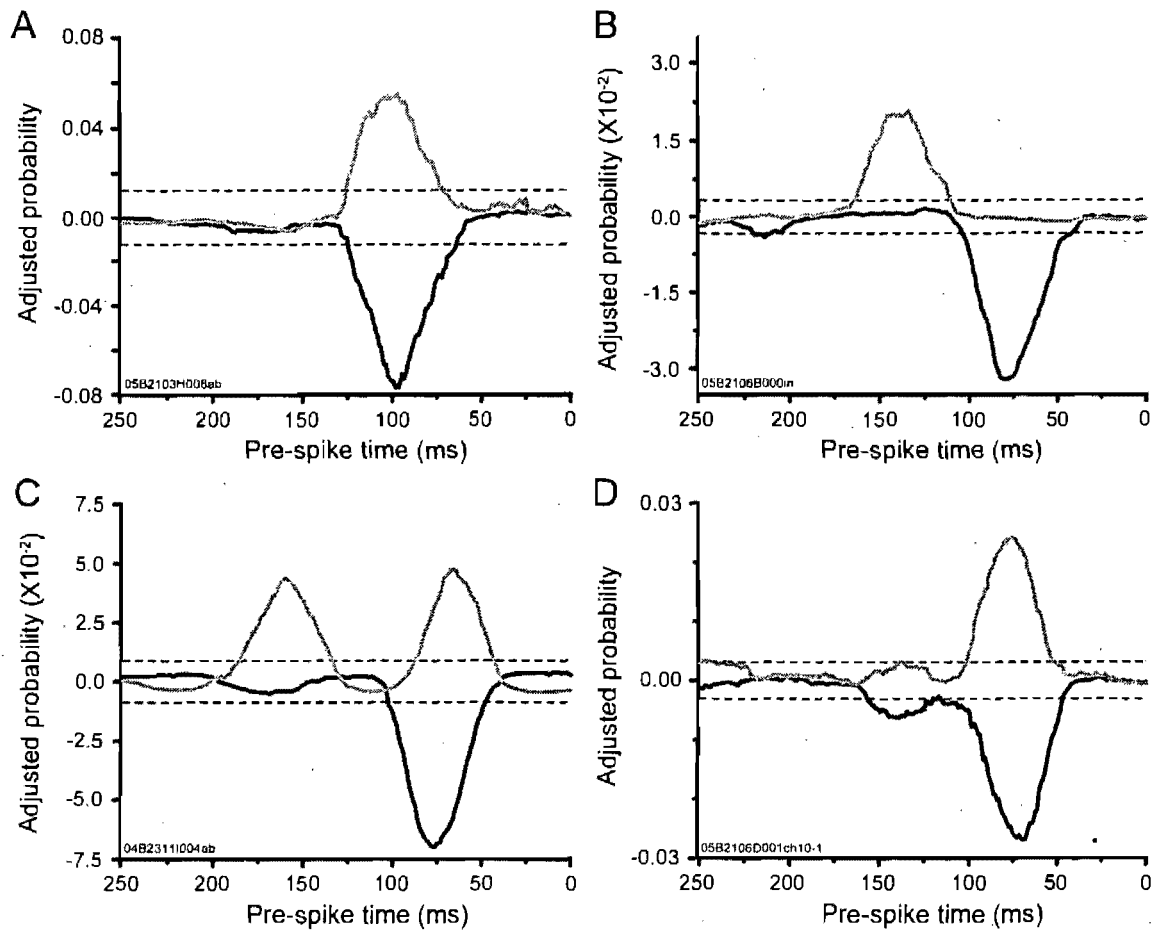


**Figure 9**

Temporal response profiles. The curves were taken from the point in the spatio-temporal profiles which exhibited the maximal response. All probabilities from that spatial position throughout the analysis period are presented. **A)** Synchronous response to bright and dark stimuli. For this and following panels, the calculated random probability has been subtracted in order to help visualise suppressive effects had they been present. **B)** Temporally out of phase response. In this case the latency for the bright stimulus is greater than that for the dark stimulus. **C)** Example of a typical bi-lobed response to bright stimuli. **D)** Typical bi-lobed response for dark stimuli. Note the small non-significant deflection of the profile in response to bright stimuli. The timing is similar to that of the curve for dark stimuli.

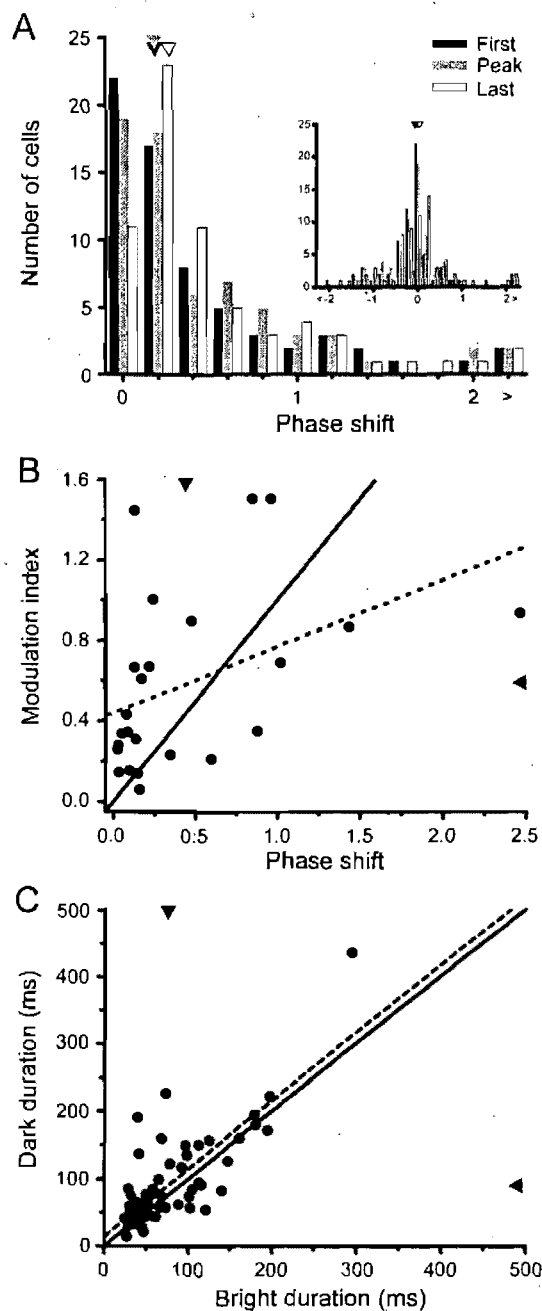


**Figure 10**

Temporal characteristics of the response. **A)** Distribution of neurons according to the temporal phase shift of the response. Inset is the same data prior to collapsing positive and negative values. Values have been collapsed for ease of viewing. **B)** Relationship between temporal phase shift and the modulation index. **C)** Duration of the response (first to last latency) to stimuli of both contrasts. Arrows and dashed lines represent means and regressions.

Despite spatially overlapping subfields, neurons with large phase shifts would be ideally suited to exhibit high MI's in response to gratings as is sometimes seen in PMLS (Zumbroich & Blakemore, 1987; Ouellette *et al.*, 2007). If this were the case, then these previous reports would not have revealed spatially separate ON and OFF RFs (or tested with overly low spatial frequencies), but rather would have observed temporally displaced contrast dependent responses. The capacity of the phase shift to predict the MI was assessed with a correlation. This was carried out for the phase shift for first, peak and last latencies. Only one significant correlation (Figure 10B) was observed between the first response phase shift (absolute value) and MI ( $r = 0.43$ ,  $p = 0.034$ ,  $n = 24$ ). The values for peak were  $r = 0.34$ ,  $p = 0.1067$ ,  $n = 24$  while that for the last response was  $r = 0.34$ ,  $p = 0.1052$ ,  $n = 24$ . This suggests that PMLS neurons, at least via the timing of their initial response, act as temporal filters, which in turn explains the occasional high MI values reported in this region.

### Response duration

In order to better grasp the temporal dynamics of the response, the duration was assessed for the two contrasts. The mean response duration to dark stimuli was greater than that to bright stimuli (bright:  $75.2\text{ms} \pm 51.5$ , dark:  $89.4\text{ms} \pm 66.2$ ;  $t = 2.79$ ,  $p = 0.0069$ ), which is reflected by the greater number of data points (40/66) above the line of unity in Figure 10C (25/66 lie below, and one neuron is on the line of unity). The proportions did not significantly differ

however ( $\chi^2 = 3.46$ ,  $p = 0.0628$ ,  $df = 1$ ), although a trend is present. The response durations to bright and dark stimuli were significantly correlated ( $r = 0.78$ ,  $p < 0.0001$ ,  $n = 66$ ) suggesting that the same or similar mechanisms are responsible for both responses.

### Multi-lobed responses

A subset of 19 neurons had more than one clearly distinct response peak in the temporal domain for at least one contrast (Figure 9C&D). The cell in panel C is representative of bright bi-lobed cells in that the probability of the secondary response is approximately equivalent to that of the first. While for the dark bi-lobed cells, including the example in panel D, the probability of the secondary peak is far below that of the first. Moreover, a non-significant secondary bright peak occurs simultaneously with that of the secondary dark peak. Of the 19 multi-lobed neurons, 5 and 12 had a secondary lobe for bright and dark stimuli respectively, while one cell had a secondary lobe for each, and a final cell exhibited many lobes (3 bright, 2 dark). The proportion of bright or dark only bi-lobed cells was not significantly different ( $\chi^2 = 2.88$ ,  $p = 0.0896$ ,  $df = 1$ ), although a trend is present for there to be a greater number of secondary peaks for dark stimuli. Regardless of the number of response lobes, of the 7 neurons which had a secondary response to bright stimuli, 3 occurred prior to the main peak, while this occurred only once among the 14 neurons with a secondary dark response. These proportions significantly differed, that is more bright than dark multi-lobed neurons' secondary response occurred prior to the

main peak ( $\chi^2 = 3.86$ ,  $p = 0.0494$ ,  $df = 1$ ). The median duration of the secondary peak was not significantly shorter than that of the first for bright stimuli ( $X_{\text{peak1}} = 72.9 \pm 48.9$ ,  $X_{\text{peak2}} = 36.8 \pm 23.4$ ;  $W = 3$ ,  $p = 0.0781$ ,  $n = 7$ ) although a strong trend was present, while the secondary peaks were significantly shorter than the first for dark stimuli ( $X_{\text{peak1}} = 83.9 \pm 43.6$ ,  $X_{\text{peak2}} = 33.6 \pm 24.0$ ;  $W = 14$ ,  $p = 0.0001$ ,  $n = 14$ ).

The bi-lobed responses could be explained via two separate mechanisms; 1- the two responses could arise from separate inputs, either from separate regions or from one region but temporally offset. 2- a response could be evoked by the onset and offset of the stimulus. In order to determine whether the latter was the case, the inter-response timing (the absolute difference between latency measures for each lobe) was compared to the duration of the stimulus. If the bi-lobed response is strictly an ON-OFF type response then stimulus duration should be an excellent predictor of the inter-response duration. A significant correlation was observed for both the inter-peak and inter-last response with stimulus duration ( $r_{\text{inter-peak}} = 0.49$ ,  $p = 0.0242$ ;  $r_{\text{inter-last}} = 0.48$ ,  $p = 0.0273$ ,  $n = 21$  for both; note that the  $n$  is greater than the number of bi-lobed cells since two cells had at least one secondary lobe for both contrasts), while only a trend was present for inter-first response timing ( $r = 0.42$ ,  $p = 0.0608$ ,  $n = 21$ ). Although these results demonstrate a significant relationship between the inter-response timing and stimulus duration, the slope of the functions (2.9, 3.2, and 3.4 for first, peak, and last response respectively) clearly demonstrate that it is not a one for one relationship. Although a slope of



1 should not be expected given the known differences in onset and offset latencies (Bair *et al.*, 2002), these large slopes are not consistent with a secondary response due to stimulus offset.

### Afferents

Both the spatial and temporal profiles described above suggest that the bright and dark stimuli are not treated in an identical manner, suggesting that different inputs may underlie these responses. This was further investigated by comparing response parameters for both contrasts. A measure of contrast dependent response amplitude was calculated (MRI: see methods) and the mean value was  $-0.13 \pm 0.25$  when cells responding to only one contrast were not included. For comparison, the cell shown in Figure 9A had a MRI of  $-0.16$ , close the mean value for the sample. On average the dark response was stronger than the bright one, as reflected by a mean MRI that was significantly below zero ( $t = 4.19$ ,  $p < 0.0001$ ,  $n = 66$ ).

Given the timing differences described in previous sections, the related measure of response slope was also compared between contrasts. The temporal profiles of both contrasts were normalised to each neuron's peak probability. The mean normalised slopes (% change in probability per ms) for the ascending portion of the response to bright and dark stimuli were  $0.0194 (\pm 0.0117)$  and  $0.0228 (\pm 0.0085)$  respectively, while for descending portion it was  $-0.0163 (\pm 0.0108)$  and  $-0.0211 (\pm 0.0116)$ . There was no strict relationship of

slopes between the two contrasts ( $r_{\text{ascending}} = 0.24$ ,  $p = 0.0525$ ;  $r_{\text{descending}} = 0.21$ ,  $p = 0.0885$ ,  $n = 66$  for both) although trends were present. As a sample, the slopes were significantly steeper for the dark stimuli as compared to those for bright stimuli ( $t_{\text{ascending}} = 2.14$ ,  $p = 0.0360$ ;  $t_{\text{descending}} = 2.78$ ,  $p = 0.0072$ ,  $n = 66$  for both). This can indirectly be seen in the lower median values (arrows) for dark stimuli in Figure 8C. The ascending portion of the curve was steeper than the descending portion for both contrasts ( $t_{\text{bright}} = 15.51$ ,  $p < 0.0001$ ;  $t_{\text{dark}} = 20.69$ ,  $p < 0.0001$ ,  $n = 66$  for both). This is reflected in the greater spacing between peak and last significant response median values (Figure 8C) than between first and peak median values.

#### RF property prediction

We sought to determine how well the appropriate parameters from the spatio-temporal RF maps could predict responses to gratings (25, 24 and 18 cells for direction, SF and TF respectively). One would expect, for example, that RFs with a low OI would have a high MI. Rapidly, the mean properties of these neurons to gratings were; a DI of  $0.76 \pm 0.32$  ( $n = 25$ ), a mean optimal SF of  $0.08 \pm 0.05$  ( $n = 24$ ) and a mean optimal TF of  $3.97 \pm 2.04$  ( $n = 18$ ), which are similar to reported values from our laboratory (Villeneuve *et al.*, 2006a; Ouellette *et al.*, 2007).

### Direction selectivity

The relationship with directional parameters will be treated first. The extent of direction selectivity, assessed with the DI, was not significantly correlated with the area of either subfield ( $r_{\text{bright}} = -0.36$ ,  $p = 0.0786$ ,  $r_{\text{dark}} = -0.08$ ,  $p = 0.6964$  and  $n = 25$ ). Similarly, the DI was not correlated with the OI ( $r = 0.11$ ,  $p = 0.6089$ ), nor with the II ( $r = 0.35$ ,  $p = 0.0861$ ,  $n = 25$ ). Interestingly, the DI significantly increases as the absolute SSI deviates from zero ( $r = 0.64$ ,  $p < 0.0006$ ), that is direction selectivity increases as the imbalance between subfield area accrues. Similar comparisons with temporal domain parameters, revealed no significant correlation of response duration with the DI ( $r_{\text{bright}} = -0.37$ ,  $p = 0.0658$ ;  $r_{\text{dark}} = -0.33$ ,  $p = 0.1117$  for  $n = 25$ ). Note that two counterintuitive trends were present. The first suggests that direction selectivity gets weaker as the area of the bright but not dark responsive subfield increases, and secondly that shorter response durations correlate with stronger directional responses.

A similar analysis was carried for direction tuning BW (half-width at half-height) and no significant relationship was observed between direction BW and subfield area ( $r_{\text{bright}} = 0.19$ ,  $p = 0.3532$ ;  $r_{\text{dark}} = 0.03$ ,  $p = 0.8752$ ,  $n = 25$  for both). Similarly, no significant correlation was observed with the different spatial measures ( $r_{\text{OI}} = -0.09$ ,  $p = 0.6633$ ;  $r_{\text{II}} = -0.13$ ,  $p = 0.524$ ;  $r_{\text{SSI}} = -0.20$ ,  $p = 0.3351$ ,  $n = 25$  for all three test). The duration of the response was not a better predictor of direction BW ( $r_{\text{bright}} = -0.30$ ,  $p = 0.1433$ ;  $r_{\text{dark}} = -0.32$ ,  $p = 0.1231$ ,  $n = 25$  for both).

### Spatial frequency

The same analysis was carried for SF, using data from 24 neurons. The subfield area was not a good predictor of the SF which evoked the maximal response ( $r_{\text{bright}} = 0.01$ ,  $p = 0.9811$ ;  $r_{\text{dark}} = -0.25$ ,  $p = 0.2314$ ,  $n = 24$  for both). No significant correlations between optimal SF and OI, II or SSI were present ( $r_{\text{OI}} = -0.13$ ,  $p = 0.5355$ ;  $r_{\text{II}} = 0.06$ ,  $p = 0.77$ ;  $r_{\text{SSI}} = -0.14$ ,  $p = 0.5118$ ,  $n = 24$  for all).

Similarly, SF BW was not correlated with subfield area ( $r_{\text{bright}} = 0.25$ ,  $p = 0.2794$ ;  $r_{\text{dark}} = 0.18$ ,  $p = 0.4551$ ,  $n = 20$  as 4 neurons were classified as low pass), nor with OI, II or SSI ( $r_{\text{OI}} = 0.08$ ,  $p = 0.7348$ ,  $r_{\text{II}} = -0.41$ ,  $p = 0.0705$ ,  $r_{\text{SSI}} = -0.37$ ,  $p = 0.1082$ ,  $n = 20$  for all). Subfield response duration was not significantly correlated with SF BW ( $r_{\text{bright}} = 0.02$ ,  $p = 0.9380$ ,  $n = 19$ ;  $r_{\text{dark}} = 0.01$ ,  $p = 0.9753$ ,  $n = 20$ ). Note that one trend is present (II), where greater independence of subfields leads to tighter tuning.

Based on the response at the optimal SF, the mean MI was calculated. This index was not correlated with any of the three indices from the spatial domain ( $r_{\text{OI}} = 0.06$ ,  $p = 0.7657$ ;  $r_{\text{II}} = 0.01$ ,  $p = 0.9814$ ;  $r_{\text{SSI}} = 0.22$ ,  $p = 0.2950$ ,  $n = 24$  for all). Similarly, the MI was not significantly correlated with response duration ( $r_{\text{bright}} = -0.11$ ,  $p = 0.5992$ ;  $r_{\text{dark}} = -0.17$ ,  $p = 0.4243$ ,  $n = 24$  for all).

## Temporal frequency

Equivalent comparisons for TF, revealed that the latter could not accurately be predicted based on response duration for either contrast ( $r_{\text{bright}} = -0.21$ ,  $p = 0.4120$ ;  $r_{\text{dark}} = -0.29$ ,  $p = 0.412$ ,  $n = 18$  for both). The same analysis was carried out with first, last and peak response latency for which no significant correlations were observed (bright:  $r_{\text{first}} = -0.27$ ,  $p = 0.9146$ ,  $r_{\text{last}} = -0.21$ ,  $p = 0.3961$ ,  $r_{\text{peak}} = -0.23$ ,  $p = 0.3568$ ; dark:  $r_{\text{first}} = 0.01$ ,  $p = 0.9805$ ,  $r_{\text{last}} = -0.30$ ,  $p = 0.2302$ ,  $r_{\text{peak}} = 0.01$ ,  $p = 0.9533$ ,  $n = 18$  for all). The inter contrast latency difference (absolute value) was calculated and no significant correlation was observed for the response latencies with the optimal TF ( $r_{\text{first}} = 0.07$ ,  $p = 0.7683$ ,  $r_{\text{last}} = -0.07$ ,  $p = 0.7919$ ,  $r_{\text{peak}} = 0.09$ ,  $p = 0.7349$ ,  $n = 18$  for all). The related measure of time between first and peak response, as well as that between peak to last response was also compared to the TF, again no significant correlations were observed (bright:  $r_{\text{first-peak}} = 0.21$ ,  $p = 0.4050$ ;  $r_{\text{peak-last}} = -0.20$ ,  $p = 0.4319$ ; dark:  $r_{\text{first-peak}} = -0.02$ ,  $p = 0.9378$ ;  $r_{\text{peak-last}} = -0.33$ ,  $p = 0.1795$ ,  $n = 18$  for all tests).

With TF BW no significant correlation was observed with response duration ( $r_{\text{bright}} = -0.06$ ,  $p = 0.8186$ ;  $r_{\text{dark}} = -0.15$ ,  $p = 0.6047$ ,  $n = 15$  for both; 2 low pass and 1 high pass cell have been eliminated). The same analysis was carried out with the response latencies and no significant correlations were found with TF BW (bright:  $r_{\text{first}} = 0.26$ ,  $p = 0.3524$ ,  $r_{\text{last}} = -0.02$ ,  $p = 0.9395$ ,  $r_{\text{peak}} = -0.07$ ,  $p = 0.8038$ ; dark:  $r_{\text{first}} = -0.16$ ,  $p = 0.5594$ ,  $r_{\text{last}} = -0.21$ ,  $p = 0.4493$ ,  $r_{\text{peak}} = -0.28$ ,  $p = 0.3184$ ,  $n = 15$  for all). Similarly, the absolute difference in latency

between contrasts was calculated and no significant correlation was observed between the response latencies and TF BW ( $r_{\text{first}} = -0.26$ ,  $p = 0.3411$ ,  $r_{\text{last}} = -0.23$ ,  $p = 0.4018$ ,  $r_{\text{peak}} = -0.22$ ,  $p = 0.4238$ ,  $n = 18$  for all). As above, the time between first and peak, as well as peak to last was not correlated to TF BW (bright:  $r_{\text{first-peak}} = 0.22$ ,  $p = 0.4256$ ,  $r_{\text{peak-last}} = -0.003$ ,  $p = 0.9908$ ; dark:  $r_{\text{first-peak}} = 0.29$ ,  $p = 0.2968$ ,  $r_{\text{peak-last}} = -0.10$ ,  $p = 0.7302$ ,  $n = 15$  for all tests).

### Test of linear model

The primary goal of this study was to determine whether PMLS neurons are involved in linear spatial integration. If PMLS neurons are linear, then it should be possible to predict their preferred properties based on their first-order spatio-temporal profiles. If not, then one must assume that they engage in some form of non-linear analysis. The previous section addressed this issue using descriptive indices based on the RF profiles. Indices are unable to entirely capture the neuronal response, therefore a further test was carried out using the entire spatio-temporal profile. In order to examine how well the first order approximation of PMLS RFs would predict the measured neuronal responses to gratings, three linear models were created. It should be noted that given the present testing paradigm only SF can be assessed with these models. Direction selectivity would require second-order analyses, and predicted TFs would be heavily influenced by stimulus duration rather than inherent neuronal processing.

The prediction from the RF based model (see methods) was not significantly correlated with the optimal SF, whether the RF width was taken from the bright, dark, or a weighted mean spatio-temporal profile ( $r_{\text{bright}} = 0.05$ ,  $p = 0.8271$ ,  $r_{\text{dark}} = 0.23$ ,  $p = 0.2762$ ,  $r_{\text{weighted\_mean}} = 0.18$ ,  $p = 0.3892$ ,  $n = 24$  for all). Given the similarity of this model with that of Movshon *et al.* (1978a), the actual RF width was divided by the predicted RF width based on half the optimal SF (the half cycle was chosen in order to remain consistent with previous work, despite deviating from what one would predict for a complex like RF). This gave a ratio of  $1.51 \pm 1.12$  and  $1.64 \pm 0.96$  for bright and dark subfields respectively. These values do not correspond to either the simple or complex cells reported by Movshon *et al.* (1978a, b).

The product model was a better predictor of the optimal SF than was the RF based model. The optimal SF was predicted for bright and dark subfields, as well as a probability normalized mixture (complex-like) and a subtraction of both (simple-like). Only the dark subfield based prediction exhibited a significant correlation with the measured optimal SF ( $r = 0.44$ ,  $p = 0.0353$ ,  $n = 24$ ), while the bright subfield based prediction exhibited a trend ( $r = 0.03$ ,  $p = 0.0892$ ,  $n = 24$ ). No correlation was observed for the mixture and subtraction versions, the values of which may be seen in Table 1.

Correlating measured optimal SF and the SF prediction of the third model (spatial correlation model) revealed no significant relationship. However, a clear trend is present for the dark subfield based prediction ( $r = 0.41$ ,  $p = 0.053$ ,  $n = 24$ ; see Table 1 for other values.). It could be argued that thresholding the

spatio-temporal maps could have biased the predictions. Therefore, the same analysis was carried out based on the probability values prior to passing the threshold. Neither the product nor the spatial correlation models showed a significant correlation with the optimal SF (see Table 1 for values). Note that the RF based model cannot be carried out prior to thresholding.

Generally the linear models were poor predictors of the actual neuronal response (Table 1). This is partly attributable to the fact that the measured SFs were higher than or equal to the predicted value, hence the predictions were biased towards low frequencies and therefore inaccurate. This is consistent with the ratio of  $\approx 1.5$  calculated (see above) for comparison with the work of Movshon *et al.* (1978a)

As demonstrated above, the first-order spatio-temporal RF maps do not allow for an accurate prediction of the optimal grating parameters. One further test to ensure that the RFs could not be described by linear mechanisms similar to simple cells was performed. This was achieved by fitting the spatio-temporal profiles with 2-D Gabor and Gaussian functions and then comparing the fits (see methods). For all cells, the index has a value greater than 0.8, which indicates that a Gaussian is a far better descriptor of the spatio-temporal maps than is a Gabor function. At first glance this unimodal distribution may seem in conflict with the presence of the juxtaposed cells mentioned above (Cellular classification section). This distribution is likely attributable to the fact that the mean SSI among the juxtaposed group was 0.41 and the absolute MRI was 0.22, hence these RFs were spatially unbalanced between contrasts as was the



amplitude of their responses. A spatially asymmetric Gabor would be required in order to obtain a better fit than a Gaussian. While in the latter, the smaller subfield may simply be lost in the tail of the larger subfield leading to little increased error.

#### Subfield fits.

During the spatio-temporal RF analysis process we were confronted with the difficult choice of how to interpolate the data. Unlike other areas, there are no quantitative descriptions of the spatial profile of PMLS neurons (although see Borghuis *et al.*, 2003). For all the above analyses, linear interpolation was chosen as a conservative estimate, although it is unlikely to be an optimal descriptor of PMLS RF profiles. Given the above fits with Gaussians, we chose to determine which of three variations of a Gaussian would best describe the data for future reference. The first was a classical 2-D Gaussian. The second function was a difference of Gaussians (DOG) for which the subtracted Gaussian was attributed a weight ( $w$ ) which was expressed as a percentage of the first. In the extreme case where a DOG is a poor descriptor of the subfields then the weight would be 0, and therefore the function reverts to a Gaussian. Such a function could account for surround suppression even if the latter was non-significant. The third possibility was a truncated Gaussian, effectively limiting the maximal probability and thereby presenting a *plateau*. Again, in an extreme case where the threshold (the level of truncation) would be set to 100% of the Gaussian's maximal probability, then the function reverts back to a

classical Gaussian. An index based on all three LMS values from the fits was calculated as  $I_{\text{Gaussian}} = E_{\text{Gaussian}} / (E_{\text{Gaussian}} + E_{\text{DOG}} + E_{\text{truncated}})$ , and so on for  $I_{\text{DOG}}$  and  $I_{\text{truncated}}$ . The ternary graph representing the relative importance of the LMS for each fit is shown in Figure 11A. Clearly, almost all neurons are described equally well by all three functions, with a few cells showing a slight bias for the truncated Gaussian. Inspection of panels B & C demonstrate that most neurons have a  $w$  of zero and a threshold of 100% (i.e. the function reverts to a Gaussian). This indicates that the spatial maps were best fit by a classical Gaussian function.

## Discussion

### General conclusions

First order reverse correlation with sparse noise stimuli elicited sufficiently robust responses to obtain spatio-temporal profiles among PMLS neurons. These profiles suggest that for the majority of neurons there is a large degree of overlap between bright and dark responsive subfields. This is consistent with complex-like RFs. Furthermore, simple models based on the first order profiles were poor predictors of the optimal parameters to gratings for these same cells. Overall, the data suggest that despite the known linear temporal integration of PMLS neurons (Vajda *et al.*, 2006) spatial integration is to a large extent non-linear.

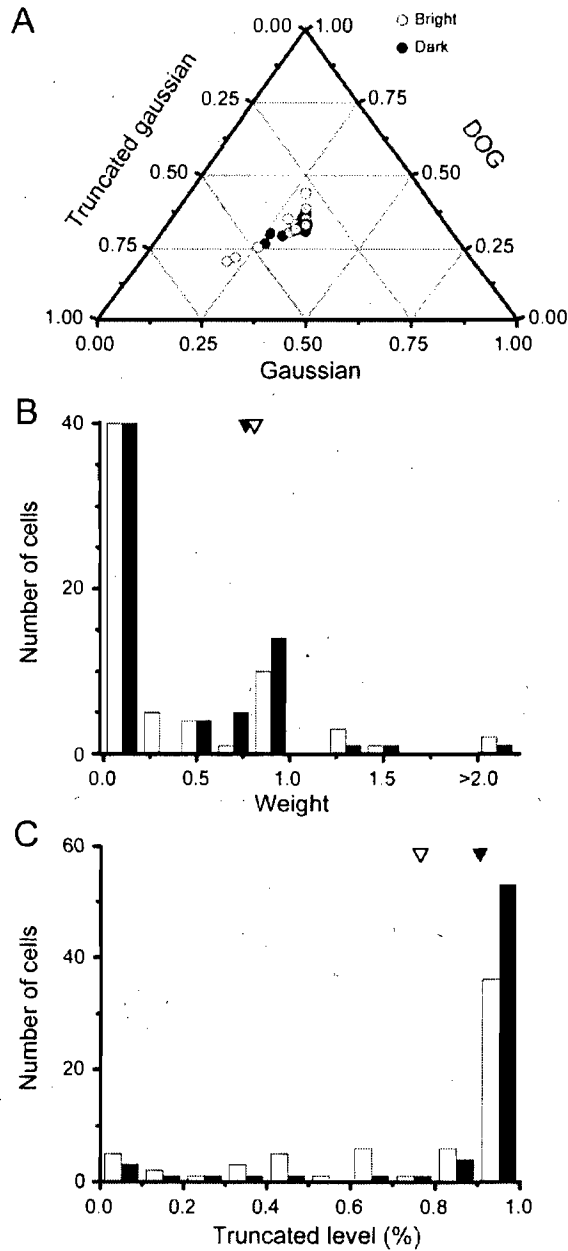


**Figure 11**

Best RF descriptor. **A)** Ternary plot representing the indices of quality of fit for the Gaussian, DOG and truncated Gaussian functions with the measured RFs. **B)** Distribution of weights for the DOG. Most neurons reverted back to a classical Gaussian function (i.e. weights of 0). **C)** Distribution of the truncation level of the best fit for the truncated Gaussian. The fits for most neurons were best when no truncation occurred (i.e. 1.0).

## Methodological considerations

The reverse correlation method used in the present experiment allows for linear analyses but not interaction terms unless unrealistically long acquisition times are used. Given the known projections of area 17 and 18 cells with complex RFs, the LPI, and connections from other extrastriate cortical areas (Berson & Graybiel, 1978; Raczkowski & Rosenquist, 1983; Symonds & Rosenquist, 1984a; Norita *et al.*, 1996) one would expect PMLS neurons to behave in a non-linear fashion. This is not a limiting factor for the present study given the question that motivated this work. Nonetheless, it should be kept in mind that the spatio-temporal profiles in the present study are incomplete descriptions and await further work. Therefore, higher-order analyses of PMLS RFs using dense noise stimuli are currently underway. Beyond its inherent value, this data should prove to be interesting given the proposed homology between area MT in primate and PMLS in cat (Payne, 1993), for which a few discrepancies exist (e.g. lack of plaid pattern motion selectivity in PMLS; Movshon *et al.*, 1985).

## Spatial domain

### Complex like RF profile

The initial question of this study was based on the surprising finding that temporal integration among PMLS neurons was devoid of non-linear interactions for most cells (Vajda *et al.*, 2006). The question therefore concerned the

presence or absence of linear integration in the spatial domain by PMLS neurons. Although there is no strict relationship between simple/complex and linear/non-linear dichotomies (e.g. Movshon *et al.*, 1978a, b), complex RFs in area 17 are non-linear and simple RFs are usually linear. The data in the present study shows that the overwhelming majority of neurons in PMLS had overlapping RFs which are consistent with complex-like RFs. Using RF parameters and derived indices we found no relationship with the preferred parameters for gratings. Moreover, it was shown that a Gaussian distribution is a far better descriptor of PMLS RFs than is a Gabor. This is exactly what one would expect based on feedforward input from supragranular layers of areas 17 and 18 (Maciewicz, 1974; Symonds & Rosenquist, 1984b; Einstein & Fitzpatrick, 1991; Lowenstein & Somogyi, 1991; Shipp & Grant, 1991; Norita *et al.*, 1996) and is consistent with qualitative hand mapping assessments (Zumbroich & Blakemore, 1987). Nor is it surprising to find complex RFs given the known motion processing properties in this area (Toyama *et al.*, 1990; Kim *et al.*, 1997; Mulligan *et al.*, 1997; Brosseau-Lachaine *et al.*, 2001; Villeneuve *et al.*, 2006a).

Similarly, our simple models based on the linear spatio-temporal profiles were generally poor predictors of optimal parameters for gratings. One exception to the poor quality of the predictions was the product model, for which the dark responsive subfields were fair predictors of the neurons preferred SF, and a similar trend was present for the bright subfields. However, when information from both subfields was linearly combined to estimate the optimal SF, the predictions were no longer accurate. This suggests that some form of

linear processing does indeed occur in PMLS, while a non-linear integration of inputs for opposite contrasts occurs. This further justifies the above mentioned interest in higher order analyses among PMLS neurons.

A distinction between the present complex-like neurons and those of previous studies is the lack of a clear response to both stimulus onset and offset (Hubel & Wiesel, 1962; Movshon *et al.*, 1978a; Palmer & Davis, 1981b; Citron & Emerson, 1983; Kagan *et al.*, 2002). It could be suggested that our bilobed cells represent such ON and OFF responses, however as was shown in the results section there was no relationship between inter response latencies of bi-lobed neurons and stimulus duration. Furthermore the majority of neurons were not of the bi-lobed type. Thus classical complex RFs were not observed in the present study.

#### Other RF profiles

Not all neurons exhibited responses that were similar to the prototypical complex like RFs as described by Hubel & Wiesel in area 17 (1962). In particular, 6 out of 72 neurons responded to only one stimulus contrast and 12/72 had a large asymmetry in subfield size between contrasts. Both of these phenomena have previously been reported in area 17 of the cat and V1 in primate (Hubel & Wiesel, 1962; Movshon *et al.*, 1978a; Emerson *et al.*, 1992; Hirsch *et al.*, 2002; Kagan *et al.*, 2002; Martinez *et al.*, 2005; Mata & Ringach, 2005; Hirsch & Martinez, 2006). Similarly, most of these studies have

mentioned, or have consistently shown examples in which the responses are dominated by dark stimuli. This is also consistent with the present data. The latter may partially be attributable to an artefact due to the stimulation protocols used in most sparse noise reverse correlation studies. In the present and other papers, the difference (in  $\text{cd/m}^2$ ) between the stimuli and the background was the same for bright and dark stimuli, which *a priori* seems appropriate. However, using our parameters as an example, the Michelson contrast of each stimulus as compared to background (as opposed to stimulus to stimulus) was 100% for the dark condition while it was 33% for the bright condition. With such parameters it is not surprising that dark stimuli evoke responses of greater probability and that cover a larger area. It is important to note however, that some neurons exhibited the opposite behavior, which was larger probability responses and greater response area to bright stimuli. Therefore, the unequal contrast values do not explain these bright super-responsive cells and presumably an equal proportion of dark super-responsive cells. The uneven contrasts simply explain the greater proportion of neurons which had stronger responses to dark stimuli. Hence under different testing conditions, the proportion of such cells may well be the same for bright and dark stimuli. Their mere presence however remains interesting and requires further study.

In regards to the above mentioned neurons which exhibited subfields of different size (i.e. large SSIs), it is intriguing to speculate as to their function. It is possible that they simply represent random fluctuations due to developmental phenomena. Another possibility is related to spatially detailed motion

processing. The larger of the two subfields could integrate motion signals from a large extent of the visual field, while the smaller subfield would allow for higher SF selectivity. This seems unlikely for four reasons; 1- the measured optimal SFs of PMLS neurons are relatively low. 2- No correlation was found between the SSI and optimal SF or its BW. 3- The ideal way to achieve this would be with a push-pull mechanism, which was not observed in the present experiments. Note that a push-push mechanism could also achieve this given the proper system dynamics. 4- The visual system would have had to evolve to respond to the simultaneous and superimposed presence of dark and bright stimuli within the RF, which seems unlikely.

#### Spatial integration of motion signal

It is generally assumed in vision research that larger RFs allow a better integration of motion signals. However this was not found to be the case in the present study, when RF profiles were compared to the neuronal tuning properties for gratings. It was shown that there was a trend for direction selectivity to increase as the area of the bright (but not dark) responsive subfields decreased. Similarly, the difference in size between both subfields (SSI) was significantly correlated with DI. Although this could be indicative of a process that differs from what is usually assumed, an alternative explanation seems more likely. The greater the motion selectivity of a PMLS neuron, the less likely that same cell is to respond to stationary stimuli. If this is the case,



then our higher-order analyses will reveal larger RFs, which may allow the demonstration of a correlation between RF size and direction selectivity.

In the papers by Movshon *et al.* (1978a, b) simple and complex cells could be distinguished by a ratio of actual RF size and predicted RF size based on optimal SF. While for simple cells the prediction was close to the measured values, complex cells had RFs three times larger than what was predicted. In the present study, we found a ratio of approximately 1.5, which does not correspond to either cell class. This ratio is consistent with the reported low SF tuning of PMLS neurons (Zumbroich & Blakemore, 1987), as well as the lack of a strict correspondence between RF size and acuity among PMLS neurons (Di Stefano *et al.*, 1985). This suggests that PMLS neurons are involved in fundamentally different computations from those found in primary visual cortex. Specifically, the high spatial resolution observed among area 17 neurons with complex RFs would not be required for large field motion processing as previously reported for PMLS neurons (Toyama *et al.*, 1985; Sherk *et al.*, 1995; Kim *et al.*, 1997; Mulligan *et al.*, 1997; Sherk *et al.*, 1997; Brosseau-Lachaine *et al.*, 2001; Sherk & Kim, 2002; Villeneuve *et al.*, 2006a).

Care should be taken in interpreting this ratio however, as the estimate of RF area, which is critical to the calculation of the ratio, is dependent upon the chosen threshold. Similarly, the ratio may also have been influenced by our choice of fullscreen stimulation with gratings, since the spatial extent of visual stimuli has been shown to influence responses in PMLS (Villeneuve *et al.*, 2006a; although this study was carried out with a different stimulus). Therefore

the ratio found among the sample of PMLS neurons is difficult to interpret, beyond the fact that PMLS neurons clearly do not exhibit simple like RFs.

Classically, the MI has been used to distinguish neurons that have or lack segregated ON and OFF subfields (Skottun *et al.*, 1991a). Previous studies have shown that a small number of PMLS neurons have an MI that is indicative of segregated RFs (Zumbroich & Blakemore, 1987; Guido *et al.*, 1990b; Ouellette *et al.*, 2007), this would have been consistent with the possibility of linear spatial integration that motivated this study. The results suggest that the high MI is attributable to factors other than segregated RF subfields. This is in keeping with recent demonstrations that the MI is not necessarily a good indicator of spatial segregation of subfields (Kagan *et al.*, 2002; although see: Mata & Ringach, 2005). It has previously been suggested that complex cells which exhibit a stronger response to one contrast, or the extreme case of monocontrast cells, could be those which also display high MI's in area 17 (Hirsch *et al.*, 2003). This hypothesis was not confirmed with the present sample. The data suggest an alternate explanation however, in that PMLS neurons with a high MI have temporally out of phase responses to each contrast. Thus the high MI values among these neurons do not reflect spatially segregated subfields, but rather are indicative of a peculiar temporal encoding scheme. Such a response profile would be ideally suited for detecting rapid changes in contrast. This is similar to the findings of Vajda *et al.* (2004) suggesting that some PMLS cells are ideally tuned to detect changes in the visual environment. What's more, they observed that approximately 14% of

their neurons changed their response in time, versus 17% of our cells that had an out of phase response (taking cells with an absolute first response phase shift greater than 1). It should be noted however, that there is a fundamental difference between the present results and theirs. In the case of Vajda *et al.* (2004) the responses were biphasic, whether to the preferred or non-preferred direction, whereas in the present study the neurons exhibited monophasic responses. It is the timing of the response of the latter which leads to the similarity of the two response profiles.

As pertains to the spatial resolution of encoding in PMLS, both in absolute and relative terms the optimal SFs that are generally observed are low (Morrone *et al.*, 1986; Zumbroich & Blakemore, 1987; Gizzi *et al.*, 1990; Guido *et al.*, 1990b; Minville & Casanova, 1998). This is likely due to two factors revealed by the present spatio-temporal profiles. Firstly, the RFs may be described as large overlapping push-push subfields. Secondly, no robust inhibitory flanking regions were observed in the first order spatio-temporal profiles. Based on these two points, such a system could be described as a low pass or a band pass filter biased towards lower SFs. This is consistent with the above mentioned optimal SF parameters observed in PMLS.

## Temporal domain

### Response duration

It is interesting to compare the present data and previously reported work concerning the measures of the temporal profile given the similarity in stimuli across reverse correlation studies. In area 17 it has been reported that few if any neurons respond to the type of stimuli used here when the duration is less than 50ms (McLean *et al.*, 1994). In the present study all neurons were tested with stimulus durations below 48ms, and most of them responded best to a 32ms presentation (data not shown). Another difference is that the mean response duration in the present study was much shorter than values reported for area 17 (DeAngelis *et al.*, 1993, 1995b). These results suggest that the input to PMLS neurons in the present study does not arise from area 17 (see below).

### Response slope

Previous work with almost identical stimuli (DeAngelis *et al.*, 1993) reported that the ascending portion of the temporal response profile had a steeper slope than that of the descending phase, which is in agreement with the present data. This suggests that the input along the temporal dimension to both these regions is similar. At first glance these results may seem to contrast with those of Bair *et al.* (2002), who demonstrated that offset latencies were shorter than their onset counterparts in the LGN, striate and extrastriate cortex of the primate. However, there is clearly a distinction to be made between latency and the slope of the

temporal profile. Upon close inspection of the examples from the Bair *et al.* (2002) study, a result similar to that in this study and that of DeAngelis *et al.* (1993) may be observed. Thus this characteristic of temporal response profiles seems to be a ubiquitous feature of visually responsive areas, even across species and is stimulus independent.

### Response latency

We wished to compare our data directly with that of Bair *et al.* (2002) and therefore calculated the offset latencies, (i.e. taking into consideration the duration of the stimulus presentation). The results contrasted with those found in the above mentioned study. That is, onset latencies were significantly shorter than offset latencies ( $W_{\text{bright}} = 3324.5$ ,  $p < 0.0001$ ,  $W_{\text{dark}} = 30925$ ,  $p < 0.0001$ ,  $n = 66$ ). The authors argued that the longer onset latency was a measure of the integration time required to analyse their motion stimulus. If this is correct and given the simple nature of our stimuli, it can be safely assumed that a much shorter integration is required for the present stimuli as compared to their directional stimuli. Although if our data are correct, their difference measure cannot directly be used as a metric of integration time given the negative values reported here. It is also possible that different parallel visual pathways may be responsible for the response to these two stimuli, especially in the highly parallel system of the cat. Therefore, our data are not necessarily at odds with those of Bair *et al.* (2002).

### Phase shifted and multi-lobed response

An interesting response profile observed here were the phase shifted cells. Although only a small percentage had extreme values, a large number of cells deviated from zero. It may be that these neurons receive input from the homogeneous type cells of the LGN described by Stevens & Gerstein (1976), which clearly treat each contrast separately. This could explain the phase shifted responses to each contrast. The latter authors suggested that such cells could act as temporal filters, and the present study in conjunction with previous descriptions of SF selectivity in PMLS suggest that neurons in this region are poor spatial filters. What's more, PMLS neurons exhibit a far wider variety of temporal than spatial response profiles, as demonstrated here. Similarly, the bi-lobed responses observed may be explained by the second excitatory peak reported by Stevens & Gerstein (1976). It is thus possible that PMLS acts as a temporal filter with low spatial acuity. Fine temporal tuning would thus be possible via phase shifted and/or bi-lobed responses as well as short response durations. Such temporal response profiles would be well suited for motion processing and detection of sudden changes in the visual environment.

### Implications for system organization

The data from the present study not only address the linear versus non-linear spatial integration of visual information among PMLS neurons but also

pose certain limitations as to which areas may supply functionally important visual input to PMLS. As stated in the introduction, it is to be expected that non-linear spatial processing occurs in PMLS. However the observed responses, although putatively non-linear, did not correspond to what one would expect based on feedforward projections from area 17 complex cells. This suggests that PMLS neurons receive functionally important input from other areas.

#### The evidence against sole area 17 input

Rapidly, in the spatial domain the area of the visual field covered by the subfields (SSI) was not equal across contrast and some cells responded uniquely to one contrast, while another subset of cells were found to have non-overlapping subfields. Likewise, the probability for the response to each contrast (MRI) was often unbalanced. Although these types of responses may be explained by previously reported data from area 17 (Hubel & Wiesel, 1962; Movshon *et al.*, 1978a; Hirsch *et al.*, 2002; Kagan *et al.*, 2002; Martinez *et al.*, 2005; Hirsch & Martinez, 2006), one would have to assume that these PMLS neurons receive exclusively from the former cells. This seems unlikely because of the connectional complexity involved, the small proportion of such cells in the above mentioned studies, and because of the spatial integration required due to the large RFs in PMLS.

In the temporal domain, the response to each contrast was not what would be expected from complex cells either. This can be seen as differences

between contrast for response latency (for example see Figure 8B), duration (Figure 10C), and the phase shift of the response (10A). Similarly, most bi-lobed responses were limited to only one of the two contrasts (Figure 9). The duration of the response was shorter in PMLS than what has been reported for area 17 (DeAngelis *et al.*, 1993, 1995b). What's more, we did not observe responses to both stimulus onset and offset in the same cell, while this has been reported in area 17 complex cells (Hubel & Wiesel, 1962; Kagan *et al.*, 2002). Taken together the data are not consistent with the notion that feedforward projections from complex area 17 neurons provide the sole major excitatory input to PMLS neurons.

Furthermore, lesions of primary visual cortex leave response properties of PMLS neurons relatively unchanged (Spear & Baumann, 1979; Spear, 1988; Guido *et al.*, 1990b). Likewise, the timing of responses between primary visual cortex and PMLS exhibit considerable overlap (Dinse & Kruger, 1994; Bullier, 2004a; Vajda *et al.*, 2004; Ouellette & Casanova, 2006a) and PMLS neurons have been shown to putatively drive or respond synchronously with area 17 neurons (Katsuyama *et al.*, 1996). Finally, behavioral tasks which elicit an increase in area 17 metabolism do not have the same effect in PMLS (Vanduffel *et al.*, 1997b). All of the preceding data would be surprising if primary visual cortex were the sole functionally important input to PMLS cortex.



### Direct LGN input

The data suggest that, at least for the impulse response, PMLS neurons receive a functionally important projection from neurons elsewhere than the supragranular layers of area 17. Given the above mentioned PMLS response properties, an alternate source of input would need to treat different contrast separately. The first and most likely possibility is input from the LGN (Raczkowski & Rosenquist, 1980; Tong *et al.*, 1982; Raczkowski & Rosenquist, 1983; Berson, 1985; Sherk, 1986; Rauschecker *et al.*, 1987b; Miceli *et al.*, 1991; MacNeil *et al.*, 1997; Kawano, 1998; Herbin *et al.*, 2000), despite the small number of terminals attributable to this projection.

Firstly, these neurons meet the above mentioned requirement of contrast dependent responses. Secondly, LGN neurons can be well excited by stationary contrast stimuli similar to those used here (Stevens & Gerstein, 1976). Thirdly, the short presentation times used would nonetheless evoke a response from LGN neurons (using the same temporal parameters as for the PMLS neurons, we evoked robust responses from 10/10 LGN neurons, data not shown). Fourthly, a direct parallel input to area 17/18 and PMLS would explain the synchronous responses in these two areas (Katsuyama *et al.*, 1996; Vajda *et al.*, 2004; Ouellette & Casanova, 2006a). Finally, the greater proportion of geniculate magnocellular/Y cells projecting to PMLS (Kawano, 1998; Herbin *et al.*, 2000) would explain the earlier responses in this region as compared to those of some area 17 neurons (Katsuyama *et al.*, 1996).

### Direct input from the Pulvinar

An alternative efferent input could be the Pulvinar nucleus. A direct projection from this thalamic nucleus to PMLS cortex has been described (Tekian & Afifi, 1981; Naito & Kawamura, 1982; Tong *et al.*, 1982; Norita *et al.*, 1996), although many authors have reported an absence of such projections (Graybiel, 1972; Maciewicz, 1974; Robertson, 1976; Raczkowski & Rosenquist, 1983). Some Pulvinar nucleus neurons have been described to have response properties similar to LGN neurons (Arutyunyan-Kozak *et al.*, 1981; Harutiunian-Kozak *et al.*, 1981b; Mason, 1981). While other Pulvinar neurons have been described to have only ON or OFF responses, some exhibit responses limited to one contrast, while others have stronger dark responsive subfields which also cover a greater area of the visual field as compared to the bright subfield (Arutyunyan-Kozak *et al.*, 1981; Harutiunian-Kozak *et al.*, 1981b, a). Furthermore, the RFs of Pulvinar neurons have been characterized as covering a large part of the visual field (Arutyunyan-Kozak *et al.*, 1981; Mason, 1981; Sudkamp & Schmidt, 2000). All of these response properties are consistent with the present results. Note however, that the reported response properties for the Pulvinar are all qualitative assessments. To get a clearer picture of the Pulvinar's functional input a quantitative study of its RFs is presently underway.

Taken together this suggests that PMLS neuronal activity is not solely dependent upon input from primary visual cortex. This could explain the putative input independent PMLS RF properties (Illig *et al.*, 2000), which would not be due to inherent computations in PMLS but rather a diversity of inputs.

Given the latency data cited above, it may be that at least the initial parts of PMLS responses arise from the LGN or the Pulvinar nucleus and only later portions of the response are influenced by area 17-18 input.

It could be argued that it is computationally inefficient to extract motion information a second time from LGN or other input rather than building upon the already treated information from areas 17 and 18. However, it may not be behaviourally efficient to have visual information pass an extra synapse prior to the commencement of motion processing by PMLS neurons. In line with such reasoning, Pasternak *et al.* (1995) have already demonstrated that area 17 is not involved in the processing of the type of motion commonly associated with PMLS response properties. Likewise, previous reverse correlation work has demonstrated that optimal parameters in area 18 and PMLS are not consistent with information flow from the former to the latter (Vajda *et al.*, 2005), but rather from the LGN to PMLS. Finally, input from the LGN to PMLS would be consistent with work carried out in the primate which suggest that non-direction selective input to MT is transformed into a direction selective response via inherent inhibitory processes (Thiele *et al.*, 2004).

As suggested by Bullier (2001), an early response in specialised extrastriate areas, in this case PMLS, would allow such areas to shape the response in primary visual cortex via cortico-cortical connections. Consistent with such a proposal are extrastriate cortex deactivation studies which show specific disruptions of processing in primary visual cortex as revealed by the organization of cortical maps (Galuske *et al.*, 2002; Huang *et al.*, 2004; Shen *et*

*al.*, 2006a). Once a structure is imposed on the map, area 17 neurons could then project back to extrastriate cortex in order to allow a more detailed analysis of the visual scene.

### Conclusion

The instigating question of this study was whether the linear temporal responses of PMLS neurons (Vajda *et al.*, 2006) would be reflected in their spatial integration. At first glance the results of the present study present contradictory streams of evidence in that the spatial structure of the RFs of PMLS neurons are homogeneous (i.e. non-linear), while the temporal profile of the responses are contrast dependent (i.e. linear). This suggests that despite the area 17 input to PMLS, other afferent regions are also functionally important. This is in part reflected by the heterogeneous temporal response profiles which do not correspond to complex like RFs in area 17 or 18. As suggested by others, PMLS neurons may be part of another visual pathway specialised in detection and behavioural orientation to moving stimuli rather than discrimination of fine detail (Kruger *et al.*, 1993b; Vanduffel *et al.*, 1997b; Lomber, 2001; Payne, 2004). It remains to be determined which of the other possible afferent inputs provides a major excitatory drive to PMLS, which would influence its response properties and hence contribution to behavior.

## Appendix

In the first alternate method for calculating the OI, a 2-D correlation of each Cartesian product at each pre-spike time for bright and dark stimulus evoked maps was calculated (e.g. for an analysis lasting 250ms pre-spike time, the result would be a 250X250 matrix of 2-D correlation coefficients). Correlation coefficients were then squared in order to obtain explained variance. Separately, a vector consisting of the variance of each contrast map at each time point was calculated (leading to two 250 item long vectors). High values in these vectors correspond to points in pre-spike time where probability exhibited spatial variation, generally indicative of the presence of a responsive subfield. The Cartesian product of the two resulting variance vectors was then calculated, leading to a second 250X250 point matrix of covariance (the term covariance is applied loosely), which was then normalized. The normalized covariance matrix was then point multiplied by the explained variance matrix mentioned above.

Although seemingly complex, the logic behind this method is straightforward when one considers a simplified version of the formula; explained variance multiplied by normalized covariance. The result is of interest if and only if both values are relatively large. If the explained variance is low, then a map with high normalized covariance is of no interest. Similarly, if there is little normalized covariance, an elevated explained variance would be of little interest. Although at first glance the latter possibility seems unlikely, the large area stimulated necessitated this precaution. Slight chance covariations outside the subfields, or at early and late pre-spike times where no or weak subfields

were present could lead to high correlation coefficients without actually being associated with a meaningful change in neuronal response. From the resulting matrix, the indices of the highest amplitude point were identified. These values represent pre-spike times for each contrast that evoked spatially varying responses (i.e. a responsive subfield surrounded by no response as opposed to the absence of a responsive subfield) and for which there was a high correlation between the spatial organization of the bright and dark maps. The maps at these pre-spike times (hereafter  $t_{max}$ ) were then used to calculate an OI using the same formula described above.

A final method of calculating the OI consisted of collapsing all the data over the temporal domain, after a frame-by-frame multiplication with the normalized spatial variance of each map. This is similar to the 2-D correlation method, by giving greater weight to those pre-spike times which evoked a spatially varying response. This method avoids any potential bias in the OI which could arise from calculating the index from a single point in time rather than considering the entire response. The data was then used to calculate the OI as above. These two OI's will be referred to as 2-D correlation and temporal summation respectively throughout the text.

## References

- ARUTYUNYAN-KOZAK, B. A., EKIMYAN, A. A., GRIGORYAN, G. E. & DEC, K. (1981). Structure of receptive fields of cat pulvina neurons sensitive to photic stimulation. *Neurosci Behav Physiol* **11**, 400-405.
- BAIR, W., CAVANAUGH, J. R., SMITH, M. A. & MOVSHON, J. A. (2002). The timing of response onset and offset in macaque visual neurons. *J Neurosci* **22**, 3189-3205.
- BAIR, W. & MOVSHON, J. A. (2004). Adaptive temporal integration of motion in direction-selective neurons in macaque visual cortex. *J Neurosci* **24**, 7305-7323.
- BERSON, D. M. (1985). Cat lateral suprasylvian cortex: Y-cell inputs and corticotectal projection. *J Neurophysiol* **53**, 544-556.
- BERSON, D. M. & GRAYBIEL, A. M. (1978). Parallel thalamic zones in the LP-pulvina complex of the cat identified by their afferent and efferent connections. *Brain Res* **147**, 139-148.
- BORGHUIS, B. G., PERGE, J. A., VAJDA, I., VAN WEZEL, R. J., VAN DE GRIND, W. A. & LANKHEET, M. J. (2003). The motion reverse correlation (MRC) method: a linear systems approach in the motion domain. *J Neurosci Methods* **123**, 153-166.
- BROSSEAU-LACHAINE, O., FAUBERT, J. & CASANOVA, C. (2001). Functional sub-regions for optic flow processing in the posteromedial lateral suprasylvian cortex of the cat. *Cereb Cortex* **11**, 989-1001.
- BULLIER, J. (2001). Integrated model of visual processing. *Brain Res Brain Res Rev* **36**, 96-107.
- BULLIER, J. (2004). Communications between cortical areas of the visual system. In *The Visual Neurosciences*, pp. 522-540. Bradford Books, Cambridge.
- CITRON, M. C. & EMERSON, R. C. (1983). White noise analysis of cortical directional selectivity in cat. *Brain Res* **279**, 271-277.
- DANILOV, Y., MOORE, R. J., KING, V. R. & SPEAR, P. D. (1995). Are neurons in cat posteromedial lateral suprasylvian visual cortex orientation sensitive? Tests with bars and gratings. *Vis Neurosci* **12**, 141-151.
- DEANGELIS, G. C., OHZAWA, I. & FREEMAN, R. D. (1993). Spatiotemporal organization of simple-cell receptive fields in the cat's striate cortex. I. General characteristics and postnatal development. *J Neurophysiol* **69**, 1091-1117.

- DEANGELIS, G. C., OHZAWA, I. & FREEMAN, R. D. (1995). Receptive-field dynamics in the central visual pathways. *Trends Neurosci* **18**, 451-458.
- DI STEFANO, M., MORRONE, M. C. & BURR, D. C. (1985). Visual acuity of neurones in the cat lateral suprasylvian cortex. *Brain Res* **331**, 382-385.
- DINSE, H. R. & KRUGER, K. (1994). The timing of processing along the visual pathway in the cat. *Neuroreport* **5**, 893-897.
- EINSTEIN, G. & FITZPATRICK, D. (1991). Distribution and morphology of area 17 neurons that project to the cat's extrastriate cortex. *J Comp Neurol* **303**, 132-149.
- EMERSON, R. C., BERGEN, J. R. & ADELSON, E. H. (1992). Directionally selective complex cells and the computation of motion energy in cat visual cortex. *Vision Res* **32**, 203-218.
- EMERSON, R. C., CITRON, M. C., VAUGHN, W. J. & KLEIN, S. A. (1987). Nonlinear directionally selective subunits in complex cells of cat striate cortex. *J Neurophysiol* **58**, 33-65.
- GALUSKE, R. A., SCHMIDT, K. E., GOEBEL, R., LOMBER, S. G. & PAYNE, B. R. (2002). The role of feedback in shaping neural representations in cat visual cortex. *Proc Natl Acad Sci U S A* **99**, 17083-17088.
- GASKA, J. P., JACOBSON, L. D., CHEN, H. W. & POLLEN, D. A. (1994). Space-time spectra of complex cell filters in the macaque monkey: a comparison of results obtained with pseudowhite noise and grating stimuli. *Vis Neurosci* **11**, 805-821.
- GILBERT, C. D. (1977). Laminar differences in receptive field properties of cells in cat primary visual cortex. *J Physiol* **268**, 391-421.
- GIZZI, M. S., KATZ, E. & MOVSHON, J. A. (1990). Spatial and temporal analysis by neurons in the representation of the central visual field in the cat's lateral suprasylvian visual cortex. *Vis Neurosci* **5**, 463-468.
- GRAYBIEL, A. M. (1972). Some extrageniculate visual pathways in the cat. *Invest Ophthalmol* **11**, 322-332.
- GUIDO, W., TONG, L. & SPEAR, P. D. (1990). Afferent bases of spatial- and temporal-frequency processing by neurons in the cat's posteromedial lateral suprasylvian cortex: effects of removing areas 17, 18, and 19. *J Neurophysiol* **64**, 1636-1651.
- HARUTIUNIAN-KOZAK, B. A., HEKIMIAN, A. A., DEC, K. & GRIGORIAN, G. E. (1981a). Responses of cat's pulvinar neurons to moving visual stimuli. *Acta Neurobiol Exp (Wars)* **41**, 147-162.



- HARUTIUNIAN-KOZAK, B. A., HEKIMIAN, A. A., DEC, K. & GRIGORIAN, G. E. (1981b). The structure of visual receptive fields of cat's pulvinar neurons. *Acta Neurobiol Exp (Wars)* **41**, 127-145.
- HERBIN, M., MICELI, D., REPERANT, J., MASSICOTTE, G. & ROY, G. (2000). Postnatal development of thalamocortical projections upon striate and extrastriate visual cortical areas in the cat. *Anat Embryol (Berl)* **202**, 431-442.
- HIRSCH, J. A. & MARTINEZ, L. M. (2006). Circuits that build visual cortical receptive fields. *Trends Neurosci* **29**, 30-39.
- HIRSCH, J. A., MARTINEZ, L. M., ALONSO, J. M., DESAI, K., PILLAI, C. & PIERRE, C. (2002). Synaptic physiology of the flow of information in the cat's visual cortex in vivo. *J Physiol* **540**, 335-350.
- HIRSCH, J. A., MARTINEZ, L. M., PILLAI, C., ALONSO, J. M., WANG, Q. & SOMMER, F. T. (2003). Functionally distinct inhibitory neurons at the first stage of visual cortical processing. *Nat Neurosci* **6**, 1300-1308.
- HUANG, L., CHEN, X. & SHOU, T. (2004). Spatial frequency-dependent feedback of visual cortical area 21a modulating functional orientation column maps in areas 17 and 18 of the cat. *Brain Res* **998**, 194-201.
- HUBEL, D. H. & WIESEL, T. N. (1962). Receptive fields, binocular interaction and functional architecture in the cat's visual cortex. *J Physiol* **160**, 106-154.
- HUBEL, D. H. & WIESEL, T. N. (1965). Receptive Fields and Functional Architecture in Two Nonstriate Visual Areas (18 and 19) of the Cat. *J Neurophysiol* **28**, 229-289.
- HUBEL, D. H. & WIESEL, T. N. (1969). Visual area of the lateral suprasylvian gyrus (Clare-Bishop area) of the cat. *J Physiol* **202**, 251-260.
- ILLIG, K. R., DANILOV, Y. P., AHMAD, A., KIM, C. B. & SPEAR, P. D. (2000). Functional plasticity in extrastriate visual cortex following neonatal visual cortex damage and monocular enucleation. *Brain Res* **882**, 241-250.
- JONES, J. P. & PALMER, L. A. (1987). The two-dimensional spatial structure of simple receptive fields in cat striate cortex. *J Neurophysiol* **58**, 1187-1211.
- KAGAN, I., GUR, M. & SNODDERLY, D. M. (2002). Spatial organization of receptive fields of V1 neurons of alert monkeys: comparison with responses to gratings. *J Neurophysiol* **88**, 2557-2574.
- KATSUYAMA, N., TSUMOTO, T., SATO, H., FUKUDA, M. & HATA, Y. (1996). Lateral suprasylvian visual cortex is activated earlier than or synchronously with primary visual cortex in the cat. *Neurosci Res* **24**, 431-435.

- KAWANO, J. (1998). Cortical projections of the parvocellular laminae C of the dorsal lateral geniculate nucleus in the cat: an anterograde wheat germ agglutinin conjugated to horseradish peroxidase study. *J Comp Neurol* **392**, 439-457.
- KIM, J. N., MULLIGAN, K. & SHERK, H. (1997). Simulated optic flow and extrastriate cortex. I. Optic flow versus texture. *J Neurophysiol* **77**, 554-561.
- KRUGER, K., KIEFER, W., GROH, A., DINSE, H. R. & VON SEELEN, W. (1993). The role of the lateral suprasylvian visual cortex of the cat in object-background interactions: permanent deficits following lesions. *Exp Brain Res* **97**, 40-60.
- LIM, J. S. (1990). *Two-dimensional signal and image processing*. Prentice Hall, Englewood Cliffs, N.J.
- LOMBER, S. G. (2001). Behavioral cartography of visual functions in cat parietal cortex: areal and laminar dissociations. *Prog Brain Res* **134**, 265-284.
- LOWENSTEIN, P. R. & SOMOGYI, P. (1991). Synaptic organization of cortico-cortical connections from the primary visual cortex to the posteromedial lateral suprasylvian visual area in the cat. *J Comp Neurol* **310**, 253-266.
- MACIEWICZ, R. J. (1974). Afferents to the lateral suprasylvian gyrus of the cat traced with horseradish peroxidase. *Brain Res* **78**, 139-143.
- MACNEIL, M. A., LOMBER, S. G. & PAYNE, B. R. (1997). Thalamic and cortical projections to middle suprasylvian cortex of cats: constancy and variation. *Exp Brain Res* **114**, 24-32.
- MARTINEZ, L. M., WANG, Q., REID, R. C., PILLAI, C., ALONSO, J. M., SOMMER, F. T. & HIRSCH, J. A. (2005). Receptive field structure varies with layer in the primary visual cortex. *Nat Neurosci* **8**, 372-379.
- MASON, R. (1981). Differential responsiveness of cells in the visual zones of the cat's LP-pulvinar complex to visual stimuli. *Exp Brain Res* **43**, 25-33.
- MATA, M. L. & RINGACH, D. L. (2005). Spatial overlap of ON and OFF subregions and its relation to response modulation ratio in macaque primary visual cortex. *J Neurophysiol* **93**, 919-928.
- MCLEAN, J., RAAB, S. & PALMER, L. A. (1994). Contribution of linear mechanisms to the specification of local motion by simple cells in areas 17 and 18 of the cat. *Vis Neurosci* **11**, 271-294.
- MERABET, L., MINVILLE, K., PTITO, M. & CASANOVA, C. (2000). Responses of neurons in the cat posteromedial lateral suprasylvian cortex to moving texture patterns. *Neuroscience* **97**, 611-623.

- MICELI, D., REPERANT, J., MARCHAND, L., WARD, R. & VESSELKIN, N. (1991). Divergence and collateral axon branching in subsystems of visual cortical projections from the cat lateral posterior nucleus. *J Hirnforsch* **32**, 165-173.
- MINVILLE, K. & CASANOVA, C. (1998). Spatial frequency processing in posteromedial lateral suprasylvian cortex does not depend on the projections from the striate-recipient zone of the cat's lateral posterior-pulvinar complex. *Neuroscience* **84**, 699-711.
- MORRONE, M. C., DI STEFANO, M. & BURR, D. C. (1986). Spatial and temporal properties of neurons of the lateral suprasylvian cortex of the cat. *J Neurophysiol* **56**, 969-986.
- MOVSHON, J. A., ADELSON, E. H., GIZZI, M. S. & NEWSOME, W. T. (1985). The analysis of moving visual patterns. In *Pontificae Academia Scientiarum Scripta Varia*. ed. CITY, V., pp. 117-151.
- MOVSHON, J. A., THOMPSON, I. D. & TOLHURST, D. J. (1978a). Receptive field organization of complex cells in the cat's striate cortex. *J Physiol* **283**, 79-99.
- MOVSHON, J. A., THOMPSON, I. D. & TOLHURST, D. J. (1978b). Spatial summation in the receptive fields of simple cells in the cat's striate cortex. *J Physiol* **283**, 53-77.
- MULLIGAN, K., KIM, J. N. & SHERK, H. (1997). Simulated optic flow and extrastriate cortex. II. Responses to bar versus large-field stimuli. *J Neurophysiol* **77**, 562-570.
- NAITO, J. & KAWAMURA, K. (1982). Thalamocortical neurons projecting to the areas surrounding the anterior and middle suprasylvian sulci in the cat. A horseradish peroxidase study. *Exp Brain Res* **45**, 59-70.
- NISHIMOTO, S., ISHIDA, T. & OHZAWA, I. (2006). Receptive field properties of neurons in the early visual cortex revealed by local spectral reverse correlation. *J Neurosci* **26**, 3269-3280.
- NORITA, M., KASE, M., HOSHINO, K., MEGURO, R., FUNAKI, S., HIRANO, S. & MCHAFFIE, J. G. (1996). Extrinsic and intrinsic connections of the cat's lateral suprasylvian visual area. *Prog Brain Res* **112**, 231-250.
- OUELLETTE, B. G. & CASANOVA, C. (2006). Overlapping visual response latency distributions in visual cortices and LP-pulvinar complex of the cat. *Exp Brain Res*.
- OUELLETTE, B. G., FAUBERT, J. & CASANOVA, C. (2005). Mapping of spatiotemporal receptive field substructure of neurons in cat

posteromedial lateral suprasylvian cortex. *Society for Neuroscience Abstracts*, 619.611.

- QUELLETTE, B. G., FAUBERT, J. & CASANOVA, C. (2006). Simple-like receptive fields in cat postero-medial lateral suprasylvian cortex? *FENS Abstracts* **3**, A216.215.
- QUELLETTE, B. G., MINVILLE, K., BOIRE, D., PTITO, M. & CASANOVA, C. (2007). Complex motion selectivity in PMLS cortex following early lesions of primary visual cortex in the cat. *Vis Neurosci* **24**, 53-64.
- PALMER, L. A. & DAVIS, T. L. (1981a). Comparison of responses to moving and stationary stimuli in cat striate cortex. *J Neurophysiol* **46**, 277-295.
- PALMER, L. A. & DAVIS, T. L. (1981b). Receptive-field structure in cat striate cortex. *J Neurophysiol* **46**, 260-276.
- PALMER, L. A., ROSENQUIST, A. C. & TUSA, R. J. (1978). The retinotopic organization of lateral suprasylvian visual areas in the cat. *J Comp Neurol* **177**, 237-256.
- PASTERNAK, T., TOMPKINS, J. & OLSON, C. R. (1995). The role of striate cortex in visual function of the cat. *J Neurosci* **15**, 1940-1950.
- PAYNE, B. R. (1993). Evidence for visual cortical area homologs in cat and macaque monkey. *Cereb Cortex* **3**, 1-25.
- PAYNE, B. R. (2004). Neuroplasticity in the cat's visual system: test of the role of the expanded retino-geniculo-parietal pathway in behavioral sparing following early lesions of visual cortex. *Exp Brain Res* **155**, 69-80.
- RACZKOWSKI, D. & ROSENQUIST, A. C. (1980). Connections of the parvocellular C laminae of the dorsal lateral geniculate nucleus with the visual cortex in the cat. *Brain Res* **199**, 447-451.
- RACZKOWSKI, D. & ROSENQUIST, A. C. (1983). Connections of the multiple visual cortical areas with the lateral posterior-pulvinar complex and adjacent thalamic nuclei in the cat. *J Neurosci* **3**, 1912-1942.
- RAUSCHECKER, J. P., VON GRUNAU, M. W. & POULIN, C. (1987). Thalamo-cortical connections and their correlation with receptive field properties in the cat's lateral suprasylvian visual cortex. *Exp Brain Res* **67**, 100-112.
- RINGACH, D. L., SAPIRO, G. & SHAPLEY, R. (1997). A subspace reverse-correlation technique for the study of visual neurons. *Vision Res* **37**, 2455-2464.
- ROBERTSON, R. T. (1976). Thalamic projections to visually responsive regions of parietal cortex. *Brain Res Bull* **1**, 459-469.

- RUST, N. C., SCHWARTZ, O., MOVSHON, J. A. & SIMONCELLI, E. P. (2005). Spatiotemporal elements of macaque v1 receptive fields. *Neuron* **46**, 945-956.
- SHEN, W., LIANG, Z., CHEN, X. & SHOU, T. (2006). Posteromedial lateral suprasylvian motion area modulates direction but not orientation preference in area 17 of cats. *Neuroscience*.
- SHERK, H. (1986). Location and connections of visual cortical areas in the cat's suprasylvian sulcus. *J Comp Neurol* **247**, 1-31.
- SHERK, H. & KIM, J. N. (2002). Responses in extrastriate cortex to optic flow during simulated turns. *Vis Neurosci* **19**, 409-419.
- SHERK, H., KIM, J. N. & MULLIGAN, K. (1995). Are the preferred directions of neurons in cat extrastriate cortex related to optic flow? *Vis Neurosci* **12**, 887-894.
- SHERK, H., MULLIGAN, K. & KIM, J. N. (1997). Neuronal responses in extrastriate cortex to objects in optic flow fields. *Vis Neurosci* **14**, 879-895.
- SHERK, H. & MULLIGAN, K. A. (1992). Retinotopic order is surprisingly good within cell columns in the cat's lateral suprasylvian cortex. *Exp Brain Res* **91**, 46-60.
- SHIPP, S. & GRANT, S. (1991). Organization of reciprocal connections between area 17 and the lateral suprasylvian area of cat visual cortex. *Vis Neurosci* **6**, 339-355.
- SKOTTUN, B. C., DE VALOIS, R. L., GROSOF, D. H., MOVSHON, J. A., ALBRECHT, D. G. & BONDS, A. B. (1991). Classifying simple and complex cells on the basis of response modulation. *Vision Res* **31**, 1079-1086.
- SPEAR, P. D. (1988). Influence of areas 17, 18, and 19 on receptive-field properties of neurons in the cat's posteromedial lateral suprasylvian visual cortex. *Prog Brain Res* **75**, 197-210.
- SPEAR, P. D. (1991). Functions of extrastriate visual cortex in non-primate species. In *The neural basis of visual function*, vol. 4. ed. LEVENTHAL, A. G., pp. 339-370. MacMillan Press, London.
- SPEAR, P. D. & BAUMANN, T. P. (1975). Receptive-field characteristics of single neurons in lateral suprasylvian visual area of the cat. *J Neurophysiol* **38**, 1403-1420.
- SPEAR, P. D. & BAUMANN, T. P. (1979). Effects of visual cortex removal on receptive-field properties of neurons in lateral suprasylvian visual area of the cat. *J Neurophysiol* **42**, 31-56.

- STEVENS, J. K. & GERSTEIN, G. L. (1976). Spatiotemporal organization of cat lateral geniculate receptive fields. *J Neurophysiol* **39**, 213-238.
- SUDKAMP, S. & SCHMIDT, M. (2000). Response characteristics of neurons in the pulvinar of awake cats to saccades and to visual stimulation. *Exp Brain Res* **133**, 209-218.
- SYMONDS, L. L. & ROSENQUIST, A. C. (1984a). Corticocortical connections among visual areas in the cat. *J Comp Neurol* **229**, 1-38.
- SYMONDS, L. L. & ROSENQUIST, A. C. (1984b). Laminar origins of visual corticocortical connections in the cat. *J Comp Neurol* **229**, 39-47.
- SZULBORSKI, R. G. & PALMER, L. A. (1990). The two-dimensional spatial structure of nonlinear subunits in the receptive fields of complex cells. *Vision Res* **30**, 249-254.
- TEKIAN, A. & AFIFI, A. K. (1981). Efferent connections of the pulvinar nucleus in the cat. *J Anat* **132**, 249-265.
- THIELE, A., DISTLER, C., KORBMACHER, H. & HOFFMANN, K. P. (2004). Contribution of inhibitory mechanisms to direction selectivity and response normalization in macaque middle temporal area. *Proc Natl Acad Sci U S A* **101**, 9810-9815.
- TONG, L., KALIL, R. E. & SPEAR, P. D. (1982). Thalamic projections to visual areas of the middle suprasylvian sulcus in the cat. *J Comp Neurol* **212**, 103-117.
- TOYAMA, K., FUJII, K. & UMETANI, K. (1990). Functional differentiation between the anterior and posterior Clare-Bishop cortex of the cat. *Exp Brain Res* **81**, 221-233.
- TOYAMA, K., KOMATSU, Y., KASAI, H., FUJII, K. & UMETANI, K. (1985). Responsiveness of Clare-Bishop neurons to visual cues associated with motion of a visual stimulus in three-dimensional space. *Vision Res* **25**, 407-414.
- VAJDA, I., BORGHUIS, B. G., VAN DE GRIND, W. A. & LANKHEET, M. J. (2006). Temporal interactions in direction-selective complex cells of area 18 and the posteromedial lateral suprasylvian cortex (PMLS) of the cat. *Vis Neurosci* **23**, 233-246.
- VAJDA, I., LANKHEET, M. J., BORGHUIS, B. G. & VAN DE GRIND, W. A. (2004). Dynamics of directional selectivity in area 18 and PMLS of the cat. *Cereb Cortex* **14**, 759-767.

- VAJDA, I., LANKHEET, M. J. & VAN DE GRIND, W. A. (2005). Spatio-temporal requirements for direction selectivity in area 18 and PMLS complex cells. *Vision Res* **45**, 1769-1779.
- VANDUFFEL, W., VANDENBUSSCHE, E., SINGER, W. & ORBAN, G. A. (1997). A metabolic mapping study of orientation discrimination and detection tasks in the cat. *Eur J Neurosci* **9**, 1314-1328.
- VILLENEUVE, M. Y., PTITO, M. & CASANOVA, C. (2006). Global motion integration in the postero-medial part of the lateral suprasylvian cortex in the cat. *Exp Brain Res* **172**, 485-497.
- ZUMBROICH, T. J. & BLAKEMORE, C. (1987). Spatial and temporal selectivity in the suprasylvian visual cortex of the cat. *J Neurosci* **7**, 482-500.

### Acknowledgements

The authors wish to thank the expert programming assistance of Jonathan Roy without whom the visual stimulation would not have been possible, as well as Matthieu Vanni for discussions throughout the development of this project.

### Grants

This work was supported by a CIHR grant to C.C. and part of C.C.'s salary was provided by FRSQ (chercheur National). B.G.O. was supported by FRSQ and NSERC scholarships, and an educational grant from Eli Lilly Canada Inc.



## Discussion

### 1. Résumé des résultats

#### 1.1 Études des effets d'une lésion de l'aire visuelle primaire

Avant d'examiner les implications théoriques des résultats de la présente thèse, résumons rapidement la conclusion de chaque étude. Le premier article porte sur les lésions de l'aire visuelle primaire chez le chaton et ses effets sur les réponses des neurones du PMLS (Ouellette *et al.*, 2007). Nous pouvons en retirer trois points majeurs. Premièrement, malgré l'utilisation de stimuli qui requièrent une intégration spatio-temporelle plus importante que dans les études antérieures (Tong *et al.*, 1984; Guido *et al.*, 1990a), la sélectivité à la direction des neurones du PMLS est maintenue. Ainsi, les conclusions des études antérieures sont confirmées et généralisées. Deuxièmement, l'amélioration comportementale observée par Rudolph et Pasternak (1996) ne semble pas être attribuable à une augmentation de la sélectivité à la direction des neurones du PMLS. Troisièmement, via un modèle simple, nous avons démontré qu'à partir d'une entrée du CGL, l'extraction d'informations directionnelles d'un stimulus de RDK complexe était possible. En résumé, cette étude a démontré, que les réponses du PMLS ne dépendaient pas exclusivement des projections des aires visuelles primaires chez le chaton.

## 1.2 Études des latences

L'analyse des latences dans diverses régions visuelles a permis d'arriver à deux conclusions majeures. Dans un premier temps, la simultanéité des réponses dans les régions visuelles suggère que la hiérarchie anatomique n'est pas reflétée au niveau fonctionnel. Il en découle qu'au niveau fonctionnel le système visuel dorsal semblerait organisé de façon parallèle. Dans une telle éventualité, il faudra alors cerner l'implication fonctionnelle des patrons d'origines et de terminaisons observés dans les études anatomiques. Par ailleurs, l'étude des latences permet également de suggérer qu'il y aurait deux types d'aires visuelles dans la voie dorsale; 1- celles qui ont une latence médiane identiques peu importe le stimulus et 2- celles dont la latence médiane varie selon le stimulus. Ces dernières ne reçoivent aucune projection directe de l'aire 17, alors que l'inverse est vrai pour les régions qui démontrent le premier patron de latences. En ce sens, il existe une correspondance des données anatomiques et physiologiques. Cela suggère que la simultanéité des réponses ne soit pas attribuable à une limitation méthodologique.

## 1.3 Étude des profils spatio-temporels

Les profils spatio-temporels linéaires des champs récepteurs des neurones du PMLS ont révélé que ce ne sont pas toutes les cellules de cette région qui correspondent aux prédictions basées sur une projection prédominante des cellules complexes de l'aire visuelle primaire. Un sous-groupe important de

champ récepteur avait plutôt des propriétés qui pourraient être héritées des projections de régions qui traitent les contrastes opposés de façon spatialement ségrégués. De plus, il a été démontré que pour certaines cellules plus d'une réponse significative est présente dans le domaine temporel. Ces multiples réponses sont incompatibles avec une projection prédominante des aires 17 et 18. Ces résultats suggèrent donc que d'autres régions pourraient avoir des projections fonctionnelles importantes vers le PMLS. Cependant, l'origine de ces multiples réponses reste à déterminer. Pour conclure, la réponse impulsionnelle des neurones du PMLS suggère que des régions autres que l'aire visuelle primaire aient une projection qui pourrait provoquer une réponse à elle seule.

## 2. Considérations méthodologiques

### 2.1 Étude de lésions de l'aire visuelle primaire

#### 2.1.1 Étendues des lésions

Rappelons que le but de cette étude était d'observer les effets d'une lésion de l'aire visuelle primaire sur les réponses des neurones du PMLS. L'un des contrôles les plus importants est de vérifier l'étendue des lésions. Deux méthodes viennent immédiatement à l'esprit afin de faire un tel contrôle, cependant celles-ci ne sont pas réalisables en pratique. Premièrement, il pourrait être suggéré que lors de la lésion, l'étendue de celle-ci soit immédiatement cartographiée et comparée avec les limites des aires corticales. Le problème avec cette idée est que, à ma connaissance, les limites des aires

corticales chez le chaton ne sont pas connues de façon précise et il n'y a aucune raison de présumer qu'elles soient proportionnellement identiques à celles chez l'adulte. La proposition alternative serait de comparer l'étendue de la lésion chez l'animal adulte, tel qu'effectuée par Rushmore et Payne (2004), par exemple. Malheureusement cette procédure est problématique pour deux raisons. D'une part, lors de la période de survie (environ un an) le cortex adjacent à la lésion envahit l'espace libérée par la lésion. Par ailleurs, rien ne garantit que ce cortex soit fonctionnel. Il devient donc impossible de déterminer directement l'étendue de la lésion après un an de survie.

Afin de contourner ce problème, la dégénérescence provoquée par la lésion a été examinée dans le CGL. Il est connu qu'aux mêmes positions rétinotopiques du CGL correspondant à la lésion, il y a une mort cellulaire (parmi d'autres : Cornwell *et al.*, 1989; Guido *et al.*, 1990a; Rushmore & Payne, 2003, 2004). Cette façon d'établir l'étendue de la lésion présente deux avantages. Dans un premier temps, l'organisation rétinotopiques très stéréotypée du CGL permet l'estimation de l'étendue du champ visuel affecté. Deuxièmement, cette méthode permet de déterminer le degré d'atteinte à chaque point du champ visuel. Cela fournit une évaluation de l'importance fonctionnelle de la lésion.

### 2.1.2 Âges des lésions

Rappelons qu'une des questions qui a motivé l'étude sur les lésions était reliée à l'étude de Rudolph et Pasternak (1996). Ces auteurs avaient

démontré qu'une lésion de l'aire visuelle primaire chez l'adulte mène à une amélioration comportementale dans des tâches de discrimination de la direction avec un stimulus de mouvement global. Les lésions effectuées dans le cadre de cette thèse étaient chez le chaton âgé de 7-9 jours. Il est concevable que la différence d'âge lors de la lésion entre notre étude et celle de Rudolph et Pasternak soit explicative de l'absence d'augmentation de la sélectivité à la direction dans le présent ouvrage. Ceci semble, néanmoins, peu probable car une augmentation de la sélectivité à la direction des cellules du PMLS suite à une lésion serait vraisemblablement attribuable à une réorganisation anatomique. Un tel changement étant plus probable chez le chaton que chez l'adulte, l'augmentation de la sélectivité, si elle existait au niveau du PMLS, devrait être présente chez le chaton.

## 2.2 Étude de latence

### 2.2.1 La nature du processus étudié

Dans l'étude des latences, il y a une présomption que la mesure du délai entre l'apparition du stimulus et le début de la réponse neuronale reflète une succession d'étapes dans la hiérarchie du système visuel ainsi qu'un temps de traitement du mouvement présent dans le stimulus (intégration neuronale). Toutefois, dans la présente étude les stimuli apparaissaient et se mettent en mouvement simultanément. Il est donc impossible de dissocier le temps nécessaire pour qu'une information reliée à un changement de luminance se

rende dans une région visuelle donnée versus le temps requis pour que celle-ci extrait l'information directionnelle. Ceci ne change en rien les conclusions de l'étude pour trois raisons. 1- La simultanéité des réponses va à l'encontre de la notion d'une hiérarchie stricte. Cet argument reste quand même valide même dans l'éventualité que nous ayons mesuré la latence reliée uniquement au changement de luminance. 2- Le fait que différents stimuli aient évoqué des réponses avec des latences variables à l'intérieur d'une même région suggère que cette mesure ne reflétait pas uniquement une réponse au changement de luminance, car elles auraient été simultanées. 3- Par ailleurs, lors de mesure de la latence avec des conditions non-optimales (direction, vitesse, fréquence, densité, etc.) la latence était supérieure à celle pour la condition optimale (ces données ne sont pas présentées dans l'article), ce qui confirme que celle-ci est reliée au traitement de l'information. En résumé, la mesure de latence semble refléter l'intégration d'indices de mouvement, bien que cette intégration ne soit pas nécessaire afin de tirer des conclusions sur la hiérarchie des aires visuelles.

### 2.2.2 La résolution temporelle

Une critique potentielle serait que la nature du phénomène mesuré ne permet pas de discriminer entre différents niveaux de la hiérarchie. Présignons, par exemple, que la somme du temps de transmission d'une région à l'autre et d'intégration soit d'au plus 10ms (Nowak & Bullier, 1997). Cet estimé est vraisemblable selon les études de stimulations anti- et orthodromiques chez le chat (entre autre : Berson, 1985; Rauschecker *et al.*, 1987b; Casanova, 1993;

Weyand & Gafka, 2001), ainsi que la mesure du délai entre le premier potentiel post-synaptique excitateur évoqué par un stimulus et le premier potentiel d'action (Creutzfeldt & Ito, 1968; Volgushev *et al.*, 1995). La variabilité des latences à l'intérieur d'une même région est nettement supérieure à cette valeur de 10ms (voir les écarts types du Tableau 1 de l'étude des latences pour des exemples). Malgré cette variabilité, s'il existait un corrélat fonctionnel entre la hiérarchie et les latences, il devrait au moins y avoir une tendance récurrente dans les données. Aucune tendance ne fût constatée parmi les mesures de latence, du moins dans ce contexte de hiérarchie. De plus, la relation claire entre la position dans la hiérarchie des régions dans la voie ventrale et les latences suggère que le problème potentiel mentionné ci-haut n'en soit pas un. C'est-à-dire que la variabilité à l'intérieur d'une même région n'est pas supérieure à celle entre les régions.

## 2.3 Profil spatio-temporel

### 2.3.1 Aspect linéaire de la méthode

Tel que nous l'avons vu dans l'introduction, le principal apport cortical au PMLS provient des cellules complexes des aires 17 et 18 (Symonds & Rosenquist, 1984a, b; Einstein & Fitzpatrick, 1991; Grant & Shipp, 1991; Shipp & Grant, 1991; Norita *et al.*, 1996; Scannell, 1997; Scannell *et al.*, 1999; Grant & Hilgetag, 2005), et celles-ci démontrent des propriétés non-linéaires (Citron & Emerson, 1983; Emerson *et al.*, 1987; Vajda *et al.*, 2006). Dans un tel contexte,

l'utilisation de corrélation rétrograde de premier ordre peut *a priori* paraître être un choix surprenant, car cette technique ne devrait pas permettre une description complète du profil spatio-temporel. Rappelons cependant que les travaux de Vajda *et al.* (2006) ont démontré une intégration temporelle non-linéaire dans l'aire 18, mais que la quasi-totalité des neurones du PMLS effectuaient une intégration temporelle linéaire. Ainsi, la question qui a motivé la présente étude était de déterminer si une intégration spatiale linéaire avait également lieu au niveau du PMLS, ce à quoi la corrélation rétrograde de premier ordre peut répondre. Enfin, notons que si les champs récepteurs du PMLS sont impliqués dans une intégration spatiale non-linéaire, alors la description de leur profil spatio-temporel avec la corrélation rétrograde est incomplète mais pas erronée. Une description des profils d'ordre supérieur est présentement en cours (voir section étude future).

### 2.3.2 La nature non-écologique de la stimulation impulsionnelle

Un des principes de la corrélation rétrograde est que celle-ci reflète la réponse impulsionnelle du système (de Boer & Kuyper, 1968; Eggermont *et al.*, 1983; Marmarelis *et al.*, 1986). Une stimulation, et donc une réponse, de plus longue durée provoquent un problème car il devient alors impossible de différencier la composante de la réponse qui est provoquée uniquement par la présentation du stimulus de la composante qui est ajoutée par l'intégration temporelle de la stimulation. Il s'en suit qu'une critique plutôt évidente de la méthode de la corrélation rétrograde est l'aspect peu écologique de la méthode



de stimulation. Il est rare dans un milieu naturel qu'un objet apparaisse et disparaisse subitement et ce de façon aléatoire. Il est donc peu probable que le système visuel ait évolué dans un environnement dans lequel une telle sorte d'analyse soit utile, par conséquent la description du champ récepteur qui en ressort est, au moins partialement, biaisée par le choix du stimulus. En reconnaissant cette limite, nous pouvons l'utiliser à bon escient afin de comprendre comment les afférences d'une cellule sont intégrées ponctuellement sans se soucier de l'intégration temporelle mentionnée ci-haut. Autrement dit, ce qui pourrait être un point faible de cette technique est en fait sa force.

### 3. Implication pour la hiérarchie des aires corticales

Bien que chaque étude dans la présente thèse ait un objectif qui lui soit propre, la question centrale qui relie les trois études est celle du corrélat fonctionnel de l'organisation hiérarchique des projections vers le cortex extrastrié. En particulier, est-ce que les propriétés physiologiques du PMLS concordent avec les prédictions basées sur les hiérarchies proposées (Rockland & Pandya, 1979; Maunsell & van Essen, 1983; Van Essen & Maunsell, 1983; Symonds & Rosenquist, 1984b; Felleman & Van Essen, 1991). Les résultats de la présente thèse suggèrent que ces hiérarchies ne soient pas en mesure d'expliquer toutes les propriétés physiologiques des neurones du PMLS, et potentiellement d'autres aires corticales de la voie dorsale.

### 3.1 La voie du CGL

Les résultats des trois études suggèrent que le transfert de l'information visuelle vers le PMLS ne doit pas obligatoirement passer par les aires 17 et 18. Quelle voie pourrait alors être responsable des réponses observées? La proposition la plus probable semble être celle du CGL. Une telle projection permettrait d'expliquer les latences simultanées dans l'aire visuelle primaire et le PMLS (Dinse & Kruger, 1994 : présente étude), ainsi que les réponses du PMLS qui précèdent ou sont synchrones avec celles de l'aire 17 (Katsuyama *et al.*, 1996). Ceci concorde avec la démonstration que les projections du CGL vers l'aire 17 et le PMLS ont la même latence de transmission et sont suffisamment fortes pour évoquer un potentiel d'action dans le PMLS (Berson, 1985; Rauschecker *et al.*, 1987b). Cela n'est guère surprenant étant donné les résultats anatomiques de Tong et Spear (1986) qui ont démontré que certaines cellules du CGL projetaient à la fois à l'aire 17 et au PMLS.

Une telle projection permettrait aussi d'expliquer les effets limités des lésions de l'aire visuelle primaire tant chez l'adulte que chez le chaton (Spear & Baumann, 1979; Tong *et al.*, 1984; Tong *et al.*, 1987; Spear, 1988; Guido *et al.*, 1990a; Guido *et al.*, 1990b; Guido *et al.*, 1992; Spear, 1995; Illig *et al.*, 2000). L'élimination d'un traitement tel que celui du modèle d'énergie (Adelson & Bergen, 1985) pourrait expliquer la réduction de la sélectivité à la direction. Parallèlement, le maintien (adulte) ou l'augmentation (chaton) de la projection du CGL (Tong *et al.*, 1984; Kalil *et al.*, 1991; Payne & Cornwell, 1994; Payne &

Lomber, 1998b) permettrait aux neurone du PMLS de conserver leurs propriétés spatio-temporelles (Tong *et al.*, 1984; Tong *et al.*, 1987; Guido *et al.*, 1990a; Guido *et al.*, 1990b; Guido *et al.*, 1992) et fournirait un apport excitateur permettant un maintien partiel de la sélectivité à la direction. Avec le modèle présenté dans l'article sur les lésions, il a été démontré qu'un apport géniculé était suffisant pour extraire de l'information directionnelle, même à partir de stimuli complexes. Il est important de noter que ce modèle est une démonstration de faisabilité et non une preuve que l'apport géniculé est responsable des réponses résiduelles observées dans le PMLS.

La question est alors de savoir si le peu de changement des propriétés du PMLS est réellement attribuable à une modulation du nombre de projections des voies qui sont présentes chez l'animal normal ou à une plasticité qui génère de nouvelles connexions. À ma connaissance aucune étude ne fait état d'une nouvelle projection suite à une lésion de l'aire visuelle primaire chez le chaton (cependant voir les données contradictoires de : Payne *et al.*, 1993; Boire *et al.*, 2004). Par contre, plusieurs études ont observées une augmentation du nombre de certaines projections suite à une lésion néo-natale, par exemple les projections du CGL vers le PMLS (Tong *et al.*, 1984; Kalil *et al.*, 1991; Spear, 1995; Payne & Lomber, 1998b). Du côté fonctionnel, la conservation de la sélectivité spatio-temporelle des cellules du PMLS, mentionnée dans le paragraphe précédent, n'est pas compatible avec une réorganisation massive des projections vers le PMLS. Pour proposer une réorganisation massive des projections vers le PMLS, il faudrait alors présumer que 1- ces nouvelles

projections existeraient et 2- qu'elles permettraient une sélectivité quasi-normale, malgré un apport fondamentalement différent entre l'animal normal et lésé. Selon le principe du rasoir d'Ockham, il faut présumer qu'une projection accrue du CGL vers le PMLS serait responsable de la sélectivité observée.

Deux autres études soutiennent cette idée d'un apport important du CGL vers le PMLS. Premièrement, suite à une lésion de l'aire visuelle primaire à P1-2, Payne (2004) a démontré qu'une fois adulte ces chats arrivaient à s'orienter vers des stimuli présentés dans l'hémi-champ lésé avec un taux de réussite qui avoisinait celui des animaux normaux. Par contre, après une injection d'acide iboténique dans le CGL les chats étaient incapables de s'orienter vers ces mêmes stimuli. Ceci démontre donc que la voie géniculo-extrastrée joue un rôle important dans les capacités comportementales résiduelles chez le chat lésé en bas âge. Il a été démontré par Lomber (2001) que chez l'animal normal, le PMLS doit être fonctionnel afin de bien accomplir cette tâche. Il est donc plausible que la manipulation de Payne (2004) ait interrompu directement une voie géniculo-extrastrée, ce qui aurait rendu les animaux incapables d'accomplir la tâche. Cette projection pourrait également servir la sélectivité résiduelle à la direction telle que mesurée dans le PMLS d'animaux lésés.

La deuxième étude a été effectuée chez le singe dans l'aire MT, cette dernière ayant été suggérée comme étant l'homologue du PMLS (Payne, 1993). Lors de la présentation de réseaux de barres, Thiele (2004) a injecté de la bicuculline dans MT afin d'éliminer l'inhibition intra-corticale dans cette région, l'hypothèse étant que la sélectivité à la direction devrait encore être présente à

cause des projections de V1 vers MT (Shipp & Zeki, 1989). La sélectivité à la direction observée durant la période initiale de la réponse neuronale était absente lors de l'injection. Ainsi, les auteurs ont conclu que l'aire MT était impliquée dans une analyse de la direction qui serait parallèle à celle de l'aire visuelle primaire et que l'apport le plus probable proviendrait du CGL. Puisque la projection du CGL vers le cortex extrastrié chez le chat est plus importante que celle du singe (Benevento & Yoshida, 1981; Fries, 1981; Niimi *et al.*, 1981; Benevento & Standage, 1982; Tong & Spear, 1986; Tong *et al.*, 1991; Kawano, 1998; Stepniewska *et al.*, 1999) cette voie est vraisemblablement fonctionnellement plus importante chez le félin.

Enfin, les champs récepteurs des neurones de l'aire visuelle primaire ont des profils spatio-temporels incompatibles avec certains profils observés dans le PMLS. Cependant, une projection du CGL vers les neurones du PMLS expliquerait ces résultats inattendus. Décrivons d'abord les deux principales caractéristiques qui rendent ces profils inattendus. Premièrement, 28% des neurones ne présentaient pas de superposition spatiale des sous-champs qui répondaient aux contrastes inversés. Ceci ne correspond pas aux attentes pour des neurones qui reçoivent leurs principaux apports des cellules complexes de l'aire visuelle primaire (Gilbert, 1977; Symonds & Rosenquist, 1984b; Einstein & Fitzpatrick, 1991). La deuxième caractéristique inattendue est la présence de réponses temporellement déphasées entre contrastes. À ma connaissance, aucune étude n'a décrit de tels profils pour les cellules complexes de l'aire 17

(Movshon *et al.*, 1978a; Citron & Emerson, 1983; Emerson *et al.*, 1987; Szulborski & Palmer, 1990; Emerson *et al.*, 1992).

Une réponse dans le PMLS construite à partir des champs récepteurs du CGL (Stevens & Gerstein, 1976) permettrait d'expliquer ces deux caractéristiques. En effet, Stevens and Gerstein (1976) ont décrit, grâce à une technique précurseur à celle de la corrélation rétrograde, l'existence de sous-populations de neurones qui démontraient une ségrégation spatiale et temporelle des réponses à différents contrastes dans le CGL. Une projection de ces sous-groupes du CGL pourrait donc expliquer les profils inattendus dans le PMLS. Notamment, des réponses spatialement et/ou temporellement distinctes selon le contraste.

### 3.2 Les voies alternatives

#### 3.2.1 Le collicule supérieur

Une des voies qui pourrait avoir un effet sur les réponses des neurones du PMLS serait celle du collicule supérieur. Notamment, nous savons qu'une élimination des apports du collicule supérieur modifie les propriétés du PMLS (Smith & Spear, 1979; Ogino & Ohtsuka, 2000; Ohtsuka & Ogino, 2001). Par contre, plusieurs éléments suggèrent que cet effet soit indirect. Les neurones du collicule supérieur ne projettent pas directement au PMLS, et donc n'ont qu'un effet indirect. Quelle est cette voie indirecte? Le collicule supérieur projette vers la partie médiane du LP-pulvinar (Berson & Graybiel, 1978;

Graybiel & Berson, 1980; Kelly *et al.*, 2003), mais comme nous avons vu dans l'introduction c'est surtout la partie latéral du LP-pulvinar qui projette au PMLS (Berson & Graybiel, 1978; Tong *et al.*, 1982; Raczkowski & Rosenquist, 1983; Tong & Spear, 1986; Norita *et al.*, 1996; MacNeil *et al.*, 1997). La conjonction de ces données anatomiques rend peu probable l'existence d'un effet majeur des neurones du collicule supérieur sur ceux du PMLS. De plus, il a été démontré que suite à une lésion de l'aire visuelle primaire, les neurones du collicule supérieur perdent leur sélectivité à la direction (Wickelgren & Sterling, 1969; Rosenquist & Palmer, 1971; Stein & Magalhaes-Castro, 1975; Mize & Murphy, 1976; Flandrin & Jeannerod, 1977; Dec & Tarnecki, 1980), il serait alors fort surprenant que le PMLS hérite sa sélectivité résiduelle du collicule supérieur suite à une lésion.

Tel que mentionné dans le paragraphe précédent, la majorité des terminaisons de la projection du collicule supérieur n'aboutissent pas dans la sous-division du LP-pulvinar qui projette massivement au PMLS. D'où provient alors l'effet de la lésion du collicule supérieur sur les neurones du PMLS? Il a été démontré que le collicule supérieur module l'amplitude de la réponse du CGL (Xue *et al.*, 1994). Si une projection du CGL est impliquée dans la sélectivité à la direction dans le PMLS, alors le collicule supérieur serait bien placé pour influencer cette sélectivité. Alternativement, la projection du collicule supérieur vers le LPm pourrait indirectement influencer les réponses dans des aires corticales tels que le PLLS, l'ALLS, l'AEV, et dans une moindre mesure l'AMLS. En fait, ces régions reçoivent des projections du LPm plutôt que du LPI

(Symonds *et al.*, 1981; Naito & Kawamura, 1982; Raczkowski & Rosenquist, 1983; Norita *et al.*, 1996). Via des voies de rétroaction à partir de ces régions corticales (Symonds & Rosenquist, 1984b, a; Miceli *et al.*, 1985; Norita *et al.*, 1996), le collicule supérieur pourrait influencer les réponses dans le PMLS. Ceci semble moins probable à cause du nombre de synapses séparant le collicule supérieur et le PMLS.

### 3.2.2 Les boucles de rétroaction

L'information visuelle pourrait être acheminée vers les aires extrastriées et ces dernières pourraient imposer une sélectivité à la direction aux neurones du PMLS via des boucles de rétroaction. Ceci semble peu probable dans le cadre d'une organisation hiérarchique. Il faudrait alors supposer que des aires de plus haut niveau que le PMLS reçoivent leurs apports principaux via un réseau indépendant de celui-ci. Cela contredirait directement la notion de hiérarchie. De plus, la nature même des boucles de rétroaction est incompatible avec l'évocation d'une réponse visuelle robuste dans le PMLS. C'est-à-dire la nature plutôt modulatrice des boucles de rétroaction impliquées versus la fonction de transmetteur (*driver*) des projections *feedforward* telles que celles présentes dans le CGL. Ces boucles pourraient servir à moduler les réponses des neurones du PMLS plutôt que de les évoquer.



### 3.2.3 La voie rétino-thalamo-corticale

Enfin, une dernière possibilité afin d'expliquer les réponses observées dans le PMLS serait la projection de la rétine vers le LP-pulvinar (Labar *et al.*, 1981; Itoh *et al.*, 1983; Boire *et al.*, 2004), quoique cette projection soit disputée (Payne *et al.*, 1993). Comme nous l'avons vue précédemment, le LPI est la partie du LP qui projette le plus au PMLS, mais les trois sous-divisions projettent à ce dernier (Symonds *et al.*, 1981; Naito & Kawamura, 1982; Raczkowski & Rosenquist, 1983; Norita *et al.*, 1996), dont le pulvinar qui reçoit la projection rétinienne. L'importance fonctionnelle de cette projection dans le contexte de l'évocation d'une réponse de la part des neurones du PMLS n'est pas claire pour deux raisons. Premièrement, il y a une surreprésentation du méridien vertical (Boire *et al.*, 2004) ce qui ne correspond pas à la représentation du champ visuel dans le PMLS (Palmer *et al.*, 1978). Deuxièmement, les synapses rétino-thalamique ont été décrites comme étant de type bouton (Boire *et al.*, 2004) plutôt que rosette comme on en retrouve dans le CGL. La capacité d'évoquer une réponse visuelle robuste dans le LP-pulvinar à partir des afférences rétinienne n'est donc pas évidente.

Il est important de noter par contre que chez l'animal normal, le LPI reçoit également une projection massive de la part des aires 17 et 18 (Berson & Graybiel, 1978; Graybiel & Berson, 1980; Berson & Graybiel, 1983b; Raczkowski & Rosenquist, 1983). Deux études portent à croire que les projections des aires 17 et 18 vers le PMLS via le LPI contribuent peu aux propriétés physiologiques des neurones du PMLS. D'une part, malgré

l'importance anatomique des projections de l'aire 17 vers le LPI, leur influence fonctionnelle n'est pas claire. Notamment, Casanova *et al.* (1997) ont démontré qu'il y avait peu de modifications des propriétés dans le LPI suite à l'élimination des apports de l'aire 17 par des techniques soit de refroidissement, soit de lésions. Il reste à déterminer si des manipulations semblables soit de l'aire 18 seule, ou en conjonction avec l'aire 17, auraient un effet plus important. D'autre part, l'inactivation pharmacologique du LPI n'a pas d'effets majeurs sur les propriétés physiologiques des neurones du PMLS telles que mesurées avec des réseaux (Minville & Casanova, 1998). En résumé, il n'est pas clair s'il existe une afférence excitatrice qui soit capable, à elle seule, d'évoquer une réponse des neurones du LPI. Cela n'exclut pas la possibilité d'une intégration de plusieurs afférences. Indirectement le PMLS recevrait donc de l'information de plusieurs voies parallèles.

### 3.3 Réconciliation de l'anatomie et de la physiologie

Faisons abstraction pour l'instant de l'origine précise des afférences du PMLS et des autres aires visuelles extrastriées. Il y a malgré tout une hiérarchie anatomique qui semble coexister avec un système physiologique qui opère en parallèle. Pour quelle raison une telle organisation existerait-elle? Deux propositions offrent un cadre dans lequel analyser cette situation et possiblement réconcilier cette situation dichotomique

### 3.3.1 La proposition sensorielle

Dans le cadre d'un système visuel organisé en parallèle, une intégration globale aurait lieu dans les diverses aires visuelles en simultanée (Bullier, 2001, 2004a). À la suite de quoi les aires visuelles renverraient l'information à l'aire visuelle primaire pour lui imposer une organisation fonctionnelle. L'aire 17 projetterait alors vers les aires extrastriées pour leur fournir des informations locales supplémentaires. Il est à noter que dans cette vision du transfert de l'information les projections feedforward évoqueraient toujours une réponse dans des aires de plus haut niveau, mais ne serait pas impliquées dans la partie initiale de la réponse.

Dans le cas du PMLS, la sélectivité à la direction extraite servirait à imposer une organisation fonctionnelle aux réponses de l'aire 17 (Bullier, 2001, 2004a). Ensuite, cette dernière projetterait de nouveau vers le PMLS afin que ses neurones puissent utiliser une information avec une plus grande résolution spatiale. Les boucles cortico-corticales rétrogrades participeraient donc au traitement de l'information avant les projections dites *feedforward*.

Cette proposition est compatible avec les études de latences chez le chat et le primate (Robinson & Rugg, 1988; Maunsell & Gibson, 1992; Dinse & Kruger, 1994; Nowak *et al.*, 1995; Schmolesky *et al.*, 1998; Schroeder *et al.*, 1998; Raiguel *et al.*, 1999; Lamme & Roelfsema, 2000; Bullier, 2001; Azzopardi *et al.*, 2003; Bullier, 2004a) ainsi que les résultats de cross-corrélation des potentiels d'action dans le PMLS et l'aire 17 (Katsuyama *et al.*, 1996). De plus, ces réponses simultanées dans les deux aires requièrent des voies parallèles

afin d'acheminer l'information vers le PMLS, ceci pourrait alors expliquer la sélectivité à la direction résiduelle observée dans cette thèse. Ces multiples voies seraient également compatibles avec la diversité de profils de champs récepteurs observés dans la troisième étude de cette thèse.

Les neurones des aires de haut niveau dicteraient alors l'organisation des propriétés physiologiques à l'aire visuelle primaire. En effet, il a été démontré que les cellules de V1 chez le macaque font une analyse initialement grossière qui devient de plus en plus précise avec le temps (Ringach *et al.*, 1997a; Bredfeldt & Ringach, 2002) pour ce qui a trait à la sélectivité à l'orientation et la fréquence spatiale. Toujours chez le primate, les boucles de rétroaction exerceraient leur effet dès le début de la réponse des cellules dans V1 (Hupe *et al.*, 2001). De plus, chez le chat il a été démontré que les cartes de sélectivités à la direction mesurées par l'imagerie des signaux intrinsèques sont compromises dans l'aire 17 et 18 (Galuske *et al.*, 2002; Shen *et al.*, 2006a) lors d'une inhibition du PMLS par refroidissement. De même, l'aire 21a aurait une relation similaire avec l'aire 17 concernant les fréquences spatiales (Huang *et al.*, 2004).

Dans un système tel que décrit ci-dessus, l'aire 17 servirait comme une *tabula rasa* (Bullier, 2001) pour intégrer l'information provenant de plusieurs aires corticales, chacune spécialisée dans l'analyse d'une composante de la scène visuelle. Ceci est similaire à la proposition de Mumford (1991) pour la fonction intégrative du LP-pulvinar. Pour faire une comparaison avec le modèle de sélection (Nowlan & Sejnowski, 1995), l'aire 17 agirait alors comme modèle

d'énergie tel que dans le modèle originel mais pourrait également agir en tant que "mécanisme de vitesse locale" qui était originellement attribué à MT. Les neurones du PMLS agiraient comme le mécanisme de sélection, c'est-à-dire un mécanisme d'extraction de direction globale.

### 3.3.2 La proposition attentionnelle

Passons maintenant à la deuxième proposition qui pourrait réconcilier la hiérarchie anatomique et un système physiologique parallèle. Cette idée, tout comme celle que nous venons de voir (Nowak & Bullier, 1997; Bullier, 2001, 2004a), implique deux étapes distinctes avec des fonctions bien différentes. La première étape serait le *rapid feedforward sweep* (Lamme & Roelfsema, 2000) qui est essentiellement une activation rapide de toutes les aires corticales visuelles suite à la présentation d'un stimulus. Selon Lamme et Roelfsema (2000), le profil d'activation temporel ne correspond pas à la hiérarchie anatomique pour trois raisons. 1- Tel que proposé dans la présente thèse, le rôle des afférences provenant d'autres structures que l'aire visuelle primaire doit être pris en considération. 2- Il y a plusieurs voies parallèles qui co-existent dans le système visuel, et celles-ci n'ont pas la même vitesse de conduction (Lennie, 1980; Dreher *et al.*, 1996a). Une des conséquences de cette multiplicité des voies et de vitesses de conduction est une augmentation de la variabilité prédite pour les distributions de latence à l'intérieur d'une même aire. Ceci pourrait donc masquer une différence dans les latences entre régions. 3- Dans chaque aire, tous les neurones ne reçoivent pas des afférences via les

connexions les plus courtes, c'est-à-dire avec le plus petit nombre de synapses à partir de la rétine. Ceci augmenterait également la variabilité des latences à l'intérieur d'une région. Ces trois points expliqueraient la différence entre l'anatomie et la physiologie, mais alors qu'est-ce que la hiérarchie nous dit à propos du système visuel?

Commençons par rendre explicite ce qui est implicitement proposé dans le paragraphe précédent. Une étude qui prendrait en compte le type d'afférences des neurones corticaux devrait être en mesure de mettre en évidence une hiérarchie basée sur les latences qui reflèterait celle provenant de l'anatomie. Les projections de type *feedforward* serviraient donc à évoquer une réponse qui suivrait l'ordre hiérarchique des structures visuelles et serait responsable des propriétés de base des champs récepteurs (taille, sélectivité à la direction, vitesse, etc.), celles-là mêmes qui sont compatibles avec la notion de traitement sériel (voir introduction). Les voies de rétroactions serviraient plutôt de modulateur de la réponse selon le contexte, notamment, via une modulation attentionnelle. Par exemple, lors de la réponse initiale, une cellule de l'aire 17 encoderait l'orientation d'un stimulus (entre autres), mais par la suite son taux de décharge pourrait encoder la saillance comportementale de ce stimulus. Un tel comportement a déjà été décrit dans l'aire 17 (Roelfsema *et al.*, 1998; Khayat *et al.*, 2006) et plus récemment il a été démontré que l'activité de ces mêmes neurones reflète plusieurs étapes d'analyse lors d'une tâche de segmentation d'image (Roelfsema *et al.*, 2007).

En résumé, les deux hypothèses mettent de l'avant l'idée qu'il y ait une activation rapide de tout le système visuel. Cette activation initiale quasi-simultanée sert à l'analyse et l'extraction de l'information visuelle. Ensuite, l'effet des boucles de rétroaction augmenterait la précision de l'analyse dans les aires de bas niveau. Cette information serait alors acheminée vers les aires de haut niveau via des voies qui suivent la hiérarchie anatomique. Ceci permet donc de réconcilier ce qui *a priori* semblait être des observations contradictoires.

Mentionnons rapidement un problème avec ces deux notions. Elles fonctionnent très bien lorsque nous tentons d'expliquer comment le système visuel effectue une analyse de l'information sur des stimuli dans un laboratoire. Cependant, comment une telle organisation traiterait-elle l'information dans un milieu naturel? Il faudrait donc expliquer comment de nouveaux signaux provenant d'une stimulation récente interagiraient avec l'information dans les boucles de rétroaction. Il est concevable que les boucles de rétroaction n'agissent pas sur les mêmes neurones que les voies *feedforward*, mais ceci pose également un problème. Si le rôle des boucles de rétroaction n'est pas d'influencer directement les neurones dont les réponses sont évoquées par les voies *feedforward* (dans l'aire 17 par exemple) alors pourquoi avoir des projections cortico-corticales de rétroaction qui sont physiologiquement coûteuses?

## 4. Intégration spatiale dans le PMLS

### 4.1 Intégration linéaire versus non-linéaire

Dans l'introduction de cette thèse nous avons vu que la corrélation rétrograde a permis de démontrer que l'intégration temporelle dans le PMLS était linéaire (Vajda *et al.*, 2006). Cette conclusion a mené à une des principales questions de cette thèse, soit est-ce que les champs récepteurs des neurones du PMLS font également une intégration spatiale linéaire. Les résultats de l'étude des profils spatio-temporels de la présente thèse suggèrent que cela n'est pas le cas. En fait, s'il y avait une intégration spatiale linéaire il devrait être possible d'utiliser les profils spatio-temporels des neurones du PMLS pour prédire leurs paramètres optimaux. Les résultats ont démontré le contraire, il n'est pas possible de prédire le profil de réponse d'un neurone du PMLS en se basant sur son profil spatio-temporel. Une description complète du profil de réponse des neurones du PMLS requiert donc une corrélation rétrograde non-linéaire (voir étude future).

### 4.2 Intégration du mouvement

Plusieurs auteurs supposent implicitement que les neurones du PMLS analysent le mouvement à partir de la sortie d'un modèle d'énergie (Adelson & Bergen, 1985), et certains, tels que Nowlan & Sejnowski (1995), l'expriment explicitement. Rappelons qu'il a été démontré que les cellules complexes ont une réponse similaire à celle de la sortie du modèle d'énergie (Emerson *et al.*,



1992) et que ce sont surtout ces cellules qui projettent vers le PMLS. Pourtant le présent ouvrage a démontré que suite à une lésion des aires visuelles primaires chez le chaton, la sélectivité à la direction est encore présente dans le PMLS. Ainsi, un autre mécanisme doit être responsable de cette sélectivité, du moins chez le chaton lésé. En utilisant un modèle très simple, une démonstration de faisabilité a mis en évidence la possibilité d'encoder la direction de stimuli de mouvement complexe à partir des réponses du CGL. Une étude potentielle qui découle de ces données sera discutée dans la section étude future.

Avant de continuer revenons rapidement sur le dernier modèle dont il est mention dans le paragraphe précédent, soit celui de Nowlan & Sejnowski (1995). Ce modèle représente simplement une auto-corrélation avec un déphasage spatio-temporel donné effectué sur les afférences d'une cellule, soit un modèle de type Reichardt (1961a). L'intérêt des modèles de ce type est à la fois leur simplicité mais également le fait que le corrélat physiologique est plutôt facile à imaginer, soit une simple intégration spatio-temporelle au niveau de l'arborisation dendritique. Une schématisation du concept se trouve à la Figure 1. Dans le panneau du haut, un stimulus (cercle noir) apparaît à différents endroits selon le moment et par conséquent sur différents récepteurs. Ce panneau décrit donc un stimulus en mouvement. Dans le panneau du bas, une schématisation de trois synapses excitatrices provenant des trois récepteurs du panneau du haut est présentée. Notez que si la stimulation visuelle passe du récepteur 1 vers le 3 et que le  $\Delta t$  est approximativement équivalent au temps de

conduction du potentiel post-synaptique entre les synapses, il y aura sommation. Cependant, si la stimulation passe du récepteur 3 vers le 1, alors il n'y aura pas de sommation des potentiels post-synaptiques. Ce processus synaptique est équivalent à une auto-corrélation du stimulus avec un délai et un déplacement précis.

Dans les paragraphes précédent il a été mentionné que ce modèle, tel qu'appliqué dans cet ouvrage, n'est qu'une démonstration de faisabilité. C'est-à-dire qu'un tel mécanisme pourrait expliquer les résultats, sans pour autant démontrer que ce mécanisme est responsable des réponses observées. Il est à noter qu'il est plus plausible qu'un mécanisme d'ordre supérieur soit responsable des réponses résiduelles dans le PMLS suite à une lésion de l'aire visuelle primaire. En fait, l'étude sur les profils spatio-temporels nous apprend que l'intégration spatiale des neurones du PMLS est non-linéaire alors que l'auto-corrélation est un outil linéaire. Ceci n'implique pas pour autant que les projections du CGL ne puissent être responsables de la sélectivité à la direction des neurones du PMLS. Cela implique par contre, que dans l'éventualité d'un apport du CGL, l'intégration soit d'ordre supérieur.

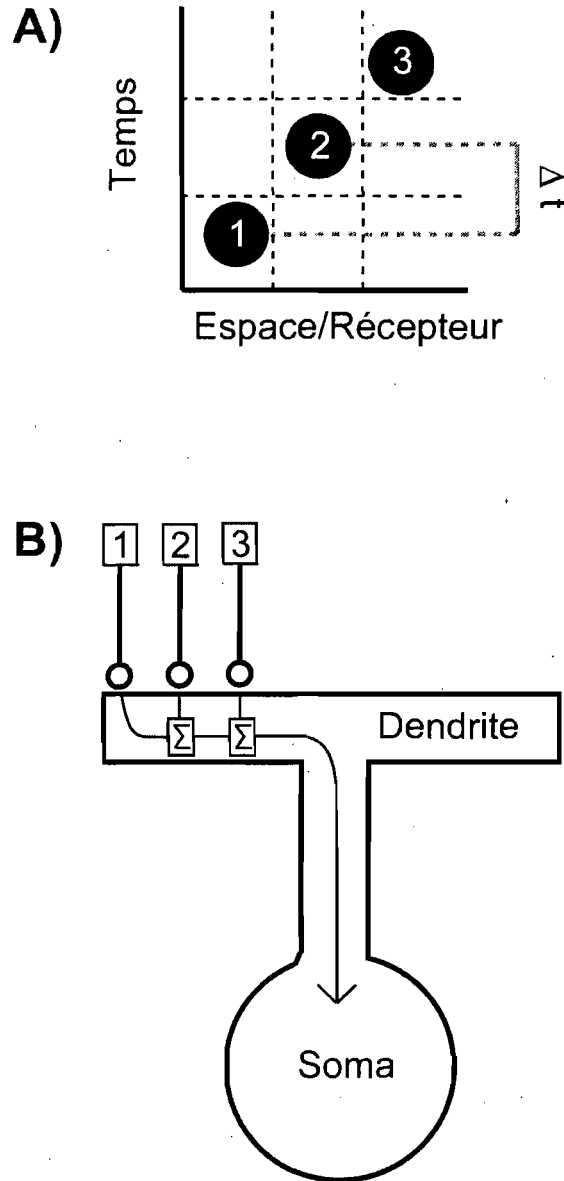


**Figure 1**

Schématisation du corrélat physiologique du modèle de Reichardt. A) La position d'un stimulus à trois moments successifs (1 à 3). Dans cette figure, chaque position dans le champ visuel représente aussi un récepteur. Les lignes pointillées représentent la séparation entre différents temps (abscisse) et la position/le récepteur (ordonné). B) Les synapses proviennent des récepteurs mentionnés dans le panneau A, et sont identifiés de 1 à 3. Lors d'une conjonction spatio-temporelle appropriée des apports synaptiques il y a une sommation des potentiels post-synaptiques.

## 5. Études futures

Les idées d'études futures seront présentées dans trois sections qui reflètent les cadres théoriques qui proviennent de chacune des trois études présentées dans ce travail. Dans une quatrième section se trouveront les idées qui proviennent de la synthèse des présentes études. Mentionnons que l'ordre de présentation des études utilisé jusqu'à ce point sera modifié pour des raisons de clarté de la présentation.

### 5.1 Idées découlant de l'étude des profils

#### 5.1.1 La corrélation rétrograde d'ordre supérieur

Tel que mentionné dans la section de considération méthodologique, la corrélation rétrograde de premier ordre utilisée dans cette thèse est une description incomplète du profil spatio-temporel des champs récepteurs du PMLS. En utilisant une corrélation rétrograde d'ordre plus élevé il serait possible de mieux comprendre l'intégration spatio-temporelle effectuée par les neurones du PMLS. En fait, de telles analyses (Szulborski & Palmer, 1990; Livingstone, 1998; Pack *et al.*, 2006) permettent d'expliquer la sélectivité à la direction et à la vitesse des neurones. À cause de leur capacité de décrire les interactions spatio-temporelles entre les sous-unités qui forment le champ récepteur de la cellule sous étude, il est possible d'estimer la fonction qui décrit le mieux l'intégration effectuée par le neurone. De plus, la nature même des stimuli utilisés dans ces études augmente le niveau d'activité spontanée de la

cellule, ce qui permet d'étudier le rôle possible de l'inhibition dans l'élaboration des propriétés du neurone. Les données pour ce type d'étude ont déjà été cueillies et l'algorithme d'analyse est présentement développé.

Passons rapidement à un exemple d'une cellule fictive qui aurait été étudiée avec cette technique. Dans la Figure 2 nous voyons une représentation de la réponse à différents intervalle spatiaux ( $\Delta$  espace) entre deux stimuli sur chacun des axes et ce pour un intervalle temporel donné ( $\Delta t$ ). Autrement dit, une schématisation de l'amplitude de la réponse neuronale pour chaque changement de position des stimuli pour un intervalle inter stimulus est présentée. Puisque nous connaissons la distance spatiale et temporelle entre la présentation de stimuli successifs qui évoquent la réponse maximale (la partie claire de la figure) nous pouvons calculer la direction et la vitesse préférées de la cellule. Dans notre exemple (panneau du haut), un déplacement vers la droite et vers le haut provoque une réponse de la part de la cellule à ce  $\Delta t$ . Un  $\Delta$  espace plus grand mène forcément à une vitesse plus élevée et *vice versa*. Il s'en suit que les positions en bas à gauche de la partie claire représentent des vitesses plus lentes que les parties en haut à droite.

### 5.1.2 La corrélation rétrograde d'ordre supérieur et l'inactivation

Une autre façon de mieux comprendre les différentes afférences du PMLS dans le cadre d'un système parallèle serait d'utiliser la corrélation rétrograde d'ordre supérieur mentionnée ci-dessus et d'y ajouter une

inactivation de l'aire 17, le CGL, le collicule supérieur et le LP-pulvinar tour à tour. Ainsi, il serait possible de voir l'apport de chacune de ces régions sur la réponse des neurones du PMLS. Comme exemple d'hypothèse, prenons les effets d'une inactivation du collicule supérieur dont la conséquence est une réduction de l'amplitude de la réponse à des vitesses élevées (Ogino & Ohtsuka, 2000; Ohtsuka & Ogino, 2001).

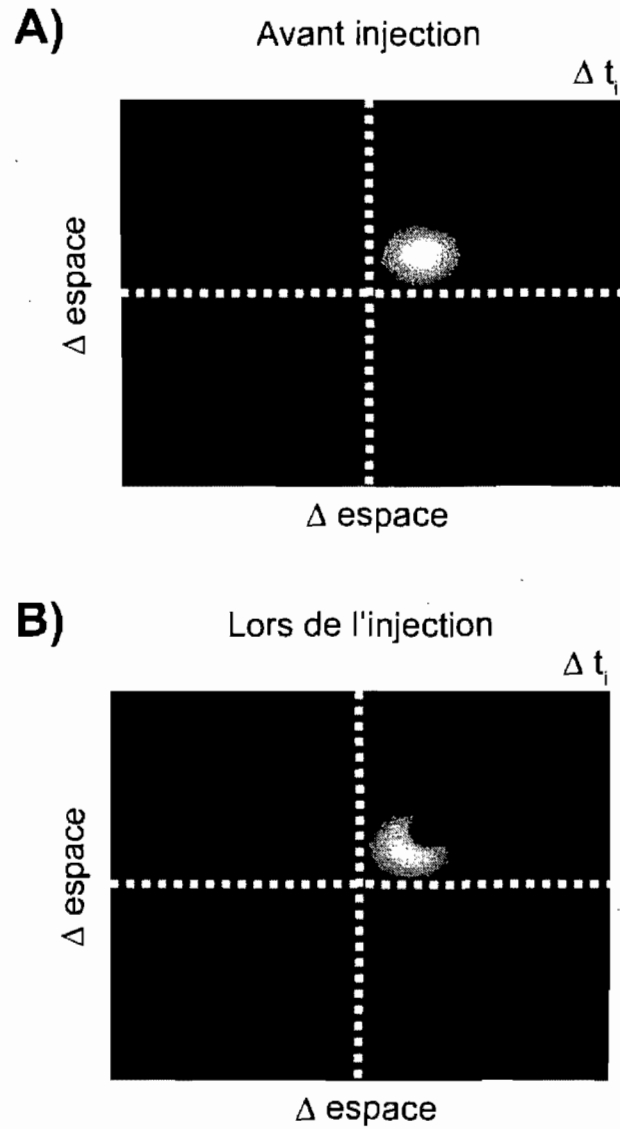


**Figure 2**

Schématisation des résultats d'une corrélation rétrograde d'ordre supérieur. A) Représentation de l'intensité d'une réponse neuronale fictive lors d'une corrélation rétrograde d'ordre supérieur. B) La réponse possible de la même cellule fictive lors d'une inactivation du collicule supérieur.

Revenons à notre cellule fictive du panneau supérieur de la Figure 2. Prêsumons que cette cellule répond de façon maximale à des vitesses moyennes. Dans le cadre de notre prédiction des changements dans le PMLS lors d'une injection dans le collicule supérieur; nous nous attendons à une réduction de la réponse à des vitesses élevées. Dans le diagramme  $\Delta$  espace pour un  $\Delta t$  qui résulterait d'une corrélation rétrograde de deuxième ordre, il devrait donc y avoir une suppression de la zone excitatrice qui représente les vitesses élevées, soit la partie de haut à droite de la zone claire dans la figure 2 (panneau B). L'avantage par rapport aux méthodes précédentes étant que nous pourrions alors déterminer si la réduction de la sélectivité aux vitesses élevées est attribuable à une intégration spatiale, temporelle, ou une conjonction des deux.

### 5.1.3 Le mouvement fronto-parallèle versus le flux optique

Il est connu que les cellules du PMLS sont sélectives aux mouvements fronto-parallèles (Spear & Baumann, 1975; Camarda & Rizzolatti, 1976; von Grunau & Frost, 1983; Minville & Casanova, 1998; Merabet *et al.*, 2000; Villeneuve *et al.*, 2006a) ainsi qu'au flux optique (Rauschecker *et al.*, 1987a; Brenner & Rauschecker, 1990; Sherk *et al.*, 1995; Kim *et al.*, 1997; Mulligan *et al.*, 1997; Sherk *et al.*, 1997; Brosseau-Lachaine *et al.*, 2001). Toutefois aucune technique à ce jour ne permet de facilement distinguer si ces cellules sont plus adaptées à l'analyse des mouvements fronto-parallèles ou au flux optique. Une façon de répondre à cette question serait d'utiliser la corrélation rétrograde avec



un stimulus qui contienne plusieurs impulsions directionnelles spatialement restreintes et indépendantes (Borghuis *et al.*, 2003; Vajda *et al.*, 2004).

L'intérêt d'un tel stimulus est que la composante directionnelle est déjà présente à chaque position testée dans le champ visuel. Donc, un estimé de la sélectivité à la direction est possible pour chaque position, car il n'y a aucun besoin d'utiliser des interactions spatio-temporelles entre les positions. Le résultat peut donc être représenté sous forme de surface dont les points sont des vecteurs moyens des réponses à la direction pour chaque position dans le champ visuel (Srinivasan *et al.*, 1993). Il est alors possible de comparer une telle surface à une prédiction pour des cellules sélectives au mouvement fronto-parallèle ou le flux optique tel que représenté dans la figure 3. Si les prédictions sont exprimées sous forme de modèle quantitatif il est alors possible d'utiliser la technique de la réduction des moindres carrés afin d'évaluer quel modèle correspond le mieux aux données de chaque cellule. Par conséquent il serait possible de quantifier la proportion de chaque type de cellule dans le PMLS ainsi que dans d'autres aires extrastriées.

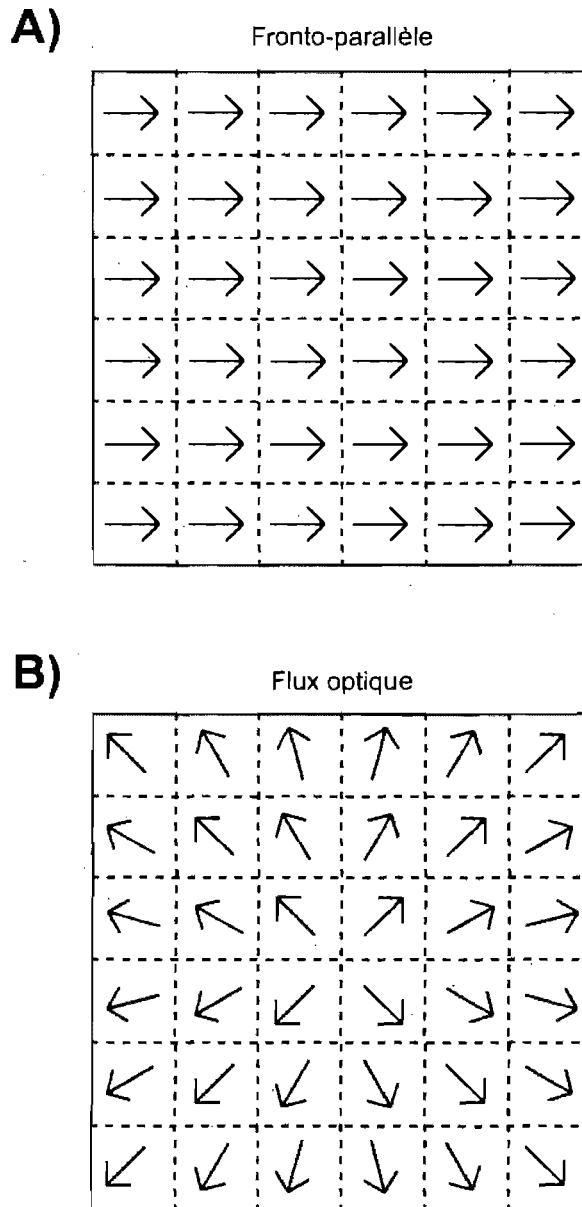


**Figure 3**

Surface de réponse de deux neurones idéalisés. La surface de vecteurs moyens pour deux neurones dont les sous-unités directionnelles seraient disposées de façon optimale pour un mouvement ; A) fronto-parallèle et B) de flux optique. Afin de simplifier, tous les vecteurs sont de même longueur. Les lignes pointillées représentent la limite entre les sous-unités directionnelles.

## 5.2 Idées découlant de l'étude de lésion

### 5.2.1 L'identification de l'origine de la sélectivité résiduelle

L'étude sur les lésions a démontré une sélectivité à la direction résiduelle dans le PMLS, et que ceci pourrait être attribuable à une augmentation de la projection du CGL vers le PMLS. Ces projections existent également chez le chat normal (Raczkowski & Rosenquist, 1980; Symonds *et al.*, 1981; Raczkowski & Rosenquist, 1983; Berson, 1985; Tong & Spear, 1986; Rauschecker *et al.*, 1987b). On pourrait alors formuler l'hypothèse selon laquelle la sélectivité à la direction dans le PMLS est au moins partiellement attribuable aux afférences du CGL même chez le chat adulte normal.

Dans un premier temps, une inactivation des aires 17, 18 et 19 avec une cryoprobe permettrait de déterminer si la sélectivité des neurones du PMLS à des stimuli complexes est présente tel que dans le modèle du chat lésé. L'intérêt d'une telle manipulation, par rapport à une lésion, serait que l'échelle de temps ne permettrait pas de plasticité tout en ne créant pas de dommages physiques majeurs.

Si la sélectivité à la direction demeure, il serait alors opportun d'effectuer une injection de GABA dans le CGL en conjonction avec le refroidissement des aires 17, 18 et 19. Notons rapidement qu'une injection dans le CGL chez le primate a déjà été effectuée (Maunsell *et al.*, 1990), le résultat étant que la sélectivité à la direction et les réponses visuelles en générales sont éliminées dans MT. Dans la mesure où un effet similaire ne serait pas observé dans le

PMLS, il faudrait alors éliminer la possibilité des voies tecto-thalamo-corticale et rétino-thalamo-corticale. Toujours en conjonction avec l'inactivation des aires 17, 18 et 19, une injection de GABA dans le LP-pulvinar permettrait d'éliminer ces deux possibilités. Seulement dans le cas où un effet serait observé faudrait-il alors identifier son origine : 1- tecto-thalamique ou 2- rétino-thalamique.

### 5.2.2 Amélioration comportementale post-lésion

Une des hypothèses de l'étude de lésion était que l'augmentation de la capacité à discriminer des stimuli de points complexes (Rudolph & Pasternak, 1996) chez le chat lésé était attribuable à une modification du traitement effectué par les neurones du PMLS. Bien que peu probable, l'absence d'une augmentation de la sélectivité des neurones du PMLS pourrait être attribuable au fait que le modèle choisit était le chaton et non l'adulte comme dans l'article de Rudolph & Pasternak (1996). Afin de répondre à cette question de façon définitive, il faudrait effectuer la même étude que dans le présent ouvrage mais chez l'adulte, et ce avec le même temps de survie que dans l'article original. De plus, un test comportemental et l'enregistrement extracellulaire chez le même animal permettrait d'assurer qu'il y a en effet une amélioration comportementale, sans quoi l'absence de changement dans le PMLS serait difficile à interpréter. Étant donné les résultats du présent ouvrage, il faut envisager des aires alternatives afin d'expliquer les données comportementales. Afin d'identifier ces aires pour ensuite faire des enregistrements électrophysiologiques, la technique de la révélation de la consommation du 2-DG lors d'une tâche comportementale

(Vanduffel *et al.*, 1995; Vanduffel *et al.*, 1997a; Vanduffel *et al.*, 1997b) pourrait être des plus utile.

### 5.2.3 Mesure de l'effet des lésions par corrélation rétrograde

Malgré l'utilisation de stimuli en mouvement de type complexe, il est possible que ces stimuli ne soient pas un bon choix pour mettre en évidence les effets sur les réponses des neurones du PMLS d'une lésion de l'aire visuelle primaire chez le chaton. Une technique très sensible aux propriétés des champs récepteurs est la corrélation rétrograde. Une étude avec cette technique pourrait mettre à jour des effets jusqu'alors passé inaperçu. De plus, la nature impulsionnelle de cette technique permettrait d'éviter de masquer un effet jusque là voilé par l'intégration temporelle. Cette dernière est une partie inhérente de la plupart des autres paradigmes de stimulation. Lors d'une étude avec une corrélation rétrograde d'ordre plus élevé (voir la section 5.1), nous pourrions nous attendre à voir une diminution de l'importance relative de sous-unités qui correspondent aux propriétés de l'aire visuelle primaire, notamment, la sélectivité à des vitesses faibles. Inversement, l'importance de d'autres types de sous-unités devrait augmenter et ce en fonction de la plasticité évoquée par la lésion. Les résultats permettraient donc de mieux cerner l'origine de la sélectivité résiduelle des neurones du PMLS aux stimuli en mouvement.

### 5.3 Idées découlant de l'étude de latences

#### 5.3.1 Latence aux stimuli stationnaires et dynamiques

Comme nous l'avons vu dans la section des considérations méthodologiques, une des critiques possibles est que le début du mouvement et l'apparition des stimuli se produisaient en simultanée. Des arguments ont déjà été présentés qui suggèrent que la mesure de latence était bien celle au mouvement et non pas de l'apparition du stimulus. Pour en être certain, les études futures devraient faire apparaître un stimulus stationnaire et suite à un délai (disons 500ms) initier le mouvement. Au-delà de la désambiguïsation des deux possibilités mentionnées ci-dessus, ce paradigme expérimental permettrait une mesure de latence pour l'apparition et le mouvement d'un même stimulus. Il serait alors possible de savoir si des régions, telle que le PMLS, reçoivent certains types d'informations plus rapidement que d'autres.

#### 5.3.2 Confirmation et identification de deux sous-voies dorsales

Dans l'article sur les latences qui fait partie de la présente thèse, il est mentionné de deux profils de distribution des latences dans les aires corticales, soit celles qui dépendent ou non des stimuli. Anatomiquement, la distinction entre ces deux profils semblait être attribuable à une projection directe ou indirecte de l'aire 17. Ces données portent à croire qu'il pourrait y avoir deux voies parallèles de traitement de l'information dans la voie dorsale du système visuel. Cependant, il y a seulement deux régions corticales qui tombent dans

chaque catégorie : 1- Aire 17 et le PMLS. L'inclusion même de l'aire 17 dans cette catégorie peut facilement être remise en cause, puisqu'il va sans dire que cette région ne reçoit pas une projection *feedforward* de l'aire 17. 2- L'AMLS et l'AEV. Afin de confirmer que les profils temporels pourraient être expliqués via la distinction anatomique il faudrait alors prendre des mesures dans d'autres aires corticales. Il serait intéressant de voir en quoi les propriétés des neurones de ces deux voies diffèrent. Notons que certains de ces paramètres sont déjà connus pour certaines régions mais demeurent peu ou pas étudiés dans le PLLS, ALLS et l'AMLS.

#### 5.4 Idées découlant de la synthèse des trois études

##### 5.4.1 Anatomie : la nature des connexions

Afin d'émettre des hypothèses plus précises pour des études électrophysiologiques, deux questions devront trouver des réponses. La première concerne l'anatomie des voies visuelles. Pour l'exemple donné ici, nous nous concentrerons sur le lien entre l'aire 17 et le PMLS, mais la question de fond s'applique à tout le système visuel. Traditionnellement les études de traçage anatomique décrivent le nombre de terminaisons (par exemple : Symonds & Rosenquist, 1984b). Ces données ne nous donnent pas accès à deux types d'informations fondamentales afin de comprendre la circuiterie du système : 1- l'importance fonctionnelle de ces connexions, notamment dans le contexte de la notion de *driver* versus *modulator* de Sherman & Guillery (1998).

Bien que cette classification réfère traditionnellement aux terminaisons dans le thalamus, il n'y a aucune raison *a priori* de croire qu'une organisation similaire n'existe pas au niveau des terminaisons dans le cortex. La compréhension du rôle de la projection de l'aire 17 vers le PMLS serait nécessairement changée selon si les terminaisons sont de type *driver* ou *modulator*. 2- Est-ce que les projections font synapse avec des cellules excitatrices ou inhibitrices ? Notons que ce travail est déjà partiellement fait par Lowenstein & Somogyi (1991), ils ont documenté le pourcentage de synapses sur des cellules excitatrices et inhibitrices pour la projection de l'aire 17 au PMLS. Dans la mesure où nous ne connaissons pas ces proportions pour les autres aires corticales, leurs données demeurent difficiles à interpréter.

Notons qu'il existe une méthode alternative pour répondre au point 1 ci-haut, soit l'utilisation de la cross-corrélation des potentiels d'action dans deux aires. En fait, la prédiction du cross-corrélogramme entre une cellule et ses afférences diffère selon la nature *driver* ou *modulator* de la cellule afférente (Sherman & Guillery, 1998). Une cross-corrélation entre deux cellules liées par une synapse soit de type *driver* ou *modulator* devrait évoquer un pic dans l'auto-corrélogramme qui serait soit étroit ou non respectivement, selon la nature de la synapse. Bien que cette technique soit une démonstration indirecte du type de synapse, elle donne une mesure directe de l'efficacité fonctionnelle du lien synaptique entre deux cellules.



#### 5.4.2 Comportement : le rôle comportemental du PMLS

Le deuxième type d'étude qui permettrait des hypothèses plus précises serait de type comportemental. Il serait plus efficace de comprendre les propriétés des neurones dans le cadre d'un rôle comportemental connu (Glimcher, 2003), plutôt que l'inverse. Ceci étant dit, il y a eu plusieurs études comportementales de lésion/inactivation du LS, mais aucune conclusion claire en découle quant au rôle comportemental précis des aires lésées/inactivées (Smith & Spear, 1979; Ptito & Lepore, 1983; Kieffer *et al.*, 1989; Pasternak *et al.*, 1989; Kruger *et al.*, 1993a; Kruger *et al.*, 1993b; Vanduffel *et al.*, 1995; Lomber & Payne, 1996; Rudolph & Pasternak, 1996; Vanduffel *et al.*, 1997b; Lomber, 2001; Huxlin & Pasternak, 2004). La plupart de ces études ont ciblé des fonctions des voies dorsales et ventrales et ont révélé des déficits qui sont spécifiques à la voie dorsale. Par contre, peu d'études ont utilisé plusieurs tâches qui ciblaient la voie dorsale. Il est donc difficile d'évaluer l'importance relative du PMLS dans plusieurs tâches. De plus, peu d'aires de la voie dorsale autre que le PMLS ont ainsi été étudiées. Il n'est donc pas clair si les effets obtenus lors de lésion/inactivation du PMLS sont des conséquences spécifiques au PMLS ou sont attribuables à l'information que le PMLS transmet aux autres aires de la voie dorsale. Dans le futur, il faudrait donc cibler spécifiquement les tâches reliées à la voie dorsale et lésé ou inactivé d'autres aires afin de voir la contribution relative de chaque aire à chaque tâche. Ceci est d'autant plus important que chaque aire extra-striée reçoit des projections d'afférences différentes.

#### 5.4.3 Physiologie : rôle des voies *feedforward* et de rétroaction

Passons maintenant à une étude qui pourrait mettre à l'épreuve les notions mises de l'avant pour expliquer le rôle des voies *feedforward* et de rétroaction (Nowak & Bullier, 1997; Lamme *et al.*, 1998; Lamme & Roelfsema, 2000; Bullier, 2001, 2004a). Une critique mentionnée ci-haut à propos de ces deux idées est le côté peu écologique des conditions expérimentales qui ont menées à leur élaboration. Spécifiquement, qu'est-ce que leur explication nous permettraient de comprendre dans un monde visuel dynamique où l'utilité des boucles de rétroaction n'est pas aussi claire. Une façon de voir comment le système réagirait serait d'enregistrer l'activité d'une cellule alors qu'un stimulus en déplacement est présenté.

Si les boucles de rétroaction changent la sélectivité des neurones de façon importante, la largeur de bande de la courbe de sélectivité à la direction devrait passer de large à étroite suite à la réponse visuelle initiale (soit la partie de la réponse attribuable à la voie *feedforward*). Suite à un délai de 250ms, qui permettrait aux boucles de rétroaction de moduler la réponse initiale du neurone, un objet passerait dans le champ récepteur. La courbe de sélectivité devrait s'élargir de nouveau suite à l'introduction de l'objet à cause d'une compétition entre les différentes boucles de rétroaction impliquées. Après le passage de l'objet, nous revenons au stimulus de départ, la largeur de bande devrait être étroite de nouveau car il n'y aurait qu'un réseau de boucles de rétroaction encore actif. Mentionnons rapidement que ce paradigme de

stimulation est similaire à une des conditions utilisées par von Grunau et Frost (1983), la différence étant dans la façon d'analyser les données.

## 6. Conclusions

Les résultats de la présente thèse s'ajoutent à un nombre croissant d'études qui remettent en question la hiérarchie des aires corticales visuelles telle que présentée habituellement. Cet état de fait force une reconsidération des voies ainsi que des mécanismes qui mènent aux propriétés des neurones dans les aires extrastriées, telle que le PMLS. En fait, les modèles d'intégration postulent habituellement au moins deux niveaux d'analyse corticale afin d'encoder l'information directionnelle. Les conclusions des présentes études suggèrent plutôt que le PMLS puisse extraire l'information directionnelle en une seule étape. Quoique excitant en soit, ces travaux ouvrent un nouveau débat quant à la fonction des voies *feedforward* et de rétroaction.

## Références

- ABRAMSON, B. P. & CHALUPA, L. M. (1985). The laminar distribution of cortical connections with the tecto- and cortico-recipient zones in the cat's lateral posterior nucleus. *Neuroscience* **15**, 81-95.
- ADELSON, E. H. & BERGEN, J. R. (1985). Spatiotemporal energy models for the perception of motion. *J Opt Soc Am A* **2**, 284-299.
- ADELSON, E. H. & MOVSHON, J. A. (1982). Phenomenal coherence of moving visual patterns. *Nature* **300**, 523-525.
- AKASE, E., INOKAWA, H. & TOYAMA, K. (1998). Neuronal responsiveness to three-dimensional motion in cat posteromedial lateral suprasylvian cortex. *Exp Brain Res* **122**, 214-226.
- ARUTYUNYAN-KOZAK, B. A., EKIMYAN, A. A., GRIGORYAN, G. E. & DEC, K. (1981). Structure of receptive fields of cat pulvinar neurons sensitive to photic stimulation. *Neurosci Behav Physiol* **11**, 400-405.
- AZZOPARDI, P., FALLAH, M., GROSS, C. G. & RODMAN, H. R. (2003). Response latencies of neurons in visual areas MT and MST of monkeys with striate cortex lesions. *Neuropsychologia* **41**, 1738-1756.
- BAIR, W., CAVANAUGH, J. R., SMITH, M. A. & MOVSHON, J. A. (2002). The timing of response onset and offset in macaque visual neurons. *J Neurosci* **22**, 3189-3205.
- BAIR, W. & MOVSHON, J. A. (2004). Adaptive temporal integration of motion in direction-selective neurons in macaque visual cortex. *J Neurosci* **24**, 7305-7323.
- BENDER, D. B. (1983). Visual activation of neurons in the primate pulvinar depends on cortex but not colliculus. *Brain Res* **279**, 258-261.
- BENEVENTO, L. A. & STANDAGE, G. P. (1982). Demonstration of lack of dorsal lateral geniculate nucleus input to extrastriate areas MT and visual 2 in the macaque monkey. *Brain Res* **252**, 161-166.
- BENEVENTO, L. A. & YOSHIDA, K. (1981). The afferent and efferent organization of the lateral geniculo-prestriate pathways in the macaque monkey. *J Comp Neurol* **203**, 455-474.
- BERSON, D. M. (1985). Cat lateral suprasylvian cortex: Y-cell inputs and corticotectal projection. *J Neurophysiol* **53**, 544-556.

- BERSON, D. M. & GRAYBIEL, A. M. (1978). Parallel thalamic zones in the LP-pulvinar complex of the cat identified by their afferent and efferent connections. *Brain Res* **147**, 139-148.
- BERSON, D. M. & GRAYBIEL, A. M. (1983a). Organization of the striate-recipient zone of the cats lateral posterior-pulvinar complex and its relations with the geniculostriate system. *Neuroscience* **9**, 337-372.
- BERSON, D. M. & GRAYBIEL, A. M. (1983b). Subsystems within the visual association cortex as delineated by their thalamic and transcortical affiliations. *Prog Brain Res* **58**, 229-238.
- BEST, J., REUSS, S. & DINSE, H. R. (1986). Lamina-specific differences of visual latencies following photic stimulation in the cat striate cortex. *Brain Res* **385**, 356-360.
- BOIRE, D., MATTEAU, I., CASANOVA, C. & PTITO, M. (2004). Retinal projections to the lateral posterior-pulvinar complex in intact and early visual cortex lesioned cats. *Exp Brain Res* **159**, 185-196.
- BORGHUIS, B. G., PERGE, J. A., VAJDA, I., VAN WEZEL, R. J., VAN DE GRIND, W. A. & LANKHEET, M. J. (2003). The motion reverse correlation (MRC) method: a linear systems approach in the motion domain. *J Neurosci Methods* **123**, 153-166.
- BREDFELDT, C. E. & RINGACH, D. L. (2002). Dynamics of spatial frequency tuning in macaque V1. *J Neurosci* **22**, 1976-1984.
- BRENNER, E. & RAUSCHECKER, J. P. (1990). Centrifugal motion bias in the cat's lateral suprasylvian visual cortex is independent of early flow field exposure. *J Physiol* **423**, 641-660.
- BRITTEN, K. H., NEWSOME, W. T., SHADLEN, M. N., CELEBRINI, S. & MOVSHON, J. A. (1996). A relationship between behavioral choice and the visual responses of neurons in macaque MT. *Vis Neurosci* **13**, 87-100.
- BROSSEAU-LACHAINE, O., FAUBERT, J. & CASANOVA, C. (2001). Functional subregions for optic flow processing in the posteromedial lateral suprasylvian cortex of the cat. *Cereb Cortex* **11**, 989-1001.
- BULLIER, J. (2001). Integrated model of visual processing. *Brain Res Brain Res Rev* **36**, 96-107.
- BULLIER, J. (2004a). Communications between cortical areas of the visual system. In *The Visual Neurosciences*, pp. 522-540. Bradford Books, Cambridge.

- BULLIER, J. (2004b). Communications between cortical areas of the visual system. In *The visual neurosciences*, vol. 2, pp. 522-540. Bradford Book, Cambridge, Massachusetts.
- CAMARDA, R. & RIZZOLATTI, G. (1976). Visual receptive fields in the lateral suprasylvian area (Clare-Bishop area) of the cat. *Brain Res* **101**, 427-443.
- CASANOVA, C. (1993). Response properties of neurons in area 17 projecting to the striate-recipient zone of the cat's lateralis posterior-pulvinar complex: comparison with cortico-tectal cells. *Exp Brain Res* **96**, 247-259.
- CASANOVA, C., MERABET, L., DESAUTELS, A. & MINVILLE, K. (2001). Higher-order motion processing in the pulvinar. In *Progress in Brain Research*, vol. 134. ed. CASANOVA, C. & PTITO, M., pp. 71-82.
- CASANOVA, C., SAVARD, T. & DARVEAU, S. (1997). Contribution of area 17 to cell responses in the striate-recipient zone of the cat's lateral posterior-pulvinar complex. *Eur J Neurosci* **9**, 1026-1036.
- CITRON, M. C. & EMERSON, R. C. (1983). White noise analysis of cortical directional selectivity in cat. *Brain Res* **279**, 271-277.
- COLLINS, C. E., LYON, D. C. & KAAS, J. H. (2003). Responses of neurons in the middle temporal visual area after long-standing lesions of the primary visual cortex in adult new world monkeys. *J Neurosci* **23**, 2251-2264.
- CORNWELL, P., HERBEIN, S., CORSO, C., ESKEW, R., WARREN, J. M. & PAYNE, B. (1989). Selective sparing after lesions of visual cortex in newborn kittens. *Behav Neurosci* **103**, 1176-1190.
- CORNWELL, P. & PAYNE, B. (1989). Visual discrimination by cats given lesions of visual cortex in one or two stages in infancy or in one stage in adulthood. *Behav Neurosci* **103**, 1191-1199.
- CREUTZFELDT, O. & ITO, M. (1968). Functional synaptic organization of primary visual cortex neurones in the cat. *Exp Brain Res* **6**, 324-352.
- DANILOV, Y., MOORE, R. J., KING, V. R. & SPEAR, P. D. (1995). Are neurons in cat posteromedial lateral suprasylvian visual cortex orientation sensitive? Tests with bars and gratings. *Vis Neurosci* **12**, 141-151.
- DE BOER, E. & KUYPER, P. (1968). Triggered correlation. *IEEE Transactions on Biomedical Engineering* **15**, 169-179.
- DEANGELIS, G. C., OHZAWA, I. & FREEMAN, R. D. (1993). Spatiotemporal organization of simple-cell receptive fields in the cat's striate cortex. I.

General characteristics and postnatal development. *J Neurophysiol* **69**, 1091-1117.

- DEANGELIS, G. C., OHZAWA, I. & FREEMAN, R. D. (1995a). Neuronal mechanisms underlying stereopsis: how do simple cells in the visual cortex encode binocular disparity? *Perception* **24**, 3-31.
- DEANGELIS, G. C., OHZAWA, I. & FREEMAN, R. D. (1995b). Receptive-field dynamics in the central visual pathways. *Trends Neurosci* **18**, 451-458.
- DEC, K. & TARNECKI, R. (1980). The response patterns of collicular neurons to moving stimuli in cats after lesion of the visual cortex. *Acta Neurobiol Exp (Wars)* **40**, 501-505.
- DESAUTELS, A. & CASANOVA, C. (2001). Response properties in the pulvinar complex after neonatal ablation of the primary visual cortex. *Prog Brain Res* **134**, 83-95.
- DI STEFANO, M., MORRONE, M. C. & BURR, D. C. (1985). Visual acuity of neurones in the cat lateral suprasylvian cortex. *Brain Res* **331**, 382-385.
- DINSE, H. R. & KRUGER, K. (1994). The timing of processing along the visual pathway in the cat. *Neuroreport* **5**, 893-897.
- DREHER, B., WANG, C. & BURKE, W. (1996a). Limits of parallel processing: excitatory convergence of different information channels on single neurons in striate and extrastriate visual cortices. *Clin Exp Pharmacol Physiol* **23**, 913-925.
- DREHER, B., WANG, C., TURLEJSKI, K. J., DJAVADIAN, R. L. & BURKE, W. (1996b). Areas PMLS and 21a of cat visual cortex: two functionally distinct areas. *Cereb Cortex* **6**, 585-599.
- DUMBRAVA, D., FAUBERT, J. & CASANOVA, C. (2001). Global motion integration in the cat's lateral posterior-pulvinar complex. *Eur J Neurosci* **13**, 2218-2226.
- EGGERMONT, J. J., JOHANNESMA, P. M. & AERTSEN, A. M. (1983). Reverse-correlation methods in auditory research. *Q Rev Biophys* **16**, 341-414.
- EINSTEIN, G. & FITZPATRICK, D. (1991). Distribution and morphology of area 17 neurons that project to the cat's extrastriate cortex. *J Comp Neurol* **303**, 132-149.
- ELLAWAY, P. H. (1978). Cumulative sum technique and its application to the analysis of peristimulus time histograms. *Electroencephalogr Clin Neurophysiol* **45**, 302-304.

- EMERSON, R. C., BERGEN, J. R. & ADELSON, E. H. (1992). Directionally selective complex cells and the computation of motion energy in cat visual cortex. *Vision Res* **32**, 203-218.
- EMERSON, R. C., CITRON, M. C., VAUGHN, W. J. & KLEIN, S. A. (1987). Nonlinear directionally selective subunits in complex cells of cat striate cortex. *J Neurophysiol* **58**, 33-65.
- EORDEGH, G., NAGY, A., BERENYI, A. & BENEDEK, G. (2005). Processing of spatial visual information along the pathway between the supragenulate nucleus and the anterior ectosylvian cortex. *Brain Res Bull* **67**, 281-289.
- ESCHWEILER, G. W. & RAUSCHECKER, J. P. (1993). Temporal integration in visual cortex of cats with surgically induced strabismus. *Eur J Neurosci* **5**, 1501-1509.
- FELLEMAN, D. J. & VAN ESSEN, D. C. (1991). Distributed hierarchical processing in the primate cerebral cortex. *Cereb Cortex* **1**, 1-47.
- FLANDRIN, J. M. & JEANNEROD, M. (1977). Lack of recovery in collicular neurons from the effects of early deprivation or neonatal cortical lesion in the kitten. *Brain Res* **120**, 362-366.
- FRIES, W. (1981). The projection from the lateral geniculate nucleus to the prestriate cortex of the macaque monkey. *Proc R Soc Lond B Biol Sci* **213**, 73-86.
- GALUSKE, R. A., SCHMIDT, K. E., GOEBEL, R., LOMBER, S. G. & PAYNE, B. R. (2002). The role of feedback in shaping neural representations in cat visual cortex. *Proc Natl Acad Sci U S A* **99**, 17083-17088.
- GASKA, J. P., JACOBSON, L. D., CHEN, H. W. & POLLEN, D. A. (1994). Space-time spectra of complex cell filters in the macaque monkey: a comparison of results obtained with pseudowhite noise and grating stimuli. *Vis Neurosci* **11**, 805-821.
- GILBERT, C. D. (1977). Laminar differences in receptive field properties of cells in cat primary visual cortex. *J Physiol* **268**, 391-421.
- GIRARD, P., SALIN, P. A. & BULLIER, J. (1992). Response selectivity of neurons in area MT of the macaque monkey during reversible inactivation of area V1. *J Neurophysiol* **67**, 1437-1446.
- GIZZI, M. S., KATZ, E. & MOVSHON, J. A. (1990). Spatial and temporal analysis by neurons in the representation of the central visual field in the cat's lateral suprasylvian visual cortex. *Vis Neurosci* **5**, 463-468.



- GLIMCHER, P. W. (2003). *Decisions, uncertainty, and the brain: The science of neuroeconomics*. MIT press, Cambridge, MA.
- GOODALE, M. A. & MILNER, A. D. (1992). Separate visual pathways for perception and action. *Trends Neurosci* **15**, 20-25.
- GRANT, S. & HILGETAG, C. C. (2005). Graded classes of cortical connections: quantitative analyses of laminar projections to motion areas of cat extrastriate cortex. *Eur J Neurosci* **22**, 681-696.
- GRANT, S. & SHIPP, S. (1991). Visuotopic organization of the lateral suprasylvian area and of an adjacent area of the ectosylvian gyrus of cat cortex: a physiological and connectional study. *Vis Neurosci* **6**, 315-338.
- GRAYBIEL, A. M. (1972). Some extrageniculate visual pathways in the cat. *Invest Ophthalmol* **11**, 322-332.
- GRAYBIEL, A. M. & BERSON, D. M. (1980). Histochemical identification and afferent connections of subdivisions in the lateralis posterior-pulvinar complex and related thalamic nuclei in the cat. *Neuroscience* **5**, 1175-1238.
- GUIDO, W., SPEAR, P. D. & TONG, L. (1990a). Functional compensation in the lateral suprasylvian visual area following bilateral visual cortex damage in kittens. *Exp Brain Res* **83**, 219-224.
- GUIDO, W., SPEAR, P. D. & TONG, L. (1992). How complete is physiological compensation in extrastriate cortex after visual cortex damage in kittens? *Exp Brain Res* **91**, 455-466.
- GUIDO, W., TONG, L. & SPEAR, P. D. (1990b). Afferent bases of spatial- and temporal-frequency processing by neurons in the cat's posteromedial lateral suprasylvian cortex: effects of removing areas 17, 18, and 19. *J Neurophysiol* **64**, 1636-1651.
- HARTING, J. K., HUERTA, M. F., HASHIKAWA, T. & VAN LIESHOUT, D. P. (1991). Projection of the mammalian superior colliculus upon the dorsal lateral geniculate nucleus: organization of tectogeniculate pathways in nineteen species. *J Comp Neurol* **304**, 275-306.
- HARUTIUNIAN-KOZAK, B. A., HEKIMIAN, A. A., DEC, K. & GRIGORIAN, G. E. (1981a). Responses of cat's pulvinar neurons to moving visual stimuli. *Acta Neurobiol Exp (Wars)* **41**, 147-162.

- HARUTIUNIAN-KOZAK, B. A., HEKIMIAN, A. A., DEC, K. & GRIGORIAN, G. E. (1981b). The structure of visual receptive fields of cat's pulvinar neurons. *Acta Neurobiol Exp (Wars)* **41**, 127-145.
- HENDRICKSON, A. & DINEEN, J. T. (1982). Hypertrophy of neurons in dorsal lateral geniculate nucleus following striate cortex lesions in infant monkeys. *Neurosci Lett* **30**, 217-222.
- HENRY, G. H., LUND, J. S. & HARVEY, A. R. (1978). Cells of the striate cortex projecting to the Clare-Bishop area of the cat. *Brain Res* **151**, 154-158.
- HERBIN, M., MICELI, D., REPERANT, J., MASSICOTTE, G. & ROY, G. (2000). Postnatal development of thalamocortical projections upon striate and extrastriate visual cortical areas in the cat. *Anat Embryol (Berl)* **202**, 431-442.
- HILGETAG, C. C., BURNS, G. A., O'NEILL, M. A., SCANNELL, J. W. & YOUNG, M. P. (2000a). Anatomical connectivity defines the organization of clusters of cortical areas in the macaque monkey and the cat. *Philos Trans R Soc Lond B Biol Sci* **355**, 91-110.
- HILGETAG, C. C., O'NEILL, M. A. & YOUNG, M. P. (2000b). Hierarchical organization of macaque and cat cortical sensory systems explored with a novel network processor. *Philos Trans R Soc Lond B Biol Sci* **355**, 71-89.
- HIRSCH, J. A. & MARTINEZ, L. M. (2006). Circuits that build visual cortical receptive fields. *Trends Neurosci* **29**, 30-39.
- HIRSCH, J. A., MARTINEZ, L. M., ALONSO, J. M., DESAI, K., PILLAI, C. & PIERRE, C. (2002). Synaptic physiology of the flow of information in the cat's visual cortex in vivo. *J Physiol* **540**, 335-350.
- HIRSCH, J. A., MARTINEZ, L. M., PILLAI, C., ALONSO, J. M., WANG, Q. & SOMMER, F. T. (2003). Functionally distinct inhibitory neurons at the first stage of visual cortical processing. *Nat Neurosci* **6**, 1300-1308.
- HUANG, L., CHEN, X. & SHOU, T. (2004). Spatial frequency-dependent feedback of visual cortical area 21a modulating functional orientation column maps in areas 17 and 18 of the cat. *Brain Res* **998**, 194-201.
- HUBEL, D. H. & WIESEL, T. N. (1962). Receptive fields, binocular interaction and functional architecture in the cat's visual cortex. *J Physiol* **160**, 106-154.
- HUBEL, D. H. & WIESEL, T. N. (1965). Receptive Fields and Functional Architecture in Two Nonstriate Visual Areas (18 and 19) of the Cat. *J Neurophysiol* **28**, 229-289.

- HUBEL, D. H. & WIESEL, T. N. (1969). Visual area of the lateral suprasylvian gyrus (Clare-Bishop area) of the cat. *J Physiol* **202**, 251-260.
- HUPE, J. M., JAMES, A. C., GIRARD, P., LOMBER, S. G., PAYNE, B. R. & BULLIER, J. (2001). Feedback connections act on the early part of the responses in monkey visual cortex. *J Neurophysiol* **85**, 134-145.
- HUPPÉ-GOURGUE, F., BICKFORD, M. E., BOIRE, D., PTITO, M. & CASANOVA, C. (2006a). Distribution, morphology and synaptic targets of corticothalamic terminals in the cat lateral posterior-pulvinar complex that originates from the posteromedial lateral suprasylvian cortex. *J Comp Neurol* **In Press**.
- HUPPÉ-GOURGUE, F., BICKFORD, M. E., BOIRE, D., PTITO, M. & CASANOVA, C. (2006b). Distribution, morphology and synaptic targets of corticothalamic terminals in the cat lateral posterior-pulvinar complex that originates from the posteromedial lateral suprasylvian cortex. *J Comp Neurol* **45**, 137-145.
- HUXLIN, K. R. & PASTERNAK, T. (2001). Long-term neurochemical changes after visual cortical lesions in the adult cat. *J Comp Neurol* **429**, 221-241.
- HUXLIN, K. R. & PASTERNAK, T. (2004). Training-induced recovery of visual motion perception after extrastriate cortical damage in the adult cat. *Cereb Cortex* **14**, 81-90.
- IKEDA, H. & WRIGHT, M. J. (1975). Retinotopic distribution. Visual latency and orientation tuning of 'sustained' and 'transient' cortical neurones in area 17 of the cat. *Exp Brain Res* **22**, 385-398.
- ILLIG, K. R., DANILOV, Y. P., AHMAD, A., KIM, C. B. & SPEAR, P. D. (2000). Functional plasticity in extrastriate visual cortex following neonatal visual cortex damage and monocular enucleation. *Brain Res* **882**, 241-250.
- ITOH, K., MIZUNO, N. & KUDO, M. (1983). Direct retinal projections to the lateroposterior and pulvinar nuclear complex (LP-Pul) in the cat, as revealed by the anterograde HRP method. *Brain Res* **276**, 325-328.
- JONES, J. P. & PALMER, L. A. (1987). The two-dimensional spatial structure of simple receptive fields in cat striate cortex. *J Neurophysiol* **58**, 1187-1211.
- KAAS, J. H. & KRUBITZER, L. A. (1992). Area 17 lesions deactivate area MT in owl monkeys. *Vis Neurosci* **9**, 399-407.

- KAGAN, I., GUR, M. & SNODDERLY, D. M. (2002). Spatial organization of receptive fields of V1 neurons of alert monkeys: comparison with responses to gratings. *J Neurophysiol* **88**, 2557-2574.
- KALIL, R. E., TONG, L. L. & SPEAR, P. D. (1991). Thalamic projections to the lateral suprasylvian visual area in cats with neonatal or adult visual cortex damage. *J Comp Neurol* **314**, 512-525.
- KATSUYAMA, N., TSUMOTO, T., SATO, H., FUKUDA, M. & HATA, Y. (1996). Lateral suprasylvian visual cortex is activated earlier than or synchronously with primary visual cortex in the cat. *Neurosci Res* **24**, 431-435.
- KAWANO, J. (1998). Cortical projections of the parvocellular laminae C of the dorsal lateral geniculate nucleus in the cat: an anterograde wheat germ agglutinin conjugated to horseradish peroxidase study. *J Comp Neurol* **392**, 439-457.
- KELLY, L. R., LI, J., CARDEN, W. B. & BICKFORD, M. E. (2003). Ultrastructure and synaptic targets of tectothalamic terminals in the cat lateral posterior nucleus. *J Comp Neurol* **464**, 472-486.
- KHAYAT, P. S., SPEKREIJSE, H. & ROELFSEMA, P. R. (2006). Attention lights up new object representations before the old ones fade away. *J Neurosci* **26**, 138-142.
- KIEFER, W., KRUGER, K., STRAUSS, G. & BERLUCCHI, G. (1989). Considerable deficits in the detection performance of the cat after lesion of the suprasylvian visual cortex. *Exp Brain Res* **75**, 208-212.
- KIM, J. N., MULLIGAN, K. & SHERK, H. (1997). Simulated optic flow and extrastriate cortex. I. Optic flow versus texture. *J Neurophysiol* **77**, 554-561.
- KRUGER, K., KIEFER, W. & GROH, A. (1993a). Lesion of the suprasylvian cortex impairs depth perception of cats. *Neuroreport* **4**, 883-886.
- KRUGER, K., KIEFER, W., GROH, A., DINSE, H. R. & VON SEELEN, W. (1993b). The role of the lateral suprasylvian visual cortex of the cat in object-background interactions: permanent deficits following lesions. *Exp Brain Res* **97**, 40-60.
- LABAR, D. R., BERMAN, N. E. & MURPHY, E. H. (1981). Short- and long-term effects of neonatal and adult visual cortex lesions on the retinal projection to the pulvinar in cats. *J Comp Neurol* **197**, 639-659.
- LAMME, V. A. & ROELFSEMA, P. R. (2000). The distinct modes of vision offered by feedforward and recurrent processing. *Trends Neurosci* **23**, 571-579.

- LAMME, V. A., SUPER, H. & SPEKREIJSE, H. (1998). Feedforward, horizontal, and feedback processing in the visual cortex. *Curr Opin Neurobiol* **8**, 529-535.
- LENNIE, P. (1980). Parallel visual pathways: a review. *Vision Res* **20**, 561-594.
- LENNIE, P. (1981). The physiological basis of variations in visual latency. *Vision Res* **21**, 815-824.
- LEVICK, W. R. (1973). Variation in the response latency of cat retinal ganglion cells. *Vision Res* **13**, 837-853.
- LIM, J. S. (1990). *Two-dimensional signal and image processing*. Prentice Hall, Englewood Cliffs, N.J.
- LIVINGSTONE, M. S. (1998). Mechanisms of direction selectivity in macaque V1. *Neuron* **20**, 509-526.
- LOMBER, S. G. (2001). Behavioral cartography of visual functions in cat parietal cortex: areal and laminar dissociations. *Prog Brain Res* **134**, 265-284.
- LOMBER, S. G. & PAYNE, B. R. (1996). Removal of two halves restores the whole: reversal of visual hemineglect during bilateral cortical or collicular inactivation in the cat. *Vis Neurosci* **13**, 1143-1156.
- LONG, K. D., LOMBER, S. G. & PAYNE, B. R. (1996). Increased oxidative metabolism in middle suprasylvian cortex following removal of areas 17 and 18 from newborn cats. *Exp Brain Res* **110**, 335-346.
- LOWENSTEIN, P. R. & SOMOGYI, P. (1991). Synaptic organization of cortico-cortical connections from the primary visual cortex to the posteromedial lateral suprasylvian visual area in the cat. *J Comp Neurol* **310**, 253-266.
- MACIEWICZ, R. J. (1974). Afferents to the lateral suprasylvian gyrus of the cat traced with horseradish peroxidase. *Brain Res* **78**, 139-143.
- MACNEIL, M. A., LOMBER, S. G. & PAYNE, B. R. (1997). Thalamic and cortical projections to middle suprasylvian cortex of cats: constancy and variation. *Exp Brain Res* **114**, 24-32.
- MAJAJ, N., CARANDINI, M., SMITH, M. A. & MOVSHON, J. A. (1999). Local integration of features for the computation of pattern direction by neurons in macaque area MT. *Society for Neuroscience Abstracts* **25**, 674.
- MARMARELIS, V. Z., CITRON, M. C. & VIVO, C. P. (1986). Minimum-order Wiener modelling of spike-output systems. *Biol Cybern* **54**, 115-123.

- MARTINEZ, L. M., WANG, Q., REID, R. C., PILLAI, C., ALONSO, J. M., SOMMER, F. T. & HIRSCH, J. A. (2005). Receptive field structure varies with layer in the primary visual cortex. *Nat Neurosci* **8**, 372-379.
- MASON, R. (1981). Differential responsiveness of cells in the visual zones of the cat's LP-pulvinar complex to visual stimuli. *Exp Brain Res* **43**, 25-33.
- MATA, M. L. & RINGACH, D. L. (2005). Spatial overlap of ON and OFF subregions and its relation to response modulation ratio in macaque primary visual cortex. *J Neurophysiol* **93**, 919-928.
- MAUNSELL, J. H. & GIBSON, J. R. (1992). Visual response latencies in striate cortex of the macaque monkey. *J Neurophysiol* **68**, 1332-1344.
- MAUNSELL, J. H., NEALEY, T. A. & DEPRIEST, D. D. (1990). Magnocellular and parvocellular contributions to responses in the middle temporal visual area (MT) of the macaque monkey. *J Neurosci* **10**, 3323-3334.
- MAUNSELL, J. H. & VAN ESSEN, D. C. (1983). The connections of the middle temporal visual area (MT) and their relationship to a cortical hierarchy in the macaque monkey. *J Neurosci* **3**, 2563-2586.
- MCLEAN, J., RAAB, S. & PALMER, L. A. (1994). Contribution of linear mechanisms to the specification of local motion by simple cells in areas 17 and 18 of the cat. *Vis Neurosci* **11**, 271-294.
- MERABET, L., DESAUTELS, A., MINVILLE, K. & CASANOVA, C. (1998). Motion integration in a thalamic visual nucleus. *Nature* **396**, 265-268.
- MERABET, L., MINVILLE, K., PTITO, M. & CASANOVA, C. (2000). Responses of neurons in the cat posteromedial lateral suprasylvian cortex to moving texture patterns. *Neuroscience* **97**, 611-623.
- MICELI, D., REPERANT, J., MARCHAND, L., WARD, R. & VESSELKIN, N. (1991). Divergence and collateral axon branching in subsystems of visual cortical projections from the cat lateral posterior nucleus. *J Hirnforsch* **32**, 165-173.
- MICELI, D., REPERANT, J. & PTITO, M. (1985). Intracortical connections of the anterior ectosylvian and lateral suprasylvian visual areas in the cat. *Brain Res* **347**, 291-298.
- MILLER, R. (1996). Cortico-thalamic interplay and the security of operation of neural assemblies and temporal chains in the cerebral cortex. *Biol Cybern* **75**, 263-275.

- MINVILLE, K. & CASANOVA, C. (1998). Spatial frequency processing in posteromedial lateral suprasylvian cortex does not depend on the projections from the striate-recipient zone of the cat's lateral posterior-pulvinar complex. *Neuroscience* **84**, 699-711.
- MISHKIN, M., UNGERLEIDER, L. G. & MACKO, K. A. (1983). Object vision and spatial vision: two cortical pathways. *Trends Neurosci* **6**, 263-275.
- MIZE, R. R. & MURPHY, E. H. (1976). Alterations in receptive field properties of superior colliculus cells produced by visual cortex ablation in infant and adult cats. *J Comp Neurol* **168**, 393-424.
- MOORE, T., RODMAN, H. R. & GROSS, C. G. (2001). Direction of motion discrimination after early lesions of striate cortex (V1) of the macaque monkey. *Proc Natl Acad Sci U S A* **98**, 325-330.
- MOORE, T., RODMAN, H. R., REPP, A. B., GROSS, C. G. & MEZRICH, R. S. (1996). Greater residual vision in monkeys after striate cortex damage in infancy. *J Neurophysiol* **76**, 3928-3933.
- MORRONE, M. C., DI STEFANO, M. & BURR, D. C. (1986). Spatial and temporal properties of neurons of the lateral suprasylvian cortex of the cat. *J Neurophysiol* **56**, 969-986.
- MOVSHON, J. A., ADELSON, E. H., GIZZI, M. S. & NEWSOME, W. T. (1985). The analysis of moving visual patterns. In *Pontificae Academia Scientiarum Scripta Varia*. ed. CITY, V., pp. 117-151.
- MOVSHON, J. A., ADELSON, E. H., GIZZI, M. S. & NEWSOME, W. T. (1986). The analysis of moving visual patterns. In *Pattern recognition mechanisms*. ed. CHAGAS, C., GATTAS, R. & GROSS, C., pp. 148-164. Springer Verlag, New York.
- MOVSHON, J. A., THOMPSON, I. D. & TOLHURST, D. J. (1978a). Receptive field organization of complex cells in the cat's striate cortex. *J Physiol* **283**, 79-99.
- MOVSHON, J. A., THOMPSON, I. D. & TOLHURST, D. J. (1978b). Spatial summation in the receptive fields of simple cells in the cat's striate cortex. *J Physiol* **283**, 53-77.
- MULLIGAN, K., KIM, J. N. & SHERK, H. (1997). Simulated optic flow and extrastriate cortex. II. Responses to bar versus large-field stimuli. *J Neurophysiol* **77**, 562-570.
- MUMFORD, D. (1991). On the computational architecture of the neocortex. I. The role of the thalamo-cortical loop. *Biol Cybern* **65**, 135-145.

- MUMFORD, D. (1992). On the computational architecture of the neocortex. II. The role of cortico-cortical loops. *Biol Cybern* **66**, 241-251.
- MURPHY, E. H. & KALIL, R. (1979). Functional organization of lateral geniculate cells following removal of visual cortex in the newborn kitten. *Science* **206**, 713-716.
- MURPHY, E. H., MIZE, R. R. & SCHECHTER, P. B. (1975). Visual discrimination following infant and adult ablation of cortical areas 17, 18, and 19 in the cat. *Exp Neurol* **49**, 386-405.
- NAITO, J. & KAWAMURA, K. (1982). Thalamocortical neurons projecting to the areas surrounding the anterior and middle suprasylvian sulci in the cat. A horseradish peroxidase study. *Exp Brain Res* **45**, 59-70.
- NEWSOME, W. T., BRITTEN, K. H., SALZMAN, C. D. & MOVSHON, J. A. (1990). Neuronal mechanisms of motion perception. *Cold Spring Harb Symp Quant Biol* **55**, 697-705.
- NEWSOME, W. T. & PARE, E. B. (1988). A selective impairment of motion perception following lesions of the middle temporal visual area (MT). *J Neurosci* **8**, 2201-2211.
- NICHOLS, M. J. & NEWSOME, W. T. (2002). Middle temporal visual area microstimulation influences veridical judgments of motion direction. *J Neurosci* **22**, 9530-9540.
- NIIMI, K., MATSUOKA, H., YAMAZAKI, Y. & MATSUMOTO, H. (1981). Thalamic afferents to the visual cortex in the cat studied by retrograde axonal transport of horseradish peroxidase. *Brain Behav Evol* **18**, 114-139.
- NISHIMOTO, S., ISHIDA, T. & OHZAWA, I. (2006). Receptive field properties of neurons in the early visual cortex revealed by local spectral reverse correlation. *J Neurosci* **26**, 3269-3280.
- NORITA, M., KASE, M., HOSHINO, K., MEGURO, R., FUNAKI, S., HIRANO, S. & MCHAFFIE, J. G. (1996). Extrinsic and intrinsic connections of the cat's lateral suprasylvian visual area. *Prog Brain Res* **112**, 231-250.
- NORITA, M., MUCKE, L., BENEDEK, G., ALBOWITZ, B., KATOH, Y. & CREUTZFELDT, O. D. (1986). Connections of the anterior ectosylvian visual area (AEV). *Exp Brain Res* **62**, 225-240.
- NOWAK, L. G. & BULLIER, J. (1997). The timing of information transfer in the visual system. In *Cerebral Cortex: Extrastriate Cortex in Primate*, vol. 12. ed.



ROCKLAND, K. S., KAAS, J. H. & PETERS, A., pp. 205-241. Plenum, New York.

NOWAK, L. G., MUNK, M. H., GIRARD, P. & BULLIER, J. (1995). Visual latencies in areas V1 and V2 of the macaque monkey. *Vis Neurosci* **12**, 371-384.

NOWLAN, S. J. & SEJNOWSKI, T. J. (1995). A selection model for motion processing in area MT of primates. *J Neurosci* **15**, 1195-1214.

OGINO, T. & OHTSUKA, K. (2000). Effects of superior colliculus inhibition on visual motion processing in the lateral suprasylvian visual area of the cat. *Invest Ophthalmol Vis Sci* **41**, 955-960.

OHTSUKA, K. & OGINO, T. (2001). Effects of superior colliculus inhibition on three-dimensional visual motion processing in the lateral suprasylvian visual area of the cat. *Jpn J Ophthalmol* **45**, 475-481.

OHZAWA, I., DEANGELIS, G. C. & FREEMAN, R. D. (1990). Stereoscopic depth discrimination in the visual cortex: neurons ideally suited as disparity detectors. *Science* **249**, 1037-1041.

OHZAWA, I., DEANGELIS, G. C. & FREEMAN, R. D. (1997). Encoding of binocular disparity by complex cells in the cat's visual cortex. *J Neurophysiol* **77**, 2879-2909.

OUELLETTE, B. G. & CASANOVA, C. (2006a). Overlapping visual response latency distributions in visual cortices and LP-pulvinar complex of the cat. *Exp Brain Res*.

OUELLETTE, B. G. & CASANOVA, C. (2006b). Overlapping visual response latency distributions in visual cortices and LP-pulvinar complex of the cat. *Exp Brain Res* **175**, 332-341.

OUELLETTE, B. G., FAUBERT, J. & CASANOVA, C. (2005). Mapping of spatiotemporal receptive field substructure of neurons in cat posteromedial lateral suprasylvian cortex. *Society for Neuroscience Abstracts*, 619.611.

OUELLETTE, B. G., FAUBERT, J. & CASANOVA, C. (2006). Simple-like receptive fields in cat postero-medial lateral suprasylvian cortex? *FENS Abstracts* **3**, A216.215.

OUELLETTE, B. G., LINDSAY, B. & CASANOVA, C. (2004a). Visual response latencies vary for different stimuli and across visual areas in cats. *Society for Neuroscience Abstracts*, 410.417.

- OUELLETTE, B. G., MINVILLE, K., BOIRE, D., PTITO, M. & CASANOVA, C. (2002). Simple and complex motion selectivity in PMLS cortex following early primary visual cortex lesions in the cat. *Society for Neuroscience Abstracts*, 657.655.
- OUELLETTE, B. G., MINVILLE, K., BOIRE, D., PTITO, M. & CASANOVA, C. (2007). Complex motion selectivity in PMLS cortex following early lesions of primary visual cortex in the cat. *Vis Neurosci* **24**, 53-64.
- OUELLETTE, B. G., MINVILLE, K., FAUBERT, J. & CASANOVA, C. (2004b). Simple and complex visual motion response properties in the anterior medial bank of the lateral suprasylvian cortex. *Neuroscience* **123**, 231-245.
- PACK, C. C., CONWAY, B. R., BORN, R. T. & LIVINGSTONE, M. S. (2006). Spatiotemporal structure of nonlinear subunits in macaque visual cortex. *J Neurosci* **26**, 893-907.
- PALMER, L. A. & DAVIS, T. L. (1981a). Comparison of responses to moving and stationary stimuli in cat striate cortex. *J Neurophysiol* **46**, 277-295.
- PALMER, L. A. & DAVIS, T. L. (1981b). Receptive-field structure in cat striate cortex. *J Neurophysiol* **46**, 260-276.
- PALMER, L. A., ROSENQUIST, A. C. & TUSA, R. J. (1978). The retinotopic organization of lateral suprasylvian visual areas in the cat. *J Comp Neurol* **177**, 237-256.
- PASCUAL-LEONE, A. & WALSH, V. (2001). Fast backprojections from the motion to the primary visual area necessary for visual awareness. *Science* **292**, 510-512.
- PASTERNAK, T., HORN, K. M. & MAUNSELL, J. H. (1989). Deficits in speed discrimination following lesions of the lateral suprasylvian cortex in the cat. *Vis Neurosci* **3**, 365-375.
- PASTERNAK, T., TOMPKINS, J. & OLSON, C. R. (1995). The role of striate cortex in visual function of the cat. *J Neurosci* **15**, 1940-1950.
- PAYNE, B. R. (1993). Evidence for visual cortical area homologs in cat and macaque monkey. *Cereb Cortex* **3**, 1-25.
- PAYNE, B. R. (2004). Neuroplasticity in the cat's visual system: test of the role of the expanded retino-geniculo-parietal pathway in behavioral sparing following early lesions of visual cortex. *Exp Brain Res* **155**, 69-80.
- PAYNE, B. R. & CORNWELL, P. (1994). System-wide repercussions of damage to the immature visual cortex. *Trends Neurosci* **17**, 126-130.

- PAYNE, B. R., FOLEY, H. A. & LOMBER, S. G. (1993). Visual cortex damage-induced growth of retinal axons into the lateral posterior nucleus of the cat. *Vis Neurosci* **10**, 747-752.
- PAYNE, B. R. & LOMBER, S. G. (1998a). Neuroplasticity in the cat's visual system. *Exp Brain Res* **12**, 334-349.
- PAYNE, B. R. & LOMBER, S. G. (1998b). Neuroplasticity in the cat's visual system. Origin, termination, expansion, and increased coupling of the retinogeniculo-middle suprasylvian visual pathway following early ablations of areas 17 and 18. *Exp Brain Res* **121**, 334-349.
- PETRONI, F., PANZERI, S., HILGETAG, C. C., KOTTER, R. & YOUNG, M. P. (2001). Simultaneity of responses in a hierarchical visual network. *Neuroreport* **12**, 2753-2759.
- PTITO, M. & LEPORE, F. (1983). Effects of unilateral and bilateral lesions of the lateral suprasylvian area on learning and interhemispheric transfer of pattern discrimination in the cat. *Behav Brain Res* **7**, 211-227.
- RACZKOWSKI, D. & ROSENQUIST, A. C. (1980). Connections of the parvocellular C laminae of the dorsal lateral geniculate nucleus with the visual cortex in the cat. *Brain Res* **199**, 447-451.
- RACZKOWSKI, D. & ROSENQUIST, A. C. (1983). Connections of the multiple visual cortical areas with the lateral posterior-pulvinar complex and adjacent thalamic nuclei in the cat. *J Neurosci* **3**, 1912-1942.
- RAIGUEL, S. E., LAGAE, L., GULYAS, B. & ORBAN, G. A. (1989). Response latencies of visual cells in macaque areas V1, V2 and V5. *Brain Res* **493**, 155-159.
- RAIGUEL, S. E., XIAO, D. K., MARCAR, V. L. & ORBAN, G. A. (1999). Response latency of macaque area MT/V5 neurons and its relationship to stimulus parameters. *J Neurophysiol* **82**, 1944-1956.
- RAUSCHECKER, J. P. (1988). Visual function of the cat's LP/LS subsystem in global motion processing. *Prog Brain Res* **75**, 95-108.
- RAUSCHECKER, J. P., VON GRUNAU, M. W. & POULIN, C. (1987a). Centrifugal organization of direction preferences in the cat's lateral suprasylvian visual cortex and its relation to flow field processing. *J Neurosci* **7**, 943-958.
- RAUSCHECKER, J. P., VON GRUNAU, M. W. & POULIN, C. (1987b). Thalamo-cortical connections and their correlation with receptive field properties in the cat's lateral suprasylvian visual cortex. *Exp Brain Res* **67**, 100-112.

- REICHARDT, W. (1961a). Autocorrelation, a principle for the evaluation of sensory information by the central nervous system. In *Sensory communication*. ed. ROSENBLICH, W., pp. 303-317. MIT Press, New York.
- REICHARDT, W. (1961b). Autocorrelation, a principle for the evaluation of sensory information by the central nervous system. In *Sensory Communication*. ed. ROSENBLICH, W., pp. 303-317. MIT Press, New York.
- RINGACH, D. L., HAWKEN, M. J. & SHAPLEY, R. (1997a). Dynamics of orientation tuning in macaque primary visual cortex. *Nature* **387**, 281-284.
- RINGACH, D. L., SAPIRO, G. & SHAPLEY, R. (1997b). A subspace reverse-correlation technique for the study of visual neurons. *Vision Res* **37**, 2455-2464.
- ROBERTSON, R. T. (1976). Thalamic projections to visually responsive regions of parietal cortex. *Brain Res Bull* **1**, 459-469.
- ROBINSON, D. L. & RUGG, M. D. (1988). Latencies of visually responsive neurons in various regions of the rhesus monkey brain and their relation to human visual responses. *Biol Psychol* **26**, 111-116.
- ROCKLAND, K. S. & PANDYA, D. N. (1979). Laminar origins and terminations of cortical connections of the occipital lobe in the rhesus monkey. *Brain Res* **179**, 3-20.
- RODMAN, H. R., GROSS, C. G. & ALBRIGHT, T. D. (1989). Afferent basis of visual response properties in area MT of the macaque. I. Effects of striate cortex removal. *J Neurosci* **9**, 2033-2050.
- RODMAN, H. R., GROSS, C. G. & ALBRIGHT, T. D. (1990). Afferent basis of visual response properties in area MT of the macaque. II. Effects of superior colliculus removal. *J Neurosci* **10**, 1154-1164.
- ROELFSEMA, P. R., LAMME, V. A. & SPEKREIJSE, H. (1998). Object-based attention in the primary visual cortex of the macaque monkey. *Nature* **395**, 376-381.
- ROELFSEMA, P. R., TOLBOOM, M. & KHAYAT, P. S. (2007). Different processing phases for features, figures, and selective attention in the primary visual cortex. *Neuron* **56**, 785-792.
- ROSA, M. G., TWEEDALE, R. & ELSTON, G. N. (2000). Visual responses of neurons in the middle temporal area of new world monkeys after lesions of striate cortex. *J Neurosci* **20**, 5552-5563.

- ROSENQUIST, A. C. & PALMER, L. A. (1971). Visual receptive field properties of cells of the superior colliculus after cortical lesions in the cat. *Exp Neurol* **33**, 629-652.
- RUDOLPH, K. K. & PASTERNAK, T. (1996). Lesions in cat lateral suprasylvian cortex affect the perception of complex motion. *Cereb Cortex* **6**, 814-822.
- RUSHMORE, R. J. & PAYNE, B. R. (2003). Bilateral impact of unilateral visual cortex lesions on the superior colliculus. *Exp Brain Res* **151**, 542-547.
- RUSHMORE, R. J. & PAYNE, B. R. (2004). Neuroplasticity after unilateral visual cortex damage in the newborn cat. *Behav Brain Res* **153**, 557-565.
- RUST, N. C., SCHWARTZ, O., MOVSHON, J. A. & SIMONCELLI, E. P. (2005). Spatiotemporal elements of macaque v1 receptive fields. *Neuron* **46**, 945-956.
- SANDERSON, K. J. (1971). The projection of the visual field to the lateral geniculate and medial interlaminar nuclei in the cat. *J Comp Neurol* **143**, 101-108.
- SCANNELL, J. W. (1997). Determining cortical landscapes. *Nature* **386**, 452.
- SCANNELL, J. W., BLAKEMORE, C. & YOUNG, M. P. (1995). Analysis of connectivity in the cat cerebral cortex. *J Neurosci* **15**, 1463-1483.
- SCANNELL, J. W., BURNS, G. A., HILGETAG, C. C., O'NEIL, M. A. & YOUNG, M. P. (1999). The connectional organization of the cortico-thalamic system of the cat. *Cereb Cortex* **9**, 277-299.
- SCANNELL, J. W., SENGPHEL, F., TOVEE, M. J., BENSON, P. J., BLAKEMORE, C. & YOUNG, M. P. (1996). Visual motion processing in the anterior ectosylvian sulcus of the cat. *J Neurophysiol* **76**, 895-907.
- SCANNELL, J. W. & YOUNG, M. P. (1993). The connectional organization of neural systems in the cat cerebral cortex. *Curr Biol* **3**, 191-200.
- SCHMOLESKY, M. T., WANG, Y., HANES, D. P., THOMPSON, K. G., LEUTGEB, S., SCHALL, J. D. & LEVENTHAL, A. G. (1998). Signal timing across the macaque visual system. *J Neurophysiol* **79**, 3272-3278.
- SCHROEDER, C. E., MEHTA, A. D. & GIVRE, S. J. (1998). A spatiotemporal profile of visual system activation revealed by current source density analysis in the awake macaque. *Cereb Cortex* **8**, 575-592.

- SHEN, W., LIANG, Z., CHEN, X. & SHOU, T. (2006a). Posteromedial lateral suprasylvian motion area modulates direction but not orientation preference in area 17 of cats. *Neuroscience*.
- SHEN, W., LIANG, Z., CHEN, X. & SHOU, T. (2006b). Posteromedial lateral suprasylvian motion area modulates direction but not orientation preference in area 17 of cats. *Neuroscience* **142**, 905-916.
- SHERK, H. (1986). Location and connections of visual cortical areas in the cat's suprasylvian sulcus. *J Comp Neurol* **247**, 1-31.
- SHERK, H. & FOWLER, G. A. (2002). Lesions of extrastriate cortex and consequences for visual guidance during locomotion. *Exp Brain Res* **144**, 159-171.
- SHERK, H. & KIM, J. N. (2002). Responses in extrastriate cortex to optic flow during simulated turns. *Vis Neurosci* **19**, 409-419.
- SHERK, H., KIM, J. N. & MULLIGAN, K. (1995). Are the preferred directions of neurons in cat extrastriate cortex related to optic flow? *Vis Neurosci* **12**, 887-894.
- SHERK, H., MULLIGAN, K. & KIM, J. N. (1997). Neuronal responses in extrastriate cortex to objects in optic flow fields. *Vis Neurosci* **14**, 879-895.
- SHERK, H. & MULLIGAN, K. A. (1992). Retinotopic order is surprisingly good within cell columns in the cat's lateral suprasylvian cortex. *Exp Brain Res* **91**, 46-60.
- SHERMAN, S. M. & GUILLERY, R. W. (1998). On the actions that one nerve cell can have on another: distinguishing "drivers" from "modulators". *Proc Natl Acad Sci U S A* **95**, 7121-7126.
- SHIPP, S. & GRANT, S. (1991). Organization of reciprocal connections between area 17 and the lateral suprasylvian area of cat visual cortex. *Vis Neurosci* **6**, 339-355.
- SHIPP, S. & ZEKI, S. (1989). The Organization of Connections between Areas V5 and V1 in Macaque Monkey Visual Cortex. *Eur J Neurosci* **1**, 309-332.
- SKOTTUN, B. C., DE VALOIS, R. L., GROSOF, D. H., MOVSHON, J. A., ALBRECHT, D. G. & BONDS, A. B. (1991a). Classifying simple and complex cells on the basis of response modulation. *Vision Res* **31**, 1079-1086.
- SKOTTUN, B. C., GROSOF, D. H. & DE VALOIS, R. L. (1991b). On the responses of simple and complex cells to random dot patterns. *Vision Res* **31**, 43-46.

- SMITH, D. C. & SPEAR, P. D. (1979). Effects of superior colliculus removal on receptive-field properties of neurons in lateral suprasylvian visual area of the cat. *J Neurophysiol* **42**, 57-75.
- SMITH, M. A., MAJAJ, N. J. & MOVSHON, J. A. (2005). Dynamics of motion signaling by neurons in macaque area MT. *Nat Neurosci* **8**, 220-228.
- SORENSEN, K. M. & RODMAN, H. R. (1999). A transient geniculo-extrastriate pathway in macaques? Implications for 'blindsight'. *Neuroreport* **10**, 3295-3299.
- SPEAR, P. D. (1988). Influence of areas 17, 18, and 19 on receptive-field properties of neurons in the cat's posteromedial lateral suprasylvian visual cortex. *Prog Brain Res* **75**, 197-210.
- SPEAR, P. D. (1991). Functions of extrastriate visual cortex in non-primate species. In *The neural basis of visual function*, vol. 4. ed. LEVENTHAL, A. G., pp. 339-370. MacMillan Press, London.
- SPEAR, P. D. (1995). Plasticity following neonatal visual cortex damage in cats. *Can J Physiol Pharmacol* **73**, 1389-1397.
- SPEAR, P. D. & BAUMANN, T. P. (1975). Receptive-field characteristics of single neurons in lateral suprasylvian visual area of the cat. *J Neurophysiol* **38**, 1403-1420.
- SPEAR, P. D. & BAUMANN, T. P. (1979). Effects of visual cortex removal on receptive-field properties of neurons in lateral suprasylvian visual area of the cat. *J Neurophysiol* **42**, 31-56.
- SPEAR, P. D., MILLER, S. & OHMAN, L. (1983). Effects of lateral suprasylvian visual cortex lesions on visual localization, discrimination, and attention in cats. *Behav Brain Res* **10**, 339-359.
- SRINIVASAN, M. V., JIN, Z. F., STANGE, G. & IBBOTSON, M. R. (1993). 'Vector white noise': a technique for mapping the motion receptive fields of direction-selective visual neurons. *Biol Cybern* **68**, 199-207.
- STEIN, B. E. & MAGALHAES-CASTRO, B. (1975). Effects of neonatal cortical lesions upon the cat superior colliculus. *Brain Res* **83**, 480-485.
- STEPNIEWSKA, I., QI, H. X. & KAAS, J. H. (1999). Do superior colliculus projection zones in the inferior pulvinar project to MT in primates? *Eur J Neurosci* **11**, 469-480.
- STEVENS, J. K. & GERSTEIN, G. L. (1976). Spatiotemporal organization of cat lateral geniculate receptive fields. *J Neurophysiol* **39**, 213-238.

- STONE, J., DREHER, B. & LEVENTHAL, A. (1979). Hierarchical and parallel mechanisms in the organization of visual cortex. *Brain Res* **180**, 345-394.
- SUDKAMP, S. & SCHMIDT, M. (2000). Response characteristics of neurons in the pulvinar of awake cats to saccades and to visual stimulation. *Exp Brain Res* **133**, 209-218.
- SYMONDS, L. L. & ROSENQUIST, A. C. (1984a). Corticocortical connections among visual areas in the cat. *J Comp Neurol* **229**, 1-38.
- SYMONDS, L. L. & ROSENQUIST, A. C. (1984b). Laminar origins of visual corticocortical connections in the cat. *J Comp Neurol* **229**, 39-47.
- SYMONDS, L. L., ROSENQUIST, A. C., EDWARDS, S. B. & PALMER, L. A. (1981). Projections of the pulvinar-lateral posterior complex to visual cortical areas in the cat. *Neuroscience* **6**, 1995-2020.
- SZULBORSKI, R. G. & PALMER, L. A. (1990). The two-dimensional spatial structure of nonlinear subunits in the receptive fields of complex cells. *Vision Res* **30**, 249-254.
- TEKIAN, A. & AFIFI, A. K. (1981). Efferent connections of the pulvinar nucleus in the cat. *J Anat* **132**, 249-265.
- THIELE, A., DISTLER, C., KORBMACHER, H. & HOFFMANN, K. P. (2004). Contribution of inhibitory mechanisms to direction selectivity and response normalization in macaque middle temporal area. *Proc Natl Acad Sci U S A* **101**, 9810-9815.
- TONG, L., KALIL, R. E. & SPEAR, P. D. (1982). Thalamic projections to visual areas of the middle suprasylvian sulcus in the cat. *J Comp Neurol* **212**, 103-117.
- TONG, L., KALIL, R. E. & SPEAR, P. D. (1984). Critical periods for functional and anatomical compensation in lateral suprasylvian visual area following removal of visual cortex in cats. *J Neurophysiol* **52**, 941-960.
- TONG, L. & SPEAR, P. D. (1986). Single thalamic neurons project to both lateral suprasylvian visual cortex and area 17: a retrograde fluorescent double-labeling study. *J Comp Neurol* **246**, 254-264.
- TONG, L., SPEAR, P. D. & KALIL, R. E. (1987). Effects of corpus callosum section on functional compensation in the posteromedial lateral suprasylvian visual area after early visual cortex damage in cats. *J Comp Neurol* **256**, 128-136.



- TONG, L. L., KALIL, R. E. & SPEAR, P. D. (1991). Development of the projections from the dorsal lateral geniculate nucleus to the lateral suprasylvian visual area of cortex in the cat. *J Comp Neurol* **314**, 526-533.
- TOYAMA, K., FUJII, K., KASAI, S. & MAEDA, K. (1986a). The responsiveness of Clare-Bishop neurons to size cues for motion stereopsis. *Neurosci Res* **4**, 110-128.
- TOYAMA, K., FUJII, K. & UMETANI, K. (1990). Functional differentiation between the anterior and posterior Clare-Bishop cortex of the cat. *Exp Brain Res* **81**, 221-233.
- TOYAMA, K., KOMATSU, Y., KASAI, H., FUJII, K. & UMETANI, K. (1985). Responsiveness of Clare-Bishop neurons to visual cues associated with motion of a visual stimulus in three-dimensional space. *Vision Res* **25**, 407-414.
- TOYAMA, K., KOMATSU, Y. & KOZASA, T. (1986b). The responsiveness of Clare-Bishop neurons to motion cues for motion stereopsis. *Neurosci Res* **4**, 83-109.
- TUCKER, T. J., KLING, A. & SCHARLOCK, D. P. (1968). Sparring of photic frequency and brightness discriminations after striatectomy in neonatal cats. *J Neurophysiol* **31**, 818-832.
- TUMOSA, N., MCCALL, M. A., GUIDO, W. & SPEAR, P. D. (1989). Responses of lateral geniculate neurons that survive long-term visual cortex damage in kittens and adult cats. *J Neurosci* **9**, 280-298.
- UNGERLEIDER, L. G. & MISHKIN, M. (1982). Two cortical visual systems. In *Analysis of visual behavior*. ed. INGLE, D., GOODALE, M. A. & MANSFIELD, R. J. W., pp. 549-586. MIT Press, Cambridge, Mass.
- UPDYKE, B. V. (1981). Projections from visual areas of the middle suprasylvian sulcus onto the lateral posterior complex and adjacent thalamic nuclei in cat. *J Comp Neurol* **201**, 477-506.
- VAJDA, I., BORGHUIS, B. G., VAN DE GRIND, W. A. & LANKHEET, M. J. (2006). Temporal interactions in direction-selective complex cells of area 18 and the posteromedial lateral suprasylvian cortex (PMLS) of the cat. *Vis Neurosci* **23**, 233-246.
- VAJDA, I., LANKHEET, M. J., BORGHUIS, B. G. & VAN DE GRIND, W. A. (2004). Dynamics of directional selectivity in area 18 and PMLS of the cat. *Cereb Cortex* **14**, 759-767.

- VAJDA, I., LANKHEET, M. J. & VAN DE GRIND, W. A. (2005). Spatio-temporal requirements for direction selectivity in area 18 and PMLS complex cells. *Vision Res* **45**, 1769-1779.
- VAN ESSEN, D. C. & MAUNSELL, J. H. (1983). Hierarchical organization and functional streams in the visual cortex. *TINS* **6**, 370-375.
- VANDUFFEL, W., PAYNE, B. R., LOMBER, S. G. & ORBAN, G. A. (1997a). Functional impact of cerebral connections. *Proc Natl Acad Sci U S A* **94**, 7617-7620.
- VANDUFFEL, W., VANDENBUSSCHE, E., SINGER, W. & ORBAN, G. A. (1995). Metabolic mapping of visual areas in the behaving cat: a [<sup>14</sup>C]2-deoxyglucose study. *J Comp Neurol* **354**, 161-180.
- VANDUFFEL, W., VANDENBUSSCHE, E., SINGER, W. & ORBAN, G. A. (1997b). A metabolic mapping study of orientation discrimination and detection tasks in the cat. *Eur J Neurosci* **9**, 1314-1328.
- VIDNYANSZKY, Z., BOROSTYANKOI, Z., GORCS, T. J. & HAMORI, J. (1996). Light and electron microscopic analysis of synaptic input from cortical area 17 to the lateral posterior nucleus in cats. *Exp Brain Res* **109**, 63-70.
- VILLENEUVE, M. Y., PTITO, M. & CASANOVA, C. (2006a). Global motion integration in the postero-medial part of the lateral suprasylvian cortex in the cat. *Exp Brain Res* **172**, 485-497.
- VILLENEUVE, M. Y., PTITO, M. & CASANOVA, C. (2006b). Global motion integration in the postero-medial part of the lateral suprasylvian cortex in the cat. *Exp Brain Res In Press*.
- VOGELS, R. & ORBAN, G. A. (1990). How well do response changes of striate neurons signal differences in orientation: a study in the discriminating monkey. *J Neurosci* **10**, 3543-3558.
- VOGELS, R. & ORBAN, G. A. (1994). Activity of inferior temporal neurons during orientation discrimination with successively presented gratings. *J Neurophysiol* **71**, 1428-1451.
- VOLGUSHEV, M., VIDYASAGAR, T. R. & PEI, X. (1995). Dynamics of the orientation tuning of postsynaptic potentials in the cat visual cortex. *Vis Neurosci* **12**, 621-628.
- VON GRUNAU, M. & FROST, B. J. (1983). Double-opponent-process mechanism underlying RF-structure of directionally specific cells of cat lateral suprasylvian visual area. *Exp Brain Res* **49**, 84-92.

- WETZEL, A. B., THOMPSON, V. E., HOREL, J. A. & MEYER, P. M. (1965). Some consequences of perinatal lesions of the visual cortex in the cat. *Psychon Sci* **3**, 381-382.
- WEYAND, T. G. & GAFKA, A. C. (2001). Visuomotor properties of corticotectal cells in area 17 and posteromedial lateral suprasylvian (PMLS) cortex of the cat. *Vis Neurosci* **18**, 77-91.
- WICKELGREN, B. G. & STERLING, P. (1969). Influence of visual cortex on receptive fields in the superior colliculus of the cat. *J Neurophysiol* **32**, 16-23.
- XUE, J. T., KIM, C. B., MOORE, R. J. & SPEAR, P. D. (1994). Influence of the superior colliculus on responses of lateral geniculate neurons in the cat. *Vis Neurosci* **11**, 1059-1076.
- ZABOURI, N., PTITO, M. & CASANOVA, C. (2003). Complex motion sensitivity of neurons in the visual part of the anterior ectosylvian cortex. *Society for Neuroscience Abstracts*, 179.174.
- ZUMBROICH, T. J. & BLAKEMORE, C. (1987). Spatial and temporal selectivity in the suprasylvian visual cortex of the cat. *J Neurosci* **7**, 482-500.

Annexe I

Permission des éditeurs